Thèse présentée pour obtenir le grade de Docteur
de l'Université Louis Pasteur - Strasbourg I

DISCIPLINE : CHIMIE

ECOLE DOCTORALE : PHYSIQUE ET CHIMIE-PHYSIQUE

Présentée par

Perrine BORDES

NANO-BIOCOMPOSITES : ÉTUDE DE SYSTÈMES STRUCTURÉS À BASE DE POLYHYDROXYALCANOATES ET MONTMORILLONITES

Soutenue le jeudi 29 novembre 2007 devant le jury composé de :

Serge BOURBIGOT	Professeur, ENSC Lille	Président du jury
Alain DUFRESNE	Professeur, INP Grenoble	Rapporteur externe
Yves GROHENS	Professeur, Université Bretagne Sud	Rapporteur externe
Guy SCHLATTER	Professeur, ULP Strasbourg	Rapporteur interne
Luc AVEROUS	Professeur, ULP Strasbourg	Directeur de thèse
Eric POLLET	Maître de Conférences, ULP Strasbourg	Examinateur

LIPHT, Laboratoire d'Ingénierie des Polymères pour les Hautes Technologies, UMR 7165
ECPM, Ecole Européenne de Chimie Polymères et Matériaux
25 Rue Becquerel – 67 087 Strasbourg Cedex 2

REMERCIEMENTS

Au terme de cette aventure, je voudrais en premier lieu remercier le Professeur Luc Avérous pour m'avoir confié ce sujet qui me tenait à cœur, et le Professeur Georges Hadziioannou pour m'avoir accueillie dans son laboratoire.

Je tiens également à remercier Messieurs les Professeurs Alain Dufresne (Institut National Polytechnique de Grenoble), Yves Grohens (Université de Bretagne Sud, Lorient) et Guy Schlatter (Université Louis Pasteur, Strasbourg) pour avoir accepté de juger ce travail de thèse. Je remercie tout particulièrement le Professeur Serge Bourbigot (ENSCLille - PERF) pour m'avoir fait l'honneur de présider ce jury de thèse. Je voudrais vous exprimer toute ma reconnaissance pour l'intérêt que vous avez porté à mon travail et vos encouragements, pour votre expertise qui a permis de faire avancer de manière significative ce projet.

D'autres collaborations ont été essentielles pour mener à bien ce travail de recherche. Je remercie donc la Société Biocycle/PHB Industrial SA (Brésil) représentée par Messieurs Ortega et Nascimento pour nous avoir fourni gracieusement les précieux PHAs, Mme Ducruet (ENSAIA - AgroParitech) pour le dosage des protéines, Mme Pourroy, directrice du GMI (IPCMS Strasbourg), pour nous avoir autorisé à utiliser les équipements de DRX et d'ATG, et enfin Mme Foussat du Service Caractérisation de l'ICS Strasbourg pour les analyses par CES.

J'adresse mes plus sincères remerciements à "chef" (Eric) pour m'avoir supportée au quotidien durant ces 3 années. Merci pour ta disponibilité et ta patience, pour tes nombreux conseils avisés et autres "trucs et astuces" toujours payants, pour ta "zénitude" et ton flegme qui m'auront toujours sidérés, pour ton inépuisable sens de la répartie…et la liste est encore longue. Bref, une personne sans qui les "bas" auraient été encore plus bas.

Je n'oublie pas les personnes qui ont participé de près ou de loin à ce projet de recherche : Zuzana et son grain de folie (rassurez-vous, juste ce qu'il faut !), Fred, Elodie et Ludovic ; ainsi que les personnes qui m'ont côtoyée au quotidien i.e. les locataires du R1N2Bu1 : Fred, déjà cité, mais aussi P^3 et la fouine masquée.

Un grand merci à tous les permanents du labo : Guy, Cyril, Nicolas, Christophe Serra et M. Muller qui ont pu me renseigner sur une question, un point crucial ; Christophe S. que je ne remercierai jamais assez, Christophe M. et Thierry le SOS dépannage du labo avec leur doigts de fée ; et enfin Chhengounette, (avec l'accent SVP !), Dju et Catherine pour leur aide dans l'intendance au quotidien.

…/…

Merci également à tous les thésards et post-docs qui m'ont montré la voie : Guillaume, Guigui, Laurent, Sophie, Doreen, Khaled et à tous les autres qui participent aujourd'hui à la vie de ce labo : Fanny et son rire inimitable, Rony, Cheveux, Laure…

Je tiens enfin à remercier l'ensemble des personnes qui m'ont conseillée et soutenue dans les moments difficiles et qui m'ont aidé à surmonter les épreuves : en tout premier lieu M'man et P'pa, M. Lopez, Rose-Anne et Jean-Charles, Gilbert, Colette, Rosine et les Jean-Claude, Virginie et Antoine et les anciens A7iens (Cyril, Hélène, Julie, Lucie, Nadège, Romain, Thorsten et Xav).

Abréviations

PHA(s)	Polyhydroxyalcanoate(s)
PHAp	Polyhydroxyalcanoate purifié
PHB	Polyhydroxybutyrate
PHBp	Polyhydroxybutyrate purifié
HV	Hydroxyvalérate
PHBV	Poly(hydroxybutyrate-co-hydroxyvalérate)
PHBVp	Poly(hydroxybutyrate-co-hydroxyvalérate) purifié
LA	Acide lactique
PLA	Poly(acide lactique) ou polylactide
ε-CL	ε-caprolactone
PCL	Polycaprolactone
o-PCL	Oligo-caprolactone
BAP	Biodegradable aliphatic polyester
PBS	Poly(butylene succinate)
PBSA	Poly(butylene succinate-co-adipate)
PBAT	Poly(butylene succinate-co-butylene terephtalate)
PEG	Polyethylene glycol
PEA	Polyesteramide
Rsd	Résidus de fermentation
S-Alk ou 2M2HT	Dimethyl dihydrogenated tallow ammonium
S-Bz ou 2MBHT	Dimethyl benzyl hydrogenated tallow ammonium
S-EtOH ou MTEtOH	Methyl bis-2-hydroxyethyl tallow ammonium
TEA	Triethylamine
TMA	Tetramethyl ammonium
MMT	Montmorillonite
MMT-Na	Montmorillonite sodique ou montmorillonite naturelle
OMMT	Montmorillonite organomodifiée
OMMT-Alk	Montmorillonite organomodifiée par S-Alk (ou 2M2HT)
OMMT-Bz	Montmorillonite organomodifiée par S-Bz (ou 2MBHT)
OMMT-OH	Montmorillonite organomodifiée par S-EtOH (ou MT2EtOH)
OLS ou OMLS	Organo-modified layered silicates
SFM	Synthetic fluoromica
CEC	Capacité d’échange cationique
CES / SEC	Chromatographie d’exclusion stérique

RMN / NMR	Résonance magnétique nucléaire
DRX / XRD	Diffraction des rayons X
WAXS	Diffraction des rayons X aux grands angles (2θ>1010°)
SAXS	Diffraction des rayons X aux petits angles (2θ=0 à 10°)
MET / TEM	Microscop(i)e électronique à transmission
ATG / TGA ou TG	Analyse thermogravimetrique, i.e. courbe de perte de masse
DTG	Dérivée de la perte de masse
DSC	Calorimétrie différentielle à balayage
DMTA ou DMA	Analyse thermo-mécanique dynamique
RDA	Analyse rhéologique dynamique
$\gamma_{S/V}$ (mJ/m²)	Energie de surface solide/vapeur
Ip / PDI	Indice de molécularité
Mn	Masse molaire moyenne en nombre
Mw	Masse molaire moyenne en poids
δ (ppm)	Déplacement chimique
d (Å ou nm)	Distance interfeuillets
λ (Å ou nm)	Longueur d'onde
2θ (°)	Angle de diffraction
Δw (%)	Taux de matière organique
T_{dmax} (°C)	Température de dégradation maximale
$T_{x\%}$ (°C)	Température à laquelle la perte de masse est égale à x% de la masse initiale
α et dα	Taux de conversion de la réaction et sa dérivée
k(T)	Constance cinétique d'Arrhénius
T et dT (°C)	Température et sa dérivée
t et dt (s)	Temps et sa dérivée
R	Constante des gaz parfaits
β	Vitesse de montée en température
n	Ordre de la réaction ou ordre de diffraction
E_a	Energie d'activation
E_m (kJ/kg)	Energie mécanique
Tg (°C)	Température de transition vitreuse
T_f ou T_m (°C)	Température de fusion

T_c (°C)	Température de cristallisation
T_{cc} (°C)	Température de cristallisation au refroidissement
T_{ch} (°C)	Température de cristallisation à la chauffe
ΔH_c (J/g)	Enthalpie de cristallisation
ΔH_{cc} (J/g)	Enthalpie de cristallisation au refroidissement
ΔH_{ch} (J/g)	Enthalpie de cristallisation à la chauffe
ΔH_m (J/g)	Enthalpie de fusion
$\Delta H_{c\ 100\%}$ (J/g)	Enthalpie de fusion du polymère 100% cristallin
χ (%)	Taux de cristallinité
E (MPa)	Module d'Young ou module élastique
σ_y (MPa)	Contrainte au seuil
ε_b (%)	Elongation à la rupture
E'	Module de conservation
E''	Module de perte
tan δ	Loss angle tangent
G'	Storage modulus
G''	Loss modulus

Communications liées à cette étude

Ce travail de thèse a donné lieu à différentes communications :

Présentations orales :

- Bordes P., Chivrac F., Kadlecova Z., Pollet E., Avérous L. (2006) « Nano-biocomposites : Nanofillers organization in biopolymer matrices » Nanocomposites 2006, 6-7 Avril 2006, Montpellier (France)
- Bordes P., Pollet E., Avérous L. (2006) «Analyse de structuration de nano-biocomposites » Journée SFC - section Grand Est. 4 Mai 2006, Strasbourg (France)

Communications par affiches :

- Bordes P., Kadlecova Z., Chivrac F., Pollet E., Avérous L. (2005) « Nano-biocomposites : de l'élaboration à la caractérisation ». 35ème Congrès annuel GFP, 22-24 Novembre 2005, Paris (France).
- Chivrac F., Bordes P., Kadlecova Z., Pollet E., Avérous L. (2006) « Elaboration and structural characterization of nano-biocomposites ». Polymer Processing Symposia PPS-22, 2-6 Juillet 2006, Yamagata (Japon).
- Bordes P., Pollet E., Avérous L. (2006) "Nano-biocomposite: an environmentally friendly material". Symposium on Bioinspired Materials for the chemical Industry, 7-9 Août 2006, Strasbourg (France).
- Bordes P., Hablot E., Pollet E., Avérous L. (2006) « PHA-based nano-biocomposites: Influence of fillers and process on biopolymer properties », Trends in Materials an Nanosciences (TMN), 21-24 Novembre 2006, Strasbourg (France).
- Bordes P., Hablot E., Pollet E., Avérous L. (2007), « Structure and properties of PHA/Clay nano-biocomposites », Polymer Processing Symposia PPS-23, 27-31 Mai 2007, San Salvador (Brésil).

Sommaire

Introduction générale

Les questions environnementales occupent de nos jours une place de plus en plus importante dans notre société. Les scientifiques ont été les premiers à pointer du doigt les problèmes de réchauffement climatique, de pollution et de disponibilité des ressources fossiles (pétrole, gaz...) auxquels nous sommes déjà confrontés et qui vont s'accroître dans les années à venir. Aussi, des politiques de développement durable sont mises en place afin de sensibiliser les populations à ces préoccupations, et solliciter leur sens civique aux travers des "petits gestes" du quotidien. Mais à plus long terme et à plus grande échelle, elles visent à promouvoir et à mettre en place de véritables solutions écologiques pérennes, que ce soit dans le domaine de l'énergie ou des matériaux. Ces orientations s'inscrivent dans un contexte de :

(i) raréfaction et forte évolution du prix des ressources fossiles,

(ii) forte dépendance nationale dans l'approvisionnement des matières premières fossiles,

(iii) forte industrie pétrolière « nationale » face à une agro-industrie organisée et puissante.

En réponse à ces différentes attentes, les polymères biodégradables notamment ceux d'origine renouvelable font l'objet de nombreuses études depuis plusieurs années. Ils sont souvent issus d'agro-ressources et se biodégradent dans la nature ou en compost contrôlé. Leur cycle de vie est en parfaite adéquation avec un contexte croissant de "développement durable" du fait que le compost généré par la dégradation de ces matériaux permet d'amender des sols, lesquels vont être le support de nouvelles cultures (cf. schéma). Ils apparaissent donc comme une alternative de plus en plus crédible pour répondre aux différentes préoccupations environnementales, et notamment pour remplacer les polymères synthétiques non dégradables classiques pour des applications à durée de vie limitée.

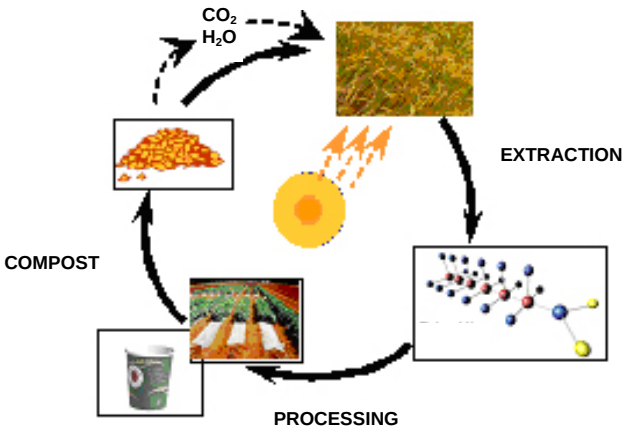

Cycle de vie des matériaux issus de ressources renouvelables et biodégradables

Bien que la demande sociétale de « matériaux biodégradables » vienne aujourd'hui en second plan, au profit d'une demande de « matériaux issus de ressources renouvelables », les « biodégradables » sont aujourd'hui une catégorie à part entière de matériaux polymères, en plein développement. Pour illustrer cela, quelques chiffres : la part mondiale des polymères biodégradables dans l'environnement était de 0,03 % en 2000, cinq ans plus tard (2005) elle était passée à 0,3 %. Sur les 10 dernières années, la capacité de leur production mondiale a présenté une très forte croissance (données IBAW). Elle est actuellement proche de 500 000 tonnes/an, ce qui correspond à une augmentation par un facteur 10 en moins de 7 ans. Cette croissance a été de l'ordre de 60% par an sur les 6 dernières années, selon une étude récente de l'ADEME (Agrice). En France, cette croissance est actuellement accélérée par la directive 2010. Les députés français ont adopté le 11 octobre 2005, un amendement au projet de loi d'orientation agricole interdisant par exemple les sachets non biodégradables en sortis de caisse à partir du 1er janvier 2010. Au niveau européen, des pays comme l'Italie sont actuellement en train de réfléchir à l'application d'une telle directive dans leur propre pays. En Europe, la consommation en polymères biodégradables était de 20 000 tonnes en 2000, elle a doublé en trois ans avec de nombreuses applications, notamment dans le domaine du packaging à courte durée de vie. Les emballages plastiques biodégradables représentent déjà près de 1 % du tonnage d'emballages plastiques mis sur le marché en Europe. On trouve aussi d'autres débouchés significatifs dans les domaines de l'agriculture et de l'horticulture (films de paillage, clips, pots …). Ces matériaux biodégradables, qu'ils soient ou non issus de ressources renouvelables, trouvent également des applications dans des domaines particuliers à hautes valeurs ajoutées comme le biomédical.

Cependant, ces matériaux présentent un certain nombre de points faibles (e.g. propriétés mécaniques) qui limitent actuellement leurs développements pour des applications technologiques industrielles viables. Afin de remédier à cela, il existe deux principales approches : (i) la modification chimique du polymère et (ii) l'association physique du polymère avec d'autres composés au travers d'une approche "formulation". L'élaboration de nano-biocomposites illustre parfaitement cette seconde voie puisqu'il s'agit de concevoir des matériaux hybrides constitués d'une matrice biopolymère dans laquelle sont dispersées des charges de taille nanométrique pour renforcer et conférer de nouvelles propriétés au matériau. Les nanocomposites conventionnels sont actuellement une partie intégrante du paysage industriel mondial. En 2003, leur production s'élevait à 12 500 tonnes soit 90,8 millions de dollars et devrait représenter 36 000 tonnes en 2008. De plus, on s'attend en 2010, à ce que cette production passe à 500 000 tonnes. Ils sont principalement utilisés dans les

secteurs de l'automobile (carrosserie, baguettes de protection latérales,…) et de l'emballage, mais également dans la construction et le câblage. La thématique autour des nano-biocomposites s'inscrit, par rapport aux nanocomposites classiques (PP, PA6,), comme une nouvelle étape technologique à forte valeur ajoutée, avec une approche d'ingénierie en éco-conception.

Le développement de ces matériaux nanostructurés s'appuie sur l'intérêt majeur des nanocharges qui est d'offrir une surface spécifique très élevée permettant d'obtenir une surface interfaciale importante avec la matrice (jusqu'à 700 m^2/g), et ceci, à de faibles taux de charges, typiquement quelques pourcents. Toutefois, une bonne affinité polymère/nanocharges ainsi qu'une répartition homogène de la charge dans la matrice sont requises pour atteindre une amélioration significative des propriétés de la matrice. La nanocharge la plus communément utilisée est une argile, la montmorillonite. Elle se présente, à l'état natif, sous la forme d'un empilement de feuillets de 1 nm d'épaisseur, séparés par une distance interfeuillets caractéristique, à la surface desquels se trouvent des cations inorganiques (Na^+, Ca^{2+}…). La montmorillonite naturelle présente ainsi un caractère hydrophile qui, bien souvent, n'est pas en adéquation avec le caractère organophile de la plupart des polymères. Toutefois, par échange cationique, l'affinité polymère/montmorillonite peut être modulée. Pour cela, on utilise des surfactants, généralement des ammoniums quaternaires portant une ou deux longues chaînes alkyles, qui permettent ainsi de conférer un caractère organophile à l'argile et de compatibiliser la charge et la matrice.

L'élaboration de tels matériaux s'inscrit parfaitement dans la thématique *"Bioplastiques-Biopolymères"* du Laboratoire d'Ingénierie des Polymères pour les Hautes Technologies (LIPHT – UMR CNRS 7165) de Strasbourg. Ce travail de thèse porte sur l'étude des relations "procédé-structure-propriétés" de matériaux nano-biocomposites, et en particulier du système Polyhydroxyalkanoate/Montmorillonite. Le choix du polymère s'inscrit dans une collaboration avec la société brésilienne Copersucar-PHB Industrial qui produit des polyhydroxyalcanoates (PHAs) désignés sous l'appellation Biocycle©. Le choix des PHAs en tant que matrice s'est également et principalement fait en raison de leurs propriétés. Ce sont des biopolyesters biodégradables et biocompatibles synthétisés par fermentation bactérienne de produits dérivés de la canne sucre. Ils présentent notamment une bonne rigidité et un taux de cristallinité très important. En revanche, le comportement mécanique fragile et la faible stabilité thermique restent des inconvénients majeurs à leurs utilisations. L'élaboration des

nano-biocomposites à base de PHA vise donc à pallier ces déficiences et pourrait permettre de lever ces verrous technologiques.

Ce document, structuré en quatre chapitres homogènes, présente les résultats de ces travaux de recherche.

L'étude bibliographique concernant les nano-biocomposites biopolyester/montmorillonite présentée au **Chapitre I** révèle que l'amélioration des propriétés du matériau est principalement conditionnée par trois facteurs : l'affinité polymère/argile, le taux de nanocharges et le procédé d'élaboration. Le procédé d'organo-modification de la montmorillonite favorise la diffusion de chaînes polymères dans l'espace interfeuillets ainsi que la déstructuration, i.e. l'exfoliation, de la nanocharge. Les feuillets individuels résultants peuvent ainsi jouer pleinement leur rôle de 'renfort'. La déstructuration et la dispersion des charges peuvent également être favorisées suivant la méthode d'élaboration utilisée. Il s'agit donc de trouver la meilleure adéquation polymère/montmorillonite/procédé d'élaboration afin d'optimiser l'exfoliation et la dispersion de l'argile au sein des PHAs et donc d'améliorer les propriétés de ces derniers.

Le **Chapitre II** présente les travaux menés sur l'élaboration des systèmes PHA/montmorillonites, la caractérisation de leur structure et de leurs propriétés. Deux voies d'élaboration ont été envisagées : la voie "solvant" (solubilisation dans le chloroforme puis évaporation) et la voie "fondu" mettant en œuvre des techniques conventionnelles de mélange des polymères à l'état fondu. De plus, afin de balayer une large gamme d'affinité polymère/nanocharges et de tester son influence sur la qualité de la dispersion, différents types de montmorillonites (naturelles ou organo-modifiées par différents surfactants) ont été sélectionnés. La caractérisation des matériaux obtenus s'est faite au travers de différentes approches micro- et macroscopique. Dans un premier temps, le degré d'intercalation/exfoliation et la répartition de la nanocharge au sein de la matrice ont été déterminés par des moyens d'investigations avancés tels que la diffraction des rayons X (DRX) aux petits angles et la microscopie électronique à transmission (MET). Une technique originale de caractérisation de la structure de matériaux nanocomposites par RMN du solide, récemment mise au point, a également permis de compléter ces résultats. Dans un second temps, les propriétés macroscopiques, i.e. thermiques, mécaniques,… ont été corrélées aux données structurales observées préalablement.

La faible stabilité thermique et thermomécanique des matériaux PHA/montmorillonites nous a conduits à mener une étude plus approfondie de la dégradation des PHAs dans de tels systèmes. Une analyse détaillée de la cinétique de dégradation et des produits de décomposition présentée au **Chapitre III** nous ont permis d'identifier les différents composés et les mécanismes mis en jeu dans les réactions de dégradation des PHAs dans de tels systèmes.

Enfin, le **Chapitre IV** fait état des différentes approches exploratoires qui ont été envisagées pour tenter de pallier les problèmes de stabilité thermique rencontrés et d'améliorer la dispersion de la charge au sein de la matrice PHA. Ces différentes approches permettent d'isoler les nanocharges minérales de la matrice, notamment par rapport aux sites acides de Lewis portés par les feuillets inorganiques. La première approche cherche à favoriser des réactions de transestérification afin de greffer le polymère à la surface des feuillets de montmorillonite et ainsi d'améliorer la compatibilité matrice/argile. La seconde approche étudiée consiste à disperser dans le polyhydroxybutyrate un mélange maître biopolyester/argile constitué de polycaprolactone greffé aux feuillets de montmorillonite par polymérisation par ouverture de cycle (ROP). Dans les deux cas, la structure des matériaux et certaines de leurs propriétés ont été caractérisées.

Chapitre I
-
Synthèse bibliographique

Introduction

Les matériaux issus de ressources naturelles et renouvelables suscitent depuis ces dernières années un intérêt considérable en raison principalement de la raréfaction des ressources fossiles et du souci grandissant de la préservation de l'environnement. Ce phénomène s'est accéléré par la mise en place récente de politiques de développement durable qui visent à promouvoir des solutions plus respectueuse de l'environnement dans le domaine des énergies et des matériaux. Les polymères biodégradables (biopolymères) qui ont fait l'objet de nombreuses recherches, apparaissent comme une alternative de plus en plus crédible pour répondre aux préoccupations environnementales. Les biopolymères se divisent en deux classes : les agro-polymères, tels que l'amidon, les protéines etc., et les biopolyesters (PHA, PLA,…). Certains de ces biopolyesters (polyesters biodégradables) peuvent être produits à partir de ressources renouvelables. Cependant, pour certaines applications, les propriétés de ces matériaux sont insuffisantes pour des applications industrielles pérennes. Par conséquent, pour améliorer leur compétitivité, notamment sur le plan technique, et développer leur champ d'application, différentes voies sont possibles, dont notamment l'incorporation de charges de taille nanométrique. Ces matériaux combinant biodégradabilité de la matrice et renfort de la charge sont appelés 'nano-biocomposites' et ont déjà fait l'objet de quelques publications.

Le travail de synthèse bibliographique, présenté dans ce chapitre au travers d'une publication, est consacré à cette nouvelle classe de matériaux, et plus particulièrement aux nano-biocomposites à base d'argile. La **Publication n°1** vise à rassembler les principales recherches et les derniers développements des nano-biocomposites biopolyester/argile menés ces dernières années.

Publication n°1.

"Nano-biocomposites: A review of biopolyester/clay systems"

Perrine Bordes, Eric Pollet, Luc Avérous*

Journal of Nanoscience and Nanotechnology, submitted.

A. Abstract

In the recent years, bio-based products have raised great interest since sustainable development politics tend to develop with the decreasing reserve of fossil fuel and the growing concern for the environment. Consequently, biodegradable polymers (biopolymers) have been the topic of many researches. Biopolymers can be mainly classified as agro-polymers (starch, protein,) or biopolyesters (PHA, PLA …). These latter can be obtained from fossil resources but main productions are obtained from renewable resources. Unfortunately for certain applications, biopolyesters (biodegradable polyesters) can not be fully competitive with conventional thermoplastics since some of their properties are too weak. Therefore, to extend their applications, these biopolymers have been formulated by incorporation of nano-sized fillers which could bring to these materials a large range of improved properties (mechanical, permeability, thermal resistance,). The resulting 'nano-biocomposites' have been the subject of many publications. This review is dedicated to this novel class of materials based on clays, which are nowadays the main nanofillers used in nanocomposites systems. This overview intends to highlight the main researches and developments in biopolyester/clay systems during the last decade.

* Corresponding author: Luc Averous.

Tel.:+33-3-90-242-707 - Fax: +33-3-90-242-716 - AverousL@ecpm.u-strasbg.fr

*Keywords***:** biopolyesters; nano-biocomposites, clay, biodegradable.

B. Introduction

In the last years, biopolymers, i.e. biodegradable polymers, have attracted more and more interest due to the increasing environmental concern and the decreasing fossil resources. This incites researchers and industrials to develop novel materials more "environmentally-friendly" i.e. materials produced from alternative resources to fossil fuel, with lower energy consumption, biodegradable and non toxic for the environment. Biopolymers are biodegradable polymers and some of them can also be produced from renewable resources such as agro-resources. Obviously, because of their biodegradable character, they can be an alternative route to common synthetic non-degradable polymers for short-life range applications. But, nowadays, they are still expensive compared to conventional thermoplastic and their properties are often too weak for certain end-uses. Therefore, it appears necessary to improve these biopolymers in order to make them competitive towards other common plastics.

Nanocomposites are novel materials with drastically improved properties due to the incorporation of small amounts of nano-sized fillers (less than 10 wt%) into a polymer matrix. These nanofillers offer high surface area (~ 700 m^2/g), i.e. huge interfaces area with the polymer (matrix). Providing strong and large polymer-nanofiller interactions as well as good dispersion of the particles into the polymer, the final materials properties can considerably be improved. Nanofillers can be considered depending on the morphology as followed: layered particles (e.g., clays), spherical (e.g., silica) or acicular ones (e.g., whiskers, carbon nanotubes). Their specific geometrical dimensions, and thus aspect ratios, partly affect the final properties of the materials. By combining biopolymers and nano-fillers, nano-biocomposites are obtained. These materials show improved properties with a preservation of the material biodegradability. Such materials are mainly destined to biomedical applications and different short term applications e.g., packaging or agriculture devices.

Nano-biocomposites are very promising materials and represent a strong and emerging answer for improved and eco-friendly materials. Till the end of the XX^e century, only few articles have been published on nano-biocomposites, but since the last years, more and more publications are available.

This review aims at reporting the state of the art in nano-biocomposites materials. Since this field is wide, this overview is limited to nano-biocomposites based on biopolyester/clay systems. Nowadays, layered silicates are widely used in nanocomposites systems. Besides and up

to now, the biopolyesters are the most promising biopolymers for main applications. In a first part, the different biopolymers are presented. The origins and characteristics of main biopolyesters are particularly focussed. In a second part, the structures and properties of nano-biocomposites based on biopolyester/clays systems are reported in detail.

C. Biodegradable polymers classification

A vast number of biodegradable polymers (biopolymers) are synthesized or are formed in nature during the growth cycles of all organisms. Some micro-organisms and enzymes capable of degrading them have been identified (Kaplan, 1993; Kaplan, 1998; Chandra, 1998; Steinbuchel, 2003). Depending on the synthesis process, Figure 1 proposes a classification with four different categories (Averous, 2004b):

(a) polymers from biomass such as the agro-polymers from agro-resources (e.g., starch, cellulose),

(b) polymers obtained by microbial production, e.g., the polyhydroxyalkanoates,

(c) polymers chemically synthesized using monomers obtained from agro-resources, e.g., the poly(lactic acid),

(d) polymers whose monomers and polymers are both obtained by chemical synthesis from fossil resources.

Only, 3 categories (a to c) are obtained from renewable resources. We can sort these different biodegradable polymers into two main families, the agro-polymers (category a) and the biodegradable polyesters (categories b to d), also called biopolyesters.

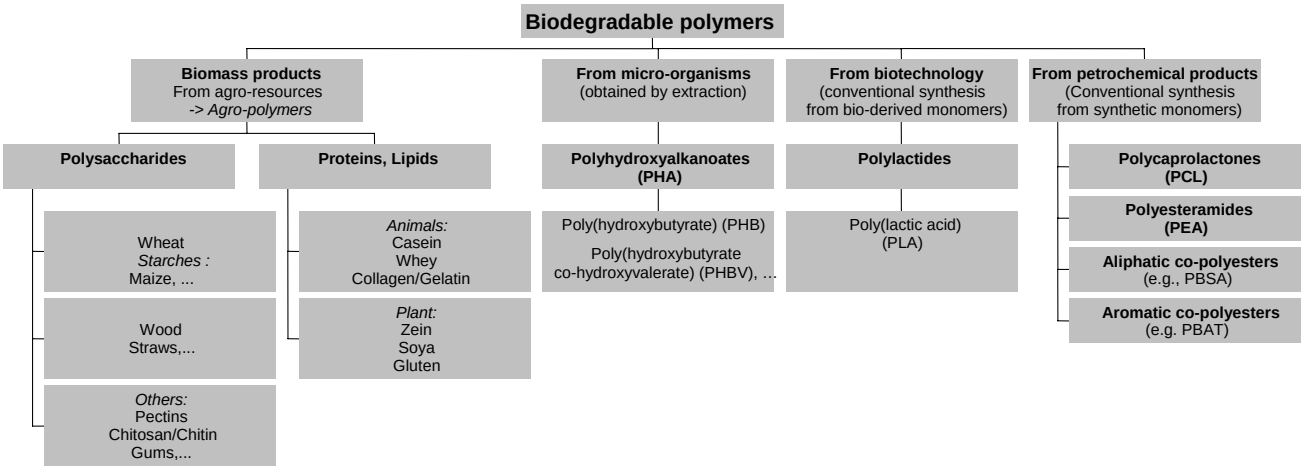

Figure 1: Classification of the biodegradable polymers (Averous, 2004a).

D. Biodegradable polyesters

Table 1 and Figure 2 show the chemical structure, trade names and main properties of commercially available biopolyesters.

D.I. Agro-resources-based polyesters

D.I.1. Poly(lactic acid)

Lactic acid is a chiral molecule existing as two stereoisomers, L- and D-lactic acid which can be produced by different ways, i.e., biologically or chemically synthesized.

In the first case, lactic acid is obtained by fermentation of carbohydrates from lactic bacteria, belonging mainly to the genus *Lactobacillus*, or fungi (Garlotta, 2001; Wee, 2006). This fermentative process requires a bacterial strain but also a carbon source (carbohydrates), a nitrogen source (yeast extract, peptides…) and mineral elements to allow the growth of bacteria and the production of lactic acid. The lactic acid as-formed exists almost exclusively as L-lactic acid and leads to poly(L-lactic acid) (PLLA) with low molecular weight by polycondensation reaction. However, Moon et al. (Moon, 2000; Moon, 2001) have proposed an alternative solution to obtain higher molecular weight PLLA by the polycondensation route.

In contrast, the chemical process could lead to various ratio of L- and D-lactic acid. Indeed, the chemical reactions leading to the formation of the cyclic dimer, the lactide, as an intermediate step to the production of PLA, could lead to macromolecular chains with L- and D-lactic acid monomers. This mechanism of ring-opening polymerisation (ROP) from the lactide explains the formation of two enantiomers. This ROP route has the advantage of reaching high molecular weight polymers (Kaplan, 1993; Garlotta, 2001; Albertsson, 2002; Okada, 2002) and allow the control of the PLA final properties by adjusting the proportions and the sequencing of L- and D-lactic acid units.

	Trade Name	Company
Agro-resources based polyesters:		
Poly(lactic acid) (PLA)		
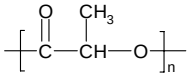	Natureworks	Cargill (USA)
	Lacty	Shimadzu (Japan)
	Lacea	Mitsui Chemicals (Japan)
	Heplon	Chronopol (USA)
	CPLA	Dainippon Ink Chem. (Japan)
	PLA	Galactic/Total (Belgium)
	Eco Plastic	Toyota (Japan)
	Treofan	Treofan (Netherland)
	PDLA	Purac (Netherland)
	Ecoloju	Mitsubishi (Japan)
	Biomer L	Biomer (Germany)
Polyhydroxyalkanoate (PHA)		
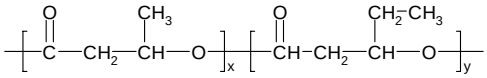		
(PHBV, PHB)	Biopol	Monsanto (USA)*
(PHBV, PHB)	Mirel	Metabolix/ADM (USA)
(PHB, PHBV)	Biocycle	PHB Industrial (Brazil)
(PHB, PHBV)	Biomer P	Biomer (Germany)
(PHB, PHBV)	Enmat	Tianan (China)
(PHBHx, PHBO, PHBOd)	Nodax	Procter & Gamble (USA)*
Petroleum-based polyesters:		
Polycaprolactone (PCL)		
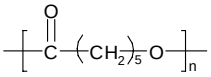	CAPA	Solvay (Belgium)
	Tone	Union Carbide (USA)
Polyesteramide (PEA)		
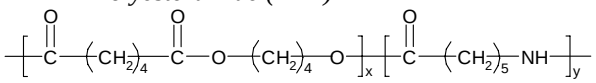	BAK	Bayer (Germany)*
Aliphatic copolyesters (e.g., PBSA)		
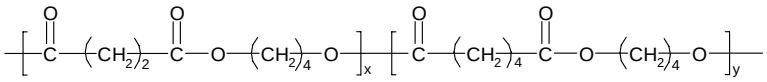		
	Bionolle	Showa Highpolymer (Japan)
	EnPol	Ire Chemical ltd (Korea)
	Skygreen	SK Chemicals (Korea)
	Lunare SE	Nippon shokubai (Japan)
Aromatic copolyesters (e.g., PBAT)		
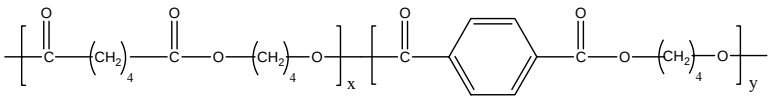	Eastar Bio	Eastman Chemical (USA) *
	Ecoflex	BASF (Germany)
	Biomax	Dupont (USA)
	Origo-Bi	Novamont (Italy)

(*) These polyesters productions have been stopped.

Figure 2: Structure, trade names and suppliers of main biodegradable polyesters commercially available (Averous, 2004a).

Table 1: Physical and mechanical data on commercial polyesters (Averous, 2004a).

	PLA	PHBV	PCL	PEA	PBSA	PBAT
	Dow-Cargill (NatureWorks)	Monsanto (Biopol D400G - HV=7 mol%)	Solvay (CAPA 680)	Bayer (BAK 1095)	Showa (Bionolle 3000)	Eastman (Eastar bio 14766)
Density	1.25	1.25	1.11	1.07	1.23	1.21
Melting point (°C)[a]	152	153	65	112	114	110-115
Glass transition (°C)[a]	58	5	-61	-29	-45	-30
Crystallinity[b] (in %)	0-1	51	67	33	41	20-35
Modulus (MPa) (NFT 51-035)	2050	900	190	262	249	52
Elongation at break (%) (NFT 51-035)	9	15	>500	420	>500	>500
Tensile stress at break or max. (MPa) (NFT 51-035)	-	-	14	17	19	9
Biodegradation[c] (Mineralization in %)	100	100	100	100	90	100
Water permeability WVTR at 25°C ($g/m^2/day$)	172	21	177	680	330	550
Surface tension (γ) (mN/m)	50	-	51	59	56	53
γ_d (dispersive component)	37	-	41	37	43	43
γ_p (polar component)	13	-	11	22	14	11

[a] measured by DSC
[b] determined on granules, before processing.
[c] after 60 days in controlled composting according to ASTM 5336.

At present, due to its availability on the market and its low price (Vert, 1995; Sinclair, 1996; Lunt, 1998; Auras, 2004), PLA has one of the highest potential among biopolyesters, particularly for packaging (Sinclair, 1996; Auras, 2004) and medical application. For instance, Cargill Dow has developed processes that use corn and other feedstock to produce different PLA grades (NatureWorks®) (Lunt, 1998; Steinbuchel, 2002). For this company, the actual production is estimated to 50-60 ktons per year although the production capacity is given at 140 ktons (www.natureworksllc.com). However, presently, it is the highest and worldwide production of biodegradable polyester. Its price was around 3€/kg in 2005, but nowadays the cost has slightly increased. Different companies such as Mitsui Chemicals (Japan), Mitsubishi (Japan), Biomer (Germany), Shimadzu (Japan), Galactic-Total (Belgium), Toyota (Japan), Purac (Netherland), Treofan (Netherland) or Dainippon Ink Chemicals (Japan) produce smaller PLAs outputs with different D/L ratios. Commercially available, we can find 100% PLLA which present a high cristallinity (C-PLA) and copolymers of PLLA and poly(D,L-lactic acid) (PDLLA) which are rather amorphous (A-PLA) (Bigg, 1996; Perego, 1996; Steinbuchel, 2002). PLA can show crystalline polymorphism (Cartier, 2000) which can lead to different melting peaks (Martin, 2001) with a main endotherm at 152°C for the PDLLA (see Table 1). Furthermore, PLA can be plasticized using oligomeric lactic acid (o-LA) (Martin, 2001), citrate ester (Labrecque, 1997) or

low molecular weight polyethylene glycol (PEG) (Jacobsen, 1999; Kranz, 2000; Martin, 2001; Ljungberg, 2003). The effect of plasticization increases the chains mobility and then favours the PLA organization and crystallization. After plasticization, we obtain a crystallinity ranging between 20 and 30%. PLA presents a medium water and oxygen permeability level (Van Tuil, 2000; Auras, 2004) comparable to polystyrene (Lehermeier, 2001). These different properties associated with its tunability and its availability favour its actual developments in different packaging applications (trays, cups, bottles, films …) (Sinclair, 1996; Steinbuchel, 2002; Auras, 2004). McCarthy (1999) (McCarthy, 1999) showed that A-PLA presents a soil degradation rate much slower compared to PBSA. PLA is presumed to be biodegradable although the role of hydrolysis vs. enzymatic depolymerization in this process remains open to debate (Bastioli, 1998a). Regarding biodegradation in compost, adequate conditions are only found in industrial units with a high temperature (above 50°C) and a high relative humidity (RH%) to promote chain hydrolysis. According to Tuominen et al. (2002) (Tuominen, 2002), PLA biodegradation does not exhibit any eco-toxicological effect.

D.I.2. Polyhydroxyalkanoates

Polyhydroxyalkanoates (PHAs) are naturally produced by micro-organisms from various carbon substrates as a carbon or energy reserve. A wide variety of prokaryotic organisms (De Koning, 1993; Madison, 1999) accumulate PHA from 30 to 80% of their cellular dry weight. Biotechnological studies revealed that PHB is produced under balanced growth conditions when the cells become limited for an essential nutrient but are exposed to an excess of carbon (Doi, 1990). Depending on the carbon substrates and the metabolism of the micro-organism, different monomers, and thus (co)polymers, could be obtained (Zinn, 2001). The main polymer of the polyhydroxyalkanoates family is the polyhydroxybutyrate homopolymer (PHB), but different poly(hydroxybutyrate-*co*-hydroxyalkanoates) copolyesters exist such as poly(hydroxybutyrate-*co*-hydroxyvalerate) (PHBV) (see Figure 2), or poly(hydroxybutyrate-*co*-hydroxyhexanoate) (PHBHx), poly(hydroxybutyrate-*co*-hydroxyoctanoate) (PHBO) and poly(hydroxybutyrate-*co*-hydroxyoctadecanoate) (PHBOd). With the progress in biotechnologies, it is possible for recombinant bacteria (Madison, 1999), but also plants (Madison, 1999; Valentin, 1999; Poirier, 2002) to produce such polymers. However, the recovery process, i.e. the extraction and purification steps, is decisive to obtain a highly pure PHA and often explains why such polymers are still expensive. Pure synthetic PHA can be produced by the ROP from butyrolactone and other lactones (Hori, 1993a; Hori, 1993b; Kobayashi, 1995; Hori, 1996; Nobes, 1996; Juzwa,

2006). Thus, according to the synthesis route, we obtain different structures, isotactic with random stereosequences for the bacterial copolyesters and with partially stereoregular block for the synthetic copolyesters. Recently, Monsanto has developed genetical modification of plants to make them produce small quantities of PHB (Valentin, 1999; Asrar, 2000, 2001).

PHB is a highly crystalline polyester (above 50%) with a high melting point, Tm=173-180°C, compared to the other biodegradable polyesters. Glass transition temperature (Tg) is around 5°C. The homopolymer shows a narrow window for the processing conditions. To ease the transformation, PHB can be plasticized with citrate ester, but the PHBV copolymer is more adapted for the process. A large range of bacterial copolymer grades had been industrially produced by Monsanto under the Biopol® trade mark, with HV contents reaching 20%. The production was stopped at the end of 1999. Metabolix bought Biopol® assets in 2001. Presently, Telles™, a joint venture between Metabolix and Archer Daniels Midlands Company (ADM), has marketed the Mirel™ product as a new bio-based biodegradable plastics from corn sugar. ADM has begun to built the first plant in Clinton, Iowa (US) which will be able to produce 50,000 tons of resin per year. The startup is scheduled for late 2008 (www.metabolix.com).

Different small companies currently produce bacterial PHA, e.g., PHB Industrial (Brazil) produces PHB and PHBV (HV=12 %) 45% crystalline, from sugar cane molasses (El-Hadi, 2002). Biocycle® production is planned to be 4,000 tons/year in 2008 and then, to be extended to 14,000 tons/year (Velho, 2006). In 2004, Procter & Gamble (US) and Kaneka Corporation (Japan) announced a joint development agreement for the completion of R&D leading to the commercialization of Nodax, a large range of polyhydroxybutyrate-*co*-hydroxyalkanoates (PHBHx, PHBO, PHBOd) (Noda, 2005). Although the industrial production was planned for 2006 with a target price around 2€/kg, the production was stopped (Philip, 2007).

The production of PHA is intended to replace synthetic non-degradable polymers for a wide range of applications (Philip, 2007): packaging, agriculture but also medicine (Williams, 1999; Zinn, 2001) since PHA are biocompatible. Figure 2 and Table 1 give the chemical structure and the properties of some PHBV, respectively. Material properties can be tailored by varying the HV content. An increase of the HV content induces an increase of the impact strength and a decrease of the melting temperature and glass transition (Amass, 1998), the crystallinity (Shogren, 1997), the water permeability (Shogren, 1997) and the tensile strength (Kotnis, 1995).

Besides, PHBV properties can evolve when plasticization occurs, e.g., with citrate ester (triacetin) (Kotnis, 1995; Shogren, 1995). The polyhydroxyalkanoates, like the PLAs, are sensitive to the processing conditions. Under extrusion, we obtain a rapid diminution of the viscosity and the molecular weight due to macromolecular chain cleavage by increasing the shear

level, the temperature and/or the residential time (Ramkumar, 1998). Regarding the biodegradable behaviour, the kinetic of enzymatic degradation is variable according to the crystallinity, the structure (Karlsson, 1998; El-Hadi, 2002) and then, to the processing history (Parikh, 1998). Bacterial copolyesters biodegrade faster than homopolymères (Dos Santos Rosa, 2004) and synthetic copolyesters (Chiellini, 1996).

D.II. Petroleum-based polyesters

A large number of biodegradable polyesters are based on petroleum resources, obtained chemically from synthetic monomers (Vert, 1995; Bigg, 1996; Sinclair, 1996; Lunt, 1998; Albertsson, 2002; Okada, 2002; Steinbuchel, 2002). According to the chemical structures (see Figure 2), we can distinguish (see Table 1) polycaprolactones, polyesteramides, aliphatic or aromatic copolyesters. All these polyesters are soft at room temperature.

D.II.1. Polycaprolactone

Poly(ε-caprolactone) (PCL) is usually obtained by ring opening polymerisation (ROP) of ε-caprolactone in the presence of metal alkoxides (aluminium isopropoxide, tin octoate,…) (Chiellini, 1996; Albertsson, 2002; Okada, 2002). PCL is widely used as a PVC solid plasticizer or for polyurethane applications, as polyols. But, it finds also some applications based on its biodegradable character in domains such as biomedicine (e.g. drugs controlled release) and environment (e.g. soft compostable packaging). Different commercial grades are produced by Solvay (CAPA®), by Union Carbide (Tone®) and by Daicel (Celgreen®). Figure 2 and Table 1 give respectively the chemical structure and the properties of this polyester. PCL shows a very low Tg (-61°C) and a low melting point (65°C), which could be a handicap in some applications. Therefore, PCL is generally blended (Bastioli, 1995; Bastioli, 1998a, 1998b; Averous, 2000) or modified (e.g., copolymerisation, crosslinking (Koenig, 1994)). Tokiwa et al. (Tokiwa, 1977) have discussed the hydrolysis of PCL and biodegradation by fungi. They have shown that PCL can be easily enzymatically degraded. According to Bastioli (Bastioli, 1998a), the biodegradability can be clearly claimed but the homopolymer hydrolysis rate is very low. The presence of starch can significantly increase the biodegradation rate of PCL (Bastioli, 1995).

D.II.2. Biodegradable aliphatic polyesters

A large number of aliphatic copolyesters are biodegradable copolymers based on petroleum resources. They are obtained by the combination of diols such as 1,2-ethanediol, 1,3-propanediol or 1,4-butadenediol, and dicarboxylic acids like adipic, sebacic or succinic acid. Showa Highpolymer (Japan) has developed a large range of polybutylene succinate (PBS) obtained by polycondensation of 1,4-butanediol and succinic acid. Polybutylene succinate/adipate (PBSA), presented on Figure 2, is obtained by addition of adipic acid. These copolymers are commercialised under the Bionolle® trademark (Steinbuchel, 2002). Table 1 shows the properties of such biopolyester. Ire chemical (Korea) commercialises exactly the same kind of copolyesters under EnPol® trademark. Skygreen®, a product from SK Chemicals (Korea) is obtained by polycondensation of 1,2-ethanediol, 1,4-butadenediol with succinic and adipic acids (Lee, 2002). Nippon Shokubai (Japan) also commercialises an aliphatic copolyester under Lunare SE® trademark. These copolyesters properties depend on the structure (Muller, 1998), i.e., the combination of diols and diacids used. These products biodegradability depends also on the structure. The addition of adipic acid, which decreases the crystallinity (Yokota, 1999) tends to increase the compost biodegradation (Fujimaki, 1998). According to Ratto et al. (Ratto, 1999), the biodegradation results demonstrate that although PBSA is inherently biodegradable, the addition of starch filler significantly improve the rate of degradation.

D.II.3. Aromatic copolyesters

Compared to totally aliphatic copolyesters, aromatic copolyesters are often based on terephthalic diacid. Figure 2 and Table 1 show respectively the chemical structure and the properties of such products (e.g, Eastar Bio® from Eastman). Besides, BASF and DuPont commercialize aromatic copolyesters under Ecoflex® (Steinbuchel, 2002) and Biomax® trademarks, respectively. Biomax® shows a high terephtalic acid content which modifies some properties such as the melting temperature (200°C). But, according to Muller et al. (Muller, 1998), an increase of terephthalic acid content tends to decrease the degradation rate. Ecoflex® biodegradation has been analysed by Witt et al. (Witt, 2001). They concluded that there is no indication for an environmental risk (ecotoxicity) when aliphatic-aromatic copolyesters of the Ecoflex®-type are introduced into composting processes.

D.II.4. Polyesteramide

Polyesteramide was industrially obtained from the statistical copolycondensation of polyamide (PA 6 or PA 6-6) monomers and adipic acid (Grigat, 1998; Steinbuchel, 2002). Bayer had developed different commercial grades under BAK® trademark but their productions stopped in 2001. Figure 2 and Table 1 show, respectively, the chemical structure and the properties of this poly(butylene adipate-*co*-amino caproate). Table 1 shows that this polyester presents the highest polar component, and then presents good compatibility with other polar products, e.g., starchy compounds. Besides, it has the highest water permeability (see Table 1). Currently, the environmental impact of this copolymer is open to discussion. Fritz (Fritz, 1999) had shown that, after composting, this biodegradable polyester presented a negative eco-toxicological impact but more recently, Bruns et al. (Bruns, 2001) have infirmed these results. These authors discussed Fritz's experiments and more precisely the composting methods used.

E. Biopolyester/clay nano-biocomposites

Before discussing about the different nano-biocomposites based on the polyesters described above, it is necessary to remind some general information about the specific properties of clays as well as the different and possible elaboration routes of such materials.

E.I. Generalities

E.I.1. Clays

The most commonly used clays in the field of nanocomposites belong to the family of 2:1 layered silicates, also called 2:1 phyllosilicates (montmorillonite, saponite,). Their crystal structure consists in layers made up of two tetrahedrally coordinated silicon atoms fused to an edge-shared octahedral sheet of either aluminium or magnesium hydroxide (see Figure 3). Each layered sheet is about 1 nm thick and its length varies from tens of nanometers to more than one micron. Layers stacking leads to a regular Van der Waals gap between the platelets called the interlayer or the gallery. Isomorphic substitution may occurs inside the sheet since Al^{3+} can be replaced by Mg^{2+} or Fe^{2+}, or Mg^{2+} by Li^{+}. Globally negatively charged platelets are counterbalanced by alkali and alkali earth cations (Na^{+}, Ca^{2+}…) located in the galleries which increase the clay hydrophilic character. But most of the polymers, and particularly the biopolyesters are considered as organophilic compounds. Thus, to obtain better affinity between

the filler and the matrix, and finally to improve final properties, the inorganic cations located inside the galleries (Na^+, Ca^{2+}…) are generally exchanged by ammonium or phosphonium cations bearing at least one long alkyl chain and possibly other substituted groups. The resulting clays are called organo-modified layered silicates (OMLS) and are abbreviated OMMT in the case of montmorillonite (MMT). By modifying the layered silicate, it is thus possible to compatibilize the matrix and the filler which will affect the material nanostructure, and consequently the properties of the nanocomposites. Tables 2 and 3 present the characteristics of the main 2:1 layered silicates and commercial clays.

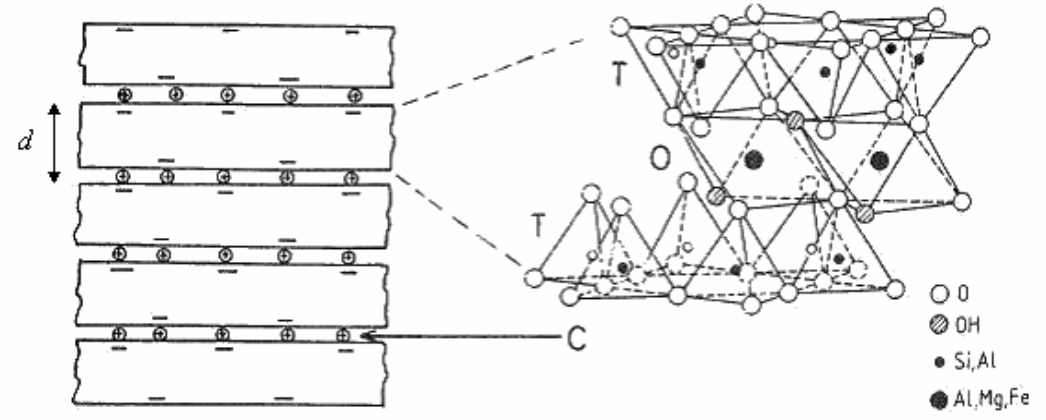

Figure 3: 2:1 layered silicate structure. T, tetrahedral sheet ; O, octahedral sheet ; C, intercalated cations ; *d*, interlayer distance (Lagaly, 1993).

Table 2: Structural characteristics of principal 2:1 layered silicates (Sinha Ray, 2003b; Utracki, 2007).

Phyllosilicates	Octahedra occupancy	Interlayer cations	CEC (meq/100 g)	Aspect ratio
Smectites				
Hectorite	Mg (3/3)	Na^+, Ca^{2+}, Mg^{2+}	120	200-300
Montmorillonite	Al (2/3)	Na^+, Ca^{2+}, Mg^{2+}	110	100-150
Saponite	Mg (3/3)	Na^+, Ca^{2+}, Mg^{2+}	86.6	50-60

Table 3: Commercial (O)MMT and their characteristics.

Commercial clays Supplier / Trade name / Designation		Clay type	Organo-modifier type	Modifier concentration (meq/100 g)	Δw[a] (%)	d-spacing (Å)
Southern Clay Products (USA)						
Cloisite®Na	CNa	MMT	-	-	7	11.7
Cloisite®15A	C15A	MMT	2M2HT	125	43	31.5
Cloisite®20A	C20A	MMT	2M2HT	95	38	24.2
Cloisite®25A	C25A	MMT	2MHTL8	95	34	18.6
Cloisite®93A	C93A	MMT	M2HT	90	37.5	23.6
Cloisite®30B	C30B	MMT	MT2EtOH	90	30	18.5
Süd-Chemie (Germany)						
Nanofil®804	N804	MMT	MT2EtOH		21	18
Laviosa Chimica Mineraria (Italy)						
Dellite® LVF	LVF	MMT	-	105	4-6	9.8
Dellite® 43B	D43B	MMT	2MBHT	95	32-35	18.6
CBC Co. (Japan)						
Somasif	MEE	SFM	MC2EtOH	120	28	
	MAE	SFM	2M2T	120	41	

[a] % Weight loss on ignition
2M2HT: dimethyl dehydrogenated tallow quaternary ammonium
2MHTL8: dimethyl dehydrogenated tallow 2-ethylhexyl quaternary ammonium
M2HT: methyl dehydrogenated tallow ammonium
MT2EtOH: methyl tallow bis-2-hydroxyethyl quaternary ammonium
2MBHT: dimethyl benzylhydrogenated tallow ammonium
MC2EtOH: bis-2-hydroxyethyl coco alkyl methyl ammonium
2M2T: dimethyl ditallow ammonium

E.I.2. Elaboration routes

An important key factor in the nanocomposites preparation is the elaboration protocol. Nowadays, three main methods are applied: (i) the solvent intercalation route which consists in swelling the layered silicates in a polymer solvent in order to make the macromolecules diffuse in the clay interlayer spacing, (ii) the in-situ intercalation method for which the layered silicates are swollen in the monomer or monomer solution before polymerization, and (iii) the melt intercalation process which is based on polymer processing in the molten state such as mixing and extrusion. Obviously, the latter method is highly preferred in the context of sustainable

development since it avoids the use of organic solvents which are not eco-friendly and then alter the life cycle analysis (LCA).

E.I.3. Nanocomposites structures

Finally, different structures of nanocomposites could be obtained such as (i) the microcomposite when the clay is aggregated and layers are stacked, the polymer is not intercalated within the (O)MMT's layers due to poor polymer-clay affinity, and thus, the material presents phase separation; (ii) the intercalated nanocomposite for which the polymer is partially intercalated between the silicate layers, these latter are still stacked but the interlayer spacing has increased; (iii) the exfoliated nanocomposite obtained when the polymer chains have delaminated the (O)MMT into individual platelets which are dispersed into the matrix, so that the layered structure does not exist anymore.

E.II. Agro-resources-based polyesters matrices

E.II.1. Poly(lactic acid)-based nano-biocomposites

PLA is a very promising material since it has good mechanical properties, thermal plasticity and biocompatibility. However, some of its properties, like flexural properties, gas permeability and heat distortion temperature, are too low for widespread applications. Therefore, many attempts were carried out to reach exfoliation state in PLA-based nanocomposites. Different organoclays with various organomodifiers were selected and different elaboration routes were tested.

Firstly, Ogata (Ogata, 1997) attempted to prepare PLA-based nanocomposites by the solvent intercalation method. Unfortunately, the layered silicates were not individually well dispersed but rather formed tactoids consisting of several stacked silicate monolayers. Consequently, although the Young's modulus increased with the clay content, the increments were small compared to conventional nanocomposites. Later, Chang et al. (Chang, 2003a; Chang, 2003b) examined the influence of the aspect ratio of the layered silicates (montmorillonite, fluorinated synthetic mica), the type of organomodifier (2MHTL8 -C25A-, hexadecylamine -C_{16}-, dodecyltrimethyl ammonium bromide -DTA) and the clay content on the nanodispersion into the PLA matrix. It was evidenced from X-Ray Diffraction (XRD) and Transmission Electron Microscope (TEM) characterizations that intercalated structures were

obtained leading to improvements in mechanical and barrier properties with only small amount of fillers. Compared to neat PLA, ultimate strength increased by about 65, 47 and 131% in the case of PLA with 2 wt% of C25A, 4 wt% of C_{16}-MMT and C_{16}-mica, respectively. However, it appeared that the mechanical enhancement was limited to a small range of clay content (up to 4-6 wt% depending on the organomodifier). Above these clay contents, properties decreased due to layered silicates agglomeration. Considering O_2 permeability, it decreased of more than a half at 10 wt% of OMMT. The initial degradation temperatures decreased linearly with an increasing amount of OMMT reaching a maximum shift of 49 and 41°C in the case of 8 wt% of C_{16}-MMT and C25A respectively, whereas the decrease was only of 16°C in the case of C_{16}-mica at the same clay loading. It was also evidenced that DTA-MMT present a particular thermal behaviour since the initial degradation temperature was not affected by the clay content (Chang, 2003b).

Finally, Krikorian et al. (Krikorian, 2003) successfully prepared exfoliated materials with randomly distributed clay platelets via solvent intercalation in the presence of C30B. Since C30B bears a long alkyl chain and hydroxyl groups, the interactions between OH functions from the clay organomodifier and C=O bonds of the PLA backbone favoured the exfoliation. Therefore, the mechanical properties were improved, e.g., the storage modulus increased by 61% with 15 wt% of C30B. A complete study about the crystallization behaviour of such materials was also conducted (Krikorian, 2004, Krikorian 2005), focusing on the role of intercalated or exfoliated layered silicates on the nucleation, the growth, and thus, the overall crystallinity. They demonstrated that addition of highly miscible clay leads to low spherulite nucleation, low bulk crystallization, and as a result, much lower extent of crystallinity compared to neat polymer. Moreover, from FTIR analyses, they described the mechanisms of crystallization and explained how the highly miscible clay hinders the crystal nuclei formation (Krikorian, 2005).

Exfoliated structure of PLA-based nanocomposites were also obtained by Wu & Wu (Wu, 2006) using a solution mixing process. They increased the interactions between the filler and the matrix by treating the montmorillonite with n-hexadecyl trimethylammonium bromide (CTAB) cations and then modified it with chitosan, a biodegradable and biocompatible polymer (see Figure 4).

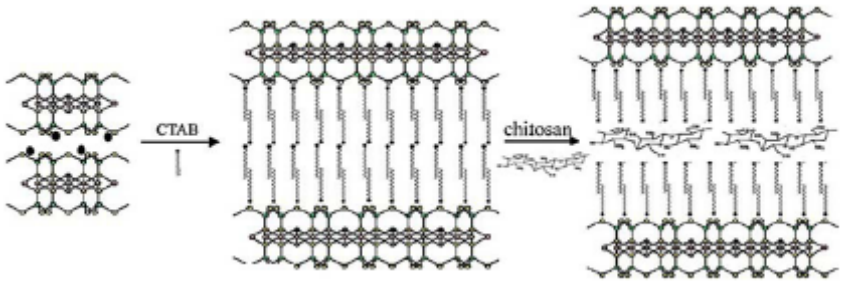

Figure 4: Schematic drawing of organo-modified montmorillonite by CTAB and chitosan (Wu, 2006).

Furthermore, many articles reported the structure and properties of PLA-based nanocomposites prepared by melt intercalation (Maiti, 2002a, 2002b; Pluta, 2002; Sinha Ray, 2002a, 2002d, 2002e; Nam, 2003b; Sinha Ray, 2003c, 2003d, 2003e, 2003f, 2003g, 2003h, 2003j; Nam, 2004; Paul, 2005a). Okamoto and his group at Toyota Technological Institute (Nagoya, Japan) tested a lot of PLA-based systems differing from the OMLS, i.e. the aspect ratio of the inorganic platelets, the nature of the organomodifier, and the clay content (Maiti, 2002b; Sinha Ray, 2002a, 2002d, 2002e; Sinha Ray, 2003c, 2003d, 2003e, 2003f, 2003g, 2003h, 2003j). Depending on these parameters, intercalated, intercalated-and-flocculated, nearly exfoliated, coexistence of intercalated and exfoliated states were obtained. They even proposed an interpretation of the nanocomposites structure related to the aspect ratio and the organomodifier chain lengths (Maiti, 2002b). Regarding the aspect ratio, it was demonstrated that the smaller the silicate layers size, the lower the physical jamming, restricting the conformation of organomodifier alkyl chains, and thus, the lower the coherency of the organoclay (see Figure 5). Due to a nicely stacked structure of organo-modified mica, the polymer chains can hardly penetrate up to the core of the silicate layers, contrary to smaller size of silicate layers like smectite and MMT (see Figure 5). The effect of organomodifiers organization in the interlayer space was also examined considering an interdigitated layer structure of the surfactants (Yoshida, 2006).

Flocculated structures were further studied by Nam et al. (Nam, 2003b; Nam, 2004) using bis(4-hydroxy butyl) methyl octadecyl ammonium modified montmorillonite. From Polarized Optical Microscopy (POM), TEM and particularly FT-IR, they showed that the formation of such nanocomposite structures could be due to hydrogen bonding among the hydroxyl groups of the surfactant, those of clay edge and those of both ends of the PLA chains.

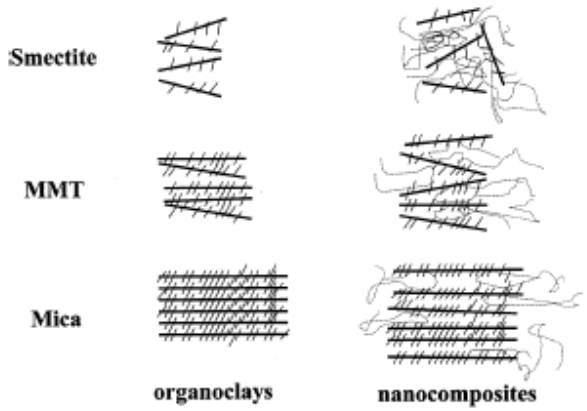

Figure 5: Stacking of silicate layers in organoclays and nanocomposites (Maiti, 2002b).

As a consequence of the nanostructure and despite of the fact that incomplete exfoliation was obtained by melt intercalation, all the nanocomposites exhibited dramatic improvement in various materials properties compared to those of neat PLA. These improvements included mechanical and flexural properties, heat distortion temperature, and O_2 gas permeability. However, it has to be noticed that the increments strongly depend on the structure of the nanocomposites. A particular study of the crystallization behaviour of the well-ordered intercalated PLA/octadecylammonium OMMT (C_{18}-MMT) nanocomposite revealed a spherulite size decrease and an overall crystallization rate enhancement compared to neat PLA (Nam, 2003a) which was attributed to the clay nucleating effect. The compostability was controlled by the crystallinity, the molecular weight and the (OM)LS dispersion and enhanced by the incorporation of layered silicates (Sinha Ray, 2003e; Sinha Ray, 2003i). Paul et al. (Paul, 2005a) studied the hydrolytic degradation in such materials and concluded that the more hydrophilic the filler, the more pronounced the degradation. This was expressed by increasing opacity and shape modification before fragmentation.

Therefore, by a judicious choice of the OMLS, it is possible to tune the materials properties as desired (Sinha Ray, 2003e).

The addition of oligo-PCL (Sinha Ray, 2002a) (o-PCL) or PCL (Hasook, 2006) to PLA-clay systems had not a beneficial effect on the interlayer spacing. However, the o-PCL, used as compatibilizer, induced a flocculated state due to hydroxylated edge-edge interactions of layered silicates leading to great enhancement of mechanical properties. Hasook et al. (Hasook, 2006) also obtained reinforced materials properties when adding 5 wt% of PCL with short chains length (<40,000).

Chen et al. (Chen, 2005c, 2005d) used the organoclay to compatibilize an immiscible PLLA/PBS blend. They introduced epoxy groups to C25A by treating the clay with (glycidoxypropyl)trimethoxy silane (GPS) to produce a twice functionalized organoclay (TFC) (see Figure 6). Reacting with epoxy groups located on the clay surface, the biopolyesters tend to delaminate the filler (see Figure 7). However, since TFC was highly compatible with PLLA rather than PBS, at small TFC content, the clays are located almost exclusively in the PLLA phase and are fully exfoliated. At higher TFC content, the clay layers were dispersed in both PBS and PLLA phases with intercalated/exfoliated coexisting morphology. The domains size of the dispersed PBS phase decreased sharply since the platelets hinders the PBS domains coalescence. The addition of TFC to the PLA/PBS blend not only improved the tensile modulus but also the elongation at break, while the incorporation of C25A to the same polymer blend increased the tensile modulus but at the cost of the elongation at break. The thermal stability of these materials, in terms of onset temperature and activation energy of degradation were also enhanced (Chen, 2005d).

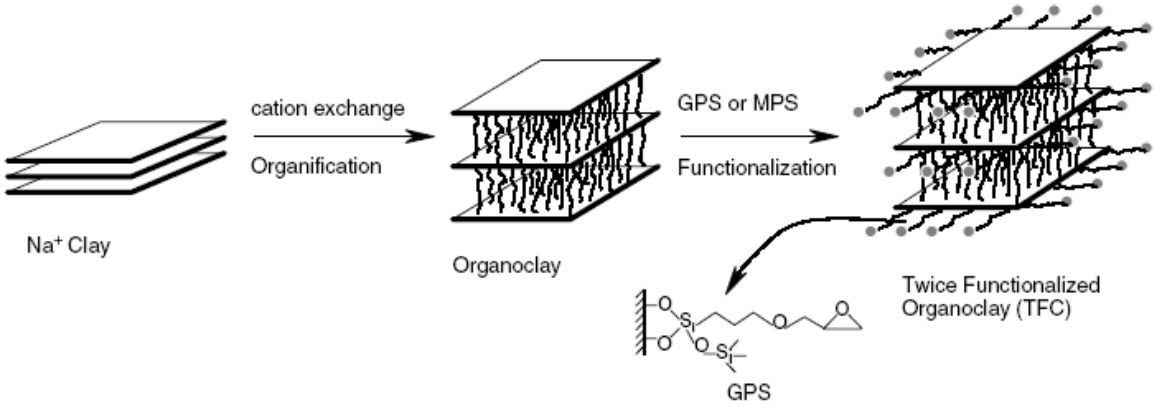

Figure 6: Schematic diagram for preparation of the twice-functionalized organoclay (TFC) (Chen, 2005a).

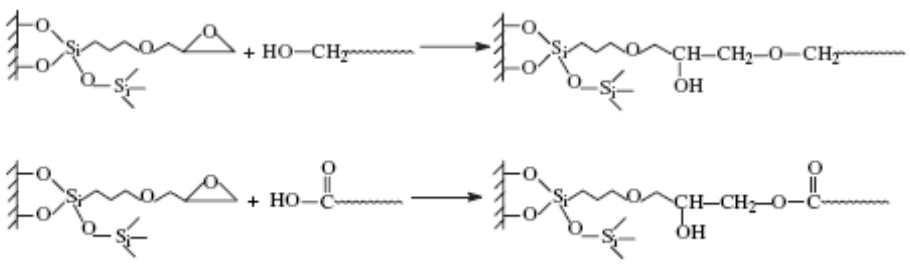

Figure 7: Reaction between the epoxy groups in TFC and the terminal functional groups of the polyesters (Chen, 2005d).

Other PLA-based nano-biocomposites were obtained via melt intercalation using cast film technique and a masterbatch process. This latter was also used to prepare PLLA-based polymer blends nano-biocomposites (PLLA-PDLLA, PLLA-PBAT) (Lewitus, 2006). Compared to neat PLLA, the PLLA nanocomposites demonstrated enhanced film properties, showing a potential extend to film applications as e.g. compostable packaging. The most significant improvements took place when the nanoclays were incorporated via masterbatch using a PLA carrier of the same grade as the PLLA matrix. In this case, the incorporation of 5 wt% of clay increased the tensile modulus and the elongation at break of PLLA by 36 and 48% respectively, while the tensile strength did not change significantly. Authors attributed this toughening effect to molecular interactions between nanoclays and PLA but also to a high degree of exfoliation. Nevertheless, without complementary characterizations of these systems, these results could not be confirmed. Regarding the thermal properties, it was proved that clays acted as nucleating agent since the cold crystallization temperature was decreased by 15°C.

Some authors were also interested in developing plasticized PLA-based nanocomposites to reduce the brittleness and improve the flowability. Thus, PLA plasticized with PEG (Paul, 2003b; Pluta, 2004; Paul, 2005b; Pluta, 2006a, 2006b; Tanoue, 2006) or diglycerine tetraacetate (Shibata, 2006) were melt compounded with different organoclay leading to intercalated structures. Paul et al. (Paul, 2003b) and Pluta et al. (Pluta, 2006a) showed that there is a real competition between PEG and PLA for the intercalation into the interlayer. Tanoue et al. (Tanoue, 2006) also studied the structure of such materials using PEG with different molecular weight. With a certain type of organoclays, i.e. dimethyl distearyl ammonium modified MMT, these authors demonstrated that the interlayer distance depend on the PEG chain length. Besides, they pointed out that addition of PEG affect the dispersion of clay in the PLA matrix resulting in more aggregated structures. Mechanical properties can be improved (Shibata, 2006; Tanoue, 2006) and crystallization enhanced (Pluta, 2004; Shibata, 2006) by selecting the right organoclay, plasticizer nature and content and chain length. Nevertheless, Pluta et al. (Pluta, 2006b) demonstrated that although the dispersed nanoclays can slow down the phase separation, particularly in the case of better PLA-clay affinity (i.e. C20A and C30B), PEG can diffuse toward the surface. Therefore, Paul et al. (Paul, 2005b) settled a protocol consisting in in-situ polymerization of lactide from end-hydroxylated PEG in presence of C30B with tin octoate ($SnOct_2$) as an activator/initiator. This polymerization method, called the "coordination-insertion" method, leads to PLA chains grafted onto the clay surface via the hydroxylated ammonium organomodifier and to PLA-b-PEG-b-PLA triblock copolymer intercalated into the clay gallery. The plasticizing effect is ensure by the PEG sequence of the triblock without phase

separation. More generally, this mechanism allows complete exfoliation by ring opening polymerization (ROP) of lactide after adequate activation (Paul, 2003a). In the particular case of activation reaction with triethylaluminium $AlEt_3$ (Paul, 2005b), the polymerization is initiated by the hydroxyl groups of the OMMT organomodifier (see Figure 8). The as-obtained PLA/OMMT nanocomposites presented enhanced thermal properties since the temperature corresponding to 50% of weight loss is shifted by ~30°C towards higher temperature. The crystallinity was also affected since the mobility of the resulting grafted chains was restricted while Tg and Tm were not influenced by the clay (Paul, 2005b).

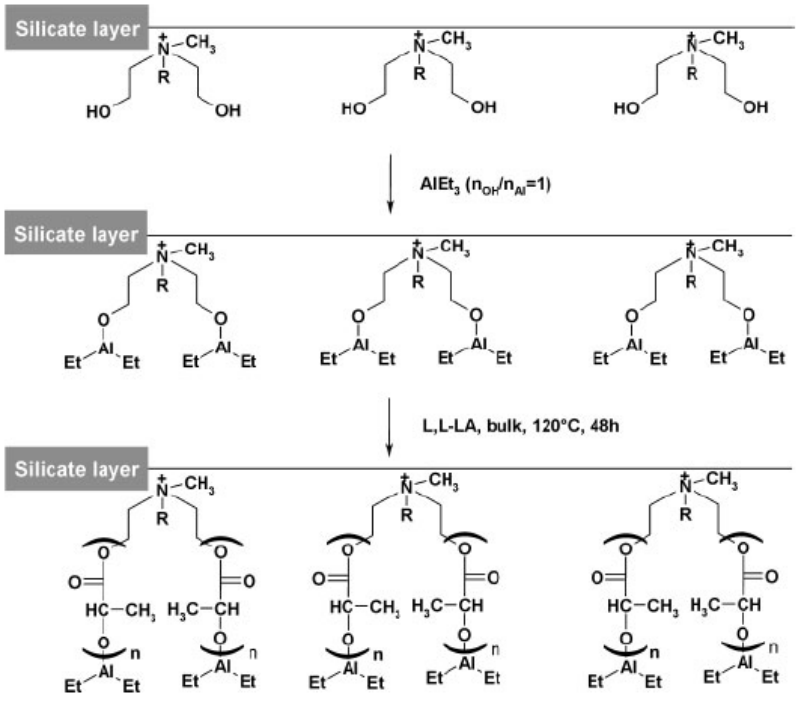

Figure 8: Schematic representation of the L,L-lactide polymerization performed in-situ from C30B using triethylaluminium ($AlEt_3$) as initiator precursor (R stands for tallow alkyl chain) (Paul, 2005b).

Recent publications reported works on more applicative researches since they deal with PLA-based nanocomposites for preparation of porous ceramic materials (Sinha Ray, 2002c) or for scaffolds as supports for tissue regeneration (Lee, 2003b; Lee, 2005b). Foams were also elaborated from PLA/OMMT nanocomposites with the aim of obtaining high cell density and a controlled morphology varying from microcellular to nanocellular structures (Ema, 2006).

To conclude, the literature shows a lot of publications on PLA-based nano-biocomposites. Several answers and strategies are proposed to improve the material properties since PLA is commercially and largely available.

E.II.2. Polyhydroxyalkanoates-based nano-biocomposites

Some drawbacks of PHA, such as brittleness and poor thermal stability still restrict their developments and uses. Therefore, nano-biocomposites appear as an answer to overcome these problems and to improve different properties as e.g., permeability.

Firstly, Maiti and al. (Maiti, 2003b) prepared PHB-based nanocomposites by melt extrusion. PHB was then reinforced using organo-modified fluoromicas or montmorillonite containing 2 wt% and up to 4 wt% of clay, respectively. MEE and MAE fluoromicas (see Table 3) as well as OMMT modified with octadecylammonium (MMT-C_{18}) were selected. XRD and TEM revealed well-ordered intercalated nanocomposites with decreasing d-spacing when clay content increases. Dynamic mechanical analyses revealed a better reinforcing effect of fluoromica compared to montmorillonite. The storage modulus E' increased with clay content reaching an increment of 35% with 3.6 wt% of MMT-C_{18}, +33% and +40% with 2 wt% of MAE and MEE, respectively. These authors explained this behaviour by degradation enhancement in presence of OMMT, due to the presence of Al Lewis acid sites in the inorganic layers which catalyze the ester linkages hydrolysis. This phenomenon does not occur in the case of fluoromica since they are based on magnesium. The biodegradation studies highlighted this difference since the initial degradation rate of PHB with MMT-C_{18} was higher than nanocomposites with fluoromica. In this case, the degradation rates have been considerably reduced and even suppressed with MEE.

A similar study on PHB-based nanocomposites was carried out by Lim et al. (Lim, 2003a). Nevertheless, they used solvent intercalation route to obtain PHB/C25A with 3, 6 and 9 wt% of clay content. XRD data led to the conclusion of intercalated structures, the interlayer distance reaching 34.8 Å, but no dependence on clay content was observed. These results were confirmed by FTIR analyses showing that two distinct different phases coexisted. These structural observations were completed by the thermal stability investigation . TGA indicated an increase of the onset temperature of weight loss and a decrease of the degradation rate with 3 wt% of C25A which was attributed to the nanoscale dispersion of OMMT layers decreasing the diffusion of volatile decomposition products. At higher clay contents (>6 wt%), although the onset of thermal degradation did not increase because of the thermal sensitivity of the organomodifiers, the nanocomposites degradation rates decreased due to restricted thermal motion of polymer in the OMMT interlayer.

Scientists were also interested in the development of PHBV-based nanocomposites since the PHBV presents better properties than PHB and better processability. In 2003, Choi et al. (Choi, 2003) described the microstructure as well as the thermal and mechanical properties of PHBV/C30B nanocomposites with low clay content. These materials were prepared by melt intercalation using a Brabender mixer. XRD and TEM clearly confirmed that intercalated nanostructures were obtained. Such structures were formed thanks to the strong hydrogen bond interactions between PHBV and the hydroxyl groups of the C30B organomodifier. They demonstated that the nanodispersed organoclay acted as a nucleating agent, increasing the temperature and rate of PHBV crystallization. Moreover, the DSC thermograms revealed that the crystallite size was reduced in the presence of nanodispered layers since the PHBV melting temperature are shifted to lower temperatures. Nanocomposites thermal stabilities were also studied. Thermogravimetric analyses revealed that the temperature corresponding to 3 wt% of weight loss increased with C30B content (+10°C with 3 wt% of filler). They explained these trends by the nanodispersion of the silicate layers into the matrix and thus concluded that the well-dispersed and layered structure account for an efficient barrier to the permeation of oxygen and combustion gas. Eventually, the mechanical properties showed that clays can also act as an effective reinforcing agent since the Young's modulus significantly increases from 480 to more than 790 MPa due to strong hydrogen bonding between PHBV and C30B.

Wang et al. (Wang, 2005) and Zhang and his group (Chen, 2002, 2004) have investigated the structure and the properties of PHBV/OMMT nanocomposites. They synthesized PHBV with 3 and 6.6 mol% of HV units as well as organo-modified MMT via cationic exchange in an aqueous solution with hexadecyl-trimethylammonium bromide. Nanocomposites were prepared by solution intercalation method adding 1, 3, 5 or 10 wt% of OMMT to a chloroform solution of PHBV and the resulting dispersions were exposed notably to an ultra-sonication treatment. These conditions led to intercalated structures evidenced by XRD, and clay aggregation occurred when increasing the clay content to 10 wt%.

A detailed study of the PHBV/OMMT crystallization behaviour was achieved. It was shown that OMMT acted as a nucleating agent in the PHBV matrix, which increased the nucleation and the overall crystallization rate, leading to more perfect PHBV crystals (Chen, 2004). With increasing amount of OMMT, the predominant crystallization mechanism of PHBV was shifted from the growth of crystals to the formation of crystalline nuclei. The nucleation effect of the organophilic clay decreased with the increase of clay content. Wang et al. (Wang, 2005) postulated that the nanoscaled OMMT layers affect the crystallization in two opposite ways. On one hand, a small part of OMMT can increase the crystalline nuclei thus causing a

more rapid crystallization rate. On the other hand, owing to the interaction of OMMT layers with PHBV chains, most of the OMMT layers restrict the motion of the PHBV chains. Therefore, the crystallization rate increased whereas the relative degree of crystallinity decreased with increasing amount of clay in the PHBV/OMMT nanocomposites. Furthermore, the PHBV processing behaviour could be improved with OMMT-based nanocomposites since the processing temperature range enlarged by lowering melting temperature with the increasing clay content. The tensile properties of the corresponding materials were improved by incorporation of 3 wt% of clay (Chen, 2002). Above this clay content, aggregation of clay occurred and tensile strength and strain at break decrease. Dynamic mechanical analysis, through the study of the modulus and the Tα relaxation temperature, highlighted that the interface was maximized because of the nanometer size which restricts segmental motion near the organic-inorganic interface. Thus, it confirmed that intercalated nanocomposites were formed. Eventually, the biodegradability of these nanocomposites systems in soil suspension decreased with increasing amount of OMMT. It was related to the interactions between PHBV and OMMT, but also to the water permeability, the degree of crystallinity, and the anti-microbial property of OMMT.

Eventually, Misra et al. developed a novel solvent-free method to prepare PHB functionalized by maleic anhydride (PHB-g-MA) (Misra, 2004). The functionalization was successfully achieved by free radical grafting of maleic anhydride using a peroxide initiator by reactive extrusion processing. Then, they have mixed PHB-g-MA with C30B to make the organomodifier hydroxyl functions react with the MA (Drzal, 2004). Although, the d-spacing was comparable to PHB/C30B prepared by melt blending, the decrease in intensity of XRD signals and TEM images showed that more delaminated platelets were obtained.

To conclude, most of the articles reported the preparation of PHA-based nanocomposite by solvent intercalation, and whatever the elaboration route, full exfoliation state was neither obtained nor clearly demonstrated.

E.III. Petroleum-based polyesters

E.III.1. Polycaprolactone-based nano-biocomposites

PCL-based nanocomposite was the first studied nano-biocomposite. In the early 90', Giannelis' group from Cornell University (Ithaca, New York, USA) started to work on the elaboration of PCL-based nanocomposite by intercalative polymerization (Messersmith, 1993; Messersmith, 1995; Krishnamoorti, 1997). Their work was motivated by previous studies

involving polymerization of ε-caprolactam in the presence of layered silicates, which suggested that lactone ROP can be catalyzed by layered silicates. Then, they decided to investigate the intercalation and polymerization of ε-caprolactone within the gallery of layered silicates. The very first PCL-based nanocomposite prepared was based on fluorohectorite, a mica-type layered silicate (Messersmith, 1993). The ROP of ε-caprolactone (ε-CL) was activated by the surface of the Cr^{3+}-exchanged fuorohectorite. Indeed, the type of interlayer cations (e.g. Cr^{3+}, Cu^{2+}, Co^{2+}, Na^{+}) is important in achieving polymerization since it proceeds through cleavage of the acyl-oxygen bond catalyzed by the interlayer Cr^{3+} ions which present a more acidic character than mono- and divalent cations. The chemical polymer-clay interactions at the interface was proved to be strong and the intercalation of the polymer irreversible. However, authors could also observed the decrease of d-spacing after polymerization. They attributed this phenomenon to a change in the intercalated molecules organization from the monomer to the polymer (see Figure 9). Similar results were also obtained later by Kiersnowski et al. (Kiersnowski, 2004a) who prepared the PCL-based composites by in-situ polymerization catalyzed by water. Afterwards, Messersmith et al. (Messersmith, 1995) attempted to prepare PCL-based nanocomposites by in-situ polymerization thermally activated and initiated by organic acid (Messersmith, 1995). This one constituted the OMMT organomodifier, namely the protonated form of 12-aminododecanoic acid, which was thus present on the clay surface and initiated the ROP by a nucleophilic attack on the ε-caprolactone carbonyl. The resulting PCL was therefore ionically bound to the silicate layers through the protonated amine chain end. XRD results suggested that individual silicate layers were dispersed in the matrix. On the contrary, OMMT layers organo-modified with a less polar ammonium (dimethyl dioctadecyl (Messersmith, 1995) or hexadecyltrimethyl (Kiersnowski, 2004b; Pucciariello, 2004a) ammonium) showed no dispersion in CL or PCL. Subsequently, the interactions occurring at the interface of a PCL/OMMT exfoliated nanocomposite were investigated (Pucciariello, 2004a, 2004b) and the crystallinity, the permeability and the rheological behaviours were examined (Messersmith, 1995; Krishnamoorti, 1997; Tortora, 2002; Pucciariello, 2004a). Both, the crystallinity and the crystallite size decreased because of the dispersed silicate layers that represent physical barriers and hinder the PCL crystal growth. The dispersion of high aspect ratio platelets also reduced the water permeability, nearly by an order of magnitude at 4.8 vol% silicate (Messersmith, 1995). Tortora et al. (Tortora, 2002) who examined the water and dichloromethane permeability, assumed that the diffusion path of the polar water molecules is slowed down compared to dichloromethane vapor, not only because of the physical barrier of the clay layers but also

because of the hydrophilic character of the platelets. Eventually, the linear viscoelastic behaviour of the nanocomposites with various OMMT contents was examined. A "pseudo-solid-like" behaviour was clearly seen at silicate loading greater than 3 wt% suggesting that domains were formed wherein some long-range order was preserved and the silicate layers were oriented in some direction. Furthermore, the non-terminal effect was more pronounced with increasing clay content. These long-range order and domain structures were hence likely to become better defined when the mean distance between the layers becomes less than the lateral dimensions of the silicate layers and thus forcing some preferential orientation between the layers.

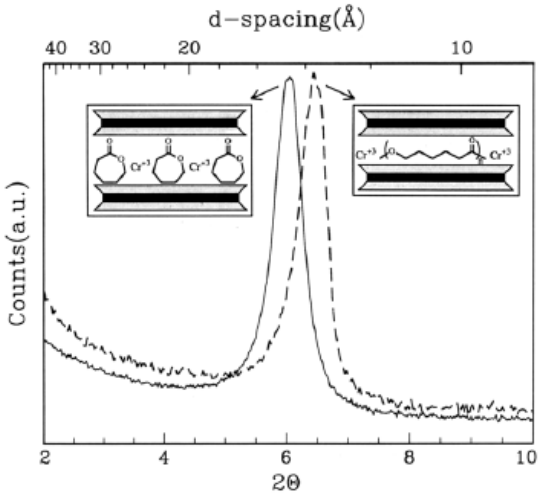

Figure 9: XRD patterns of PCL nanocomposite before (solid lines) and after (dashed lines) polymerization (Messersmith, 1993).

Jimenez et al. (Jimenez, 1997) then tested the solvent intercalation route by mixing PCL with distearyldimelthyammonium organo-modified montmorillonite. However, it was proved that PCL chains were not largely intercalated between the layers.

Dubois' group (Belgium) has worked a lot on PCL nanocomposite issues. They were interested in the in-situ ε-CL ROP and in the melt intercalation route. They demonstrated that the formation of PCL-based nanocomposites depends not only on the ammonium cation and related functionality but also on the elaboration route. Contrary to Messersmith & Giannelis (Messersmith, 1993; Messersmith, 1995), PCL-based nanocomposites were prepared by in-situ ROP according to a "coordination-insertion" mechanism (Kubies, 2002; Lepoittevin, 2002b, 2002c, 2002d; Pantoustier, 2002; Pantoustier, 2003; Viville, 2003) (see Figure 10), as for PLA (Paul, 2003a; Paul, 2005b). This reaction consists in swelling the OMMT organo-modified by alkylammonium bearing hydroxyl groups (OMMT-$(OH)_2$) and then in adding an initiator/activator such as tin(II) octoate ($Sn(Oct)_2$), dibutyltin-(IV) dimethoxide ($Bu_2Sn(OMe)_2$) or triethylaluminium ($AlEt_3$). The ammonium is thus activated and can yield surface grafted PCL

chains. Every hydroxyl function generates a PCL chain. Consequently, the higher the OMMT-$(OH)_2$, the lower the PCL average molar masses. It is worth noting that, in the presence of tin(IV) catalysts, since they are more efficient towards ε-CL ROP, the preparation took place in milder conditions compared to $Sn(Oct)_2$ (Pantoustier, 2002). Moreover, in all cases, the nanocomposites exhibited a continuous decrease of molar masses with clay concentration. This can be explained by OH functions, which can act both as co-initiator and chain transfer agent. This in-situ polymerization process led to well-exfoliated PCL/OMMT-$(OH)_2$ nanocomposites with 3 wt% of clay while with higher content (10 wt%) partially exfoliated/partially intercalated structures were observed. Further morphological observations were carried out by scanning probe microscopy (SPM), while surface analysis was examined by X-ray photoelectron spectroscopy (XPS) and Fourier transform infrared spectroscopy in the reflection absorption mode (FT-IRAS) (Viville, 2003). Taking into account the structure, the thermal stability increased and the water permeability decreased since the well dispersed fillers with high aspect ratio acted as barriers to oxygen and volatile degradation products (Pantoustier, 2002; Gorrasi, 2003). In contrast, nanocomposites filled with non-hydroxyl functional clays exhibited only intercalated structures (Kubies, 2002; Lepoittevin, 2002d; Pantoustier, 2003).

Since ε-CL polymerization is initiated by OH groups, polymer chains lengths can be predetermined and controlled by the clay loading. Thus, the clay content is limited to a certain range of concentrations to prevent from obtaining too short PCL chain lengths. Nevertheless, this can be modulated by tuning the number of OH groups i.e. by modifying the clay surface by a mixture of non-functional alkylammonium and monohydroxylated ammonium cations (Lepoittevin, 2002b, 2002c; Viville, 2004). Thus, using this interesting in-situ intercalative process, the inorganic content, the quantitative surface grafting, the number of polyester chains per clay surface as well as the polymer chain length and molecular weight distribution are well controlled (Lepoittevin, 2002c). Viville et al. (Viville, 2004) also studied the morphology of PCL grafted chains on the silicate layer surface depending on the OH content. They showed that the grafting density drastically increased as the proportion of OH-substituted alkylammonium cations used to organo-modify the clay increased. Besides, since separate polymer islands were formed in the low OH content systems (see Figure 11), they assumed that a phase separation process occurred between the ammonium ions induced by the polymerization reaction. Homogeneous coverage and subsequent thicknening only take place from 50% OH content. When this situation was achieved, adjacent platelets become fully independent of each, which greatly favoured exfoliation.

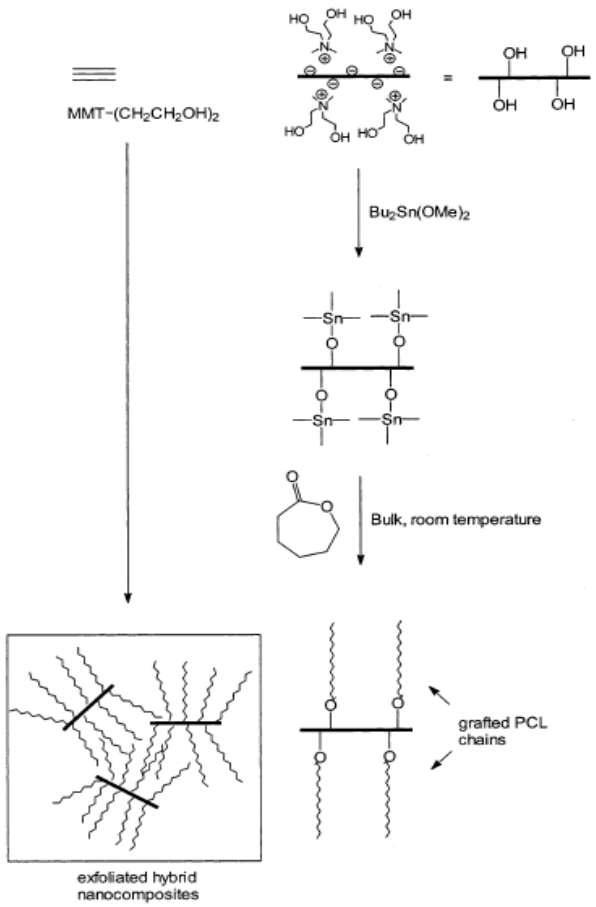

Figure 10: ROP of ε-CL by the "coordination-insertion" mechanism (Lepoittevin, 2002d).

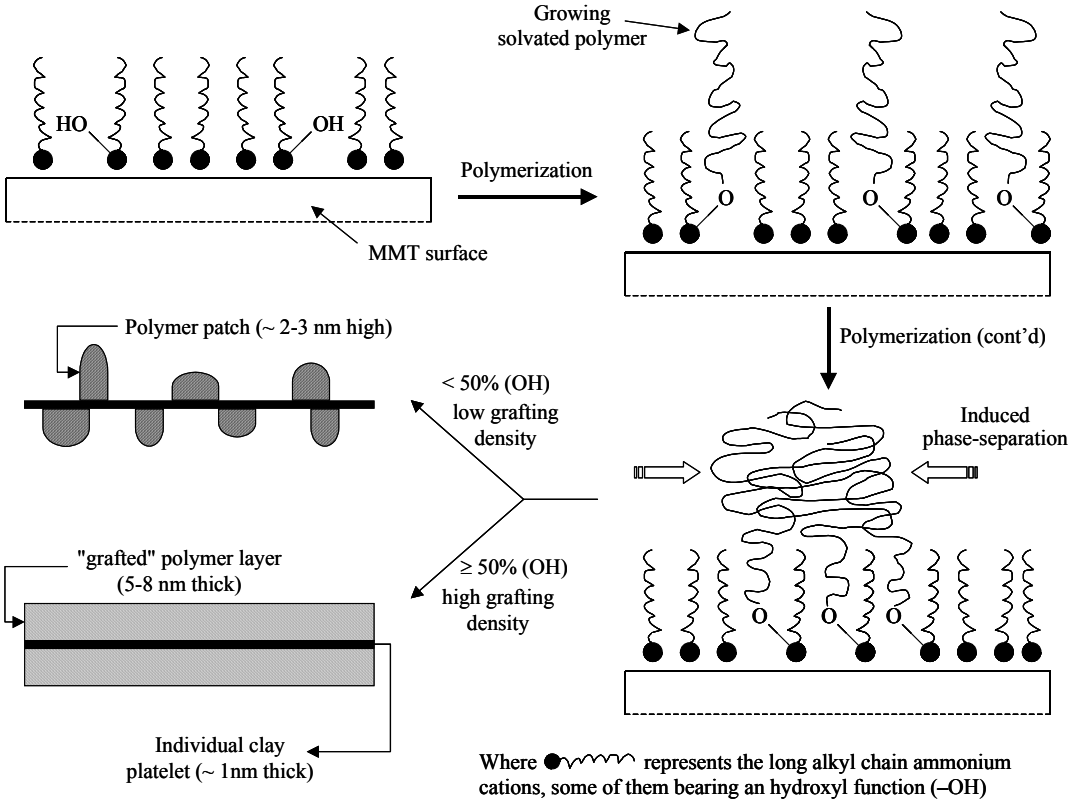

Figure 11: Polymer surface grafting onto individual clay platelets and phase separation (Viville, 2004).

The "coordination-insertion" mechanism, i.e. in-situ intercalation catalyzed by initiators, was compared to the thermally activated in-situ intercalation with various OMMT (Pantoustier, 2003). First, they confirmed Giannelis' results (Messersmith, 1995) that large catalytic surface of montmorillonite can contribute to polymerization of ε-CL. Exchanged cations bearing protic functions like NH_3^+, OH, COOH significantly favoured the polymerization and lead to similar structures than those obtained by the "coordination-insertion" mechanism. Nevertheless, the PCL molecular weights remained low and the polydispersity index at high conversion reached values higher than 2, confirming that the in-situ intercalation in presence of OH groups and initiators allows a better polymerization control.

Eventually, the melt intercalation route led to intercalated/exfoliated structures when PCL was associated with OMMT bearing quaternized octadecylamine (MMT-C_{18}), di(hydrogenated tallow) dimethyl ammonium (MMT-$2C_2C_{18}$), dimethyl 2-ethylhexyl(hydrogenated tallow alkyl) (MMT-Alk), or methyl bis(2-hydroxyethyl) (hydrogenated tallow alkyl) (OMMT-$(OH)_2$) (Lepoittevin, 2002a; Pantoustier, 2002). On the contrary, MMT-Na and ammonium bearing 12-aminododecanoic acid OMMT (MMT-COOH) formed microcomposites since no change of interlayer gap was observed whereas the in-situ intercalation showed exfoliation in the case of MMT-COOH (Messersmith, 1995). Although complete exfoliation was not reached, on the contrary to in-situ intercalative process, the tensile and thermal properties were improved. For instance, the modulus increased from 210 MPa for unfilled PCL to 280 MPa or 400 MPa with 3 wt% of MMT-C_{18} or MMT-Alk, and 10 wt% of MMT-$(OH)_2$ respectively, attesting for an almost two-fold increase of the PCL rigidity in the latter case (Pantoustier, 2001; Lepoittevin, 2002a). Chen & Evans (Chen, 2006) demonstrated on similar systems that the elastic modulus trends according to clay volume fraction can be interpreted using well-established theory for conventional composites, namely the Hashin-Shtrikman bounds. At OMMT content higher than 5 wt%, the elongation at break dropped off due to clay aggregation (Pantoustier, 2001; Lepoittevin, 2002a).

Dynamic mechanical measurements also revealed that with 1 wt% of clay, nanocomposites materials exhibited a pseudo-solid like behaviour (Lepoittevin, 2002a). However, Kwak et al. (Kwak, 2003) demonstrated that PCL chains can diffuse further into the silicate gallery due to additionally subjecting the samples to heat during the analyses and finally, extended exfoliation are achieved. The 50% weight loss temperature is shifted by 60°C towards higher temperature upon the addition of 1 wt% of clay whereas the temperature shift is only of

30°C at 10 wt%. Thus, PCL nanocomposites combine high stiffness, good ductility and improved thermal stability at low clay content (<5 wt%).

Only Di et al. (Di, 2003) reached exfoliated state in the case of PCL/OMMT-$(OH)_2$ systems prepared by direct melt intercalation with 2 to 5 wt% of clay. Obviously, they reported great enhancements of mechanical and thermal properties as well as a pseudo-solid like rheological behaviour caused by the strong interactions between the organoclay layers and PCL, and by the good dispersion of exfoliated organoclay platelets. Moreover, the results on the isothermal crystallization behaviour (Di Maio, 2004) revealed that the well dispersed organoclay platelets acted as nucleating agents but also affected the crystals quality by the restricted chains mobility.

Since the direct melt intercalation suffers a lack of efficiency towards clay dispersion, an elaboration route combining in-situ ε-CL polymerization and material redispersion by melt intercalation was settled. This masterbatch process allowed yielding exfoliated/intercalated structure that are rather difficult to reach by direct melt blending (Lepoittevin, 2003; Shibata, 2007). This process also turned out to be a good way to compatibilize and thus to reinforce other thermoplastics like conventional polymers (SAN (Kim, 2001; Kiersnowski, 2004b), PVC (Lepoittevin, 2003), PC (Gonzalez, 2006), PP, PE, PS and ABS (Zheng, 2003),) or biopolymers (PBS, PBAT (Pollet, 2006),). Conversely, PCL was blended by a reactive process with thermoplastic-clay systems (Kalambur, 2004; Yoshioka, 2006) to improve the properties of the final material.

Eventually, a remarkable study on the nanocomposite preparation of oligo-PCL/OMMT by simply mechanical mixing was reported by Maiti (Maiti, 2003a). Different types of clays having different aspect ratios (hectorite, mica, smectite) organo-modified with various phosphonium cations were selected to investigate their influence on the miscibility with oligo-PCL (o-PCL). The alkyl phosphonium cations were *n*-octyltri-*n*-butylphosphonium, *n*-dodecyltri-*n*-butylphosphonium, *n*-hexadecyltri-*n*-butylphosphonium and methyltriphenylphosphonium, noted respectively $C_{8,}$ C_{12}, C_{16} and C_{Ph}. Immiscible, intercalated, and exfoliated nanostructures were observed in o-PCL nanocomposites, depending on the nature of the organic modifier as well as the aspect ratio. Figure 12 sums up their interpretation according to experimental results but also to thermodynamic considerations. According to Maiti, when o-PCL is immiscible with a certain organic modifier, it cannot intercalate into the silicate gallery, while, for a short chain miscible modifier, o-PCL intercalates and, in the case of a long chain modifier, the modifier orients itself away from the silicate surface and is solubilized into the o-PCL phase, resulting in the collapse of the silicate gallery (see Figure 12a).

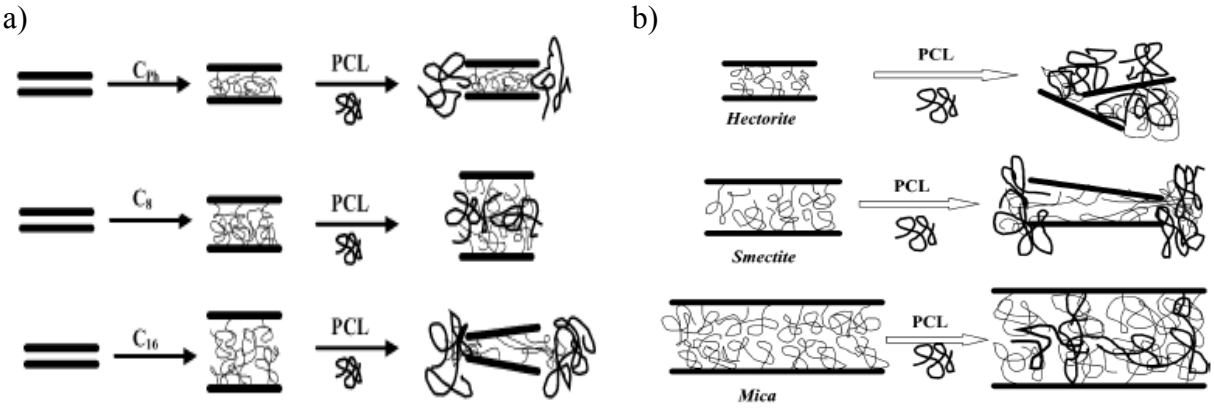

Figure 12: Schematic representation of PCL oligomers nanocomposites depending (a) on the nature of the organomodifier and (b) on the clay aspect ratio (Maiti, 2003a)

Considering the effect of the aspect ratio with a given organomodifier, when the aspect ratio is low, combined with a high CEC, the organic modifier is favoured to diffuse out the gallery and to interact with o-PCL leading to exfoliated structure. For higher aspect ratio, i.e. for larger lateral dimensions of the silicate layers, the organic modifier hardly access outside the gallery, and thus, the o-PCL must intercalate (see Figure 12b).

Other works attempted to better understand the mechanism of intercalation/exfoliation process either by melt intercalation or in-situ ε-CL polymerization by molecular dynamics simulations (Calberg, 2004; Gardebien, 2004; Gardebien, 2005). Very recently, solid-state NMR has emerged as a new tool to characterize clay/polymer nanocomposites in complement to data from classical methods (XRD, TEM) since it is a powerful technique for probing the molecular structure, conformation, and dynamics of species at interfaces. Therefore, solid state NMR was used in PCL-based nanocomposites to investigate how the surfactant conformation and mobility are changed by the polymer adsorption and how the polymer motion is perturbed after intercalation in the nanocomposites (Calberg, 2004; Hrobarikova, 2004; Urbanczyk, 2006). Finally, Calberg et al. (Calberg, 2004) validated this characterization method to determine the structure of PCL-based nanocomposites since they demonstrated that there was a correlation between variations in the proton relaxation times $T_1(H)$ and the quality of clay dispersion.

To conclude, PCL-based nanocomposites have been widely studied and several well controlled routes have been settled to reach exfoliated state. Elaboration of such materials turned out to be very useful not only for PCL properties enhancement but also for other thermoplastics one.

E.III.2. Biodegradable aliphatic copolyester-based nano-biocomposites

E.III.2.1. Polybutylene succinate

PBS presents many interesting properties, including biodegradability, melt processability, and thermal and chemical resistance, but low gas barrier properties and softness still limit their use. Therefore, particular attention have been paid to the elaboration of PBS-based nano-biocomposites to overcome these issues and to improve the material properties.

S.S. Ray et al. (Sinha Ray, 2002b) first reported structure and properties of PBS/clay nanocomposites (PBSCN) obtained by melt intercalation. Other studies (Okamoto, 2003; Sinha Ray, 2003a, Sinha Ray 2006b) investigated the effect of the organoclay type on the composites structures and properties. High molecular weight PBS were synthesized by a coupling reaction with a chain extender, namely the hexamethylene diisocyanate (OCN-C_6H_{12}-NCO) resulting in urethane type bonds (see Figure 13) and terminal hydroxyl groups. Different OMMT types were tested such as octadecylammonium and octadecyltrimethylammonium modified montmorillonite (C_{18}-MMT and qC_{18}-MMT respectively) and hexadecyltributylphosphonium modified saponite (qC_{16}-SAP). Intercalated and extended flocculated nanocomposites were obtained with the PBS/C_{18}-MMT systems. For qC_{18}-MMT reinforced materials, nanocomposites showed an intercalated and flocculated structure, whereas the coexistence of the stacked intercalated and delaminated structure was observed in PBS/qC_{16}-SAP nanocomposite. According to the authors, the flocculation was possible thanks to urethane bonds of PBS that make hydrogen bonds with the silicate hydroxylated edge groups leading to very strong interactions between matrix and silicate layers (Sinha Ray, 2003a, 2006b) (see Figure 14).

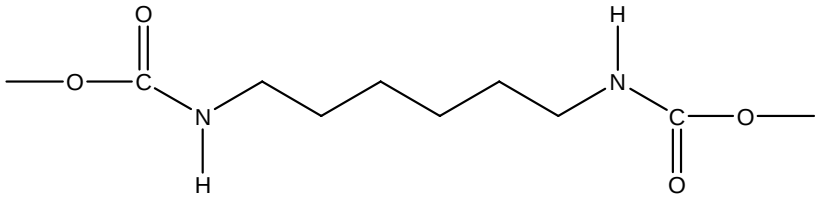

Figure 13: PBS chain extension by coupling reaction

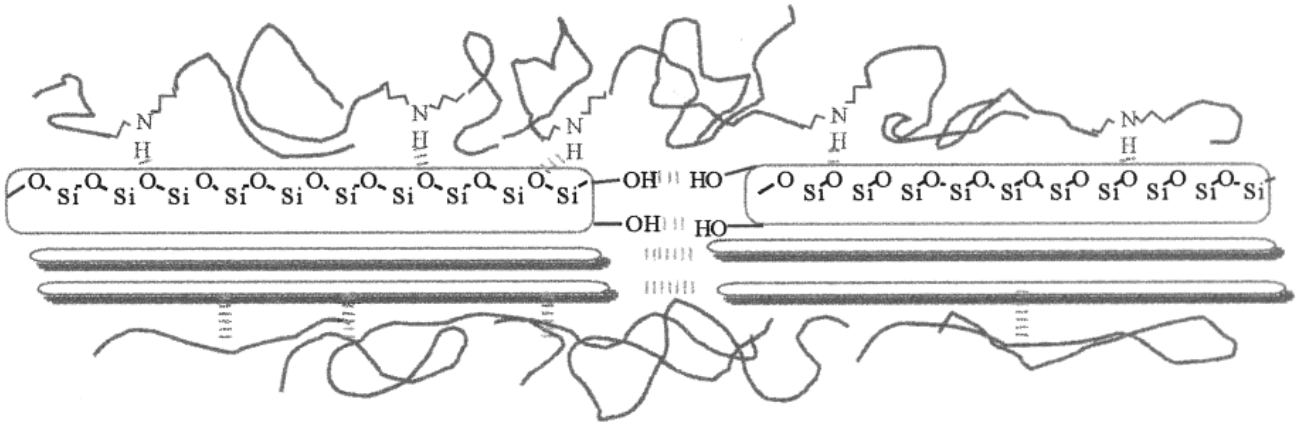

Figure 14: Formation of hydrogen bonds between PBS and clay, which leads to flocculation of the dispersed silicate layers (Sinha Ray, 2003a)

These structures were evidenced by mechanical, both in solids and melts, and barrier properties. For instance, G' determined by DMA presented significant enhancements with increasing clay loading, particularly with C_{18}-MMT and qC_{18}-MMT since increments reached more than 200% (Okamoto, 2003). Furthermore, since they noticed that properties of PBS/C_{18}-MMT and PBS/qC_{18}-MMT suddenly increased beyond a certain clay content, they concluded to the existence of a percolation threshold value (3.3 wt% for C_{18}-MMT (Sinha Ray, 2003a), and less than 3.6 wt% for qC_{18}-MMT (Sinha Ray, 2006b)). Above this clay content, dispersed and flocculated silicate layers form a network and contribute to reinforce considerably the matrix. The structures obtained affected the tensile properties and the rheological behaviour of the PBS. With increasing clay content, it was shown that the tensile modulus increased while the tensile strength decreased (Sinha Ray, 2006b). Eventually, rheological measurements revealed pseudo-solid-like behaviour of PBSCNs at high clay content suggesting a prevented relaxation due to the highly geometric constraints or physical jamming of the stacked silicate layers. This PBSCNs structure was also confirmed by the lower slope values and the higher absolute values of the dynamic moduli (Sinha Ray, 2003a). Barrier properties were also consistent with flocculated and percolated structures since the O_2 permeability decreased of 52% with 3.6 wt% of C_{18}-MMT (Okamoto, 2003) i.e. above the percolation threshold. Eventually, on the basis of compost results and GPC data, authors concluded that the PBS fragmentation was significantly improved generating higher surface area for further micro-organisms attack (Sinha Ray, 2003a).

Someya et al. (Someya, 2004) have tested different OMMT to determine the effect of variations in hydrophobicity and polar/steric interactions onto the nanostructures. Five OMMT organo-modifed with primary amines (dodecylamine DA-M, octadecylamine ODA-M, 12-aminolauric acid ALA) or tertiary amines (*N*-lauryldiethanolamine LEA-M, and 1-[*N*,*N*-bis(2-

hydroxyethyl)amino]-2-propanol HEA-M) were prepared and added to PBS by melt intercalation at different contents (from 1.0 to 10.0 wt%) and then the samples were injection molded. Highly intercalated structures and homogeneous clay dispersion were observed with DA-M, ODA-M, and LEA-M. On the contrary, some clusters or agglomerated particles were observed with ALA-M, HEA-M, and unmodified MMT. Authors showed that the enlargement of the d-spacing determined by XRD were well correlated with the clay dispersion improvement and with the increase of tensile and flexural moduli and the decrease of tensile strength. Dynamic viscoelastic measurements were also consistent with structural results since PBS/LEA-M nanocomposite had higher storage modulus and glass-transition temperature. This indicated that intercalation of PBS within the OMMT layers affected the molecular motion.

Another group achieved to improve PBS properties using compatibilization approach. Chen et al. (Chen, 2005b) proposed to graft epoxy groups onto C25A (Southern Clay Products, USA) with (glycidoxypropyl)trimethoxy silane leading to twice functionalized organoclay (TFC), as for PLA (Chen, 2005c). Tethering PBS molecules to the epoxy groups on the surface of TFC was attempted through melt compounding. Higher exfoliation degrees and properties were reached in PBS/TFC nanocomposites compared to those of PBS/C25A due to the increased PBS-TFC interfacial interactions. XRD results showed that d-spacing values were comparable when 10 wt% of C25A or TFC were added, but the difference of peak intensity attested that partial disruption of parallel stacking of TFC had occurred. The intercalation/exfoliation coexistence in the PBS/TFC systems have been also demonstrated by TEM images whereas intercalated clay tactoids have been observed with C25A. Till 10 wt% of filler, the mechanical properties are increased. Dynamic mechanical analyses also showed that E' was higher than neat PBS and increase with the clay content. Furthermore, it has to be noticed that a weak shoulder peak appearing at ~50°C in the tan δ profile was attributed to the relaxation of PBS segments confined within the clay layers on agreement with the structure deduced from morphological characterizations. Eventually, the study of the non-isothermal crystallization behaviour pointed out that the well dispersed TFC layers enhanced the nucleation and the crystallization rate of the PBS matrix (Chen, 2005e).

C30B was also used for the preparation of 3 wt% filled PBS-based nanocomposites by melt intercalation (Pollet, 2006). Since the measured d-spacing increased, intercalated structure was obtained resulting in PBS rigidity improvement (+25% Young's modulus). Furthermore, authors also tested metal-based catalysts (dibutyltin dilaurate $Sn(Bu)_2(Lau)_2$, titanium (IV) butoxide $Ti(OBu)_4$ and antimony (III) oxide Sb_2O_3) to promote transesterification between the ester moiety of the PBS and the organomodifier OH groups to graft PBS chains onto the organo-

clay surface. $Sn(Bu)_2(Lau)_2$ appeared to be the most appropriate catalyst since XRD and TEM clearly evidenced higher levels of clay exfoliation. Extraction process followed by TGA showed that grafting reaction had occurred. Consequently, material stiffness improved considerably by a Young's modulus increase of + 60% compared to neat PBS.

Recently, Shih et al. (Shih, 2007) investigated different organoclays functionalized by ammonium salts such as cetylpyridinium chloride (CPC-MMT) and cetyltrimethylammonium bromide (CTAB-MMT), which were mixed with PBS by solvent intercalation at 1, 3 and 5 wt%. The enhancement of E' and E'' evidenced that the stiffness and toughness of PBS were simultaneously improved. Weak shoulders on tan δ peaks at 5 wt% of clay were observed corresponding to the relaxation of PBS segments confined within the clay platelets suggesting an intercalated structure and inhomogeneous dispersion due to clay aggregation as mentioned by Chen et al. (Chen, 2005b). However, PBS/CTAB-MMT nanocomposites exhibited higher storage and loss moduli than PBS/CPC-MMT ones. Thus, aliphatic chain in CTAB, compared to the aromatic group in CPC, might interact more favourably with the aliphatic PBS because of their similar structures. Morphological characterizations were consistent with mechanical properties namely intercalated structures were obtained and better extent of d-spacing was observed with CTAB-MMT. Furthermore, TEM confirmed the coexistence of intercalated and exfoliated structures with 3 wt% of CTAB-MMT nanocomposite whereas aggregation was obtained with 5 wt% OMMT.

E.III.2.2. Polybutylene succinate-co-adipate

S.S. Ray et al. also reported PBSA-based nanocomposites studies (Sinha Ray, 2005a, 2005b; Sinha Ray, 2007a, 2007b). First, they have investigated various types of organoclays from Southern Clay Products (C15A, C93A and C30B) which present different polarity (Sinha Ray, 2005a). XRD and TEM have shown that the polymer-clay compatibility plays a key role to reach high d-spacing and high quality of dispersion. Finally, C30B appeared the most suitable nanofiller for PBSA-based nanocomposites prepared by melt intercalation. Highly disordered and exfoliated platelets were coexisting with few stacked intercalated layers due to interactions between C=O groups (PBSA backbone) and OH functions (C30B). Nevertheless, the dispersion quality was lowered with increasing clay content (Sinha Ray, 2005b). Consequently, thermal and mechanical properties were affected by the clay structuration according to the organoclay nature and content. First, although the PBSA crystal structure was not altered by the incorporation of clay, the crystallinity systematically decreased with the increasing dispersion degree of silicate

layers into PBSA matrix. In the case of strong polymer-clay interactions, mobility and flexibility of the polymer chains are hindered to fold and participate to the crystallization growth front. A significant increase in E' was observed due to the intercalation of chains within the silicate layers and this increase was more important with higher C30B content (Sinha Ray, 2005b). Furthermore, it was also shown substantial increase for E" suggesting the presence of strong internal friction between homogeneously dispersed intercalated silicate particles. Tensile properties were also examined. Tensile modulus and elongation at break increased in presence of organoclay but the improvement was strongly dependent on the degree of dispersion and on the C30B content. These improvements were only due to the structuration since the decrease of crystallinity with the addition of clays was demonstrated. The rheological properties also pointed out a gradual change of behaviour from liquid-like to solid-like with the increasing polymer-OMMT affinity. These results were mainly attributed to the extent of dispersion and distribution of the clay lamellae that form, beyond threshold concentration (3 wt% in the case of C30B), three dimensional percolating networks rendering the system highly elastic. Eventually, better thermal stability was obtained for PBSA/C30B but this increase was limited to low clay content since a drop was observed at 9 wt%. This was probably due to the excess of organic modifier containing OH groups on the clay surface which undergo Hofmann degradation at around 200°C.

Lee et al. (Lee, 2002) also tested C30B dispersion in Skygreen® at various clay content ranging from 1 to 30 wt% by melt intercalation. The highest values are unusual for nanocomposites since high content promotes aggregation. Nevertheless, in this case, exfoliated states were achieved above 15 wt% whereas intercalation was obtained with lower clay contents. Authors attributed this phenomenon to the combination of high shear rate reached during melt intercalation and the polymer-OMMT affinity. As seen before (Choi, 2003; Nam, 2003b; Nam, 2004), strong interactions or miscibility exist between the polymer and the C30B, due to strong hydrogen bonding between the carboxyl group from the biodegradable polyester and the OH group from C30B. These results were confirmed by TEM since the nanocomposites showed ordered intercalated structures with expanded layer gap and good dispersion at 10 wt%. Tensile properties enhancements were consistent with the structural results. Nanocomposites biodegradability decreased with increasing organoclay amount. This behaviour was explained by the existence of dispersed layers with large aspect ratio which force the micro-organisms diffusing in the matrix into a more tortuous paths.

Later, Lee et al. (Lee, 2003a) and Lim et al. (Lim, 2002; Lim, 2003b; Lim, 2004) chose C25A (Southern Clay Products, USA) as a nanofiller. Regardless the elaboration route, solvent (Lim, 2002; Lee, 2003a) or melt intercalation (Lim, 2003b), and the organoclay content studied

(<15 wt%), intercalated structures were observed. Lee et al. (Lee, 2005a) blended Skygreen® with polyepichlorohydrin (PECH) since the interlayer gap of PECH/OMMT nanocomposites can attain high values (>55 Å). Nevertheless, no larger d-spacing was obtained. Moreover, TEM observations but also the decrease and the broadening of d_{001} peak intensity with the decreasing clay content supposed that structures were much more inhomogeneous at low clay content showing exfoliated platelets at 3 wt% of C25A. Rheological measurements evidenced that shear-thinning behaviour and solid-like transition in low frequency region was enhanced by the addition of organoclay. This characterization technique also led to define a critical volume fraction. Beyond this threshold, the tactoids and individual layers are prevented from relaxing completely when subjected to shear, due to physical jamming or percolation leading to the solid-like behaviour observed in both intercalated and exfoliated nanocomposites. Creep and recovery tests were found consistent with these conclusions. Eventually, although the tensile modulus dramatically increases with the clay content, the tensile strength, the elongation at break and the onset temperature of thermal decomposition dropped beyond a certain clay loading. The collapse of mechanical and thermal properties is attributed to the OMMT aggregation. However, regarding the thermal stability in the presence of C25A with or without PECH, the decomposition phenomenon in terms of onset temperature and degradation rate is not fully understood yet. In this case, the decomposition rate increased with the increasing clay content while the onset degradation temperature was improved (Lim, 2002). Authors then supposed that, in a first step, the clay acts as a heat barrier and leads to the char formation after thermal decomposition. However, in a second step, the tactoids domain could hold accumulated heat which could be a source, in conjunction with the heat flow supplied by the external heat source, to accelerate the decomposition process.

The C25A was further modified by Chen et al. (Chen, 2005a) based on the same protocol established for PLLA-based (Chen, 2005c) and PBS-based nanocomposites (Chen, 2005b). The C25A was functionalized by grafting epoxy group at the surface using silane coupling agent. In this case, they tested (glycidyloxypropyl)trimethoxy silane (GPS) and (methacryloyloxypropyl)trimethoxy silane (MPS) as coupling agents. According to the authors, the silane compounds are located mainly on the edge of the silicate layers where the concentration of the silanol groups is higher than that on the plain surface. The preparation of the resulting twice functionalized clay (TFC) is shown on Figures 6 & 7. From XRD and TEM, it was concluded that both reaction between the PBSA end-groups and the TFC–GPS epoxy groups, and the polar interaction between the ester groups in TFC–MPS and PBSA, should have enhanced the compatibility. Larger increase of d-spacing were observed with 2 wt% of TFC–

GPS or TFC-MPS, compared to same C25A loading. TEM showed well dispersed stacks layers with multiple ordered platelets. The macroscopic properties were improved too. The storage modulus of PBSA/TFC was much higher than that of PBSA/C25A, especially in the low-frequency region, and non-terminal behaviour was observed at the terminal zone as a result of the enhanced PBSA-TFC interactions. Tensile modulus and strength at break were greatly improved with TFC–GPS and TFC–MPS due to the increased interfacial interaction.

Eventually, a particular study on PBSA/synthetic fluorinated mica nanocomposites was carried out by Sinha Ray et al. (Sinha Ray, 2006a; Sinha Ray, 2007b). Organo-modified SFM (OSFM, Somasif from CO-OP Chemicals Ltd.) was melt mixed with Bionolle®. Resulting nanocomposites showed that some intercalated stacked and disordered and/or exfoliated silicate layers coexist. The thermo-mechanical measurements were improved over all the temperature range investigated, and particularly above the Tg since E' increased by more than 100% compared to neat PBSA. Considering the crystallization behaviour (Sinha Ray, 2006a), the non-isothermal crystallization kinetics of the nanocomposite and its higher activation energy value calculated from model were on agreement with results given before (Sinha Ray, 2005b). Namely, the incorporation of OSFM decelerates the nucleation mechanism and PBSA crystal growth of as a result of the full dispersion of silicate layers into the matrix, which act as obstacles. The homogeneous dispersion was shown to increase the cold crystallization temperature of the nanocomposite. Regarding the thermal properties, the three prominent melting endotherms of PBSA, resulting from the melting–re-crystallization process, were shifted towards lower temperature and decrease in intensity due to the dispersion of the clay that restricted the motions of polymer chains. Besides, the thermal stability of PBSA was moderately increased in the presence of OSFM under both nitrogen and air atmospheres overall thermal degradation temperature range. In the early stage of the decomposition, although the surfactant, and thus the nanocomposite, seemed to be more prone to degrade in thermo-oxidative conditions than pyrolytic conditions, the main degradation temperature and char formation were increased in air compared to nitrogen. According to authors, the different types of char formation mechanisms under oxidative environment actually slow down the oxygen diffusion, thus hindering the oxidation procedure under thermo-oxidative conditions. Consequently, the flame retardance property of the nanocomposite was improved. To conclude, the activation energy of the nanocomposite thermal degradation calculated from the Kissinger model was slightly higher than that of neat PBSA, on agreement with previous results (Lim, 2002; Sinha Ray, 2005a).

Classical and original processes were investigated to reach exfoliated state and improved aliphatic copolyester-based nano-biocomposites properties with more or less success. Whatever the systems considered, the properties were well correlated to the materials structures.

E.III.3. Aromatic copolyester-based nano-biocomposites

PBAT is flexible and has a higher elongation at break than most biodegradable polyesters such as PLA and PBS, and therefore is more suitable for food packaging and agricultural films. Only few articles report the study of PBAT/clay nano-biocomposites.

Recently, Someya et al. (Someya, 2005b) have prepared OMMT which have been proved to be the more efficient with PBS (Someya, 2004), i.e. DA-M, ODA-M, LEA-M. They investigated the morphology and the properties of PBAT/clay nanocomposites prepared by melt intercalation containing 3 to 10 wt% of OMMT. The intercalation occurred in the case of DA-M and LEA-M and the exfoliation, in addition to some intercalation, occurred with ODA-M, which was also more finely dispersed in the matrix. Authors demonstrated that the mechanical properties were related to the structure as well as the crystallinity of the nanocomposites, leading globally to higher properties for PBAT/ODA-M. Furthermore, they showed that the clay reinforcing effect is really effective above Tg, because of the restricted polymer chains motions. Biodegradability was evaluated by the aerobic tests both in the soil and the aqueous medium containing activated sludge (Someya, 2005a). Compared to neat PBAT, the microcomposite based on unmodified montmorillonite exhibited a higher weight loss than PBAT/ODA-M nanocomposites.

Chivrac et al. (Chivrac, 2006; Chivrac, 2007) have expanded this work testing various commercial organoclays such as C20A, D43B and N804. The results relating to the structure and properties were compared to neat PBAT and the PBAT/MMT-Na, i.e. with non-modified montmorillonite LVF. They also compared the elaboration processes, i.e. solvent or melt intercalation. This study revealed that higher intercalation degrees have been obtained from solvent intercalation, C20A and D43B presented better affinity with PBAT. No impact of the clay have been noticed on the Tg and Tm whereas the crystallinity was affected by increasing clay content. Thus, they investigated the influence of the clay on the PBAT crystallization (Chivrac, 2007). Kinetics models were applied and it was concluded that addition of a small amount of MMT enhances the PBAT nucleation mechanism but also hinders the crystallite growth. These two antagonist phenomena lead to different crystallization behaviour depending on the clay dispersion. Furthermore, tensile tests have shown that the stiffness increases

continuously with clay content. This was attributed to the existence of strong interactions between PBAT and nanofillers, particularly with C20A, since the crystallinity decreases with increasing clay content. Nevertheless, decreases of the strain at yield and at break have been observed due to more aggregated structures at higher clay contents. Eventually, the onset degradation temperatures have been examined by TGA. The highest improvements were observed for nano-biocomposites filled with 3 wt% of MMT-Na. However, a decrease of the onset degradation temperatures is observed for higher clay contents, both with melt and solvent intercalations. This phenomenon is similar to the one described before by Lim et al. (Lim, 2002) i.e. clays act as heat barrier and lead to char formation after thermal decomposition, but unfortunately, tactoids can accumulated heat which could be used to accelerate the decomposition reaction.

To conclude, a large range of OMMT was tested leading to different PBAT-based nanocomposites structures. These studies thus highlighted the relationship between the materials structures and their properties.

E.III.4. Polyesteramide-based nano-biocomposites

Because, the polyesteramide present the higher water permeability (see Table 1), it appears necessary to improve this property, particularly if such materials is aimed at packaging applications.

Krook et al. (Krook, 2002; Krook, 2005) studied the barrier and mechanical properties of biodegradable melt-mixed polyesteramide/octadecylamine-treated montmorillonite containing 5 or 13 wt% of clay processed in different conditions (temperature, extruder screw speed). An increase of d-spacing was observed suggesting that intercalated structures were reached upon extrusion. A decrease in XRD peak intensity with increasing screw speed was observed, which implied that higher shear rates promoted delamination. TEM observations indicated that clay stacks were delaminated into smaller aggregates, containing generally one to three clay sheets. They also showed the presence of shear-induced voids almost exclusively located between the clay layers, which was confirmed by density measurements. These voids limited the improvement in barrier properties. The oxygen and water vapor transmission rates decreased with increasing clay content. According to the authors, the presence of voids prevents from the diffusion transport through the film. The low barrier properties improvement was due to the non-uniformly dispersed clay particles. However, the large improvement in stiffness and strength with filler content indicated that the mechanical properties were unaffected by the voids.

Authors also highlighted that the void content was reduced by compression moulding after extrusion. This further treatment led to higher crystallinity. This behaviour induces lower gas transmission rates and better mechanical properties (stiffness, yield point at higher stress levels and break at lower strains).

These results were completed with a series of injection-molded samples (Krook, 2005). XRD and TEM showed that these samples contained clay stacks. However, TEM also revealed that clay layers were largely delaminated and oriented "unidirectionally" over several microns. The transport and mechanical properties were greatly improved. This was attributed to a combined effect of a lower void content, higher crystallinity and greater degree of orientation.

To conclude, since packaging applications are considered for these materials, characterizations were focused on mechanical and barrier properties. The elaboration process was optimized to ensure good dispersion of clay and to avoid defects. Further properties were tested like optical transparency, weld strength, hot tack and transport properties (Krook, 2002).

F. Conclusion

This review presented the state of the art of biopolyester/clay nano-biocomposites. It has been clearly demonstrated that different parameters such as elaboration route, polymer/clay affinity and clay content can affect the structure and the nano-biocomposites properties. These latter can consequently be tuned as desired by controlling the parameters previously mentioned. In the case of good delamination and dispersion of clays, the mechanical reinforcement, thermal stability, biodegradability and barrier properties were improved. Rheological measurements also reveal that nanobiocomposites could present a more or less pronounced pseudo-solid-like behaviour indicating restricted motions of the biopolymer matrix. Obviously, the higher reinforcing effect is reached for exfoliated state which is not so trivial to obtain. Moreover, this enhancement is generally limited to small clay amounts (<~5 wt%) because at higher content, agglomeration takes place, resulting in lower properties.

Finally, nano-biocomposites present concurrent improvement in various material properties at very low filler content with no more inconvenient in the elaboration since conventional plastic processing can be used. Nano-biocomposites usefulness is no longer in question and more and more reports are focussed on applicative aspects in the environment, packaging, agriculture devices, biomedical fields, etc. Moreover, since industrials were concerned about sustainable developments, production cost of biopolymers goes on decreasing which will allow strong developments of biopolymers-based materials, such as the nano-

biocomposites. Therefore, these materials will be technically and financially competitive towards synthetic polymer-based nanocomposites. Then, this new class of material opens a new dimension for plastic industry.

Future research will address some actual issues such as the difficulty to exfoliate the clay with some biopolyester matrixes (e.g., PHA,). Further works should furnish valuable insight into new methods of nano-biocomposites design to establish new approaches to tailor novel nano-architectures.

Conclusion sur la partie bibliographique

Ce chapitre présente l'état de l'art dans le domaine des matériaux nano-biocomposites biopolyester/montmorillonite. Il a clairement été mis en évidence l'influence de trois facteurs clé, à savoir l'affinité polymère/argile, le taux de nanocharges et l'impact du procédé d'élaboration, sur la structure et les propriétés des nano-biocomposites. Le contrôle de ces différents paramètres peuvent ainsi permettre de moduler les propriétés finales des matériaux. Dans les cas d'une bonne dispersion de la charge au sein de la matrice biopolymère, les propriétés mécaniques, rhéologiques, thermiques, barrières et même la biodégradabilité sont améliorées. Les meilleurs effets de 'renfort' ont été observés dans le cas de structures exfoliées mais se limite généralement aux faibles taux de charges, i.e. <5 %pds. En effet, à des taux plus élevés, l'argile tend à s'agglomérer, conduisant ainsi à une diminution des propriétés.

En conclusion, les nano-biocomposites présentent un intérêt majeur en terme de performances techniques et s'adaptent aux techniques de mise en œuvre conventionnelles des plastiques. La nécessité de développer de tels matériaux n'est donc plus à démontrer. Aussi, de plus en plus de travaux s'intéressent aux applications possibles de ces matériaux nanostructurés, notamment dans le domaine de l'environnement, de l'emballage, de l'agriculture et du biomédical. Par ailleurs, les coûts de production des biopolymères tendent à diminuer du fait des développements actuels dans ce secteur. Ainsi, les matériaux à base de biopolymères tels que les nano-biocomposites seront techniquement et financièrement compétitifs face à des solutions plus classiques basées sur des polymères synthétiques conventionnels. De manière analogue aux nanocomposites conventionnels, les nano-biocomposites ouvrent une nouvelle ère et constituent donc une nouvelle classe de matériaux prometteurs pour l'industrie des matières plastiques.

Bibliographie

Albertsson, A.-C., Varma, I. K. (2002). Aliphatic polyesters: Synthesis, properties and applications. *Advances in Polymer Science,* 157, 1-40.

Amass, W., Amass, A., Tighe, B. (1998). A review of biodegradable polymers: Uses, current developments in the synthesis and characterization of biodegradable polyesters, blends of biodegradable polymers and recent advances in biodegradation studies. *Polymer International,* 47(2), 89-144.

Asrar, J., Mitsky, T. A., Shah, D. T. (2000). *Polyhydroxyalkanoates of narrow molecular weight distribution prepared in transgenic plants*. US6091002, Monsanto Company, St Louis, MO, United States

Asrar, J., Mitsky, T. A., Shah, D. T. (2001). *Polyhydroxyalkanoates of narrow molecular weight distribution prepared in transgenic plants*. US6228623, Monsanto Company, St Louis, MO, United States

Auras, R., Harte, B., Selke, S. (2004). An overview of polylactides as packaging materials. *Macromolecular Bioscience,* 4(9), 835-864.

Averous, L., Moro, L., Dole, P., Fringant, C. (2000). Properties of thermoplastic blends: Starch-polycaprolactone. *Polymer,* 41(11), 4157-4167.

Averous, L. (2004a). Biodegradable multiphase systems based on plasticized starch: A review. *Journal of Macromolecular Science-Polymer Reviews,* C44(3), 231-274.

Averous, L., Boquillon, N. (2004b). Biocomposites based on plasticized starch: Thermal and mechanical behaviours. *Carbohydrate Polymers,* 56(2), 111-122.

Bastioli, C., Cerutti, A., Guanella, I., Romano, G. C., Tosin, M. (1995). Physical state and biodegradation behavior of starch-polycaprolactone systems. *Journal of Environmental Polymer Degradation,* 3(2), 81-95.

Bastioli, C. (1998a). Biodegradable Materials - Present Situation and Future Perspectives. *Macromolecular Symposia,* 135, 193-204.

Bastioli, C. (1998b). Properties and applications of mater-Bi starch-based materials. *Polymer Degradation and Stability,* 59(1-3), 263-272.

Bigg, D. M. (1996). Effect of copolymer ratio on the crystallinity and properties of polylactic acid copolymers. *Journal of Engineering and Applied Science,* 2, 2028-2039.

Bruns, C., Gottschall, R., De Wilde, B. (2001). Ecotoxicological trials with BAK 1095 according to DIN V 54900. *Orbit J.,* 1(1), 1-10.

Calberg, C., Jerome, R., Grandjean, J. (2004). Solid-state NMR study of poly(e-caprolactone)/clay nanocomposites. *Langmuir,* 20(5), 2039-2041.

Cartier, L., Okihara, T., Ikada, Y., Tsuji, H., Puiggali, J., Lotz, B. (2000). Epitaxial crystallization and crystalline polymorphism of polylactides. *Polymer,* 41(25), 8909-8919.

Chandra, R., Rustgi, R. (1998). Biodegradable polymers. *Progress in Polymer Science (Oxford),* 23(7), 1273-1335.

Chang, J.-H., An, Y. U., Cho, D., Giannelis, E. P. (2003a). Poly(lactic acid) nanocomposites: Comparison of their properties with montmorillonite and synthetic mica (II). *Polymer,* 44(13), 3715-3720.

Chang, J.-H., An, Y. U., Sur, G. S. (2003b). Poly(lactic acid) nanocomposites with various organoclays. I. Thermomechanical properties, morphology, and gas permeability. *Journal of Polymer Science, Part B: Polymer Physics,* 41(1), 94-103.

Chen, B., Evans, J. R. G. (2006). Poly(e-caprolactone)-clay nanocomposites: Structure and mechanical properties. *Macromolecules,* 39(2), 747-754.

Chen, G., Yoon, J.-S. (2005a). Nanocomposites of poly[(butylene succinate)-co-(butylene adipate)] (PBSA) and twice-functionalized organoclay. *Polymer International,* 54(6), 939-945.

Chen, G. X., Hao, G. J., Guo, T. Y., Song, M. D., Zhang, B. H. (2002). Structure and mechanical properties of poly(3-hydroxybutyrate-co-3-hydroxyvalerate) (PHBV)/clay nanocomposites. *Journal of Materials Science Letters,* 21(20), 1587-1589.

Chen, G. X., Hao, G. J., Guo, T. Y., Song, M. D., Zhang, B. H. (2004). Crystallization kinetics of poly(3-hydroxybutyrate-co-3-hydroxyvalerate)/clay nanocomposites. *Journal of Applied Polymer Science,* 93(2), 655-661.

Chen, G.-X., Kim, E.-S., Yoon, J.-S. (2005b). Poly(butylene succinate)/twice functionalized organoclay nanocomposites: Preparation, characterization, and properties. *Journal of Applied Polymer Science,* 98(4), 1727-1732.

Chen, G.-X., Kim, H.-S., Kim, E.-S., Yoon, J.-S. (2005c). Compatibilization-like effect of reactive organoclay on the poly(L-lactide)/poly(butylene succinate) blends. *Polymer,* 46(25), 11829-11836.

Chen, G.-X., Yoon, J.-S. (2005d). Thermal stability of poly(L-lactide)/poly(butylene succinate)/clay nanocomposites. *Polymer Degradation and Stability,* 88(2), 206-212.

Chen, G.-X., Yoon, J.-S. (2005e). Non-isothermal crystallization kinetics of poly(butylene succinate) composites with a twice functionalized organoclay. *Journal of Polymer Science, Part B: Polymer Physics,* 43(7), 817-826.

Chiellini, E., Solaro, R. (1996). Biodegradable polymeric materials. *Advanced Materials,* 8(4), 305-313.

Chivrac, F., Kadlecova, Z., Pollet, E., Averous, L. (2006). Aromatic copolyester-based nano-biocomposites: Elaboration, structural characterization and properties. *Journal of Polymers and the Environment,* 14(4), 393-401.

Chivrac, F., Pollet, E., Averous, L. (2007). Nonisothermal crystallization behavior of poly(butylene adipate-co-terephthalate)/clay nano-biocomposites. *Journal of Polymer Science, Part B: Polymer Physics,* 45(13), 1503-1510.

Choi, W. M., Kim, T. W., Park, O. O., Chang, Y. K., Lee, J. W. (2003). Preparation and characterization of poly(hydroxybutyrate-co-hydroxyvalerate)-organoclay nanocomposites. *Journal of Applied Polymer Science,* 90(2), 525-529.

De Koning, G. J. M. (1993). Thesis.Prospects of bacterial poly[(R)-3-hydroxyalkanoates]. Center for Polymers and Composites (CPC) Eindhoven University of Technology Eindhoven

Di Maio, E., Iannace, S., Sorrentino, L., Nicolais, L. (2004). Isothermal crystallization in PCL/clay nanocomposites investigated with thermal and rheometric methods. *Polymer,* 45(26), 8893-8900.

Di, Y., Iannace, S., Di Maio, E., Nicolais, L. (2003). Nanocomposites by melt intercalation based on polycaprolactone and organoclay. *Journal of Polymer Science, Part B: Polymer Physics,* 41(7), 670-678.

Doi, Y. (1990). *Microbial polyesters*. New York: John Wiley & Sons, Inc.

Dos Santos Rosa, D., Calil, M. R., Fassina Guedes, C. d. G., Rodrigues, T. C. (2004). Biodegradability of thermally aged PHB, PHB-V, and PCL in soil compostage. *Journal of Polymers and the Environment,* 12(4), 239-245.

Drzal, L. T., Misra, M., Mohanty, A. K. (2004). Sustainable Biodegradable Green Nanocomposites From Bacterial Bioplastic for Automotive Applications. *U.S. EPA STAR Progress Review Workshop - Nanotechnology and the Environment II* (p. 23). Philadelphia.

El-Hadi, A., Schnabel, R., Straube, E., Müller, G., Henning, S. (2002). Correlation between degree of crystallinity, morphology, glass temperature, mechanical properties and biodegradation of poly(3-hydroxyalkanoate) PHAs and their blends. *Polymer Testing,* 21(6), 665-674.

Ema, Y., Ikeya, M., Okamoto, M. (2006). Foam processing and cellular structure of polylactide-based nanocomposites. *Polymer,* 47(15), 5350-5359.

Fritz, J. (1999). Thesis.Ecotoxicity of Biogenic Materials During and After their Biodegradation. University of Agriculture Vienna, Austria

Fujimaki, T. (1998). Processability and properties of aliphatic polyesters, 'Bionolle', synthesized by polycondensation reaction. *Polymer Degradation and Stability,* 59(1-3), 209-214.

Gardebien, F., Gaudel-Siri, A., Bredas, J.-L., Lazzaroni, R. (2004). Molecular dynamics simulations of intercalated poly(e-caprolactone)-montmorillonite clay nanocomposites. *Journal of Physical Chemistry B,* 108(30), 10678-10686.

Gardebien, F., Bredas, J.-L., Lazzaroni, R. (2005). Molecular dynamics simulations of nanocomposites based on poly(e-caprolactone) grafted on montmorillonite clay. *Journal of Physical Chemistry B,* 109(25), 12287-12296.

Garlotta, D. (2001). A literature review of poly(lactic acid). *Journal of Polymers and the Environment,* 9(2), 63-84.

Gonzalez, I., Eguiazabal, J. I., Nazabal, J. (2006). New clay-reinforced nanocomposites based on a polycarbonate/ polycaprolactone blend. *Polymer Engineering and Science,* 46(7), 864-873.

Gorrasi, G., Tortora, M., Vittoria, V., Pollet, E., Lepoittevin, B., Alexandre, M., Dubois, P. (2003). Vapor barrier properties of polycaprolactone montmorillonite nanocomposites: Effect of clay dispersion. *Polymer,* 44(8), 2271-2279.

Grigat, E., Koch, R., Timmermann, R. (1998). BAK 1095 and BAK 2195: Completely biodegradable synthetic thermoplastics. *Polymer Degradation and Stability,* 59(1-3), 223-226.

Hasook, A., Tanoue, S., Lemoto, Y., Unryu, T. (2006). Characterization and mechanical properties of poly(lactic acid)/poly(e-caprolactone)/organoclay nanocomposites prepared by melt compounding. *Polymer Engineering and Science,* 46(8), 1001-1007.

Hori, Y., Suzuki, M., Yamaguchi, A., Nishishita, T. (1993a). Ring-opening polymerization of optically active β-butyrolactone using distannoxane catalysts: synthesis of high-molecular-weight poly(3-hydroxybutyrate). *Macromolecules,* 26(20), 5533.

Hori, Y., Takahashi, Y., Yamaguchi, A., Nishishita, T. (1993b). Ring-opening copolymerization of optically active β-butyrolactone with several lactones catalyzed by distannoxane complexes: synthesis of new biodegradable polyesters. *Macromolecules,* 26(16), 4388.

Hori, Y., Hagiwara, T. (1996). Ring-opening polymerisation of β-butyrolactone catalysed by distannoxane complexes: study of the mechanism. *International Journal of Biological Macromolecules,* 25(1-3), 235-247.

Hrobarikova, J., Robert, J.-L., Calberg, C., Jerome, R., Grandjean, J. (2004). Solid-state NMR study of intercalated species in poly(e-caprolactone)/clay nanocomposites. *Langmuir,* 20(22), 9828-9833.

Jacobsen, S., Fritz, H. G. (1999). Plasticizing polylactide - the effect of different plasticizers on the mechanical properties. *Polymer Engineering and Science,* 39(7), 1303-1310.

Jimenez, G., Ogata, N., Kawai, H., Ogihara, T. (1997). Structure and thermal/mechanical properties of poly(e-caprolactone)-clay blend. *Journal of Applied Polymer Science,* 64(11), 2211-2220.

Juzwa, M., Jedlinski, Z. (2006). Novel Synthesis of Poly(3-hydroxybutyrate). *Macromolecules,* 39(13), 4627.

Kalambur, S. B., Rizvi, S. S. (2004). Starch-based nanocomposites by reactive extrusion processing. *Polymer International,* 53(10), 1413-1416.

Kaplan, D. L., Mayer, J. M., Ball, D., McCassie, J., Allen, A. L., Stenhouse, P. (1993). Fundamentals of biodegradable polymers. In C. Ching, D. L. Kaplan, & E. L. Thomas. *Biodegradable Polymers and Packaging* (p. 1-42): Lancaster, Technomic Pub. Co.

Kaplan, D. L. (1998). *Biopolymers from Renewable Resources*. Berlin: Springer Verlag.

Karlsson, S., Albertsson, A.-C. (1998). Biodegradable polymers and environmental interaction. *Polymer Engineering and Science,* 38(8), 1251-1253.

Kiersnowski, A., Dabrowski, P., Budde, H., Kressler, J., Piglowski, J. (2004a). Synthesis and structure of poly(e-caprolactone)/synthetic montmorillonite nano-intercalates. *European Polymer Journal,* 40(11), 2591-2598.

Kiersnowski, A., Piglowski, J. (2004b). Polymer-layered silicate nanocomposites based on poly(e-caprolactone). *European Polymer Journal,* 40(6), 1199-1207.

Kim, S. W., Jo, W. H., Lee, M. S., Ko, M. B., Jho, J. Y. (2001). Preparation of clay-dispersed poly(styrene-co-acrylonitrile) nanocomposites using poly(e-caprolactone) as a compatibilizer. *Polymer,* 42(24), 9837-9842.

Kobayashi, T., Yamaguchi, A., Hagiwara, T., Hori, Y. (1995). Synthesis of poly(3-hydroxyalkanoate)s by ring-opening copolymerization of (R)-β-butyrolactone with other four-membered lactones using a distannoxane complex as a catalyst. *Polymer,* 36(24), 4707-4710.

Koenig, M. F., Huang, S. J. (1994). Evaluation of crosslinked poly(caprolactone) as a biodegradable, hydrophobic coating. *Polymer Degradation and Stability,* 45(1), 139-144.

Kotnis, M. A., O'Brien, G. S., Willett, J. L. (1995). Processing and mechanical properties of biodegradable poly(hydroxybutyrate-co-valerate)-starch compositions. *Journal of Environmental Polymer Degradation,* 3(2), 97-105.

Kranz, H., Ubrich, N., Maincent, P., Bodmeier, R. (2000). Physicomechanical properties of biodegradable poly(D,L-lactide) and poly(D,L-lactide-co-glycolide) films in the dry and wet states. *Journal of Pharmaceutical Sciences,* 89(12), 1558-1566.

Krikorian, V., Pochan, D. J. (2003). Poly (L-Lactic Acid)/Layered Silicate Nanocomposite: Fabrication, Characterization, and Properties. *Chemistry of Materials,* 15(22), 4317-4324.

Krikorian, V., Pochan, D. J. (2004). Unusual crystallization behavior of organoclay reinforced poly(L-lactic acid) nanocomposites. *Macromolecules,* 37(17), 6480-6491.

Krikorian, V., Pochan, D. J. (2005). Crystallization behavior of poly(L-lactic acid) nanocomposites: Nucleation and growth probed by infrared spectroscopy. *Macromolecules,* 38(15), 6520-6527.

Krishnamoorti, R., Giannelis, E. P. (1997). Rheology of end-tethered polymer layered silicate nanocomposites. *Macromolecules,* 30(14), 4097-4102.

Krook, M., Albertsson, A.-C., Gedde, U. W., Hedenqvist, M. S. (2002). Barrier and mechanical properties of montmorillonite/polyesteramide nanocomposites. *Polymer Engineering and Science,* 42(6), 1238-1246.

Krook, M., Morgan, G., Hedenqvist, M. S. (2005). Barrier and mechanical properties of injection molded montmorillonite/polyesteramide nanocomposites. *Polymer Engineering and Science,* 45(1), 135-141.

Kubies, D., Pantoustier, N., Dubois, P., Rulmont, A., Jerome, R. (2002). Controlled ring-opening polymerization of e-caprolactone in the presence of layered silicates and formation of nanocomposites. *Macromolecules,* 35(9), 3318-3320.

Kwak, S.-Y., Oh, K. S. (2003). Effect of thermal history on structural changes in melt-intercalated poly(e-caprolactone)/organoclay nanocomposites investigated by dynamic viscoelastic relaxation measurements. *Macromolecular Materials and Engineering,* 288(6), 503-508.

Labrecque, L. V., Kumar, R. A., Dave, V., Gross, R. A., McCarthy, S. P. (1997). Citrate esters as plasticizers for poly(lactic acid). *Journal of Applied Polymer Science,* 66(8), 1507-1513.

Lagaly, G. (1993). From clay mineral crystals to colloidal clay mineral dispersions. In B. Dobias. *Coagulation and floculation - Theory and applications* (p. 427). New York: Dekker, M.

Lee, C. H., Lim, S. T., Hyun, Y. H., Choi, H. J., Jhon, M. S. (2003a). Fabrication and viscoelastic properties of biodegradable polymer/organophilic clay nanocomposites. *Journal of Materials Science Letters,* 22(1), 53-55.

Lee, C. H., Kim, H. B., Lim, S. T., Choi, H. J., Jhon, M. S. (2005a). Biodegradable aliphatic polyester-poly(epichlorohydrin) blend/organoclay nanocomposites: Synthesis and rheological characterization. *Journal of Materials Science,* 40(15), 3981-3985.

Lee, J. H., Park, T. G., Park, H. S., Lee, D. S., Lee, Y. K., Yoon, S. C., Nam, J.-D. (2003b). Thermal and mechanical characteristics of poly(L-lactic acid) nanocomposite scaffold. *Biomaterials,* 24(16), 2773-2778.

Lee, S.-R., Park, H.-M., Lim, H., Kang, T., Li, X., Cho, W.-J., Ha, C.-S. (2002). Microstructure, tensile properties, and biodegradability of aliphatic polyester/clay nanocomposites. *Polymer,* 43(8), 2495-2500.

Lee, Y. H., Lee, J. H., An, I.-G., Kim, C., Lee, D. S., Lee, Y. K., Nam, J.-D. (2005b). Electrospun dual-porosity structure and biodegradation morphology of Montmorillonite reinforced PLLA nanocomposite scaffolds. *Biomaterials,* 26(16), 3165-3172.

Lehermeier, H. J., Dorgan, J. R., Way, J. D. (2001). Gas permeation properties of poly(lactic acid). *Journal of Membrane Science,* 190(2), 243-251.

Lepoittevin, B., Devalckenaere, M., Pantoustier, N., Alexandre, M., Kubies, D., Calberg, C., Jerome, R., Dubois, P. (2002a). Poly(e-caprolactone)/clay nanocomposites prepared by melt intercalation: mechanical, thermal and rheological properties. *Polymer,* 43(14), 4017-4023.

Lepoittevin, B., Pantoustier, N., Alexandre, M., Calberg, C., Jerome, R., Dubois, P. (2002b). Polyester layered silicate nanohybrids by controlled grafting polymerization. *Journal of Materials Chemistry,* 12(12), 3528-3532.

Lepoittevin, B., Pantoustier, N., Alexandre, M., Calberg, C., Jerome, R., Dubois, P. (2002c). Layered silicate/polyester nanohybrids by controlled ring-opening polymerization. *Macromolecular Symposia,* 183, 95-102.

Lepoittevin, B., Pantoustier, N., Devalckenaere, M., Alexandre, M., Kubies, D., Calberg, C., Jerome, R., Dubois, P. (2002d). Poly(e-caprolactone)/clay nanocomposites by in-situ intercalative polymerization catalyzed by dibutyltin dimethoxide. *Macromolecules,* 35(22), 8385-8390.

Lepoittevin, B., Pantoustier, N., Devalckenaere, M., Alexandre, M., Calberg, C., Jerome, R., Henrist, C., Rulmont, A., Dubois, P. (2003). Polymer/layered silicate nanocomposites by combined intercalative polymerization and melt intercalation: A masterbatch process. *Polymer,* 44(7), 2033-2040.

Lewitus, D., McCarthy, S., Ophir, A., Kenig, S. (2006). The effect of nanoclays on the properties of PLLA-modified polymers Part 1: Mechanical and thermal properties. *Journal of Polymers and the Environment,* 14(2), 171-177.

Lim, S. T., Hyun, Y. H., Choi, H. J., Jhon, M. S. (2002). Synthetic biodegradable aliphatic polyester/montmorillonite nanocomposites. *Chemistry of Materials,* 14(4), 1839-1844.

Lim, S. T., Hyun, Y. H., Lee, C. H., Choi, H. J. (2003a). Preparation and characterization of microbial biodegradable poly(3-hydroxybutyrate)/organoclay nanocomposite. *Journal of Materials Science Letters,* 22(4), 299-302.

Lim, S. T., Lee, C. H., Choi, H. J., Jhon, M. S. (2003b). Solidlike transition of melt-intercalated biodegradable polymer/clay nanocomposites. *Journal of Polymer Science, Part B: Polymer Physics,* 41(17), 2052-2061.

Lim, S. T., Lee, C. H., Kim, H. B., Choi, H. J., Jhon, M. S. (2004). Polymer/organoclay nanocomposites with biodegradable aliphatic polyester and its blends: Preparation and characterization. *E-Polymers* n°026.

Ljungberg, N., Andersson, T., Wesslen, B. (2003). Film extrusion and film weldability of poly(lactic acid) plasticized with triacetine and tributyl citrate. *Journal of Applied Polymer Science,* 88(14), 3239-3247.

Lunt, J. (1998). Large-scale production, properties and commercial applications of polylactic acid polymers. *Polymer Degradation and Stability,* 59(1-3), 145-152.

Madison, L. L., Huisman, G. W. (1999). Metabolic engineering of poly(3-hydroxyalkanoates): From DNA to plastic. *Microbiology and Molecular Biology Reviews,* 63(1), 21-53.

Maiti, P., Giannelis, E. P., Batt, C. A. (2002a). Biodegradable polyester/layered silicate nanocomposites. *Materials Research Society Symposium - Proceedings,* 740, 141-145.

Maiti, P., Yamada, K., Okamoto, M., Ueda, K., Okamoto, K. (2002b). New polylactide/layered silicate nanocomposites: Role of organoclays. *Chemistry of Materials,* 14(11), 4654-4661.

Maiti, P. (2003a). Influence of miscibility on viscoelasticity, structure, and intercalation of oligo-poly(caprolactone)/layered silicate nanocomposites. *Langmuir,* 19(13), 5502-5510.

Maiti, P., Batt, C. A., Giannelis, E. P. (2003b). Renewable plastics: Synthesis and properties of PHB nanocomposites. *Polymeric Materials Science and Engineering* pp. 58-59.

Martin, O., Averous, L. (2001). Poly(lactic acid): Plasticization and properties of biodegradable multiphase systems. *Polymer,* 42(14), 6209-6219.

McCarthy, S. P., Ranganthan, A., Ma, W. (1999). Advances in properties and biodegradabilility of co-continuous, immiscible, biodegradable, polymer blends. *Macromolecular Symposia,* 144, 63-72.

Messersmith, P. B., Giannelis, E. P. (1993). Polymer-layered silicate nanocomposites: In situ intercalative polymerization of e-caprolactone in layered silicates. *Chemistry of Materials,* 5(8), 1064-1066.

Messersmith, P. B., Giannelis, E. P. (1995). Synthesis and barrier properties of polycaprolactone-layered silicate nanocomposites. *Journal of Polymer Science: Part A: Polymer Chemistry,* 33(7), 1047-1057.

Misra, M., Desai, S. M., Mohanty, A. K., Drzal, L. T. (2004). Novel solvent-free method for functionalization of polyhydroxyalkanoates: Synthesis and characterizations. *Annual Technical Conference - ANTEC, Conference Proceedings* pp. 2442-2446).

Moon, S. I., Lee, C. W., Miyamoto, M., Kimura, Y. (2000). Melt polycondensation of L-lactic acid with Sn(II) catalysts activated by various proton acids: A direct manufacturing route to high molecular weight poly(L-lactic acid). *Journal of Polymer Science, Part A: Polymer Chemistry,* 38(9), 1673-1679.

Moon, S.-I., Lee, C.-W., Taniguchi, I., Miyamoto, M., Kimura, Y. (2001). Melt/solid polycondensation of L-lactic acid: An alternative route to poly(L-lactic acid) with high molecular weight. *Polymer,* 42(11), 5059-5062.

Muller, R.-J., Witt, U., Rantze, E., Deckwer, W.-D. (1998). Architecture of biodegradable copolyesters containing aromatic constituents. *Polymer Degradation and Stability,* 59(1-3), 203-208.

Nam, J. Y., Sinha Ray, S., Okamoto, M. (2003a). Crystallization behavior and morphology of biodegradable polylactide/layered silicate nanocomposite. *Macromolecules,* 36(19), 7126-7131.

Nam, P. H., Fujimori, A., Masuko, T. (2003b). Flocculation characteristics of OM clay particles in PLA-MMT hybrid systems. *E-Polymers* n°5.

Nam, P. H., Fujimori, A., Masuko, T. (2004). The dispersion behavior of clay particles in poly(L-lactide)/organo-modified montmorillonite hybrid systems. *Journal of Applied Polymer Science,* 93(6), 2711-2720.

Nobes, G. A. R., Kazlauskas, R. J., Marchessault, R. H. (1996). Lipase-catalyzed ring-opening polymerization of lactones: a novel route to poly(hydroxyalkanoate)s. *Macromolecules,* 29(14), 4829.

Noda, I., Green, P. R., Satkowski, M. M., Schechtman, L. A. (2005). Preparation and properties of a novel class of polyhydroxyalkanoate copolymers. *Biomacromolecules,* 6(2), 580-586.

Ogata, N., Jimenez, G., Kawai, H., Ogihara, T. (1997). Structure and thermal/mechanical properties of poly(L-lactide)-clay blend. *Journal of Polymer Science, Part B: Polymer Physics,* 35(2), 389-396.

Okada, M. (2002). Chemical syntheses of biodegradable polymers. *Progress in Polymer Science (Oxford),* 27(1), 87-133.

Okamoto, K., Ray, S. S., Okamoto, M. (2003). New poly(butylene succinate)/layered silicate nanocomposites. II. Effect of organically modified layered silicates on structure, properties, melt rheology, and biodegradability. *Journal of Polymer Science, Part B: Polymer Physics,* 41(24), 3160-3172.

Pantoustier, N., Alexandre, M., Degée, P., Calberg, C., Jerome, R., Henrist, C., Cloots, R., Rulmont, A., Dubois, P. (2001). Poly(e-caprolactone) layered silicate nanocomposites: effect of clay surface modifiers on the melt intercalation process. *E-Polymers* n° 009.

Pantoustier, N., Lepoittevin, B., Alexandre, M., Kubies, D., Calberg, C., Jerome, R., Dubois, P. (2002). Biodegradable polyester layered silicate nanocomposites based on poly(e-caprolactone). *Polymer Engineering and Science,* 42(9), 1928-1937.

Pantoustier, N., Alexandre, M., Degée, P., Kubies, D., Jerome, R., Henrist, C., Rulmont, A., Dubois, P. (2003). Intercalative polymerization of cyclic esters in layered silicates: thermal vs. catalytic activation. *Composite Interfaces,* 10(4), 423-433.

Parikh, M., Gross, R. A., McCarthy, S. P. (1998). The influence of injection molding conditions on biodegradable polymers. *Journal of Injection Molding Technology,* 2(1), 30.

Paul, M.-A., Alexandre, M., Degée, P., Calberg, C., Jerome, R., Dubois, P. (2003a). Exfoliated polylactide/clay nanocomposites by in-situ coordination-insertion polymerization. *Macromolecular Rapid Communications,* 24(9), 561-566.

Paul, M.-A., Alexandre, M., Degée, P., Henrist, C., Rulmont, A., Dubois, P. (2003b). New nanocomposite materials based on plasticized poly(L-lactide) and organo-modified montmorillonites: Thermal and morphological study. *Polymer,* 44(2), 443-450.

Paul, M.-A., Delcourt, C., Alexandre, M., Degée, P., Monteverde, F., Dubois, P. (2005a). Polylactide/montmorillonite nanocomposites: study of the hydrolytic degradation. *Polymer Degradation and Stability,* 87(3), 535-542.

Paul, M.-A., Delcourt, C., Alexandre, M., Degée, P., Monteverde, F., Rulmont, A., Dubois, P. (2005b). (Plasticized) polylactide/(organo-)clay nanocomposites by in situ intercalative polymerization. *Macromolecular Chemistry and Physics,* 206(4), 484-498.

Perego, G., Cella, G. D., Bastioli, C. (1996). Effect of molecular weight and crystallinity on poly(lactic acid) mechanical properties. *Journal of Applied Polymer Science,* 59(1), 37-43.

Philip, S., Keshavarz, T., Roy, I. (2007). Polyhydroxyalkanoates: Biodegradable polymers with a range of applications. *Journal of Chemical Technology and Biotechnology,* 82(3), 233-247.

Pluta, M., Galeski, A., Alexandre, M., Paul, M.-A., Dubois, P. (2002). Polylactide/montmorillonite nanocomposites and microcomposites prepared by melt blending: Structure and some physical properties. *Journal of Applied Polymer Science,* 86(6), 1497-1506.

Pluta, M. (2004). Morphology and properties of polylactide modified by thermal treatment, filling with layered silicates and plasticization. *Polymer,* 45(24), 8239-8251.

Pluta, M., Paul, M.-A., Alexandre, M., Dubois, P. (2006a). Plasticized polylactide/clay nanocomposites. I. The role of filler content and its surface organo-modification on the physico-chemical properties. *Journal of Polymer Science, Part B: Polymer Physics,* 44(2), 299-311.

Pluta, M., Paul, M.-A., Alexandre, M., Dubois, P. (2006b). Plasticized polylactide/clay nanocomposites. II. The effect of aging on structure and properties in relation to the filler content and the nature of its organo-modification. *Journal of Polymer Science, Part B: Polymer Physics,* 44(2), 312-325.

Poirier, Y. (2002). Polyhydroxyalknoate synthesis in plants as a tool for biotechnology and basic studies of lipid metabolism. *Progress in Lipid Research,* 41(2), 131-155.

Pollet, E., Delcourt, C., Alexandre, M., Dubois, P. (2006). Transesterification catalysts to improve clay exfoliation in synthetic biodegradable polyester nanocomposites. *European Polymer Journal,* 42(6), 1330-1341.

Pucciariello, R., Villani, V., Belviso, S., Gorrasi, G., Tortora, M., Vittoria, V. (2004a). Phase behavior of modified montmorillonite-poly(e-caprolactone) nanocomposites. *Journal of Polymer Science - Part B: Polymer Physics,* 42(7), 1321–1332.

Pucciariello, R., Villani, V., Langerame, F., Gorrasi, G., Vittoria, V. (2004b). Interfacial effects in organophilic montmorillonite-poly(e- caprolactone) nanocomposites. *Journal of Polymer Science, Part B: Polymer Physics,* 42(21), 3907-3919.

Ramkumar, D. H. S., Bhattacharya, M. (1998). Steady shear and dynamic properties of biodegradable polyesters. *Polymer Engineering and Science,* 38(9), 1426-1435.

Ratto, J. A., Stenhouse, P. J., Auerbach, M., Mitchell, J., Farrell, R. (1999). Processing, performance and biodegradability of a thermoplastic aliphatic polyester/starch system. *Polymer,* 40(24), 6777-6788.

Shibata, M., Someya, Y., Orihara, M., Miyoshi, M. (2006). Thermal and mechanical properties of plasticized poly(L-lactide) nanocomposites with organo-modified montmorillonites. *Journal of Applied Polymer Science,* 99(5), 2594-2602.

Shibata, M., Teramoto, N., Someya, Y., Tsukao, R. (2007). Nanocomposites based on poly(e-caprolactone) and the montmorillonite treated with dibutylamine-terminated e-caprolactone oligomer. *Journal of Applied Polymer Science,* 104(5), 3112-3119.

Shih, Y. F., Wang, T. Y., Jeng, R. J., Wu, J. Y., Teng, C. C. (2007). Biodegradable nanocomposites based on poly(butylene succinate)/organoclay. *Journal of Polymers and the Environment,* 15(2), 151-158.

Shogren, R. (1997). Water vapor permeability of biodegradable polymers. *Journal of Environmental Polymer Degradation,* 5(2), 91-95.

Shogren, R. L. (1995). Poly(ethylene oxide)-coated granular starch-poly(hydroxybutyrate-co-hydroxyvalerate) composite materials. *Journal of Environmental Polymer Degradation,* 3(2), 75-80.

Sinclair, R. G. (1996). The case for polylactic acid as a commodity packaging plastic. *Journal of Macromolecular Science - Pure and Applied Chemistry,* 33(5), 585-597.

Sinha Ray, S., Maiti, P., Okamoto, M., Yamada, K., Ueda, K. (2002a). New Polylactide/Layered Silicate Nanocomposites. 1. Preparation, Characterization, and Properties. *Macromolecules,* 35(8), 3104-3110.

Sinha Ray, S., Okamoto, K., Maiti, P., Okamoto, M. (2002b). New Poly(butylene succinate)/Layered Silicate Nanocomposites: Preparation and Mechanical Properties. *Journal of Nanoscience and Nanotechnology,* 2(2), 171-176.

Sinha Ray, S., Okamoto, K., Yamada, K., Okamoto, M. (2002c). Novel Porous Ceramic Material via Burning of Polylactide/Layered Silicate Nanocomposite. *Nano Letters,* 2(4), 423-425.

Sinha Ray, S., Yamada, K., Ogami, A., Okamoto, M., Ueda, K. (2002d). New polylactide/layered silicate nanocomposite: Nanoscale control over multiple properties. *Macromolecular Rapid Communications,* 23(16), 943-947.

Sinha Ray, S., Yamada, K., Okamoto, M., Ueda, K. (2002e). Polylactide-Layered Silicate Nanocomposite: A Novel Biodegradable Material. *Nano Letters,* 2(10), 1093-1096.

Sinha Ray, S., Okamoto, K., Okamoto, M. (2003a). Structure-property relationship in biodegradable poly(butylene succinate)/layered silicate nanocomposites. *Macromolecules,* 36(7), 2355-2367.

Sinha Ray, S., Okamoto, M. (2003b). Polymer/layered silicate nanocomposites: A review from preparation to processing. *Progress in Polymer Science (Oxford),* 28(11), 1539-1641.

Sinha Ray, S., Okamoto, M. (2003c). New Polylactide/Layered Silicate Nanocomposites. 6. Melt Rheology and Foam Processing. *Macromolecular Materials and Engineering,* 288(12), 936-944.

Sinha Ray, S., Okamoto, M. (2003d). Biodegradable polylactide and its nanocomposites: Opening a new dimension for plastics and composites. *Macromolecular Rapid Communications,* 24(14), 815-840.

Sinha Ray, S., Yamada, K., Okamoto, M., Fujimoto, Y., Ogami, A., Ueda, K. (2003e). New polylactide/layered silicate nanocomposites. 5. Designing of materials with desired properties. *Polymer,* 44(21), 6633-6646.

Sinha Ray, S., Yamada, K., Okamoto, M., Ogami, A., Ueda, K. (2003f). New Polylactide/Layered Silicate Nanocomposites. 3. High-Performance Biodegradable Materials. *Chem. Mater.,* 15(7), 1456-1465.

Sinha Ray, S., Yamada, K., Okamoto, M., Ogami, A., Ueda, K. (2003g). New polylactide/layered silicate nanocomposites. 4. Structure, properties and biodegradability. *Composite Interfaces,* 10(4-5), 435-450.

Sinha Ray, S., Yamada, K., Okamoto, M., Ueda, K. (2003h). Biodegradable polylactide/montmorillonite nanocomposites. *Journal of Nanoscience and Nanotechnology,* 3(6), 503-510.

Sinha Ray, S., Yamada, K., Okamoto, M., Ueda, K. (2003i). Control of biodegradability of polylactide via nanocomposite technology. *Macromolecular Materials and Engineering,* 288(3), 203-208.

Sinha Ray, S., Yamada, K., Okamoto, M., Ueda, K. (2003j). New polylactide-layered silicate nanocomposites. 2. Concurrent improvements of material properties, biodegradability and melt rheology. *Polymer,* 44(3), 857-866.

Sinha Ray, S., Bousmina, M. (2005a). Poly(butylene sucinate-co-adipate)/montmorillonite nanocomposites: Effect of organic modifier miscibility on structure, properties, and viscoelasticity. *Polymer,* 46(26), 12430-12439.

Sinha Ray, S., Bousmina, M., Okamoto, K. (2005b). Structure and properties of nanocomposites based on poly(butylene succinate-co-adipate) and organically modified montmorillonite. *Macromolecular Materials and Engineering,* 290(8), 759-768.

Sinha Ray, S., Bousmina, M. (2006a). Crystallization behavior of poly[(butylene succinate)-co-adipate] nanocomposite. *Macromolecular Chemistry and Physics,* 207(14), 1207-1219.

Sinha Ray, S., Okamoto, K., Okamoto, M. (2006b). Structure and properties of nanocomposites based on poly(butylene succinate) and organically modified montmorillonite. *Journal of Applied Polymer Science,* 102(1), 777-785.

Sinha Ray, S., Bandyopadhyay, J., Bousmina, M. (2007a). Effect of organoclay on the morphology and properties of poly(propylene)/poly[(butylene succinate)-co-adipate] blends. *Macromolecular Materials and Engineering,* 292(6), 729-747.

Sinha Ray, S., Bandyopadhyay, J., Bousmina, M. (2007b). Thermal and thermomechanical properties of poly[(butylene succinate)-co-adipate] nanocomposite. *Polymer Degradation and Stability,* 92(5), 802-812.

Someya, Y., Nakazato, T., Teramoto, N., Shibata, M. (2004). Thermal and mechanical properties of poly(butylene succinate) nanocomposites with various organo-modified montmorillonites. *Journal of Applied Polymer Science,* 91(3), 1463-1475.

Someya, Y., Kondo, N., Teramoto, N., Shibata, M. (2005a). Studies of biodegradation of poly (butylene adipate-co-butylene terephtharate) / layered silicatenanocomposites. *Polymer Preprints, Japan* (p. 5362).

Someya, Y., Sugahara, Y., Shibata, M. (2005b). Nanocomposites based on poly(butylene adipate-co-terephthalate) and montmorillonite. *Journal of Applied Polymer Science,* 95(2), 386-392.

Steinbuchel, A., Doi, Y. (2002). *Polyesters III - Applications and Commercial Products*. Wiley-VCH, Weinheim, Germany.

Steinbuchel, A. (2003). *Biopolymers, General Aspects and Special Applications*. Wiley-VCH, Weinheim, Germany.

Tanoue, S., Hasook, A., Iemoto, Y., Unryu, T. (2006). Preparation of poly(lactic acid)/poly(ethylene glycol)/ organoclay nanocomposites by melt compounding. *Polymer Composites,* 27(3), 256-263.

Tokiwa, Y., Suzuki, T. (1977). Hydrolysis of polyesters by lipases. *Nature,* 270(5632), 76-78.

Tortora, M., Vittoria, V., Galli, G., Ritrovati, S., Chiellini, E. (2002). Transport properties of modified montmorillonite-poly(e-caprolactone) nanocomposites. *Macromolecular Materials and Engineering,* 287(4), 243-249.

Tuominen, J., Kylma, J., Kapanen, A., Venelampi, O., Itävaara, M., Seppälä, J. (2002). Biodegradation of lactic acid based polymers under controlled composting conditions and evaluation of the ecotoxicological impact. *Biomacromolecules,* 3(3), 445-455.

Urbanczyk, L., Hrobarikova, J., Calberg, C., Jerome, R., Grandjean, J. (2006). Motional heterogeneity of intercalated species in modified clays and poly(e-caprolactone)/clay nanocomposites. *Langmuir,* 22(10), 4818-4824.

Utracki, L. A., Sepehr, M., Boccaleri, E. (2007). Synthetic, layered nanoparticles for polymeric nanocomposites (PNCs). *Polymers for Advanced Technologies,* 18(1), 1–37.

Valentin, H. E., Broyles, D. L., Casagrande, L. A., Colburn, S. M., Creely, W. L., DeLaquil, P. A., Felton, H. M., Gonzalez, K. A., Houmiel, K. H., Lutke, K., Mahadeo, D. A., Timothy A. Mitsky, Padgette, S. R., Reiser, S. E., Slater, S., Stark, D. M., Stock, R. T., Stone, D. A., Taylor, N. B., Thorne, G. M., Tran, M., Gruys, K. J. (1999). PHA production, from bacteria to plants. *International Journal of Biological Macromolecules,* 25(1-3), 303-306.

Van Tuil, R., Fowler, P., Lawther, M., Weber, C. J. (2000). Properties of biobased packaging materials. *Biobased Packaging Materials for the Food Industry - Status and Perspectives* pp. 8-33): KVL, Frederiksberg, Denmark.

Velho, L., Velho, P. (2006). Innovation in Resource-Based Technology Clusters: Investigating the Lateral Migration Thesis - The development of a sugar-based plastic in Brazil. *Employment growth & development initiative*: Human Science Research Council.

Vert, M., Schwarch, G., Coudane, J. (1995). Present and future of PLA polymers. *J. Macromol. Sci., Pure Appl. Chem.,* A32(4), 787-796.

Viville, P., Lazzaroni, R., Pollet, E., Alexandre, M., Dubois, P., Borcia, G., Pireaux, J.-J. (2003). Surface Characterization of Poly(e-caprolactone)-Based Nanocomposites. *Langmuir,* 19(22), 9425-9433.

Viville, P., Lazzaroni, R., Pollet, E., Alexandre, M., Dubois, P. (2004). Controlled polymer grafting on single clay nanoplatelets. *Journal of the American Chemical Society,* 126(29), 9007-9012.

Wang, S., Song, C., Chen, G., Guo, T., Liu, J., Zhang, B., Takeuchi, S. (2005). Characteristics and biodegradation properties of poly(3-hydroxybutyrate-co-3-hydroxyvalerate)/organophilic montmorillonite (PHBV/OMMT) nanocomposite. *Polymer Degradation and Stability,* 87(1), 69-76.

Wee, Y.-J., Kim, J.-N., Ryu, H.-W. (2006). Biotechnological production of lactic acid and its recent applications. *Food Technology and Biotechnology,* 44(2), 163-172.

Williams, S. F., Martin, D. P., Horowitz, D. M., Peoples, O. P. (1999). PHA applications: addressing the price performance issue I. Tissue engineering. *International Journal of Biological Macromolecules,* 25(1-3), 111–121.

Witt, U., Einig, T., Yamamoto, M., Kleeberg, I., Deckwer, W.-D., Muller, R.-J. (2001). Biodegradation of aliphatic-aromatic copolyesters: Evaluation of the final biodegradability and ecotoxicological impact of degradation intermediates. *Chemosphere,* 44(2), 289-299.

Wu, T.-M., Wu, C.-Y. (2006). Biodegradable poly(lactic acid)/chitosan-modified montmorillonite nanocomposites: Preparation and characterization. *Polymer Degradation and Stability,* 91(9), 2198-2204.

Yokota, Y., Marechal, H. (1999). Processability of biodegradable poly(butylene) succinate and its derivates. A case study. *Biopolymer Conference*. Wurzburg, Germany.

Yoshida, O., Okamoto, M. (2006). Direct melt intercalation of polylactide chains into nano-galleries: Interlayer expansion and nano-composite structure. *Macromolecular Rapid Communications,* 27(10), 751-757.

Yoshioka, M., Takabe, K., Sugiyama, J., Nishio, Y. (2006). Newly developed nanocomposites from cellulose acetate/layered silicate/poly(e-caprolactone): Synthesis and morphological characterization. *Journal of Wood Science,* 52(2), 121-127.

Zheng, X., Wilkie, C. A. (2003). Nanocomposites based on poly (e-caprolactone) (PCL)/clay hybrid: Polystyrene, high impact polystyrene, ABS, polypropylene and polyethylene. *Polymer Degradation and Stability,* 82(3), 441-450.

Zinn, M., Witholt, B., Egli, T. (2001). Occurrence, synthesis and medical application of bacterial polyhydroxyalkanoate. *Advanced Drug Delivery Reviews,* 53(1), 5-21.

Chapitre II
-
Nano-biocomposites PHA/Montmorillonite

Introduction

Nous avons vu dans le chapitre précédent qu'il existe trois méthodes conventionnelles d'élaboration des nanocomposites : la voie "solvant", la voie "fondu" et la polymérisation in-situ. Cette étude porte sur des polymères produits par fermentation bactérienne de sucre issu de la canne à sucre, les polyhydroxyalcanoates. Aussi, la voie par polymérisation in-situ n'a pas été envisagée. Dans ce chapitre, seule l'élaboration des nano-biocomposites PHB-montmorillonite et PHBV-montmorillonite obtenus par voie "solvant" et/ou par voie "fondu" sera présentée.

Dans un premier temps, les caractéristiques des montmorillonites et le procédé de compatibilisation seront exposés. Par la suite, pour chacune des voies d'élaboration, les résultats des caractérisations structurales correspondantes seront présentés. Pour les systèmes ayant des propriétés macroscopiques intéressantes, une étude approfondie a été menée afin d'établir les relations "mise en œuvre-structure-propriétés" de ces matériaux.

A. Structure et propriétés des montmorillonites

Les montmorillonites sont des argiles présentes en abondance à l'état naturel. Elles suscitent depuis longtemps l'intérêt des chercheurs pour des applications dans la dépollution (Nistor, 2004) et la catalyse (Laszlo, 1987; Sposito, 1999). Mais plus récemment, elles font l'objet de nombreuses attentions en tant que nanocharges pour renforcer des matrices polymères. En effet, nous l'avons vu au chapitre I, en raison de leur structure, elles peuvent notamment améliorer les propriétés mécaniques, la stabilité thermique ou encore les propriétés barrières de certains biopolyesters.

A.I. Les montmorillonites naturelles (MMT)

La montmorillonite fait partie de la famille des phyllosilicates 2:1. Cela signifie qu'elle présente une structure en feuillets constitués chacun par deux couches de sites tétraédriques [SiO_3] séparées par une couche de sites octaédriques occupés par des atomes d'aluminium (cf. Publication n°1 Figure 3). Chaque feuillet individuel a une épaisseur d'environ 1 nm et sa longueur varie de 0,1 µm à 500 nm ce qui leur confère un facteur de forme (longueur/épaisseur) très élevé. L'empilement des feuillets forme des structures appelées tactoïdes. Les feuillets sont alors séparés par une distance caractéristique, appelée

distance ou espace interfeuillets *d* (d-spacing), régie par les forces de Van der Waals. Lorsqu'on déstructure ces tactoïdes, i.e. lorsqu'on atteint un état exfolié, les feuillets présentent alors une surface spécifique très importante (~700 m²/g).

Par ailleurs, des substitutions isomorphiques peuvent apparaître notamment au niveau des sites octaédriques des feuillets, par exemple des ions Al^{3+} peuvent être remplacés par des ions Mg^{2+} ou Fe^{2+}. Ce phénomène génère alors des charges négatives au cœur du feuillet qui sont contrebalancées par des ions alcalins ou alcalino-terreux (Na^{+}, Ca^{2+},…) dans l'espace interfeuillets. Ces ions confèrent un caractère hydrophile à la montmorillonite, la plus commune étant la montmorillonite sodique, notée MMT-Na.

A.II. Les montmorillonites organophiles (OMMT)

A.II.1. L'organomodification

La majorité des polymères étant organophiles, des études visant à améliorer la compatibilité entre la matrice et la charge ont donc été menées. Le procédé, appelé "organomodification", consiste à modifier les montmorillonites de façon à abaisser leur énergie de surface et donc à améliorer la mouillabilité. Les cations inorganiques (Na^{+} ou Ca^{2+}) dans l'espace interfeuillets sont alors échangés par des tensioactifs (appelés organomodifiants), généralement de type alkylammonium ou alkylphosphonium. Le nombre total de cations échangeables, correspondant également au nombre de sites négatifs dans les feuillets de montmorillonite, est appelée "capacité d'échange cationique" (CEC) et s'exprime en milliéquivalent par 100 g d'argile (meq/100 g). Les montmorillonites résultantes sont dites organomodifiées (OMMT). Leur CEC, i.e. la quantité d'organomodifiants, peut être inférieure, égale voire même supérieure à celle de la montmorillonite non modifiée (env. 90 meq/100 g). Dans ce dernier cas, les organomodifiants sont présents en excès parmi les feuillets d'argile.

Les OMMT modifiées par des ammonium quaternaires comprenant au minimum une longue chaîne alkyle sont les plus utilisées du fait de leur disponibilité et de leur faible coût. Dans le cadre de cette étude, les autres groupes substituants sont des groupes alkyles (noté OMMT-Alk), un groupe benzyle (noté OMMT-Bz) ou deux groupes hydroxyéthyle (noté OMMT-OH). Quant aux longues chaînes alkyles, elles sont constituées de chaînes en C_{18} (~65%), C_{16} (~30%) et C_{14} (~5%). Les (O)MMT utilisées lors de notre étude et leurs principales caractéristiques sont récapitulées dans l'Annexe I.

A.II.2. Organisation des organomodifiants

Nous avons vu dans le paragraphe précédent que la CEC de l'OMMT pouvait être supérieure à la CEC de la MMT-Na. Une partie des ions ammonium est alors intercalée entre les feuillets inorganiques tandis qu'une autre sera présente autour de ces feuillets (Kadar, 2006). Plusieurs études ont déterminé avec plus de précision la localisation des surfactants dans les montmorillonites organomodifiées (Xie, 2001; Xi, 2004; Xi, 2005), qui est fonction notamment de la CEC. En effet, au fur et à mesure que la CEC de l'OMMT augmente, les ions s'intercalent préférentiellement dans la région interfeuillets par échange cationique ; ils sont liés aux sites présents à la surface du feuillet inorganique par les interactions électrostatiques. Lorsque la CEC excède la CEC de l'argile non modifiée, les molécules de surfactants en excès se placent dans l'espace interfeuillets et interagissent avec les cations adsorbés à la surface des feuillets inorganiques par des forces de Van der Waals (Xi, 2004).

Par ailleurs, plusieurs publications (Lagaly, 1986; Vaia, 1994; Bonczek, 2002; Xi, 2004; Kadar, 2006) font état de l'organisation des organomodifiants intercalés. Selon la densité, la longueur des chaînes et la température, les chaînes alkyles s'orientent parallèlement ou s'écartent de la surface du feuillet pour former des monocouches ou des bicouches. Il existe également une configuration "hybride" i.e. combinant les deux types de configuration. Mais selon Vaia et al. (Vaia, 1994), ces configurations sont moins "figées" car ces modèles ne tiennent pas compte de la conformation *trans* ou *gauche* des chaînes alkyles. Les chaînes intercalées s'organiseraient de façon plus ou moins ordonnée en fonction du ratio de conformères, conduisant ainsi à des comportements de type liquide ou solide de ces chaînes. En général, lorsque la densité ou la longueur de chaînes diminue ou lorsque la température augmente, les chaînes adoptent une structure plus désordonnée (type liquide). Dans les cas intermédiaires, elles peuvent avoir un caractère cristal liquide.

Selon la quantité d'organomodifiants, la longueur et la configuration de(s) chaîne(s) alkyle(s) substituée(s), la distance interfeuillets de la montmorillonite peut augmenter (Vaia, 1994; Burgentzlé, 2004). Globalement, cet espace, initialement d'environ 10 Å dans le cas de la montmorillonite naturelle MMT-Na, peut augmenter jusqu'à ~30 Å dans le cas d'OMMT modifiées par des ammoniums quaternaires.

Des simulations numériques (He, 2005; Heinz, 2005; Heinz, 2006) ont également permis de montrer l'influence de la fonctionnalité des ammonium, du nombre de carbones de la chaîne alkyle, et de la CEC sur l'agencement de ces chaînes et donc sur la distance interfeuillets.

B. Elaboration des nano-biocomposites : la voie "solvant"

Cette voie d'élaboration fait intervenir un autre composé dans la préparation des nano-biocomposites : le solvant. Dans cette partie, les résultats relatifs aux systèmes PHB/(O)MMT préparés par voie solvant seront présentés et il sera montré que le solvant joue un rôle particulier sur la structure finale des matériaux. Il faut noter que cette voie ne répond pas à une approche de développement durable dans lequel s'inscrit principalement ce projet, du fait de l'utilisation importante de solvant organique "non vert". Cette voie est envisagée comme élément de comparaison, notamment pour établir des relations entre structuration et voie d'élaboration.

B.I. Généralités

Comme mentionné dans le chapitre I, le PHB et, dans une moindre mesure, le PHBV présentent des limites importantes liées à leur faible stabilité thermique au voisinage de leur point de fusion. De ce point de vue, la voie "solvant" apparaît comme une alternative intéressante à la voie "fondu". Cela explique certainement que les quelques travaux publiés à ce jour sur les systèmes PHA/montmorillonites concerne majoritairement la voie "solvant" (Chen, 2002; Lim, 2003; Chen, 2004; Wang, 2005). Pour obtenir une structuration optimisée et donc améliorer les propriétés finales des matériaux, il est nécessaire de connaître et maitriser les différents phénomènes mis en jeu. Ces derniers vont être décrits dans le paragraphe suivant.

B.I.1. Principe

Préparer des nanocomposites polymère-argile par voie solvant consiste, dans un premier temps, à faire diffuser les chaînes polymères en solution entre les feuillets d'argile puis, dans un second temps, à éliminer le solvant pour obtenir un film. Le solvant en "gonflant" la charge, i.e. en augmentant l'espace interfeuillets, peut favoriser l'exfoliation de l'argile. Cependant, ceci n'est possible que si les composants du système ternaire polymère-solvant-montmorillonite présentent une bonne affinité.

B.I.2. Dispersion d'OMMT en milieu organique

Cette affinité dépend en partie de l'organomodification qui a, non seulement un effet de compatibilisation entre le polymère et la charge, mais qui permet également de faciliter l'insertion des molécules organiques (solvant, monomère ou polymère). En effet, l'augmentation de la distance interfeuillets due à la longueur et/ou à la configuration des chaînes (e.g. chaînes alkyles) portées par les surfactants peut favoriser la solvatation des chaînes carbonées intercalées. L'excès de surfactants (Xi, 2004) ou encore le caractère pseudo-cristallin (Burgentzlé, 2004) des chaînes alkyles dans l'espace interfeuillets jouent également un rôle sur la solvatation des OMMT i.e. sur l'augmentation de la distance interfeuillets en milieu organique.

Le comportement de ces charges organomodifiées dans divers solvants organiques a été étudié au travers de différents paramètres.

Jordan (Jordan, 1949) a été le premier à démontrer que la solvatation de l'OMMT dépend de la quantité d'organomodifiants, en terme de CEC et de taux de recouvrement, présents à la surface du feuillet inorganique. La nature chimique du solvant apparaît également être un facteur important. Slabaugh et Hiltner (Slabaugh, 1968) ont proposé une interprétation du phénomène de solvatation des OMMT en deux étapes. Dans un premier temps, les molécules de solvants diffusent dans l'espace interfeuillets et recouvrent les feuillets sans pour autant augmenter *d*. Ensuite, les organomodifiants sont solvatés et les interactions de Van der Waals existant entre les surfactants sont annihilées. Il apparaît donc que les solvants les plus efficaces présentent aussi bien un fort caractère organophile compte tenu du taux d'organomodifiants (env. 20 à 30%) situés dans l'espace interfeuillets, qu'un caractère polaire en raison des interactions possibles avec la surface des feuillets inorganiques et les groupes hydroxyle présents à leurs extrémités (Burgentzlé, 2004; Connelly, 2006). Mais les principales interactions qui conditionnent la solvatation de l'OMMT dans le système ternaire sont les interactions organomodifiant-solvant. La détermination des paramètres pertinents contrôlant la solvatation des OMMT, et donc leur dispersion dans les solvants organiques, est complexe.

Ho & Glinka (Ho, 2003) ont corrélé le degré d'exfoliation de la Cloisite®15A (cf. Annexe I) aux paramètres de solubilité de Hansen (composantes dispersives et polaires, liaison H) de certains solvants. Ils ont alors démontré que la composante dispersive du solvant est le principal facteur mis en jeu pour obtenir une suspension stable d'argile. En revanche,

les composantes relatives à la polarité et aux liaisons hydrogène interviennent plutôt sur la structure de l'argile dans la solution. Par conséquent, ils ont pu en déduire les caractéristiques requises et donc identifier le solvant adéquat pour exfolier la Cloisite®15A.

Moraru (Moraru, 2001) s'est lui intéressé à l'aspect thermodynamique du phénomène mouillabilité-solvatation des OMMT. Il a établit que le degré de solvatation et de dispersion des OMMT par le solvant organique sont régis par l'énergie de cohésion entre les feuillets, l'énergie de solvatation, les forces de répulsions électrostatiques et les effets entropiques.

Par ailleurs, Burgentzlé et al. (Burgentzlé, 2004) ont démontré que pour comprendre et maîtriser les paramètres mis en jeu dans la dispersion des argiles en milieu organique, il est nécessaire d'envisager le phénomène dans une approche multi-échelle. A l'échelle nanométrique, l'augmentation de la distance interfeuillets est favorisée lorsque le solvant présente le caractère ambivalent polaire et organophile, i.e. lorsque la tension de surface du solvant est supérieure à celle de l'OMMT. Ensuite, ces résultats doivent être corrélés avec les résultats d'études rhéologiques et d'observations faites sur le gonflement de l'OMMT à l'échelle macroscopique.

Il faut également noter que d'autres études ont été menées sur la dispersion des OMMT dans des mélanges binaires de solvants organiques (Jordan, 1949; Slabaugh, 1968; Moraru, 2001; Vaia, 2003; Burgentzlé, 2004), l'un présentant le caractère polaire, l'autre le caractère fortement organophile. Dans notre cas, nous nous sommes limités à l'utilisation d'un seul solvant choisi parmi les plus communément utilisés.

B.II. Matériel et méthodes

B.II.1. Matériel

En raison des masses molaires importantes des grades de PHB dont nous disposons, et des problèmes de solubilité que cela implique, les expériences par voie "solvant" ont été effectuées sur le PHB470 fournit par Copersucar-PHB Industrial (Brésil), i.e. le PHB ayant les plus faibles masses molaires (Mw=470 000, cf. Annexe I).

Les montmorillonites commerciales testées ont été sélectionnées de façon à offrir une large gamme d'affinité polymère-argile. Il s'agit des montmorillonites de type MMT-Na (Dellite®LVF), OMMT-Bz (Dellite®43B) ou OMMT-OH (Cloisite®30B), ou encore différentes argiles de type OMMT-Alk (Cloisite®15A ou Cloisite®20A).

B.II.2. Préparation des nano-biocomposites

Comme étape préliminaire à toute dissolution, polymère et nanocharges sont préalablement séchés sous vide à 80°C pendant toute une nuit pour éliminer au maximum l'eau adsorbée.

B.II.2.1. Solubilisation du PHB470

Parmi les solvants usuels, seul le chloroforme est capable de dissoudre le PHB. Cependant, cette étape de solubilisation reste difficile, même avec des masses molaires réduites. Cela nécessite de travailler sous pression, à chaud et à des concentrations relativement faibles. La solution de PHB470 dans le chloroforme a donc été préparée dans un tube sous pression à chaud ($T_{consigne}$=60°C) et à une concentration de 1 %pds/vol.

B.II.2.2. Préparation des nano-biocomposites

Après solubilisation, la nanocharge est ajoutée à la solution de polymère dans les proportions souhaitées (3, 5 et 10 %pds de matière inorganique). Les tubes sous pression sont ensuite maintenus dans un bac à ultrasons à 50°C pendant 4h afin de favoriser le gonflement et l'exfoliation de la charge. Enfin, la solution est versée dans un cristallisoir, couvert et laissé sous hotte jusqu'à évaporation complète du solvant (~24h), c'est l'étape de "casting".

B.II.2.3. Caractérisation par DRX

Les films obtenus sont découpés et placés sur le porte-échantillon pour mesurer l'espace interfeuillets par Diffraction des Rayons X (DRX) aux petits angles (ou SAXS en anglais ; cf. Annexe II). Le balayage des angles 2θ entre 1,5 et 10° s'effectue à une vitesse de 0,03°/s. On notera $\mathbf{d_f}$ l'espace interfeuillets du nanocomposite obtenu par voie "solvant" après "casting".

B.II.3. Détermination des distances interfeuillets des montmorillonites

B.II.3.1. Protocole

Afin de déterminer la valeur référence de l'espace interfeuillets, les nanocharges testées (cf. Annexe I) sont soumises à un protocole précis. Une première série de nanocharges est séchée à l'étuve sous vide durant une nuit puis analysée par DRX. Ensuite, deux autres séries de nanocharges, traitées séparément, sont préparées. Pour cela, 1 g de nanocharges est dispersé dans 35 ml de chloroforme. Les argiles sont ensuite soumises à un traitement aux ultrasons similaire à celui effectué lors de la préparation des nanocomposites i.e. à 50°C pendant 4h, puis laissées au repos dans des cristallisoirs de façon à évaporer le solvant (env. 36h). La deuxième série est alors directement analysée en DRX, la troisième est préalablement séchée à l'étuve (80°C) sous vide de façon à éliminer le solvant résiduel.

B.II.3.2. Caractérisations par DRX

Les distances interfeuillets des montmorillonites fournies et séchées ($\mathbf{d_{sec}}$) ainsi que celles des montmorillonites traitées avant ($\mathbf{d_{US}}$) et après séchage ($\mathbf{d_{USS}}$) sont déterminées par DRX aux petits angles. Le protocole d'analyse est alors le même que celui utilisé pour les matériaux nanocomposites, à savoir on procède à un balayage en 2θ de 1,5 à 10° à une vitesse de 0,03°/s.

B.III. Résultats et discussion

B.III.1. Distances interfeuillets référence des montmorillonites.

Avant de discuter la structure des nanocomposites, il est nécessaire d'étudier les distances interfeuillets initiales des montmorillonites ($\mathbf{d_{sec}}$) mais également celles ayant subi un traitement analogue à la préparation des nanocomposites ($\mathbf{d_{US}}$ et $\mathbf{d_{USS}}$). Ainsi, cela va permettre de déterminer la valeur référence de l'espace interfeuillets qui sera comparée aux résultats obtenus sur les nano-biocomposites ($\mathbf{d_f}$).

Tout d'abord, les expériences relatives aux traitements des montmorillonites seules ont permis de distinguer deux comportements différents vis-à-vis du solvant. En effet, d'une part, la MMT-Na (LVF) et l'OMMT-OH (Cloisite®30B) sédimentent au fond du tube sous

pression en raison de leur énergie de surface. Burgentzlé et al. (Burgentzlé, 2004) ont mesuré les tensions de surface de différentes montmorillonites organomodifiées ou non (cf. Tableau 1). Si on se réfère à ces données, la MMT-Na et l'OMMT-OH présentent des tensions de surface plus élevées ($\gamma_{MMT\text{-}Na}$ =44,0± 2,0 mJ/m² -plus hydrophile- et $\gamma_{OMMT\text{-}OH}$=34,5 ± 2,0 mJ/m²) que celle du solvant (γ_{CHCl3}=27,1 mJ/m²). Ceci signifie donc que l'OMMT-OH n'est pas solvatée par le chloroforme et qu'il est donc difficile d'obtenir une suspension stable. D'autre part, les OMMT-Alk (Cloisite®15A et Cloisite®20A) et l'OMMT-Bz (Dellite®43B) forment une suspension stable d'argiles dans le chloroforme, ce qui est en accord avec les valeurs proches des énergies de surface de ces OMMT et du solvant ($\gamma_{OMMT\text{-}Alk}$=25,4 mJ/m² ; $\gamma_{OMMT\text{-}Bz}$=30,0 mJ/m² et γ_{CHCl3}=27,1 mJ/m²).

Tableau 1 : Paramètres caractéristiques des montmorillonites (Burgentzlé, 2004)

Type	Montmorillonite	Cation	d_{001} (Å)	Δw (%)[a]	$\gamma_{S/V}$ (mJ/m²)
MMT-Na	Cloisite®Na	Na^+	11,4	-	44,0 ± 2,0
OMMT-Alk	Cloisite®15A	2M2HT	33,0	43,4	25,4 ± 1,0
OMMT-Bz	Cloisite®10A	2MBHT	18,7	38,9	30,0 ± 2,0
OMMT-OH	Cloisite®30B	MT2EtOH	18,4	30,6	34,5 ± 2,0

[a] Taux de matière organique mesuré par analyse thermogravimétrique en considérant la perte de masse entre 150 et 500°C.

Tableau 2 : Comparaison des distances interfeuillets des argiles traitées (d_{US} et d_{USS}) ou non traitées (d_{sec})

Charge	**d_{sec}(Å)**	**d_{US} (Å)**	**d_{USS} (Å)**
Dellite®LVF	12,1	14,1	10,0
Cloisite®15A	31,0	25,9[a]	24,1[a]
Cloisite®20A	22,0	25,7	22,6
Dellite®43B	32,3	25,5[a]	23,5[a]
Cloisite®30B	17,7	18,3	17,8

[a] distance interfeuillets calculée à partir de la valeur 2θ du pic d_{002}

Dans le Tableau 2, les mesures des distances interfeuillets mettent en évidence l'excès de surfactants dans le cas de la Cloisite®15A et de la Cloisite®43B. En effet, nous avons vu au paragraphe A.II.2. que le surplus de surfactant participe à l'augmentation significative de la distance interfeuillets *d*. Or, dans notre cas, nous pouvons différencier la Cloisite®15A et la Dellite®43B des autres charges car leur valeur d_{sec} atteint des valeurs supérieures à 30Å. Ceci

est tout à fait en accord avec d'une part, les données de CEC ($CEC_{Cloisite®15A}$=125 meq/100g ; $CEC_{Dellite®43B}$>95 meq/100g vs. CEC≈90meq/100g pour les autres (O)MMT cf. Annexe I), et d'autre part, les taux de matière organique obtenus par analyse thermogravimétrique (cf. Annexe I - Δw%≈29% pour la Cloisite®15A et la Cloisite®43B alors que Δw%≈20% pour les autres OMMT). Ces OMMT présentent également une forte diminution de la distance interfeuillets entre d_{sec} et d_{US} (cf. Tableau 2). Ceci semble montrer que le chloroforme solvate les organomodifiants mais extrait de la région interfeuillets les molécules intercalées mais non adsorbées à la surface du feuillet inorganique. En effet, les valeurs des énergies de surface des OMMT et du solvant sont relativement proches ($\gamma_{OMMT-Alk}$=25,4mJ/m² ; $\gamma_{OMMT-Bz}$=30,0mJ/m² et γ_{CHCl3}=27,1mJ/m²) ce qui signifie qu'il y a bien solvatation des surfactants et éventuellement augmentation de la distance *d* par le chloroforme (Slabaugh, 1968; Burgentzlé, 2004). De plus, le fait que les valeurs finales des distances interfeuillets soient similaires aux autres OMMT démontre que cet excédent de surfactants n'est plus présent pour assurer un espace interfeuillets élevé. Comme il est mentionné dans le Tableau 2, il faut noter que ces valeurs sont mesurées à partir des pics d_{002} du fait de l'étalement du pic d_{001}. Cela confirme le départ des surfactants et indique qu'il se fait de façon inhomogène dans l'ensemble des espaces interfeuillets conduisant ainsi à une disparité des distances entre deux feuillets. Vaia et al. (Vaia, 2003) avaient déjà constaté ce phénomène de "rinçage" des organomodifiants en excès par le solvant sur la série des Cloisite®6A, 15A et 20A dans le toluène.

Enfin, la différence entre les valeurs des distances interfeuillets avant ($\mathbf{d_{US}}$) et après séchage ($\mathbf{d_{USS}}$) montre que cette dernière étape permet d'éliminer le solvant résiduel sans doute intercalé dans la région interfeuillets. Les distances interfeuillets de référence seront donc les valeurs $\mathbf{d_{USS}}$ correspondant aux argiles ayant subi les étapes de traitement aux ultrasons puis de séchage.

B.III.2. Structure des nanocomposites obtenus par voie solvant

Pour les mêmes raisons que celles citées au paragraphe précédent, un phénomène de sédimentation ou de suspension des argiles dans la solution de polymère est également observé pour les mêmes types de charges. Ces comportements différents vis-à-vis du solvant ont donc conduit, comme on pouvait s'y attendre, à différentes structurations de l'argile au sein de la matrice polymère.

Tout d'abord, la sédimentation des charges MMT-Na et OMMT-OH a conduit à leur agrégation dans la matrice PHB470 (cf. Figure 1). De plus, l'absence de pic de diffraction sur les spectres de DRX aux petits angles des matériaux PHB470/MMT-Na et PHB470/OMMT-OH, et ce, quelle que soit la concentration en nanocharges, conforte ce résultat (cf. Tableau 3). En effet, lors de la découpe des films pour la caractérisation par DRX, les amas de charges localisés au cœur ou en bordure du film ne sont pas englobés dans l'échantillon prélevé. Ce dernier n'est donc pas représentatif de l'échantillon et par conséquent, aucun signal correspondant à l'argile ne peut être détecté. La MMT-Na et l'OMMT-OH n'étant pas solvatées par le chloroforme, il est donc difficile d'obtenir une suspension et a fortiori une augmentation de la distance interfeuillets.

a) b)

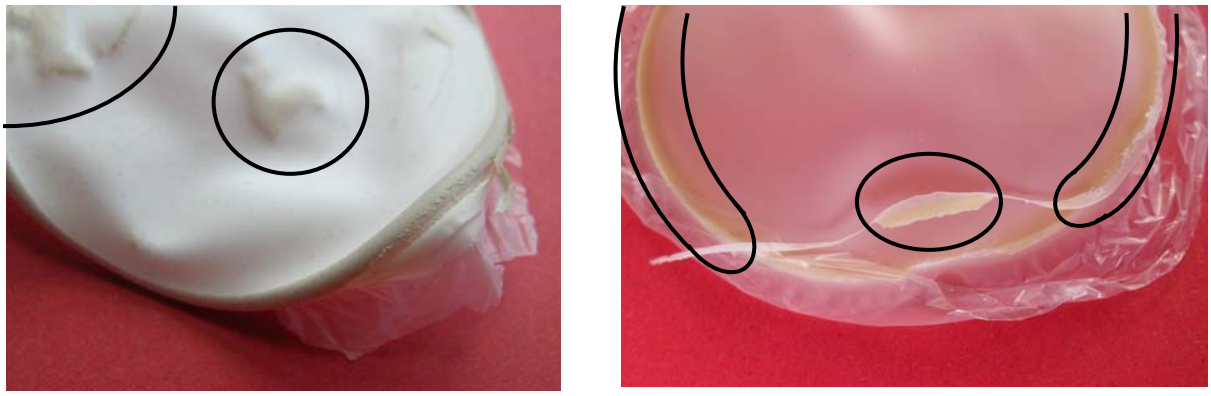

Figure 15 : Films obtenus par voie solvant avec 10%pds/vol de a) MMT-Na et b) C30B

Tableau 3 : Distance interfeuillets des nanocomposites à base de PHB470 obtenus par voie solvant

Charge	Type	d_{USS}(Å)	%wt/v	d_f (Å)
LVF	MMT-Na	10,0	3 - 5 - 10	-
Cloisite®30B	OMMT-OH	17,8		
Cloisite®15A	OMMT-Alk	24,1	3 5 10	- 24,3 24,4
Cloisite®20A	OMMT-Alk	22,6	3 5 10	- 24,2 24,1
Dellite®43B	OMMT-Bz	23,5	3 5 10	- 25,8 25,6

En revanche, dans le cas des autres argiles (OMMT-Alk et OMMT-Bz), la suspension dans la solution de polymère conduit à la bonne dispersion de ces charges dans la matrice. En effet, les diffractogrammes obtenus sur les matériaux composites correspondant mettent en évidence des pics de diffraction pour les taux de charge de 5 et 10 %pds (cf. Figure 2). La concentration de 3 %pds semble quant à elle trop faible pour pouvoir détecter le signal caractéristique de la charge.

Pour déterminer la structure des nanocomposites, i.e. connaître le degré d'intercalation, nous nous sommes intéressés à la distance interfeuillets $\mathbf{d_f}$ déduite de la caractérisation par DRX aux petits angles (cf. Tableau 3) et nous l'avons comparée à l'espace interfeuillets référence des OMMT, d_{USS}. On constate alors que les distances interfeuillets d_f sont similaires, suggérant ainsi que le polymère ne s'est pas intercalé entre les feuillets des OMMT malgré la solvatation de ces dernières par le chloroforme. On obtient ainsi des matériaux **microcomposites**.

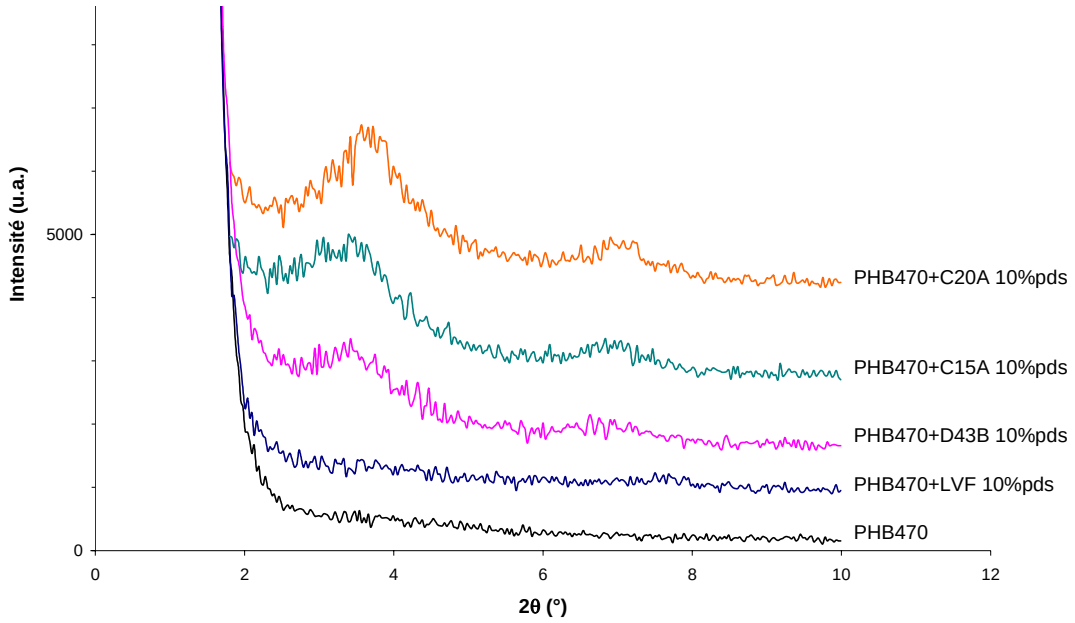

Figure 16 : SAXS des films à 10%pds de charges obtenus par voie solvant

Plusieurs travaux utilisant des systèmes similaires mais non équivalents ont montré l'intercalation de chaînes PHB et PHBV, dans des systèmes nanocomposites préparés par voie "solvant" (Chen, 2002; Lim, 2003; Chen, 2004; Wang, 2005) dans le chloroforme. Dans ces systèmes, les OMMT utilisées étaient respectivement organomodifiées par des ammoniums diméthyle(2-éthylhexyle) suif hydrogéné (Cloisite®25A, Southern Clay Products, Inc., CEC=95 g/100 g d'argile), ou de l'hexadecyltriéthylamine. Les distances interfeuillets ont

ainsi augmenté de 21,8 Å à environ 34,8 Å et de 18 Å à 24 Å respectivement, attestant de la structure intercalée et non exfoliée des matériaux nanocomposites obtenus.

Au vu de ses observations, il apparaît dans nos systèmes que la solvatation des OMMT par le chloroforme n'entraîne pas d'augmentation significative de la distance interfeuillets, soit en raison d'une relative mauvaise affinité organomodifiant-solvant, soit à cause du "rinçage" de l'excès de surfactants. Ainsi, l'insertion et la diffusion de chaînes polymères dans la région interfeuillets restent difficiles. On peut également penser que le départ d'une partie des surfactants intercalés diminue l'affinité OMMT-matrice, limitant donc l'intercalation des chaînes polymères.

En conclusion, du fait de la sédimentation de certaines charges dans le chloroforme et de la mauvaise affinité polymère/solvant/OMMT, la voie "solvant" n'apparaît pas comme étant une approche adéquate à la dispersion d'argile au sein de la matrice PHB. De plus, cette voie d'élaboration présente quelques limites induites par le choix restreint de solvants et les problèmes de solubilité qui contraignent à travailler à chaud, sous pression, à des concentrations relativement faibles, i.e. avec de grandes quantités de solvant. Tout cela ne favorise donc pas le développement de cette méthode, et ceci sans rappeler les aspects peu environnementaux de cette approche. Par conséquent, la voie "fondu" a davantage retenu notre attention.

La **publication n°2** présente l'élaboration des nano-biocomposites PHA/montmorillonite par voie "fondu", c'est-à-dire en utilisant les moyens classiques de mise en œuvre des polymères. Pour cette étude, le poly(3-hydroxybutyrate) (PHB) et le poly(3-hydroxybutyrate-co-3-hydroxyvalérate) (PHBV) contenant 4 % d'unités hydroxyvalérate (HV) ont chacun été mélangé à des montmorillonites non modifiées (Dellite®HPS et Cloisite®Na) et organomodifiées. Nous nous sommes particulièrement intéressés à un type d'OMMT, à savoir la Cloisite®30B qui est une montmorillonite modifiée par des ammoniums quaternaires comportant des groupes hydroxyles (cf. Annexe I). La structure de la montmorillonite a été déterminée par diffraction des rayons X aux petits angles comme dans le cas de la voie "solvant". Ces résultats ont été complétés par des observations au microscope électronique à balayage (MET). Nous avons également appliqué à nos systèmes une nouvelle méthode récemment mise au point utilisant la résonance magnétique nucléaire (RMN) à l'état

solide permettant de quantifier les degrés d'intercalation et de dispersion de l'argile au sein d'une matrice polymère. Ces résultats ont ensuite été corrélés aux phénomènes de cristallisation/fusion observés mais également aux comportements mécaniques et thermiques afin de mettre en évidence les relations "procédé-structure-propriétés" de ces matériaux.

C. Elaboration des nano-biocomposites : la voie "fondu"

Publication n°2.

"Structure and properties of PHA/clay nano-biocomposites obtained by melt intercalation"

Perrine Bordes[1], Eric Pollet[1], Serge Bourbigot[2], Luc Avérous[1]*

Macromolecular Chemistry and Physics, submitted.

A. Abstract

Polyhydroxyalkanoates (PHA)-based nano-biocomposites were prepared by the melt intercalation route. Two main PHAs, the poly(3-hydroxybutyrate) (PHB) homopolymer and the poly(3-hydroxybutyrate-co-3-hydroxyvalerate) (PHBV) copolyester containing 4% of HV units, were studied. Structural characterizations were conducted by advanced techniques like SAXS and TEM, but also by a recent method allowing the quantification of the degrees of clay intercalation and dispersion using solid-state NMR spectroscopy. Well intercalated small tactoids (3-10 layers) more or less homogeneously dispersed into the polymer were obtained when relatively good PHA-clay affinity existed, i.e. with the Cloisite®30B organo-modified montmorillonite (OMMT). In the case of non-modified montmorillonite, microcomposites have been evidenced. Crystallization behavior, mechanical and thermal properties were determined and correlated to the materials structure to demonstrate the "process-structure-properties" relationship.

[1]LIPHT-ECPM, UMR 7165, Université Louis Pasteur, 25 rue Becquerel, 67087 Strasbourg Cedex 2, France

[2]PERF LSPES UMR 8008, Ecole Nationale Supérieure de Chimie de Lille, BP 90108, 59652 Villeneuve d'Ascq Cedex

Keywords: polyhydroxyalkanoates; nanocomposites; structure-process-properties relationship.

B. Introduction

Biopolymers are a growing research issue since they appear as a solution to the emerging environmental concern that have risen in the recent years, representing an interesting alternative to synthetic polymers for short-life range applications.

Polyhydroxyalkanoates (PHAs) are biopolyesters produced from renewable resources (Doi, 1990; Madison, 1999; Valentin, 1999; Poirier, 2002; Lenz, 2005), mainly by bacterial fermentation. The bacteria store the biopolymer as an energy or carbon resource. The main PHAs are the polyhydroxybutyrate (PHB) and the copolymer poly(hydroxybutyrate-*co*-hydroxyvalerate) (PHBV) which have particular interesting properties such as biodegradability and biocompatibility. The physical properties of PHB are often compared to isotactic polypropylene ones since they have similar melting temperature and crystallinity (Doi, 1990). Nevertheless, they are not well competitive compared to conventional polymers since they present high crystallinity, brittleness and poor thermal stability just above their melting temperature (Grassie, 1984a, 1984b, 1984c). Therefore, to improve their properties, it is possible to either modify them or associate them to another material. However, chemical modification can affect the material biodegradability. Furthermore, many investigations were conducted on nanocomposites based either on synthetic polymers (Sinha Ray, 2003) or biopolymers (Pandey, 2005; Bordes, 2008a) (nano-biocomposites) and reported successful results like reinforced mechanical properties, better thermal and barrier properties with only a small amount of nano-sized filler. The most commonly used nanofiller in such materials is the montmorillonite (MMT), a layered silicate clay. MMT presents a high aspect ratio, which can lead to a high interface area with the matrix, as well as the possibility to be organo-modified by cationic exchange, resulting in an organo-modified MMT (OMMT). Both characteristics contribute to improve the polymer-clay affinity, and thus, the interface properties.

The aim of this paper is to analyze the nano-structuration and the structure-properties relationships of nano-biocomposites elaborated by melt intercalation method and based on different PHAs, namely PHB and PHBV. Since final properties are strongly dependent on the structure, this paper is firstly dedicated to the determination of clay organization into the matrix using advanced characterization techniques such as X-Ray diffraction (XRD) and

transmission electronic microscopy (TEM). Besides, a recent method based on solid-state NMR spectroscopy has been carried out. Secondly, crystallization behavior as well as the thermal, mechanical properties were determined and correlated to the structure to establish the structure-properties relationships.

C. Experimental Section

C.I. Materials

Two types of polyhydroxyalkanoates, produced by bacterial fermentation, were kindly supplied by Biocycle PHB Industrial S/A, Brazil. %HV units was calculated from nuclear magnetic resonance (NMR) spectra in $CDCl_3$. The weight average molecular weight (M_w) and the polydispersity index (PDI) have been determined by size exclusion chromatography (SEC) (see Table 1) and the melting point (Tm) by differential scanning calorimetry (DSC).

Regarding the nanofillers, two kinds of montmorillonite were used: (i) non-modified montmorillonite MMT-Na, namely Dellite®HPS (HPS) from Laviosa Chimica Mineraria S.p.A. (Italy), or Cloisite®Na (CNa) from Southern Clay Products (USA), (ii) montmorillonite organo-modified by methyl tallow bis-2-hydroxyethyl quaternary ammonium produced by Southern Clay Products, Inc. (Cloisite®30B, noted C30B). The corresponding organomodifier, the oleylbis(2-hydroxyethyl)methylammonium chloride (S-EtOH) from Akzo Nobel, was kindly supplied by Brenntag Specialities.

Table 1: Characteristics of the PHB and PHBV samples

Polymer	Reference	%HV	Mw	PDI	d	Tm (°C)
PHB	PHB	0	650,000	2	1.22	175
PHBV	PHBV4	4	930,000	2	1.22	173

C.II. Samples preparation

Before processing, polymer and clays were dried overnight at 80°C under vacuum. PHB- and PHBV-based nano-biocomposites containing 1, 3 and 5 wt% of inorganic matter were prepared as followed. Since the different compounds are powders, they were mixed manually before introduction in an internal mixer Haake Rheocord 9000. They were processed at T_p=170°C and 160°C for PHB- and PHBV4-based nanocomposites, respectively.

The initial roller rotors speed was adjusted to 100 rpm to introduce rapidly the whole volume of powder. As soon as the polymer-clay powder was introduced into the chamber, the speed is reduced to 50 rpm and the mixing is stopped after 5 min. Such protocol was settled as a compromise between high shear rate required for clay delamination and high viscous dissipation which could enhance PHA degradation. After mixing, the mechanical energy (E_m) and the final torque value (TQ_5) were recorded and the materials were further processed (injection moulding, compression,) to obtain adequate samples for the different characterizations.

Samples based on C30B organomodifier were also prepared. About 0.5 wt% of S-EtOH was first dispersed into diethyl ether (SDS Carlo Erba) and mixed to the PHA powder. Then, after solvent evaporation, the mixture was dried and processed according to the protocol mentioned above.

Neat polymers were also processed under same conditions and were considered as references.

C.III. Characterizations

C.III.1. Materials structure

Small Angle X-Ray Scattering (SAXS) data were recorded on a Siemens D5000 (Germany) diffractometer using Cu (Kα) radiation (1.5406 Å) at room temperature in the range of 2θ=1.5-10° at 0.1°/min. Wide Angle X-Ray Scattering (WAXS) patterns were obtained on the same apparatus with a scanning range of 2θ=4-60° at 0.6°/min.

Bright-field Transmission Electron Microscopy (TEM) images of nanocomposites were obtained at 200 kV under low dose conditions with a FEI Tecnai G2 20 electron microscope, using a Gatan CCD camera. The materials were sampled by taking several images (at least 20 images) of various magnifications over 2-3 sections per grid to ensure that analysis was based on a representative sample area.

Solid-state NMR spectroscopy was recently applied to nanocomposite materials to quantify the degree of delamination and nanodispersion of clay into the bulk polymer. This approach was fully described in a previous article (Bourbigot, 2003). The method is based on the direct influence of paramagnetic Fe^{3+} located in the clay inorganic layers on polymer protons present within ~1 nm from clay surfaces. The Fe^{3+} create 'relaxation sources' which, via spin diffusion, significantly affect the overall relaxation time T_1^H of polymer protons. The

better the clay dispersion, i.e., the larger the interface area, the shorter the average relaxation time. Therefore, T_1^H appears as an indicator of the clay nanodispersion, which can be quantified thanks to spin diffusion modelling. Eventually, the NMR measurements lead to the determination of two coefficients, f and ε, calculated from experimental relaxation times T_1^H through a computational model already validated on other nanocomposite systems (VanderHart, 2001a, 2001b, 2001c; Bourbigot, 2003; Bourbigot, 2004). f is deduced from short relaxation time (T_{1s}^H) corresponding to the spin influence at the clay platelet-polymer interface indicating the degree of intercalation/exfoliation, f=1 corresponding to a complete exfoliation. On the contrary, ε is obtained from long relaxation time (T_{1l}^H) and represents the dispersion quality (ε=100% when the dispersion is perfectly homogeneous). Solid-state NMR measurements were performed on small chips samples using Bruker Avance 400 spectrometer at the protons Larmor frequency of 400 MHz. Before analysis, the samples placed in 5 mm glass tubes were deoxygenated by heating them at 50°C under vacuum for 2h and then the tubes were sealed. T_1^H recovery curves were then measured using the saturation-recovery sequence with direct proton observation. As a semi empirical approach, these saturation-recovery curves were fitted to a two-exponential equation according to:

$$M(t) = M_{0s}.(1 - e^{-t/T_{1s}^H}) + M_{0l}.(1 - e^{-t/T_{1l}^H})$$

where M(t) is the magnetization at time t, M_{0s} and M_{0l} are the magnetizations of the short and long components, respectively, and T_{1s}^H and T_{1l}^H are the proton longitudinal relaxation times of the short and long components, respectively. The accuracy of the relaxation time measurements is lower than 2%. This characterization technique requires considering neat PHA prepared in the same conditions as a reference. PHA with non-modified montmorillonite stemming from the same clay source as Cloisite®30B, i.e. Cloisite®Na, can also be analyzed to compare the impact of the clay type, and thus the affinity, on the PHA-based nanocomposites structure.

C.III.2. Material properties

Size Exclusion Chromatography (SEC) measurements were performed using a Shimadzu apparatus equipped with a RID-10A refractive index detector and a SPD-M10A UV detector. The columns used were PLGel Mixed-B 10µm. The calibration was realized with PS standard from 580 to 1,650,000 g/mol. Chloroform (puriss p.a. Riedel-de Haën) was the mobile phase and the analyses were carried out at 25°C with a solvent flow rate of

0.8 ml/min. The SEC measurements were performed on the supernatants of nanocomposite samples dissolved in chloroform and centrifuged to sediment the layered silicates.

Differential Scanning Calorimetry measurements were carried out on DSC 2910 (TA Instruments) under nitrogen flow. The samples (5-10 mg placed in an aluminium pan) were heated up to 200°C at 10°C/min and were maintained for 1 min at this temperature. Eventually, samples were cooled down to -50°C at 10°C/min and heated up again to 200°C at 10°C/min. The melting temperatures (T_m), the melting and the crystallization enthalpies (ΔH_m and ΔH_c respectively) were determined. The enthalpy values were corrected depending on the polymer content and the crystallinity χ was calculated using the ΔH_m of the 100% crystalline PHB (146 J/g according to Biocycle). Same value was considered to calculate the PHBV4 crystallinity since various values are found in the literature due to the HV content dependence.

To better understand the crystallization stage, PHA-based nanocomposites samples were heated at 190°C for 1 min and observed during natural cooling with Polarized Optical Microscope (POM) equipped with a AVT Pike F-032B fiber S800 camera and a Nikon Coolpix 4300 digital camera.

Thermal stability was studied by thermogravimetric analyses (TGA). The analyses were conducted under nitrogen flow using a Hi-Res TGA 2950 apparatus from TA Instruments. The samples (10-20 mg placed in an aluminium pan) were heated up to 600°C at 20°C/min.

Tensile tests were carried out on five replicates of dumbbell specimens according to ISO 527-2-5A. Those samples were obtained by injection molding using Haake Minijet, the temperature of the cylinder and the mold were respectively 190°C and 60°C. The measurements were performed on a universal testing machine (MTS 2/M) at 30°C at a crosshead speed of 5 mm/min.

D. Results and discussion

D.I. Structure of PHA-based nanocomposites

Nano-structure of nanocomposite materials was characterized by two complementary techniques, SAXS and TEM. In our study, the structural characterization was completed by solid state NMR measurements since a recent method has been developed and applied to

nanocomposites (VanderHart, 2001a, 2001b, 2001c; Bourbigot, 2003; Bourbigot, 2004). TEM images were used to confirm the SAXS and solid-state NMR quantitative results.

SAXS spectra and the calculated interlayer spaces of the materials obtained are shown in Figure 1 and Table 2.

a) b)

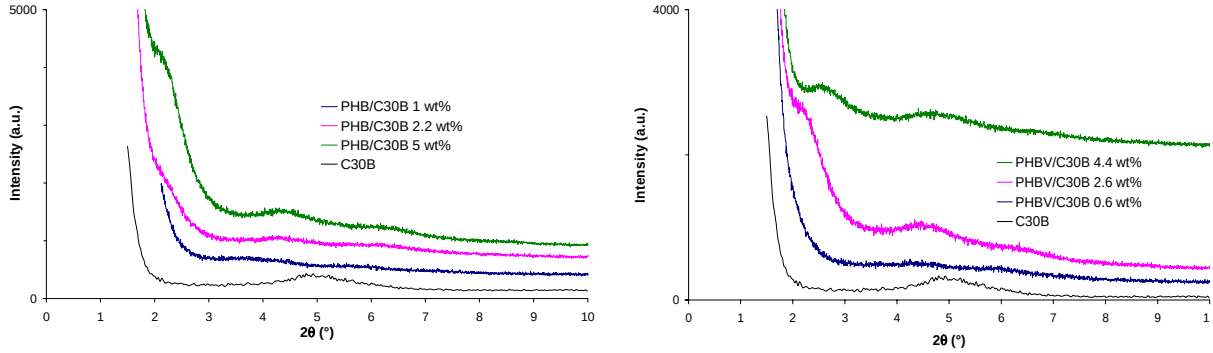

Figure 1: SAXS patterns of a) PHB/C30B and b) PHBV4/C30B at 1, 3 and 5 wt% of inorganic content

Table 2 : Interlayer distances (d_{001}) of PHA-based nanocomposites obtained from SAXS

Polymer	∅		PHB				PHBV4			
Nanofiller	HPS	C30B	HPS	C30B			HPS	C30B		
wt%[a] inorganic	-	-	2.7	1.0	2.2	5.0	2.8	0.6	2.6	4.4
d_{001} (Å)[b]	9.9	17.7	-	46.8	40.4	39.9	-	39.2	38.5	36.6

[a] content of inorganic matter determined from the weight loss of TG curves at 600°C.
[b] for nanocomposites materials, d_{001} was determined from the d_{002} peak

SAXS patterns of PHB and PHBV4 with ~3 wt% of non-modified montmorillonite (PHB/HPS and PHBV4/HPS) do not show any diffraction peak whereas HPS patterns exhibits a peak at 2θ=7.3°, corresponding to d_{001}=9.9 Å. Taking into account the hydrophilic character of the HPS clay, the absence of diffraction peak could be explained by the poor dispersion quality and the low HPS content, rather than exfoliation. Similar observation was reported by Pluta et al. (Pluta, 2002) on PLA/CNa microcomposites.

On the contrary, diffraction peaks are detected for PHB/C30B and PHBV4/C30B systems (see Figure 1 and Table 2). These peaks appear at lower angles compared to C30B suggesting intercalated structures. The interlayer distances are increased from 17.7 Å for C30B to 46.8, 40.4 and 39.9 Å for PHB/C30B containing respectively 1.0, 2.2 and 5.0 wt% of inorganic content. Same trends are obtained for PHBV/C30B nanocomposites although interlayer distances reached were lower compared to PHB/C30B ones. d_{001} equals 39.2, 38.5

and 36.6 Å for PHBV4-based systems with respectively 0.6, 2.6 and 4.4 wt% of inorganic content. It has to be noted that interlayer spacing values of the nano-biocomposites systems were calculated from the d_{002} peaks, and correlated with d_{003} one when possible, since the great shift of the d_{001} diffraction peak to lower angles (2θ=~2°) caused poor peak definition. The great d_{001} increase, particularly for PHB/C30B with 1 wt% of clay content (d_{001}=46.8 Å), and the weak intensity of diffraction peaks (see Figure 1) both suggested important polymer intercalation with probably exfoliated clay domains, or at least small tactoids. Furthermore, the peak intensity of the intercalated clay gradually increases with organoclay content indicating that the number and the size of tactoids slightly increase.

These results were complemented by a recent method using solid-state NMR which allows to obtain quantitative information about the nanocomposite structure, i.e. the degree f and the quality ε of clay dispersion. As far as we know, it is the first time that such a technique is reported on bacterial polyester-based systems. The results of solid-state NMR measurements are reported in Table 3. First, the non-modified montmorillonite (CNa) is still aggregated in PHA matrix since the f coefficients equal 0.1 in both cases (PHB/CNa and PHBV4/CNa). Nevertheless, these large tactoids are rather well dispersed showing ε coefficients equal to 50 and 60% for PHB/CNa and PHBV4/CNa, respectively. Regarding PHBV4-based samples, we can note that the relaxation times decrease with the incorporation of clay, particularly with the C30B increasing content. The f coefficient of PHBV4/C30B with 1 wt% of clay indicates the presence of very small tactoids (f=0.7) with a relatively good nanodispersion (ε=45%). However, at higher C30B content, the f and ε coefficients decrease, suggesting bigger tactoids and poorer nanodispersion (20<ε<30%). For the PHB-based systems, the data analysis is more complex since the relaxation times of PHB/C30B ($T_1^H{}_{PHB/C30B}$ = 2.46 and 2.43 s, for PHB/C30B with 1.0 and 2.2 wt%, respectively) increase compared to the neat PHB reference ($T_1^H{}_{PHB}$=2.42 s); this will be further discussed later. Therefore, the calculation of the ε parameter becomes obsolete but it still possible to reason about the degree of clay dispersion. It appears that the calculated f coefficients are lower than 0.5 indicating slightly delaminated tactoids.

TEM characterization on PHB-based materials are on agreement with the results obtained from solid-state NMR, i.e., CNa is not intercalated showing well stacked tactoids of hundreds of platelets (see Figure 2a), while small tactoids of about 3 to 10 platelets are present in the PHB/C30B nanocomposites (see Figure 2b as an example). This emphasizes the higher compatibility of C30B with PHA, compared to CNa.

Table 3: Solid-state NMR results for PHB- and PHBV4-based materials and their structure determined from XRD, TEM and solid-state NMR.

	wt% clay	T_1^H (s)	f	ε (%)	Nanocomposite structure
PHB	-	2.42	-	-	-
PHB/CNa	2.7	2.39	0.1	50	Microcomposite
PHB/C30B	1.0	2.46	0.27	-	Small and well intercalated tactoids (3/10 layers)
	2.2	2.43	0.4	-	Small and well intercalated tactoids (3/10 layers)
	5.0	2.34	0.3	-	Small and well intercalated tactoids (3/10 layers)
PHBV4	-	2.50	-	-	-
PHBV4/CNa	2.8	2.35	0.1	60	Microcomposite
PHBV4/C30B	0.6	2.32	0.7	42	Small and well intercalated tactoids with good nanodispersion
	2.6	2.19	0.45	27	Small intercalated tactoids with poor nanodispersion
	4.4	2.13	0.43	21	Small intercalated tactoids with poor nanodispersion

a) b)

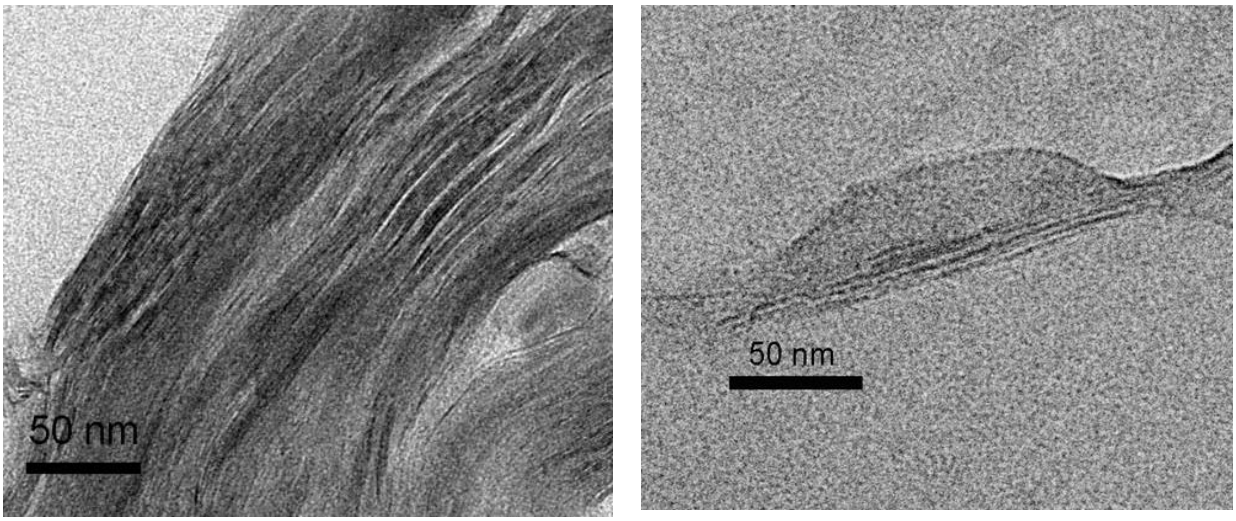

Figure 2: TEM images of a) PHB/CNa with 2.9 wt% of inorganic content, and b) PHB/C30B with 2.2 wt% of inorganic content

Since the mobility, and thus, the chains relaxation time can be affected by the crystallinity and the polymer molecular weight, these two parameters were measured to determine whether if their variations, depending on the nature and the clay content could be significant. On one hand, the crystallinity χ_1 determined from the melting enthalpy during the

first DSC scan is slightly lowered in the case of nanocomposites, regardless the clay nature (see Table 4). However, all values are still in the same range compared to neat PHA since χ_1 is about 48-55% and 40-52% for PHB-based and PHBV4-based systems, respectively. On the other hand, the weight average molecular weights are considerably reduced with C30B (see Table 4). When C30B content is about 5 wt%, the Mw decreases by 40% and 60% for the PHB- and PHBV4-based systems, respectively, compared to the corresponding processed polymer. It is well-known that PHA are highly temperature sensitive degrading according to a random chain scission process, even just above their melting temperature (Grassie, 1984a, 1984b, 1984c). But in our case, it appears that the C30B organomodifier (S-EtOH), and even the inorganic montmorillonite layer, i.e. the non-modified montmorillonite CNa, enhance PHA degradation. The Mw of PHA/CNa and PHA/S-EtOH have decreased by 20% and 32% with CNa and S-EtOH, respectively, compared to the corresponding processed polymer. Although, the effect of non-modified layered silicates has already been reported and explained by the presence of Al Lewis acid sites in the inorganic layers (Xie, 2001; Pandey, 2005), the organomodifier influence on PHA degradation had not been investigated till recently (Hablot 2007; Bordes, 2008b).

If both PHA are compared, it can be noticed that the degree of degradation was higher for PHBV4-based systems. However, the final molecular weights of PHBV4-based samples after processing are higher than the PHB ones since the initial Mw was higher than the PHB one (Mw_{PHBV4}=930,000 and Mw_{PHB}=650,000 - see Table 1). Moreover, the calculated mechanical energy (E_m) supplied to the PHBV4-based systems as well as the final torque (TQ_5) were higher suggesting higher viscosities at the processing temperature, and thus, higher shear rates. As high shear rates favour the delamination and the dispersion of clay into the matrix, it could explain the better structural results obtained from solid-state NMR compared to PHB-based nano-biocomposites.

To conclude, microcomposites are obtained with non-modified montmorillonite whereas a nanostructure is reached with small amounts (1-5 wt%) of C30B due to higher polymer-clay affinity. All the nanocomposites are well-intercalated as demonstrated by XRD characterization, while the nanodispersion was poor for PHB/C30B systems, and quite good for PHBV4/C30B samples. These particular structurations are explained by the higher viscosity of PHBV4-based systems which leads to better clay delamination. Eventually, the discrepancy of solid-state NMR results about PHB/C30B samples could be attributed to the degradation phenomenon that occurs during processing and that could affect the polymer

relaxation time. Then, concerning NMR results and discussion, we cannot compared PHB/C30B and neat PHB samples.

Table 4: SEC results, crystallinity (χ_1) and processing characteristics (Em -mechanical energy- and TQ_5 - final torque value) of PHB- and PHBV4-based systems.

System	PHB (T_p=170°C)						PHBV4 (T_p=160°C)					
	∅	S-EtOH	CNa	C30B			∅	S-EtOH	CNa	C30B		
%wt clay	-	-	2.9	1.0	2.2	5.0	-	-	2.3	0.6	2.6	4.4
$Mw.10^{-3}$	320	217	258	297	209	194	542	364	418	437	324	220
PDI	2.1	2.1	2.0	2.0	2.0	2.2	2.2	2.1	2.2	2.1	2.3	2.4
χ_1 (%)[a]	55	-	48	51	49	53	52	-	46	40	43	41
E_m (kJ/kg)	499	430	470	479	465	374	597	506	514	562	463	423
TQ_5 (N.m)	6.5	3.2	3.6	5.3	3.6	2.7	10.7	7.1	9.1	10.2	6.2	3.8

[a] χ_1 calculated from the ratio of experimental melting enthalpy measured on the first scan (not reported here) and $\Delta Hm_{100\%\ crystalline}$=146 J/g for PHB and PHBV4

D.II. Nanocomposites properties

The clay dispersion quality plays a key role in the degree of enhancement of the matrix properties. Therefore, the crystallization behaviour as well as the mechanical and thermal properties of the PHA/clay systems were determined and correlated to their structure.

D.II.1. Crystallization

WAXS spectra (not shown here) reveal no change in the crystalline structure of polyhydroxyalkanoates regardless the nature and the content of clay. This result indicates that addition of clay do not significantly modify the crystalline phase.

DSC and POM measurements were carried out in order to study the influence of clays on the non-isothermal crystallization kinetics and the resulting crystallinity of both PHB and PHBV4. The characteristic temperatures and the different enthalpies were determined from DSC (see Figure 3 and Table 5). The latter were corrected from the filler dilution effect.

The thermal behaviours of PHB with and without non-modified montmorillonite are similar since the crystallization (Tc_c and Tc_h) and melting temperatures (Tm_1 and Tm_2) are comparable. Nevertheless, the crystallization during cooling starts earlier and the corresponding enthalpy increased while the cold crystallization is considerably reduced, suggesting that the clay enhances the crystallization. In the case of PHA/C30B, the increase of the crystallization temperature (Tc_c) and enthalpy (ΔHc_c) during the cooling are largely higher

and no more cold crystallization is observed. For example, the crystallization temperature during cooling are about 70°C for neat PHB and PHB/HPS while it reaches more than 90°C

A

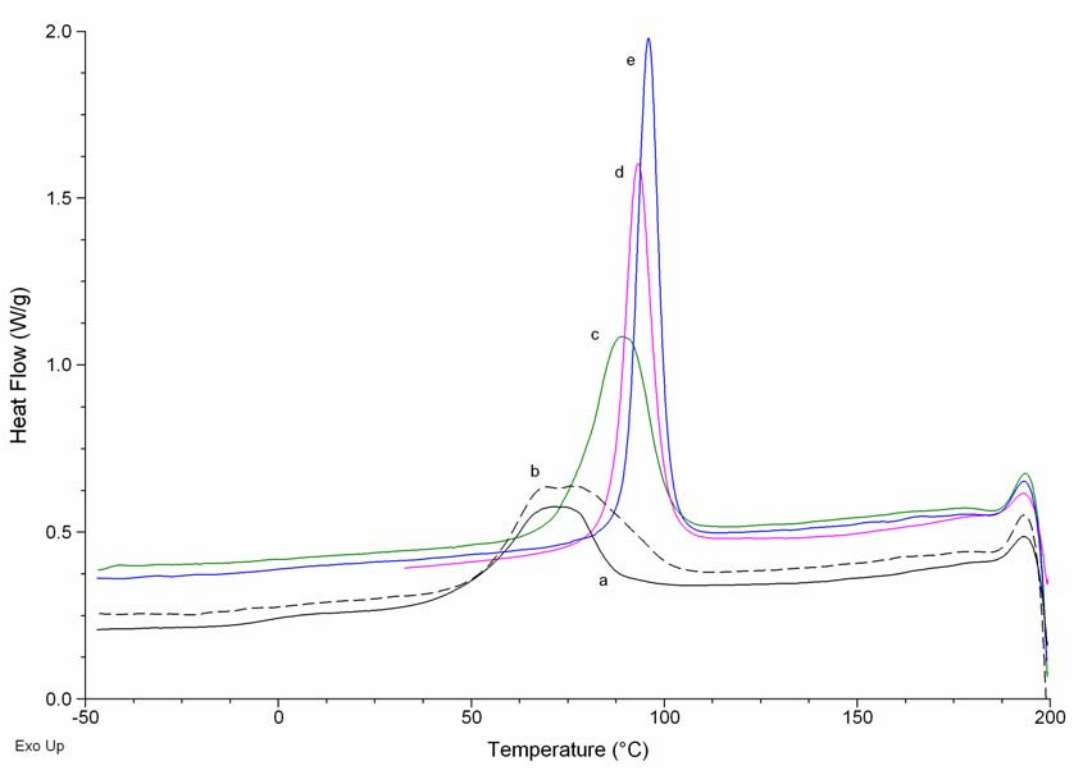

B

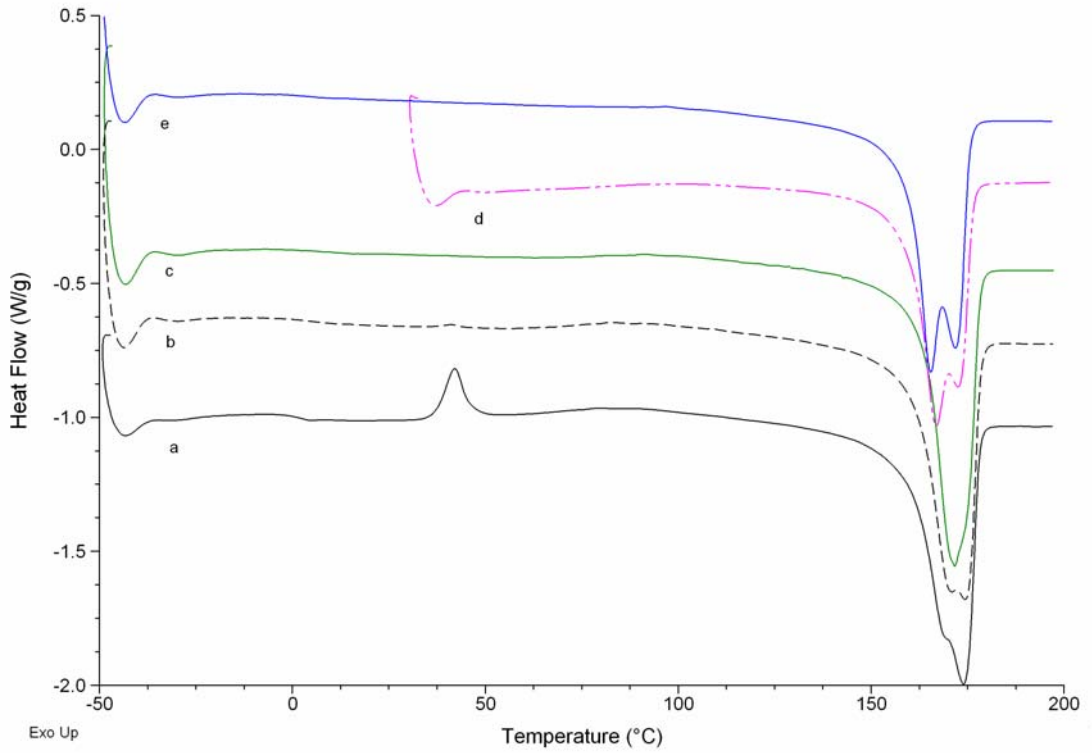

Figure 3: (A) DSC cooling and (B) second heating scans for a) PHB, b) PHB/HPS 2.7 wt%, c) PHB/C30B 1 wt%, d) PHB/C30B 2.2 wt% and e) PHB/C30B 5 wt%.

Table 5: DSC data of PHB- and PHBV4-based nanocomposites

System	%wt clay	Tg (°C)	Tm_1 [a] (°C)	Tm_2 [a] (°C)	χ_2 [b] (%)	Tc_c (°C)	ΔHc_c (J/g)	Tc_h (°C)	ΔHc_h (J/g)
PHB	-	1.5	169*	174	62	71	50	42	6.7
PHB/HPS	2.7	4	171	174	60	73	57	41	0.2
PHB/C30B	1.0	6	171		59	89	65	-	-
	2.2	3	167	173	50	93	63	-	-
	5.0	3	165	172	55	96	63	-	-
PHBV4	-	3	161*	172	52	61	28	51	11
PHBV4/HPS	2.8	4	159*	173	47	62	40	55	17
PHBV4/C30B	0.6	5	163	173	43	75	48	43	0.1
	2.6	5	161	171	49	91	59	72	0.1
	4.4	7	158	170	45	92	59	-	-

[a] Tm_1, Tm_2 determined at the second scan

[b] χ_2 calculated from the ratio of experimental melting enthalpy measured on the second scan (not reported here) and $\Delta Hm_{PHB\ 100\%\ crystalline}$=146 J/g for PHB

* melting peak shoulder

for PHB/C30B. The crystallization enthalpy ΔHc_c increases compared to neat PHB or PHB/HPS and even reaches a maximal value (ΔHc_c=63-65 J/g) since ΔHc_c was constant regardless the C30B content. This crystallization behaviour can be attributed to the nucleating effect of clay which is much more pronounced in the case of C30B. This is linked to the higher degree of C30B dispersion, compared to the non-modified montmorillonite. This phenomenon is on agreement with previous reported studies on addition of nucleating agents to PHBV (Liu, 2002) or on other nanocomposites (Choi, 2003; Nam, 2003; Di Maio, 2004; Chivrac, 2007). Regarding the crystallization kinetics during the cooling scan, the crystallization time (tc_c) was reduced to 5.5, 3.6 and 3.2 min with 1, 2.2 and 5 wt% of clay respectively, compared to the neat PHB one (11.8 min). Therefore, the higher the C30B content, the faster the crystallization. Moreover, if both PHB/HPS and PHB/C30B with similar inorganic content are considered, the crystallization rate is also enhanced by the clay dispersion (tc_c=6.6 min for PHB/HPS with 2.7 wt% of clay).

In other words, the nucleation step and the overall crystallization rate are greatly enhanced by the clay. Moreover, the enhanced and faster nucleation step leads to slightly smaller spherulites with narrow size distribution, as controlled by POM observations (see Figure 4). For neat PHB, the spherulites diameter varies from 8 to 110 µm. For nanocomposites, it ranges respectively from 60 to 300 µm and from 110 to 200 µm for the

PHB/C30B with 1 wt% and 2.2 wt% of clay. On the contrary, with 5 wt% of clay, only one population of crystallites is observed, displaying a diameter of ca. 130 µm.

Another noteworthy phenomenon, i.e. the double melting endotherms, appearing during melting has to be explained. This behavior can surely be attributed to the well-known recrystallization phenomenon (Renstad, 1997; Fujita, 2005; Hsu, 2007) rather than a consequence of the existence of bimodal size of crystallite or different types of crystallization as described by Wang et al. in PHBV/OMMT systems (Wang, 2005). Firstly, for PHB/C30B with 5 wt% of clay, the crystallite size is homogeneous (∅ 42 nm - see Figure 4d) but the DSC curves still display two well defined melting peaks. Secondly, the melting temperature Tm_2 is independent of the clay content due to the melting of the reorganized crystals during heating (Liu, 2002). Furthermore, it is worth pointing out the change in the ratio of the melting peaks intensities with the clay content. Tm_1 peak intensity becomes preponderant in comparison with the one corresponding to the second melting peak while the clay content increases. These trends can be explained by the presence of clay platelets that hinder the recrystallization phenomenon, leading to less recrystallized crystals during melting and thus to the decreasing intensity of the second melting peak with the increasing clay content. Such phenomenon of clay platelets hindering crystal growth while enhancing nucleation step has already been observed in other nano-biocomposite systems (Di Maio, 2004; Chivrac, 2007).

Clay platelets and a fast crystallization under cooling may induce less perfect crystals leading to lower melting temperatures (Tm_1) with increasing clay content, as reported in Table 5.

Eventually, glass transition temperature (Tg) does not seem affected by the presence of clay. It has also to be noticed that crystallinity (χ_2), calculated from the melting enthalpies (ΔHm) during second scan, and total crystallization enthalpies ($\Delta Hc=\Delta Hc_c+\Delta Hc_h$) do not surprisingly follow the same trends. This could be explained by the lack of reliability on ΔHm_2 values since degradation, superposed to melting phenomenon, may occur.

The crystallization and melting behaviour of PHBV4-based materials can also be interpreted as described above for PHB-based systems since similar trends from DSC and POM are shown.

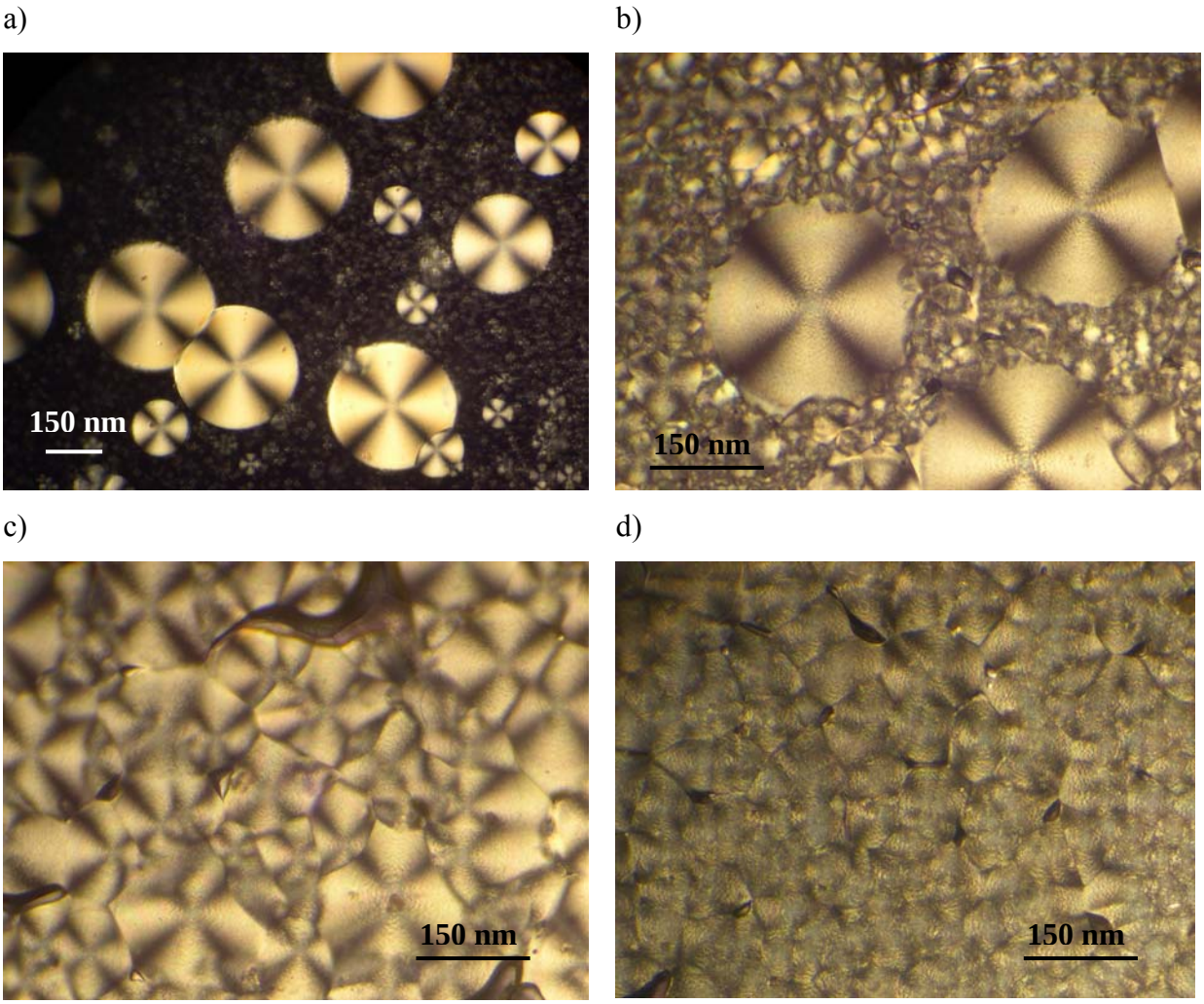

Figure 4: POM photographs of a) neat PHB, b) PHB/C30B 1 wt%, c) PHB/C30B 2.2 wt% and d) PHB/C30B 5 wt%

In conclusion, the crystallization and melting behaviour of PHA-based nanocomposites is quite difficult to analyze since several superposed phenomena can occur. It is certain that addition of clay enhance the nucleation step leading to faster polymer crystallization and smaller spherulites displaying monomodal size distribution. Nevertheless, the presence of these clay platelets seems to induce crystal defects leading to lower melting temperatures. However, the melting behaviour is more complex since double melting endotherms are observed. This is attributed to the recrystallization phenomenon which is hindered with the increasing clay content. Unfortunately, the resulting crystallinity cannot be discussed since significant degradation may occur during the second scan melting, and thus, may overestimate the melting enthalpies values.

D.II.2. Mechanical properties

Regarding the tensile properties, the Young's modulus globally shows a linear increase with C30B content, with 14 and 17% improvements for PHB/C30B and PHBV4/C30B with 5 wt% of clay, respectively. Nevertheless, this enhancement was at the expense of the elongation at break which first increased with the addition of about 1 wt% of clay (+21 and +85% for PHB- and PHBV-based nanocomposites, compared to the neat corresponding polymer), but then decreased with increasing clay content. The material becomes thus more brittle at high clay contents. Considering the tensile strength, it was almost constant with C30B regardless the clay content, reaching an increase of about +15% and +30% for PHB/C30B and PHBV4/C30, respectively. The tensile strength of the PHBV4/C30B containing only 0.6 wt% of inorganic matter is not as high as expected probably due to the low clay content. More generally, the enhancement of the tensile properties of PHA/C30B at low clay content (<3 wt%) can be attributed to a good compatibility between the PHA and the C30B clay that leads to intercalated structures with small tactoids dispersed in the polymer matrix. At higher clay content, the addition of clay is no more a benefit since the clay tends to form bigger tactoids with poorer nanodispersion. Consequently, higher increments were obtained in the case of PHBV4/C30B nanocomposites with low clay content due to better delaminated and nanodispersed clay as demonstrated by structural characterizations, particularly from solid-state NMR results.

Table 6: Tensile tests results of PHB- and PHBV4-based nanocomposites (number in brackets indicated the difference in % between the sample considered and the neat polymer values)

System	%wt clay	E (MPa)	Tensile strength (MPa)	Elongation at break (%)
PHB	-	1884	24	1.56
PHB/C30B	1.0	1904 (1)	28 (16.3)	1.98 (21)
	2.1	1981 (5)	27 (11.3)	1.56 (0)
	5.0	2201 (14)	28 (16.6)	1.47 (-6)
PHBV4	-	1689	23	1.6
PHBV4/C30B	0.6	1622 (-4)	24 (6)	2.95 (85)
	2.6	1824 (8)	30 (34)	2.51 (57)
	4.4	1971 (17)	29 (30)	1.97 (23)

D.II.3. Thermal stability

Thermogrametric analyses were performed on the PHB- and PHBV4-based materials to determine the influence of the addition of clay on the thermal stability. These results were compared to the corresponding processed polymer since SEC measurements have shown that PHA are prone to a considerable degradation during processing. Table 7 reports the different characteristic temperatures T_0, T_f and $T_{d\ max}$ which correspond respectively to the onset and the offset decomposition temperatures, and eventually, to the maximal decomposition rate temperature measured at the DTG peak maximum.

Table 7: Characteristic decomposition temperatures of PHB- and PHBV4-based materials obtained from TG analyses

System	%wt clay	T_0 (°C)	$T_{d\ max}$ (°C)	T_f (°C)
PHB	-	275	300	337
PHB/HPS	2.7	272	302	329
PHB/C30B	1.0	270	303	335
	2.2	268	301	332
	5.0	264	302	335
PHBV4	-	269	302	318
PHBV4/HPS	2.8	265	297	314
PHBV4/C30B	0.6	266	305	322
	2.6	267	303	324
	4.4	260	303	325

T_0 decreases with the addition of clay, particularly in the case of C30B, probably due to the polymer degradation which seems to be enhanced by the presence of both inorganic layers and C30B organomodifier (S-EtOH), as previously shown from SEC results. Moreover, the onset decomposition temperature could also be affected by the organomodifier degradation itself since it was demonstrated that such compounds, i.e. quaternary ammonium surfactant, start to degrade in this temperature range (Xie, 2001). Regarding the offset decomposition temperatures, we can differentiate the materials filled with non-modified montmorillonite (HPS) from those based on the C30B. It appears that T_f are lowered for PHB/HPS and PHBV4/HPS compared to neat processed polymers. On the contrary, regarding PHA/C30B nanocomposites, T_f are in the same range for PHB (~335°C) or are slightly

increase in the case of PHBV4-based samples (from 318 to 325°C). Therefore, the decomposition temperature range is enlarged with C30B suggesting that degradation is slowed down, probably by the small tactoids better dispersed into the PHA compared to large aggregated tactoids of PHA/HPS samples. The dispersed nanofillers then appear as barriers to thermal diffusion.

E. Conclusion

Structural characterizations were first carried out on PHB and PHBV-based systems prepared by melt intercalation using non-modified and organo-modified montmorillonite bearing hydroxyl groups (Cloisite®30B). SAXS, TEM but also an original technique based on solid-state NMR evidenced microcomposites in the case of non-modified montmorillonites, while well-intercalated nanocomposites were shown with the OMMT. In this case, the nanocomposites were mainly constituted of small tactoids (3-10 layers) relatively well dispersed into the polymer bulk at low clay content (<3 wt%). With increasing clay content, the tactoids show less dispersion homogeneity.

Regarding the role of the clays on the PHA properties, we have shown that clay acts as nucleating agents affecting the crystal size of PHA. In the studied conditions, the non-isothermal crystallization rate was enhanced with the clay, whereas it hindered the recrystallization phenomenon during melting. The tensile properties revealed that optimum clay content around 1% induces improved elongation at break while keeping high stiffness. Nevertheless more brittle materials are obtained with the increasing clay content. Thermal properties were affected by the polymer degradation occurring during processing that probably counterbalance the improving effect of the clay.

Consequently, melt intercalation route is a promising way for PHA/OMMT nano-biocomposites development but polymer degradation in the molten state has to be controlled first.

F. Acknowledgements

The authors thank the GMI-IPCMS (Institut de Physique et Chimie des Matériaux de Strasbourg) for their technical support. Biocycle (Copersucar-Brazil) is acknowledged for providing the PHA.

G. Discussion et commentaires

Des systèmes PHA/argile ont été préparés par voie "fondu" en mélangeant PHB et PHBV à des montmorillonites organo-modifiées (Cloisite®30B, i.e. type OMMT-OH) ou non (type MMT-Na). La diffraction des rayons X aux petits angles, ainsi qu'une méthode récemment développée mettant en œuvre la RMN à l'état solide nous ont permis de déterminer de manière quantitative les degrés d'intercalation et de dispersion de l'argile au sein de la matrice. Les observations par MET ont confirmé et complété les premiers résultats. Ainsi, en présence de montmorillonite non modifiée, il a été mis en évidence de gros tactoïdes bien dispersés mais sans intercalation de polymère, témoignant donc de structures **microcomposites**. En revanche, dans le cas de la Cloisite®30B, les résultats ont révélé la présence de petits tactoïdes composés de quelques feuillets présentant une meilleure intercalation et nanodispersion à des faibles taux de charges, caractéristiques de matériaux **nanocomposites**.

L'étude de la cristallisation des nanocomposites PHA/OMMT a révélé l'effet nucléant des nanocharges. Dans les conditions expérimentales testées, il a été démontré que la présence de charge tend à augmenter la vitesse de cristallisation (mode non-isotherme) alors que le phénomène de recristallisation qui se produit lors de la fusion est quant à lui ralenti. Par ailleurs, l'incorporation de faibles taux de Cloisite®30B, environ 1%pds, s'avère être un excellent compromis en terme de propriétés mécaniques (rigidité et déformation) des PHA puisque les nanocomposites deviennent plus fragile lorsque le taux de charge augmente. Enfin, la détermination des propriétés thermiques nous ont démontré combien la dégradation que subit le polymère lors de la mise en œuvre peut avoir un effet néfaste sur les propriétés du matériau. D'une part, l'OMMT participe à la diminution de la stabilité thermique du polymère du fait que ses composés, feuillet inorganique et organomodifiant, entrent en jeu dans les mécanismes de dégradation. D'autre part, l'OMMT permet d'améliorer les propriétés de la matrice de par sa structuration -délamination et dispersion- au sein de la matrice en créant de fortes interactions avec celui-ci. Globalement, il semble donc que l'effet de 'renfort' de l'argile soit contrebalancé par la dégradation qu'elle induit.

Des informations complémentaires justifiant le choix des systèmes présentés ci-dessus et relatives à la stabilité thermique des matériaux PHA/montmorillonites méritent d'être apportées.

Avant d'engager l'étude complète des systèmes PHA/Cloisite®30B présenté ci-dessus, un large panel d'OMMT a été testé afin d'étudier l'influence de l'organomodifiant sur la structure et les propriétés des matériaux nanocomposites à base de PHA. Pour cela, les Cloisite®15A, 20A et la Dellite®67G (type OMMT-Alk - cf. Annexe I) ainsi que la Dellite®43B (type OMMT-Bz) ont été mélangées au PHB dans des conditions identiques à celles présentées précédemment, à savoir un mélange par voie "fondu" au mélangeur interne à 180°C pendant 5 minutes avec une vitesse de rotation des pales de 100 rpm réduite à 50 rpm après introduction de la matière. Le tableau ci-dessous (Tableau 8) rassemble les paramètres étudiés lors de la mise en œuvre, à savoir le couple (TQ_5) et la masse molaire moyenne en poids du PHB (Mw) en fin de mise en œuvre ainsi que le temps ($t_{TQ0,5}$) à partir duquel le couple est considéré nul, i.e. lorsqu'il est inférieur à 0,5 N.m. Les données relatives aux mélanges à base de Cloisite®Na et Cloisite®C30B ainsi que l'échantillon référence, constitué par le PHB seul mis en œuvre, ont également été reportées dans ce tableau. Il s'avère que la viscosité du mélange chute rapidement au regard des variations du couple enregistré lors de la mise en œuvre. Cette diminution est d'autant plus prononcée dans le cas des OMMT-Alk et OMMT-Bz compte tenu des valeurs de couples (TQ_5<1 N.m) et des masses molaires moyennes en poids (Mw<100 000) atteintes en fin de mise en œuvre. De plus, la comparaison du comportement des mélanges à base de Cloisite®15A et 20A confirme le rôle de l'organomodifiant dans le phénomène observé puisqu'un taux plus élevé d'organomodifiant conduit à une diminution plus rapide du couple. Enfin, la Dellite®67G a été testée et comparée notamment à l'influence de la Cloisite®15A afin de contrôler que le phénomène observé est indépendant du fournisseur et donc de l'origine de l'argile.

Cette étude montre donc que nous avons été rapidement confrontés au problème de la dégradation du polymère lors de la mise en œuvre de systèmes PHA/montmorillonites. Afin de conserver des propriétés acceptables pour la matrice, et étant donné que la délamination et la dispersion de l'argile sont en partie assurées par le cisaillement auquel est soumis le mélange polymère/argile lors de la mise en œuvre, nous devions sélectionner des systèmes peu enclins à la dégradation thermo-mécanique. Ainsi, au vu des résultats présentés, la Cloisite®30B est apparue comme étant l'OMMT la plus adéquate dans le cadre de cette étude, non seulement du fait de la bonne compatibilité polymère-nanocharge mais également en terme de processabilité.

Tableau 8 : Valeurs de couples et masses molaires moyennes en poids lors de la mise en œuvre des matériaux PHA/OMMT

Argiles	Type	Δw^a (%)	$t_{TQ0,5}{}^b$ (s)	$TQ_5{}^c$ (N.m)	$Mw.10^{-3}$
∅	-	-	> 300	6,5	320
Cloisite®Na	MMT-Na	-	> 300	3,6	258
Cloisite®20A	OMMT-Alk	23,1	> 300	0,76	93
Cloisite®15A	OMMT-Alk	29,4	200	0,21	51
Dellite®67G	OMMT-Alk	29,2	200	0,16	45
Dellite®43B	OMMT-Bz	29,2	150	0,10	37
Cloisite®30B	OMMT-OH	16,0	> 300	3,6	209

[a] Taux de matière organique de l'OMMT mesuré par analyse thermogravimétrique en considérant la perte de masse entre 150 et 500°C
[b] $t_{TQ0,5}$ temps à partir duquel le couple est considéré nul (<0,5 N.m)
[c] TQ_5 valeur du couple après 5 minutes de mise en œuvre

L'étude de l'influence de la sollicitation mécanique (vitesse de rotation des pales) a également été menée avant d'établir le protocole de mise en œuvre décrit dans la publication n°2. Les contraintes relatives à nos systèmes étaient (i) d'introduire rapidement la matière pour s'assurer de l'homogénéité du mélange (ii) d'éviter ou de limiter la dégradation du polymère durant cette phase de mise en œuvre. Nous nous sommes donc particulièrement intéressés à la vitesse de rotation pendant le procédé de mélangeage. La caractérisation par DRX aux petits angles du matériau chargé à 3 wt% de C30B et mis en œuvre à une vitesse constante de 100 rpm montre un espace interfeuillet légèrement plus élevé (42.3 Å) que celui obtenu lorsque la vitesse à été réduite à 50 rpm après introduction (40.4 Å). Dans le cas du PHB seul, maintenir une vitesse de rotation de 100 rpm entraine une diminution significative de la masse molaire moyenne en poids (-70% contre -50% par rapport à la masse molaire moyenne en poids initiale). Dans le cas des nano-biocomposites, on doit ajouter notamment à cet effet, la dégradation engendrée par la présence du feuillet inorganique et/ou de l'organomodifiant.

A partir de ces différentes analyses, nous avons donc établi un protocole de mélange avec une diminution de la vitesse à partir de l'introduction de la matière pour préserver les propriétés intrinsèques du PHA tout en conservant une bonne structuration des nanocharges au sein de la matrice.

Conclusion du chapitre II

Au travers des deux études (voies solvant et fondu) présentées dans ce chapitre, nous avons mis en évidence les relations ‘procédé-structure-propriétés’ dans les systèmes nanocomposites à base de PHA. Nous avons montré comment les paramètres ‘affinité polymère-argile’, ‘voie d’élaboration’ et ‘taux de charge’ peuvent conditionner la structuration des nanocharges au sein de la matrice PHA et affecter les propriétés finales du matériau. Nous avons également mis en exergue les limites que présentent chacune des voies d’élaboration envisagée, à savoir les problèmes de compatibilité polymère/solvant/OMMT pour l’une, et la faible stabilité thermique des PHA, pour l’autre.

La voie "fondu" laisse entrevoir un avenir prometteur aux nanocomposites PHA/montmorillonite à condition de mieux maîtriser les phénomènes de dégradation. L’étude préliminaire de la dégradation thermique et thermomécanique des PHAs a mis en évidence l’influence de certains composés apportés par l’addition de la charge, à savoir le feuillet inorganique et l’organomodifiant. Pour contrôler cette dégradation et la limiter, il apparaît donc indispensable de mieux connaître les composés et les différents mécanismes mis en jeu. Ces études font l’objet du chapitre suivant.

Bibliographie

Bonczek, J. L., Harris, W. G., Nkedi-Kizza, P. (2002). Monolayer to bilayer transitional arrangements of hexadecyltrimethylammonium cations on Na-montmorillonite. *Clays and clay minerals,* 50(1), 11-17.

Bordes, P., Pollet, E., Averous, L. (2008a). Nano-biocomposites: A review of biopolyester/clay systems, ***submitted.***

Bordes, P., Hablot, E., Pollet, E., Avérous, L. (2008b). Effect of clay organomodifiers on polyhydroxyalkanoates degradation, ***submitted.***

Bourbigot, S., VanderHart, D. L., Gilman, J. W., Awad, W. H., Davis, R. D., Morgan, A. B., Wilkie, C. A. (2003). Investigation of nanodispersion in Polystyrene-Montmorillonite nanocomposites by solid-state NMR. *Journal of Polymer Science - Part B Polymer Physics,* 41, 3188.

Bourbigot, S., Vanderhart, D. L., Gilman, J. W., Bellayer, S., Stretz, H., Paul, D. R. (2004). Solid state NMR characterization and flammability of styrene-acrylonitrile copolymer montmorillonite nanocomposite. *Polymer,* 45(22), 7627-7638.

Burgentzlé, D., Duchet, J., Gerard, J. F., Jupin, A., Fillon, B. (2004). Solvent-based nanocomposite coatings: I. Dispersion of organophilic montmorillonite in organic solvents. *Journal of Colloid and Interface Science,* 278(1), 26-39.

Chen, G. X., Hao, G. J., Guo, T. Y., Song, M. D., Zhang, B. H. (2002). Structure and mechanical properties of poly(3-hydroxybutyrate-co-3-hydroxyvalerate) (PHBV)/clay nanocomposites. *Journal of Materials Science Letters,* 21(20), 1587-1589.

Chen, G. X., Hao, G. J., Guo, T. Y., Song, M. D., Zhang, B. H. (2004). Crystallization kinetics of poly(3-hydroxybutyrate-co-3-hydroxyvalerate)/clay nanocomposites. *Journal of Applied Polymer Science,* 93(2), 655-661.

Chivrac, F., Pollet, E., Averous, L. (2007). Nonisothermal crystallization behavior of poly(butylene adipate-co-terephthalate)/clay nano-biocomposites. *Journal of Polymer Science, Part B: Polymer Physics,* 45(13), 1503-1510.

Choi, W. M., Kim, T. W., Park, O. O., Chang, Y. K., Lee, J. W. (2003). Preparation and characterization of poly(hydroxybutyrate-co-hydroxyvalerate)-organoclay nanocomposites. *Journal of Applied Polymer Science,* 90(2), 525-529.

Connelly, J., Van Duijneveldt, J. S., Klein, S., Pizzey, C., Richardson, R. M. (2006). Effect of surfactant and solvent properties on the stacking behavior of non-aqueous suspensions of organically modified clays. *Langmuir,* 22(15), 6531-6538.

Di Maio, E., Iannace, S., Sorrentino, L., Nicolais, L. (2004). Isothermal crystallization in PCL/clay nanocomposites investigated with thermal and rheometric methods. *Polymer,* 45(26), 8893-8900.

Doi, Y. (1990). *Microbial polyesters*. New York: John Wiley & Sons, Inc.

Fujita, M., Sawayanagi, T., Tanaka, T., Iwata, T., Abe, H., Doi, Y., Ito, K., Fujisawa, T. (2005). Synchrotron SAXS and WAXS studies on changes in structural and thermal properties of poly[(R)-3-hydroxybutyrate] single crystals during heating. *Macromolecular Rapid Communications,* 26(9), 678-683.

Grassie, N., Murray, E. J., Holmes, P. A. (1984a). Thermal degradation of poly(-(D)- beta - hydroxybutyric acid): Part 3 - The reaction mechanism. *Polymer Degradation and Stability,* 6(3), 127-134.

Grassie, N., Murray, E. J., Holmes, P. A. (1984b). Thermal degradation of poly(-(D)- beta - hydroxybutyric acid): Part 1 - Identification and quantitative analysis of products. *Polymer Degradation and Stability,* 6(1), 47-61.

Grassie, N., Murray, E. J., Holmes, P. A. (1984c). Thermal degradation of poly(-(D)- beta - hydroxybutyric acid): Part 2 - Changes in molecular weight. *Polymer Degradation and Stability,* 6(2), 95-103.

Hablot, E., Bordes, P., Pollet, E., Avérous, L. (2007). Thermal and thermo-mechanical degradation of PHB-based multiphase systems, *Polymer Degradation and Stability*, In Press (doi: 10.1016/j.polymdegradstab.2007.11.018).

He, H., Galy, J., Gérard, J.-F. (2005). Molecular simulation of the interlayer structure and the mobility of alkyl chains in HDTMA+/montmorillonite hybrids. *Journal of Physics and Chemistry,* 109(27), 13301-13306.

Heinz, H., Koerner, H., Anderson, K. L., Vaia, R. A., Farmer, B. L. (2005). Force field for mica-type silicates and dynamics of octadecylammonium chains grafted to montmorillonite. *Chemistry of Materials,* 17(23), 5658-5669.

Heinz, H., Vaia, R. A., Farmer, B. L. (2006). Interaction energy and surface reconstruction between sheets of layered silicates. *Journal of Chemical Physics,* 124, 224713.

Ho, D. L., Glinka, C. J., Ho, D. L. (2003). Effects of solvent solubility parameters on organoclay dispersions. *Chemistry of Materials,* 15(6), 1309-1312.

Hsu, S.-F., Wu, T.-M., Liao, C.-S. (2007). Nonisothermal crystallization behavior and crystalline structure of poly(3-hydroxybutyrate)/layered double hydroxide nanocomposites. *Journal of Polymer Science, Part B: Polymer Physics,* 45(9), 995-1002.

Jordan, J. W. (1949). Organophilic bentonites: I - Swelling in organic liquids. *Journal of Physics and Colloid Chemistry,* 53(2), 294-306.

Kadar, F., Szazdi, L., Fekete, E., Pukanszky, B. (2006). Surface characteristics of layered silicates: Influence on the properties of clay/polymer Nanocomposites. *Langmuir,* 22(18), 7848-7854.

Lagaly, G. (1986). Interaction of alkylamines with different types of layered compounds. *Solid State Ionics,* 22(1), 43-51.

Laszlo, P. (1987). Chemical reactions on clays. *Science,* 235(4795), 1473-1477.

Lenz, R. W., Marchessault, R. H. (2005). Bacterial polyesters: Biosynthesis, biodegradable plastics and biotechnology. *Biomacromolecules,* 6(1), 1-8.

Lim, S. T., Hyun, Y. H., Lee, C. H., Choi, H. J. (2003). Preparation and characterization of microbial biodegradable poly(3-hydroxybutyrate)/organoclay nanocomposite. *Journal of Materials Science Letters,* 22(4), 299-302.

Liu, W. J., Yang, H. L., Wang, Z., Dong, L. S., Liu, J. J. (2002). Effect of nucleating agents on the crystallization of poly(3-hydroxybutyrate-co-3-hydroxyvalerate). *Journal of Applied Polymer Science,* 86(9), 2145-2152.

Madison, L. L., Huisman, G. W. (1999). Metabolic engineering of poly(3-hydroxyalkanoates): From DNA to plastic. *Microbiology and Molecular Biology Reviews,* 63(1), 21-53.

Moraru, V. N. (2001). Structure formation of alkylammonium montmorillonites in organic media. *Applied Clay Science,* 19(1-6), 11-26.

Nam, J. Y., Sinha Ray, S., Okamoto, M. (2003). Crystallization behavior and morphology of biodegradable polylactide/layered silicate nanocomposite. *Macromolecules,* 36(19), 7126-7131.

Nistor, D., Miron, N. D., Surpateanu, G. G., Azzouz, A. (2004). Study by thermal programmed desorption of the properties of modified clays on their impact on environmental pollution. *Journal of Thermal Analysis and Calorimetry,* 76(3), 913-920.

Pandey, J. K., Kumar, A. P., Misra, M., Mohanty, A. K., Drzal, L. T., Singh, R. P. (2005). Recent advances in biodegradable nanocomposites. *Journal of Nanoscience and Nanotechnology,* 5(4), 497-526.

Pluta, M., Galeski, A., Alexandre, M., Paul, M.-A., Dubois, P. (2002). Polylactide/montmorillonite nanocomposites and microcomposites prepared by melt blending: Structure and some physical properties. *Journal of Applied Polymer Science,* 86(6), 1497-1506.

Poirier, Y. (2002). Polyhydroxyalknoate synthesis in plants as a tool for biotechnology and basic studies of lipid metabolism. *Progress in Lipid Research,* 41(2), 131-155.

Renstad, R., Karlsson, S., Albertsson, A.-C., Werner, P.-E., Westdahl, M. (1997). Influence of processing parameters on the mass crystallinity of poly(3-hydroxybutyrate-co-3-hydroxyvalerate). *Polymer International,* 43(3), 201-209.

Sinha Ray, S., Okamoto, M. (2003). Polymer/layered silicate nanocomposites: A review from preparation to processing. *Progress in Polymer Science (Oxford),* 28(11), 1539-1641.

Slabaugh, W. H., Hiltner, A. (1968). The swelling of alkylammonium montmorillonites. *Journal of Physical Chemistry,* 72(12), 4295-4298.

Sposito, G., Skipper, N. T., Sutton, R., Park, S.-H., Soper, A. K., Greathouse, J. A. (1999). Surface geochemistry of the clay minerals. *Proceedings of the National Academy of Sciences of the United States of America,* 96(7), 3358-3364.

Vaia, R. A., Teukolsky, R. K., Giannelis, E. P. (1994). Interlayer structure and molecular environment of alkylammonium layered silicates. *Chemistry of Materials,* 6(7), 1017-1022.

Vaia, R. A., Liu, W., Koerner, H. (2003). Analysis of Small-Angle Scattering of Suspensions of Organically Modified Montmorillonite: Implications to Phase Behavior of Polymer Nanocomposites. *Journal of Polymer Science: Part B: Polymer Physics,* 41, 3214–3236.

Valentin, H. E., Broyles, D. L., Casagrande, L. A., Colburn, S. M., Creely, W. L., DeLaquil, P. A., Felton, H. M., Gonzalez, K. A., Houmiel, K. H., Lutke, K., Mahadeo, D. A., Timothy A. Mitsky, Padgette, S. R., Reiser, S. E., Slater, S., Stark, D. M., Stock, R. T., Stone, D. A., Taylor, N. B., Thorne, G. M., Tran, M., Gruys, K. J. (1999). PHA production, from bacteria to plants. *International Journal of Biological Macromolecules,* 25(1-3), 303-306.

VanderHart, D. L., Asano, A., Gilman, J. W. (2001a). Solid-state NMR investigation of paramagnetic nylon-6 clay nanocomposites. 1. Crystallinity, morphology, and the direct influence of Fe3+ on nuclear spins. *Chemistry of Materials,* 13(10), 3781-3795.

VanderHart, D. L., Asano, A., Gilman, J. W. (2001b). NMR measurements related to clay-dispersion quality and organic-modifier stability in nylon-6/clay nanocomposites. *Macromolecules,* 34(12), 3819-3822.

VanderHart, D. L., Asano, A., Gilman, J. W. (2001c). Solid-state NMR investigation of paramagnetic nylon-6 clay nanocomposites. 2. Measurement of clay dispersion, crystal stratification, and stability of organic modifiers. *Chemistry of Materials,* 13(10), 3796-3809.

Wang, S., Song, C., Chen, G., Guo, T., Liu, J., Zhang, B., Takeuchi, S. (2005). Characteristics and biodegradation properties of poly(3-hydroxybutyrate-co-3-hydroxyvalerate)/organophilic montmorillonite (PHBV/OMMT) nanocomposite. *Polymer Degradation and Stability,* 87(1), 69-76.

Xi, Y., Ding, Z., He, H., Frost, R. L. (2004). Structure of organoclays - An X-ray diffraction and thermogravimetric analysis study. *Journal of Colloid and Interface Science,* 277(1), 116–120.

Xi, Y., Frost, R. L., He, H., Kloprogge, T., Bostrom, T. (2005). Modification of Wyoming montmorillonite surfaces using a cationic surfactant. *Langmuir,* 21(19), 8675-8680.

Xie, W., Gao, Z., Pan, W.-P., Hunter, D., Singh, A., Vaia, R. (2001). Thermal degradation chemistry of alkyl quaternary ammonium montmorillonite. *Chemistry of Materials,* 13(9), 2979-2990.

Chapitre III
-
Etude de la dégradation thermique et thermomécanique dans les systèmes nano-biocomposites PHA/OMMT

Introduction

Dans le chapitre précédent, nous avons mis en évidence que la stabilité thermique du PHB et du PHBV génère de fortes limitations dans l'élaboration des nano-biocomposites par voie "fondu" ainsi que sur leurs propriétés finales. Aussi, une étude spécifique et approfondie sur la tenue thermique et thermomécanique de ces polyesters dans de tels systèmes a été menée. L'ossature de ce chapitre est principalement basée sur deux publications.

Dans cette étude, nous nous sommes plus particulièrement intéressés aux composés organiques présents dans les systèmes nanocomposites et susceptibles de réagir avec la matrice et d'en accélérer sa dégradation lors de la mise en œuvre. En effet, bien que plusieurs publications évoquent le rôle des feuillets inorganiques de la montmorillonite dans la dégradation de thermoplastiques (Maiti, 2003), quelques très rares publications décrivent, par exemple, la stabilité thermique intrinsèque des ammoniums quaternaires utilisés comme organomodifiants dans les nanocomposites (Xie, 2001).

Nous avons testé d'une part, l'influence des organomodifiants, i.e. des sels d'ammonium quaternaire, et d'autre part, des résidus de fermentation sur la dégradation thermique et thermomécanique des différents PHAs étudiés. En effet, les organomodifiants sont des composés indispensables à l'élaboration de matériaux nanocomposites performants car ils assurent une meilleure affinité entre la charge et la matrice. Quant aux résidus de fermentation, ce sont des composés issus de la production industrielle par fermentation bactérienne des polyhydroxyalcanoates que les procédés d'extraction et de purification n'ont pu éliminer (acides gras, …).

La **publication n°3** présentée dans la première partie de ce chapitre fait état de la dégradation du PHB en présence de résidus de fermentation et/ou d'ammoniums quaternaires, ces derniers étant utilisés comme organomodifiants de la montmorillonite. L'étude a été menée en absence de charge minérale afin de se focaliser principalement sur les effets intrinsèques de ces composés. L'analyse de la cinétique de dégradation fondée sur des modèles établis, ainsi que la détermination des produits de décomposition, notamment par caractérisation par RMN de produits dégradés, nous ont conduit à identifier les composés et à proposer les mécanismes mis en jeu dans les réactions de dégradation du PHB.

La **publication n°4** vient étendre et compléter les conclusions de la publication n°3. Les PHBV, de par des températures de mise en œuvre plus basses, montrent une sensibilité moindre à

la dégradation thermique. Cet article présente l'étude comparative de la dégradation de deux grades de PHBV (taux de HV de 4 et 8%) et du PHB (étudié dans la publication n°3), en présence des mêmes surfactants dans un système simulant les nano-biocomposites. Ainsi, une étude originale mettant en exergue l'effet des résidus de bioproduction et des organomodifiants sur la dégradation des principaux PHAs a pu être réalisée.

Publication n°3.

"Thermal and thermo-mechanical degradation of poly(3-hydroxybutyrate)-based multiphase systems"

E. Hablot, P. Bordes, E. Pollet, L. Avérous*

Polymer Degradation and Stability, Accepted

Abstract

The influence of fermentation residues and quaternary ammonium salts on the thermal and thermo-mechanical degradation of a biodegradable bacterial poly(3-hydroxybutyrate), PHB, was studied. The results obtained from DSC, SEC and TG analyses performed on blends reveal that ammonium cations greatly enhance the degradation leading to a dramatic decrease in PHB molecular weight. These results are confirmed by the thermo-mechanical study. Besides, we show that the presence of fermentation residues does not affect significantly the PHB thermal stability in comparison to the ammonium cations. A kinetic analysis based on the Coats & Redfern model was applied to the non-isothermal TGA data. This method completed by NMR characterizations lead us to determine the most probable mechanism for PHB degradation in presence of the ammonium salts. The results demonstrate that ammonium surfactants commonly found in commercial nanoclays (for nanocomposites elaboration) effectively have a catalytic effect on the PHB degradation.

*Keywords***:** polyhydroxybutyrate ; thermal degradation ; ammonium surfactants

* Corresponding author: Luc Averous.

Tel.:+33-3-90-242-707 - Fax: +33-3-90-242-716 - AverousL@ecpm.u-strasbg.fr

B. Introduction

Polyhydroxyalkanoates (PHAs) represent an interesting alternative to synthetic polymers due to many advantages. Not only they are biodegradable and biocompatible, but they can also be produced from renewable resources. The poly(3-hydroxybutyrate) (PHB), the most common PHA, was first discovered in 1926 by Lemoigne (Lemoigne, 1926; Lenz, 2005). But, PHAs were really exploited since the 80's and particularly in the last decade considering the decreasing reserves of fossil fuel and the increasing public concern in the environment protection.

The PHB accumulation by various bacteria strains (De Koning, 1993; Tagushi, 2002; Reddy, 2003) from different biomass substrates (Lee, 2002; Reddy, 2003) has been widely described in the literature as well as the recovery process (Lee, 2002; Ramsay, 2002). The extraction and purification processes are the decisive production steps since fermentation residues (metal, crude biomass,) could remain and then alter the PHAs properties (Kopinke, 1996; Kim, 2006). PHB is already produced at the industrial scale but this material shows some drawbacks compared to conventional polymers, such as a high stiffness and brittleness. Besides, PHB shows poor thermal stability at temperature above the melting point (Grassie, 1984a, 1984b, 1984c; Kopinke, 1996; Li, 2001; Aoyagi, 2002; Li, 2003; Abe, 2006; Carrasco, 2006).

To improve the PHAs properties, nano-biocomposites (Pandey, 2005; Chivrac, 2006) (nanocomposites based on biodegradable matrices) seem to be a good answer since they have raised great interest in recent years thanks to the enhancement of material properties. Few studies were dedicated to nano-biocomposites based on PHB or PHBV with montmorillonite (MMT) (Chen, 2002; Choi, 2003; Lim, 2003; Chen, 2004; Wang, 2005). Most of them use the environmentally unfriendly route of solvent intercalation (Chen, 2002; Lim, 2003; Chen, 2004; Wang, 2005), due to the particular temperature sensitivity of these biopolymers that restricts the use of the melt processing way. Many studies dedicated to thermal (Grassie, 1984a, 1984b, 1984c; Kunioka, 1990; Aoyagi, 2002; Li, 2003; Abe, 2006; Carrasco, 2006) and thermo-mechanical (Melik, 1995; Renstad, 1997) degradation of neat PHB and PHBV have revealed that the degradation occurs rapidly near the melting point according to mainly a random chain scission process (Scheme 1). They have also shown that melt processing parameters must be optimized to limit this phenomenon resulting in a really narrow processing window. Some authors have shown that fermentation residues (Kopinke, 1996; Kim, 2006) or plasticizers (Fernandes, 2004; Erceg, 2005) have an influence on the PHAs degradation. Recently, Maiti et al. (Maiti, 2003) have reported that, in the case of PHB-based nano-biocomposites reinforced by MMT, the presence of Aluminium Lewis acid sites in the silicate layers enhances the thermal degradation of PHB by

catalyzing the hydrolysis of ester linkages. Xie et al. (Xie, 2001) have studied the thermal degradation of montmorillonites organo-modified (OMMT) by quaternary ammonium surfactants. This recent work has pointed out the complex degradation reactions that could exist in organically modified MMT and consequently, in polymer-(O)MMT nanocomposite systems.

This paper aims at investigating the influence of both the addition of ammonium salts (used in common commercial OMMT) and the presence of organic fermentation residues on the PHB thermal and thermo-mechanical degradation. Differential Scanning Calorimetry (DSC) analyses and Size Exclusion Chromatography (SEC) measurements were performed to compare the melting temperatures and the weight average molecular weights of the different systems. Eventually, a kinetic analytical model (Coats, 1964) was applied to non-isothermal thermogravimetric (TG) measurements. This method completed by Nuclear Magnetic Resonance (NMR) characterizations lead us to propose the possible mechanism for PHB degradation in presence of ammonium salts.

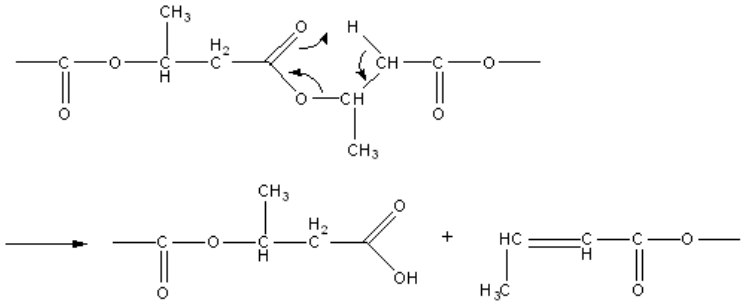

Scheme 1. PHB random chain scission

C. Experimental Section

C.I. Materials

Poly(3-hydroxybutyrate) (PHB), produced by bacterial fermentation, was kindly supplied by Biocycle PHB Industrial S/A, Brazil. The PHB production plant is entirely integrated into the sugar mill to obtain an environmentally sound plastic resin (Nonato, 2001): the *Ralstonia eutropha* bacterial strains growing and the fermentation steps are made from cane sugar, and the recovery process uses exclusively natural solvents, by-products of ethanolic fermentation. The weight average molecular weight (M_w) and the polydispersity index (PDI) have been determined by size exclusion chromatography (SEC) (M_w=650,000 and PDI=2). Melt flow index (MFI) and density are equal to 12 g/10 min and 1.22 g/cm^3, respectively.

The quaternary ammonium salts - di(hydrogenated tallow)dimethylammonium chloride (S-Alk), (vegetable oil)benzyldimethylammonium chloride (S-Bz) and oleylbis(2-hydroxyethyl)methylammonium chloride (S-EtOH) in isopropyl alcohol - from Akzo Nobel were kindly supplied by Brenntag Specialities (see Table 1). The tetramethylammonium chloride (TMA) (reagent grade, 97%) was supplied by Sigma-Aldrich and the pentadecane (puriss p.a. ≥99.8%) by Fluka. Triethylamine 99% pure purchased from Acros Organics was distilled on CaH_2.

Table 4. Structure of the ammonium cations

Ammonium cations	Structure
S-Alk	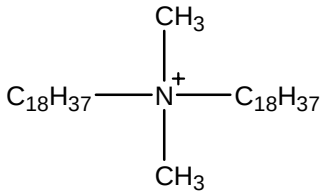
S- Bz	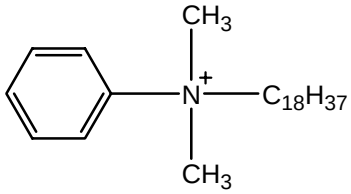
S-EtOH	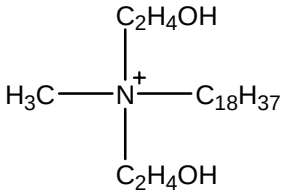
TMA	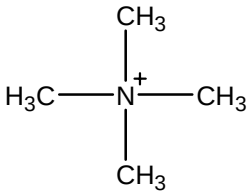

C.II.Polymer purification

Purification of PHB was performed by soxhlet extraction with diethyl ether (SDS Carlo Erba) for 24h. The purified PHB (PHBp) was then recovered and dried at 80°C under vacuum. The liquid phase was collected and the extracted fermentation residues (Rsd) were recovered after

solvent evaporation. The initial amount of fermentation residues in the raw PHB is equal to ca. 2 wt%, as determined by gravimetry.

These residues were identified by thin-layer chromatography (TLC). The solvent elution system used was hexane-diethyl ether-formic acid (80:20:2 by volume). The separation revealed that the residues are a mixing of lipids like free fatty acids, mono-, di- and triacylglycerols, phospholipids, cholesterol and cholesterol esters. The total amount of nitrogen in the extracted residues was also determined. The titration leads to about 0.5% of nitrogen in the extract that corresponds to less than 50 ppm in the raw PHB.

C.III. Samples preparation

To remove isopropyl alcohol and water from the commercial ammonium solutions, S-Alk and S-Bz were dispersed into diethyl ether, filtered and dried under vacuum in order to obtain white powders. Then, they were added and intimately mixed to the dried PHBp. Regarding the fermentation residues (Rsd) and the S-EtOH surfactant, the pasty nature of these compounds makes difficult the homogeneous mixing with the PHBp powder. Thus, they were dispersed into diethyl ether and mixed to the purified PHB. Then, once the solvent was evaporated, the mixture was dried under vacuum. A ternary blend was prepared by adding the S-Alk powder to the binary mixture PHBp+Rsd.

For the thermo-mechanical degradation study, the samples were prepared in an internal mixer Haake Rheocord 9000 at 170°C. Because of the technical difficulty to obtain large amounts of purified PHB, this study was performed on samples prepared with the "as-received" raw PHB i.e., PHB containing 2 wt% of fermentation residues. Different rotation speeds and processing times were tested, ranging from 50 to 150 rpm and from 3 to 15 min, respectively. The torque and the melt temperature were recorded during the processing. The mechanical energy was calculated using Equation 1 where N is the rotation speed (rad.s^{-1}), M the sample mass (kg) introduced in the mixing chamber and S is the area defined by the torque vs. time curve.

$$E_m\ (kJ/kg) = \left(\frac{N}{M}\right) \times S \quad (1)$$

Additives contents in the PHB-based samples are 10 wt% for the residues and 3 wt% for the ammonium cations, respectively. Such high amounts were chosen to have more pronounced degradation and thus to observe and identify more easily the occurring phenomena.

To determine the degradation mechanism, further experiments were performed on polymer-additives (97:3) blends. The raw PHB was directly mixed to pentadecane, to tetramethyl

ammonium (PHB+TMA) and to distilled triethylamine (PHB+TEA) and each blend was processed at 170°C and 50 rpm for 15 min. Another PHB+S-Bz sample containing 30 %wt of surfactant was also prepared. Eventually, S-Bz was degraded by annealing at 170°C for 15 min.

C.IV. Characterizations

Thermal degradation was studied by differential scanning calorimetry (DSC 2910 TA Instruments) under air flow. To determine the influence of the additives (fermentation residues or surfactants) on the neat polymer, the samples (5-10 mg placed in an aluminium pan) were heated up to 200°C at 10°C/min. Then, the temperature was maintained for 10 min to get rid of thermal history and to promote the degradation. Finally, samples were cooled down to room temperature at 10°C/min and heated up again to 220°C at 10°C/min. The PHB melting temperature was determined on the second heating scan.

Thermogravimetric analyses (TGA) were conducted under nitrogen flow using a Hi-Res TGA 2950 apparatus from TA Instruments. The samples (10-20 mg placed in an aluminium pan) were heated up to 500°C at different heating rates, ranging from 5 to 20°C/min.

Size Exclusion Chromatrography (SEC) measurements were performed using a Shimadzu apparatus equipped with a RID-10A refractive index detector and a SPD-M10A UV detector. The columns used were PLGel Mixed-C and PLGel 100Å. The calibration was realized with PS standard from 580 to 1,650,000 g/mol. Chloroform (puriss p.a. Riedel-de Haën) was the mobile phase and the analyses were carried out at 40°C with a solvent flow rate of 1 ml/min. The SEC measurements were performed on the samples recovered at the end of the DSC analyses and after given processing times in the internal mixer.

The ^{1}H and ^{13}C Nuclear Magnetic Resonance (NMR) analyses were carried out on a Bruker Ultrashield^{TM} 300 MHz spectrometer. The spectra were recorded at room temperature using sample solutions in $CDCl_3$ (20mg/ml).

D. Coats & Redfern model

In this part are exposed the theoretical bases of the Coats & Redfern method applied to the experimental TGA data. This model assumes that the isothermal rate of conversion can be

expressed by Equation 2, where α represents the fractional extent of conversion (i.e. weight loss), dα/dt is the isothermal rate of conversion, f(α) is a temperature-independent function of conversion that depends on the degradation mechanism and k(T) is a temperature-dependent function (Starink, 2003).

$$\frac{d\alpha}{dt} = k(T)\,f(\alpha) \quad (2)$$

According to Arrhenius equation, the expression of k(T) is given by Equation 3, where A is the pre-exponential factor independent of temperature, E_a the activation energy, R the gas constant and T the absolute temperature. By combining Equations 2 and 3, Equation 4 is obtained.

$$k(T) = A\exp\left(-\frac{E_a}{RT}\right) \quad (3)$$

$$\frac{d\alpha}{dt} = A\exp\left(-\frac{E_a}{RT}\right) f(\alpha) \quad (4)$$

For non-isothermal measurements at constant heating rate β = dT/dt, we obtain Equation 5.

$$\beta\frac{d\alpha}{dT} = A\exp\left(-\frac{E_a}{RT}\right) f(\alpha) \quad (5)$$

By multiple integration and combination of these equations, the Coats & Redfern method (Coats, 1964) is expressed by Equation 6, where g(α) is a function depending on the type of degradation mechanism and is related to f(α) by Equation 7. By plotting $\ln[g(\alpha)/T^2]$ as a function of 1/T, the slope of the obtained straight line is directly proportional to E_a.

$$\ln\left[\frac{g(\alpha)}{T^2}\right] = \ln\left(\frac{AR}{\beta E}\right) - \frac{E_a}{RT} \quad (6)$$

$$g(\alpha) = \int_0^{\alpha}\left[f(\alpha)\right]^{-1} d\alpha \quad (7)$$

E. Results and discussion

E.I. Effect of annealing on PHB characteristics

The key step of the DSC thermal treatment consists in annealing the samples for 10 min at 200°C to promote chain scission reactions. The influence of the different additives on the PHB thermal degradation has been studied by monitoring the evolution of both the polymer melting temperature and its weight average molecular weight after this thermal treatment. Table 2

summarizes the melting temperatures (T_m) and weight average molecular weights (M_w) of the polymer-additives samples compared to the annealed purified polymer (PHBp) as a reference.

Table 5. Influence of additives on the PHB melting temperature (T_m) and weight average molecular weight (Mw)

System	T_m (°C)	Mw
PHBp	174	63,200
PHBp+S-Alk	149	3,500
PHBp+S-Bz	133	1,200
PHBp+S-EtOH	146	2,500
PHBp+Rsd	171	51,700

DSC analyses show that the melting temperature of purified PHB with fermentation residues (PHBp+Rsd) displays only a slight T_m decrease (3°C). But PHBp with S-Alk, S-Bz or S-EtOH present considerable T_m decreases of 25°C, 41°C and 28°C, respectively. These significant T_m decreases are likely due to lower PHB weight average molecular weight as a direct consequence of the chain scission reactions occurring. This is confirmed by the SEC analyses performed on the samples after the thermal treatment. Table 2 shows a dramatic decrease in M_w for PHB added with surfactants, compared to neat PHBp. Indeed, PHBp+S-Alk, PHBp+S-Bz or PHBp+S-EtOH samples show M_w divided by 18, 52 and 25, respectively. These results demonstrate that the polymer degradation is strongly enhanced in presence of surfactants. On the contrary, it seems that the fermentation residues only have a small influence on the PHB thermal degradation, at least in the experimental conditions of this study. Besides, through these different results, one can conclude that S-Bz seems to be more degrading than S-Alk and S-EtOH.

E.I.1. Thermogravimetric analyses on PHB-based systems

To better understand the thermal degradation of PHB-based systems, their related reaction mechanisms and kinetic parameters, a specific study was performed on the mass loss data obtained from dynamic thermogravimetric analyses. Figure 1 shows the weight loss curves (TG) for all the systems obtained at a heating rate of 10°C/min. It can be seen that the fermentation residues have only little influence, whereas the surfactants favour the PHB degradation since the corresponding

TG curves are shifted towards lower temperatures. This is on agreement with previous results obtained from DSC and SEC analyses.

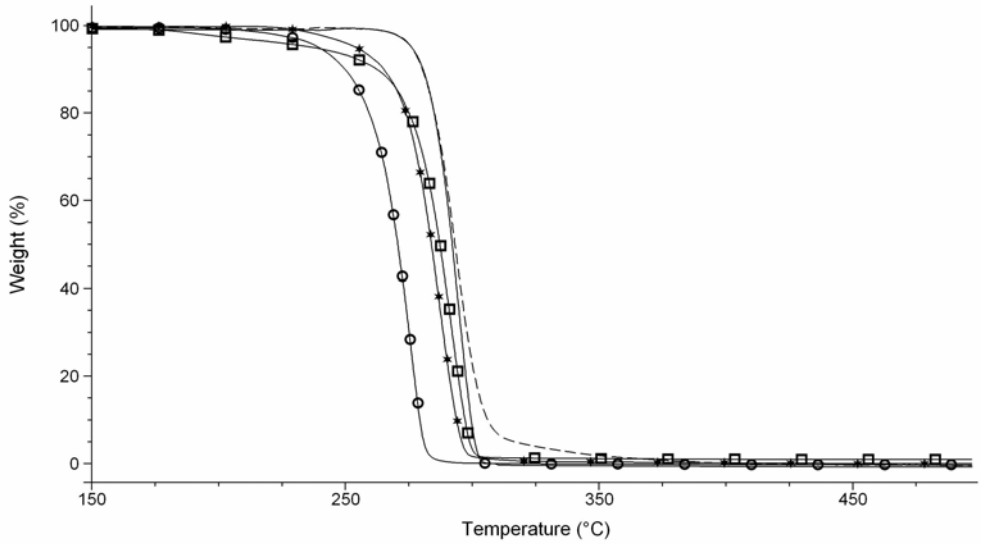

Figure 1. TG curves at 10°C/min for PHBp (—), PHBp+Rsd (---), PHBp+S-Alk (○), PHBp+S-Bz (□) and PHBp+S-EtOH (✶).

Looking attentively to the TG curves, one can see that there is a main degradation step corresponding to the PHB degradation but also secondary degradations occurring before and/or after the principal one. When superposing the TG curves of neat PHBp, the surfactant and the corresponding blend (see Figure 2 for a representative example), we can rationally attribute these secondary mechanisms to the degradation of the additive itself. Indeed, the ammonium surfactants degrade on a wide range of temperatures (150°C - 460°C), compared to neat PHBp.

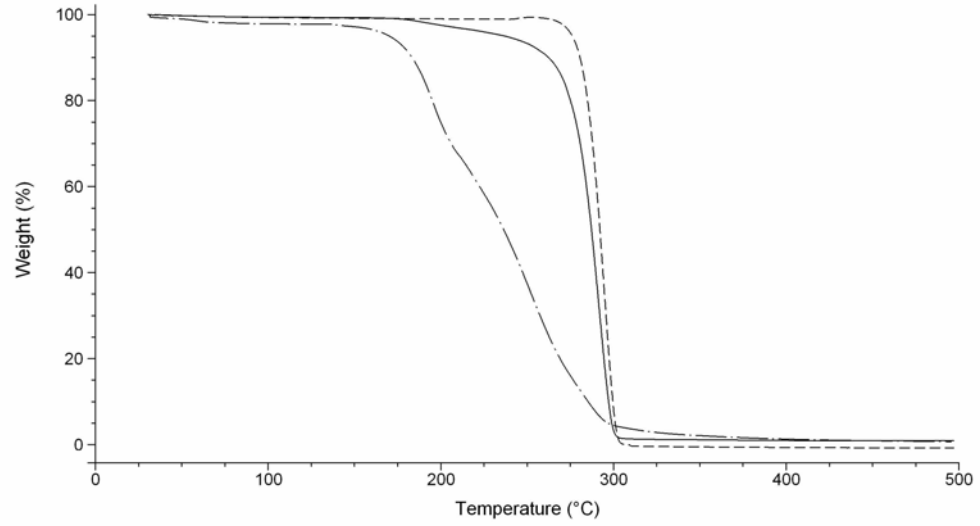

Figure 2. Superposition of PHBp (---), PHBp+S-Bz (—) and S-Bz (– · –) TG curves recorded at 10°C/min

After these observations about the influence of additives on the PHB degradation, the dependence, if any, between the degradation mechanisms of both the polymer and the additive has to be analysed.

According to Torre et al. (Torre, 1998), if the degradations of each compound of a blend are independent, the weight loss obtained by TGA is given by Equation 8, where W is the residual weight fraction of the blend. W_a and W_{PHBp} are the residual weight fractions of the additive and the purified PHB respectively, and x_a and x_{PHBp} the original weight fractions of the additive and the purified PHB in the blend, respectively.

$$W = W_a x_a + W_{PHBp} x_{PHBp} \quad (8)$$

Thus, starting from the experimental TGA of PHBp and each additive, one can build up the calculated TG curve for all respective blends. For the PHB-surfactant systems, the calculated and the experimental curves (not shown here) are not superposed. For the PHBp+S-Alk sample, the experimental curve is shifted of 20°C towards lower temperatures, compared to the calculated curve. For PHBp+S-Bz and PHBp+S-EtOH, the same observation has been noticed and experimental curves are slightly shifted towards lower temperatures. Moreover, we can observe that both experimental and calculated curves do not present exactly the same shape. Thus, we can conclude that, in such a blend, the degradation of purified PHB and the degradation of surfactants are dependent. This phenomenon highlights that surfactants play a key role in the PHB thermal degradation.

Concerning the effect of the fermentation residues on the PHB degradation, we can assume that these impurities have a limited influence on the main degradation step since the experimental and calculated TG curves (not shown here) are almost superposed with a quite similar shape. This is on perfect agreement with the previous results based on T_m and M_w determinations.

An additional experiment was done on a ternary mixture of purified PHB with S-Alk and fermentation residues (PHBp+S-Alk+Rsd) to determine whether the additives have a synergistic effect on the polymer degradation. In this case, the experimental curve is shifted of 10°C towards lower temperatures compared to the calculated one determined from the experimental thermograms of the binary mixture (PHBp+S-Alk) and the fermentation residues. Thus, the surfactants seem to act in synergy with the fermentation residues to degrade the PHB but the corresponding mechanism is still unexplained.

E.I.2. Analytical treatment of TGA data by Coats & Redfern method

To obtain additional information about the degradation mechanism, the activation energy has been calculated with the Coats & Redfern method, for each system. These values are obtained by plotting $\ln[g(\alpha)/T^2]$ as a function of 1/T. Table 3 presents twelve different probable forms of $g(\alpha)$ among the most commonly used functions of solid-state processes (Hatakeyama, 1999; Vyazovkin, 1999; Swain, 2005). Typically, for each TG curve, all the $g(\alpha)$ functions were tested and the one which presents the best linearity (r^2 closest to 1) is considered as the most probable reaction mechanism for the thermal degradation. The analysis has been performed from TG data obtained at the lowest heating rate (5°C/min), to better observe the degradation phenomenon and thus to have a better discrimination between the possible mechanisms.

Table 6. Set of solid-state reactions (g(α)) used for kinetic parameters calculation

Mechanism	Code	g(α)
Exponential law	-	$-\ln(\alpha)$
Avrami-Erofeev law	$A_{1.5}$	$[-\ln(1-\alpha)]^{2/3}$
	A_2	$[-\ln(1-\alpha)]^{1/2}$
	A_3	$[-\ln(1-\alpha)]^{1/3}$
	A_4	$[-\ln(1-\alpha)]^{1/4}$
Prout-Tompkins law	B_1	$\ln[\alpha/(1-\alpha)]$
Chemical reaction of n^{th} order (F_n)	F_1	$-\ln(1-\alpha)$
	F_2	$1/(1-\alpha)$
	F_3	$1/(1-\alpha)^2$
Phase boundary controlled reaction (contracting area)	R_2	$[1-(1-\alpha)^{1/2}]$
Phase boundary controlled reaction (contracting volume)	R_3	$[1-(1-\alpha)^{1/3}]$
Three dimensional diffusion spherical symmetry (Jander equation)	D_3	$[1-(1-\alpha)^{1/3}]^2$

Table 4 shows the main results obtained with the Coats & Redfern method, by plotting $\ln[g(\alpha)/T^2]$ vs. 1/T for each system. For each system, the most suitable reaction mechanism and its related values for the activation energy E_a and the pre-exponential factor A are presented. Regarding these results, several points can be discussed. First, the activation energy of PHBp and PHBp+Rsd i.e., 395 kJ/mol and 327 kJ/mol respectively, are close and relatively high compared to

the other systems. Moreover, it appears that the thermal degradation of these two samples follows the same mechanism, namely a first order reaction (F1 type). This statement is on agreement with previously published results (Carrasco, 2006) and it can also be concluded that residues have just a little influence on PHB thermal degradation. Surfactants have a stronger influence on the thermal degradation of PHBp. This is confirmed by the activation energy values obtained for these systems which are greatly inferior to the PHBp activation energy (see Table 4). Even if these calculated values of activation energy can hardly be regarded as having a real chemical significance, they allow us to compare the thermal stability of the different systems.

Table 7. Kinetic parameters of PHB degradation according to the Coats & Redfern method

System	Temperature range		Model	E_a (kJ/mol)	r^2	A (s^{-1})
	Start (°C)	End (°C)				
PHBp	230	305	F1	395	0.9962	3.25E+35
PHBp+S-Alk	200	240	R3	200	0.9948	1.07E+18
PHBp+S-Bz	220	290	R2	166	0.9796	1,47E+13
PHBp+S-EtOH	210	280	R2	161	0.9860	5,13E+12
PHBp+Rsd	255	290	F1	327	0.9900	7.42E+28

Finally, from the most probable reaction mechanisms which are determined for these systems, one can conclude that the studied surfactants favour and enhance the PHBp thermal degradation through a phase boundary controlled process (R type).

E.II. Thermo-mechanical degradation

By analogy and to simulate the preparation of nano-biocomposites, the thermo-mechanical degradation was also studied to analyse the PHB degradation during processing. The torque and the temperature have been monitored during the experiment. Samples have been taken from the mixer during the experiment at 3, 5 and 10 min to determine the weight average molecular weight (M_w) by SEC.

On one hand, the torque, the temperature and the weight average molecular weight curves follow the expected trends. On the other hand, we can notice some strong differences between PHB and PHB with additives (Figure 3 and Table 5). First, in the case of the PHB sample, the maximum torque value is higher and is reached earlier. Secondly, the torque decreases more

rapidly for the PHB-surfactant samples compared to neat PHB or PHB+Rsd. At 50 rpm, the torque reaches a constant value (a plateau) at ca. 700 s, in the case of PHB and PHB+Rsd samples whereas a zero-torque is recorded at around 590, 280 and 230 s, for PHB+S-EtOH, PHB+S-Alk and PHB+S-Bz, respectively. This zero-torque is probably a direct consequence of the PHB degradation. Indeed, Table 6 shows that the samples collected after 5 min of processing already show a significant M_w decrease for PHB+S-Alk and PHB+S-Bz.

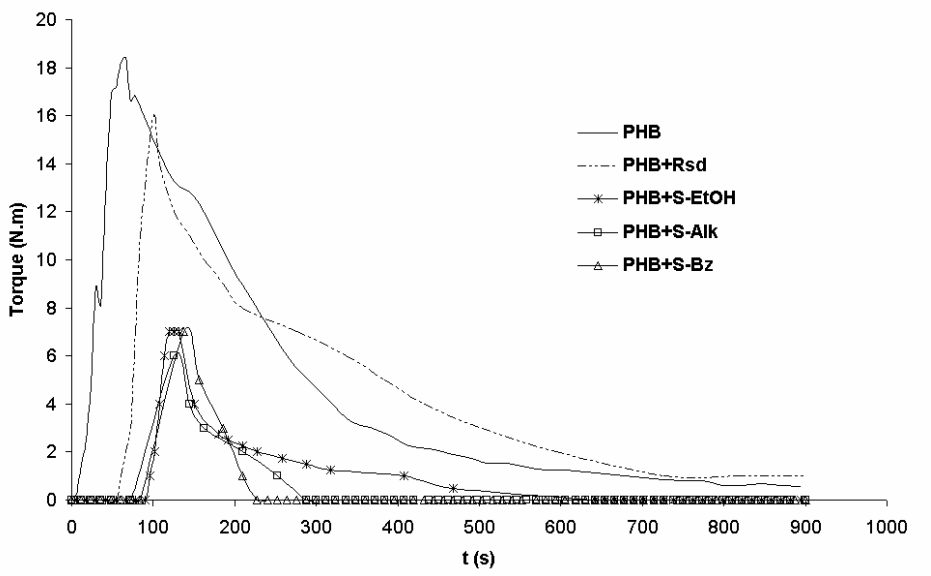

Figure 3. Evolution of the torque at 170°C and 50 rpm for 15 minutes for the different systems

Table 8. Maximal torque, time to reach it (t_{max}) and time to reach the constant torque value ($t_{plateau}$) at 170°C and 50 rpm

System	Maximal torque (Nm)	t_{max} (s)	$t_{plateau}$ (s)
PHB	24	114	700
PHB+S-Alk	6	126	280
PHB+S-Bz	7	138	230
PHB+S-EtOH	7	126	590
PHB+Rsd	16	102	700
PHB+TMA	15	90	500
PHB+TEA	16	65	200

Table 9. Weight average molecular weights (Mw) of PHB as a function of time during processing at 170°C and 50 rpm

t (s)	$Mw.10^{-3}$				
	PHB	PHB+S-Alk	PHB+S-Bz	PHB+S-EtOH	PHB+Rsd
180	625	527	286	680	753
300	412	106	39	263	605
600	337	21	15	210	313

All these observations show that in the presence of surfactant, the melt is less viscous due to an enhanced degradation. This phenomenon is particularly favoured with S-Bz and S-Alk. On the contrary, the fermentation residues do not affect significantly the viscosity, and then, the degradation. All these observations are on total agreement with the previous results.

A zero-torque value is observed in the early stage of processing in the case of PHB-surfactant systems. This unusual phenomenon could be explained by lower T_m for these blends and by a possible lubricant behaviour of the surfactants.

Same trends have been also observed at 100 and 150 rpm (not reported here). Nevertheless, it can be concluded that the rotation speed plays a significant role in the thermo-mechanical degradation of PHB since the higher the rotation speed, the earlier and the greater the degradation.

To emphasize these results, the mechanical energies (E_m) provided to the different systems for 5 and 15 minutes of processing have been determined and are presented in Table 7. The mechanical energy, which is connected to the viscosity, is greatly superior for PHB and PHB+Rsd than for PHB with surfactants. These results confirm the conclusions drawn before indicating that PHB with surfactants, particularly S-Alk and S-Bz, present a really lower viscosity compared to PHB and PHB+Rsd, due to the great ability of these surfactants to enhance the PHB degradation.

Table 10. Mechanical energy provided to each system for 5 (E_{m5}) and 15 minutes (E_{m15}) at 170°C and 50 rpm

System	E_{m5} (kJ/kg)	E_{m15} (kJ/kg)
PHB	400	640
PHB+Rsd	235	420
PHB+S-EtOH	70	130
PHB+S-Bz	50	50
PHB+S-Alk	50	50

Further experiments were performed to find out the functional group of the surfactant which could be responsible for the polymer degradation. Two entities were considered, namely the ammonium function and the long alkyl chain. First, the PHB was processed in presence of long alkyl chains (pentadecane). The results (not reported here) show that, under the experimental conditions, this chemical entity has no influence on PHB thermal stability. Then, PHB was mixed to tetramethylammonium chloride (TMA) to determine whether the quaternary ammonium cation could favour or not the polymer degradation. This system was processed in the internal mixer (170°C – 50 rpm – 15 min) and the PHB weight average molecular weight after 5 minutes was determined by SEC. Like the other polymer-surfactant systems, the M_w of PHB in presence of TMA (M_w=117,000) has considerably decreased compared to the PHB sample (M_w=412,000 at 5 min, see Table 6). This observation attests that the quaternary ammonium cation chemical entity has a significant effect on the polymer degradation.

According to Xie et al. (Xie, 2001), the well-known Hofmann elimination could take place at these temperatures (around 170°C), turning the quaternary ammonium salt into an amine (Xie, 2001), creating alkenes and releasing a proton (see Scheme 2). This proton could then enhance the polymer chain scission by an acidic catalytic reaction (Zanetti, 2001). Another possible reaction that could occur at these temperatures is the nucleophilic attack of the chloride (counter-ion of the S-Bz ammonium salt) on the quaternary ammonium yielding chloroalkanes and tertiary amine (Xie, 2001) (see Scheme 3). Furthermore, the amines resulting from either Hofmann elimination or from nucleophilic attack could then enhance the mechanism of random chain scission due to their nucleophilic character. The formed amines could also react according to an aminolysis, and aminoglycolysis in the particular case of PHB+S-EtOH blend, as recently reported by Spychaj et al. (Spychaj, 2001) for PET. This last case leading to the formation of amides.

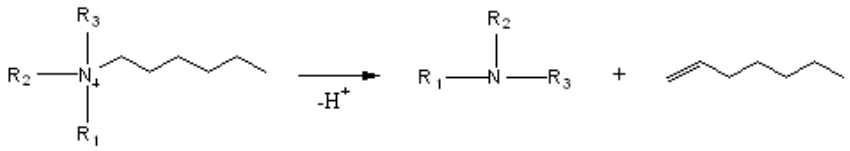

Scheme 2. Hofmann elimination

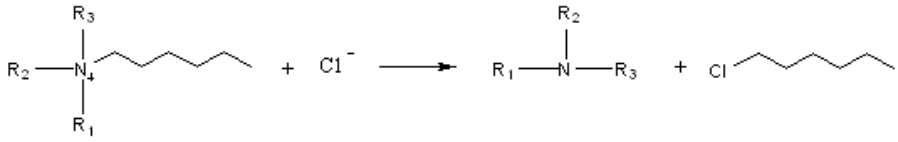

Scheme 3. Nucleophilic attack of chloride

To verify these hypotheses regarding the role of the ammonium salts or their degradation products, further experiments were conducted. Triethylamine (TEA) was mixed to PHB and processed in the same conditions as mentioned before (170°C – 50 rpm). The M_w of the PHB+TEA blend processed for 5 min revealed a considerable decrease (M_w=54,400) compared to the PHB and PHB+TMA samples, M_w=412,000 and 117,000 respectively. Besides, the PHB+TEA torque curve is similar to the PHB+TMA one but shifted to shorter times (see Table 5). This experiment demonstrates that the enhanced PHB degradation is certainly caused by amines resulting from the in-situ degradation of ammonium surfactants.

To emphasize the presence of amines as degradation products, the S-Bz surfactant was annealed at 170°C for 15 min. The ^{1}H NMR spectrum of the obtained material (see Figure 4) revealed typical peaks of the initial product S-Bz (* indexes) as well as characteristic peaks of amines (δ_B=2.2 ppm and δ_c=2.35 ppm for the two methyl groups of the N,N-dimethylalkylamine and N,N-dimethylbenzylamine respectively, δ_D=3.45 ppm for the methylene protons of the benzyl group), chloroalkanes (δ_D=3.5 ppm for the CH_2-Cl methylene protons and δ_A=1.5-2.0 ppm for the methylene protons in β and γ of the chloride) and benzyl chloride (δ_E=4.59 ppm for the methylene protons). No peaks that could be attributed to alkenes were detected. Thus, we can conclude that S-Bz degrades rather by nucleophilic attack of the chloride on the quaternary ammonium (R_4N^+) than by Hofmann elimination. Nevertheless, this last mechanism can not be totally excluded. Indeed, its products (e.g. octadecene, b.p.~180°C) could evaporate during processing and the S-Bz TG curve indicates a 3% wt of weight loss at 170°C that proves that some matter has vaporized at these temperatures. Eventually, the ^{13}C NMR spectrum (not shown here) revealed small peaks at 112-113 ppm, typically attributed to alkene carbons.

With the aim to determine the role of the surfactant on the PHB degradation mechanism, a blend with a very high S-Bz content was prepared. The degradation products of PHB+S-Bz (70:30) were studied by ^{1}H and ^{13}C NMR (not shown here). The ^{1}H NMR spectrum of PHB+S-Bz (70:30) show peaks of each compounds of the blend but also additional peaks resulting from the degradation products. These additional peaks can easily be attributed to the typical chain ends crotonyl groups (δ=1.84-1.87 ppm and 2.1-2.5 ppm for the trans and cis methyl protons respectively, δ=5.76-5.82 ppm and δ=6.9-7.0 ppm for the olefinic protons) resulting from the PHB random chain scission (see Scheme 1). We note that the trans configuration is favoured (trans/cis ratio equals to 13) as described in the literature (Grassie, 1984a; Kopinke, 1996). Furthermore, the ^{13}C NMR spectrum does not show any specific peak of amide. Thus, we can conclude that the

surfactant acts, through the formation of amines, as a catalyst of the PHB random chain scission and that aminolysis can be neglected.

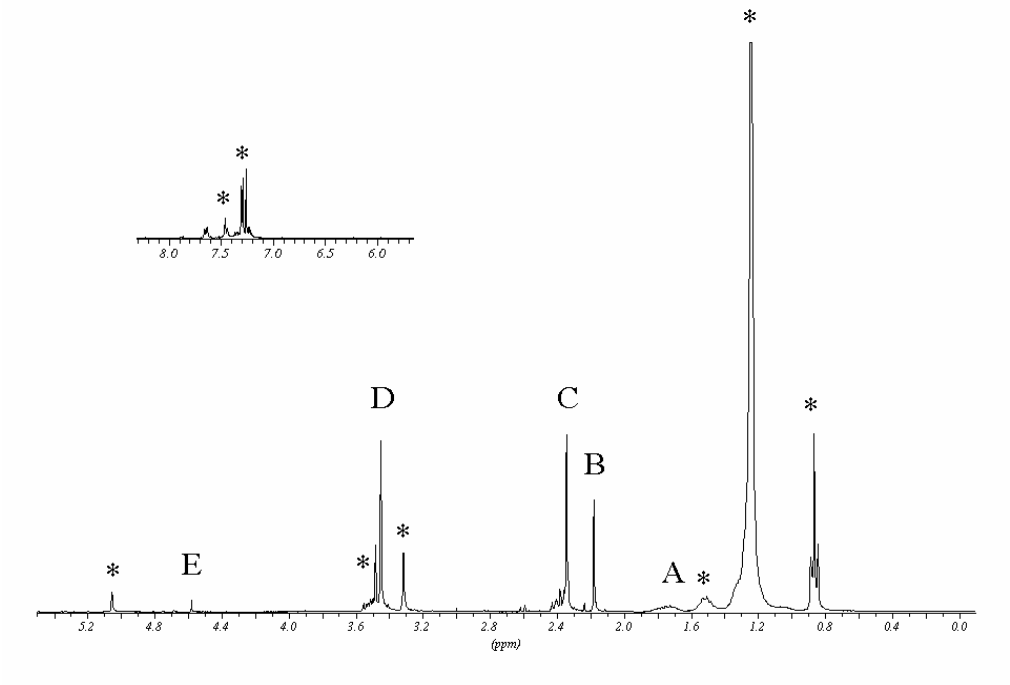

Figure 4. ^{1}H NMR spectrum of the degraded S-Bz (* indexes indicate the original peaks of S-Bz)

As a result, we can reasonably assume that the difference of influence on PHB degradation observed between S-EtOH, S-Alk and S-Bz can be explained by their ability to turn into amine. Nevertheless, the reactions can vary depending on the ammonium substituent groups and thus, additional experiments are needed to determine precisely their role on the ammonium thermal stability, the type of amines formed and their activity towards PHB degradation.

F. Conclusions

The first part of this work is based on the analysis of the thermal degradation of purified PHB and blends containing fermentation residues (Rsd) or quaternary ammonium surfactants (S-Alk, S-Bz or S-EtOH). DSC analyses associated with SEC and TGA measurements showed that the fermentation residues have low influence on the PHB degradation. On the contrary, the addition of ammonium surfactants greatly boosts the PHB degradation. To quantify the thermal degradation, the activation energy and the degradation reaction mechanism of each system have been determined from TGA results using the Coats & Redfern model.

Several conclusions have been drawn: (i) the degradation mechanisms of both the purified PHB and the surfactant in the blend are dependent whereas the fermentation residues have almost

no influence on the polymer main degradation step, (ii) both unpurified and purified PHB (i.e., with and without fermentation residues) degrade according to a first-order reaction whereas PHBp with surfactant likely degrades following a phase boundary controlled mechanism, (iii) S-Alk and S-Bz appear to be the most degrading surfactants compared to S-EtOH.

The thermo-mechanical study has led to the same conclusions regarding the influence of surfactants and fermentation residues on the polymer degradation. Nevertheless, these results have also shown that processing conditions have a great influence on the PHB thermal stability since the higher the mixer rotation speed, the faster and the greater the degradation.

Besides, TG analysis on a ternary mixture has shown that a synergistic effect between surfactants and fermentation residues occurs and favours the polymer degradation.

A possible mechanism of degradation has been proposed based on NMR characterizations. The R_4N^+ surfactant turns into an amine through either nucleophilic attack of the ammonium counter-ion or Hofmann elimination. Then, the released acidic proton and/or the nucleophilic amine formed act as catalysts of the PHB random chain scission. Thus, the differences in surfactants activity towards PHB degradation are directly linked to the variations in ammonium thermal stability stemming from the different substituent groups.

These conclusions are remarkable because they demonstrate why it is presently difficult to obtain PHB/OMMT nano-biocomposites by a melt intercalation process. Indeed, it has been demonstrated that quaternary ammonium surfactants used as montmorillonite organo-modifiers for nano-biocomposites purposes increase the PHB thermal sensitivity so that their presence during melt processing of such materials is thus not favourable. On the contrary, fermentation residues have quite no influence on the PHB thermal degradation and thus, do not hinder the use of the melt processing way.

Using the same approaches, this study could easily be extended to other thermally sensitive biodegradable polymers (e.g. polyhydroxybutyrate-co-hydroxyvalerate, polysaccharides, polylactide…) for which the elaboration of nano-biocomposites based on organo-modified montmorillonites is also of great interest.

G. Acknowledgments

The authors thank the GMI-IPCMS (Institut de Physique et Chimie des Matériaux de Strasbourg), the ICS (Institut Charles Sadron) in Strasbourg (France) and Mrs Ducruet from the ENSIA-INRA in Massy (France) for their technical support. Biocycle (Copersucar-Brazil) is acknowledged for providing the PHA.

H. Discussion et commentaires

Le but de cette étude était de déterminer le rôle des résidus de fermentation et des organomodifiants de type ammonium quaternaire sur la dégradation thermique et thermomécanique du polyhydroxybutyrate (PHB) pour mieux appréhender la stabilité thermique du même polymère dans les matériaux nanocomposites.

Dans un premier temps, la dégradation du PHB a été étudiée lors de traitements thermiques (calorimétrie différentielle et thermogravimétrie) auxquels ont été soumis le PHB purifié, seul ou en présence des résidus de fermentation ou des ammoniums quaternaires (S-Alk, S-Bz ou S-EtOH). Ces approches originales ont montré que, contrairement à ce que l'on pourrait penser, les résidus de fermentation semblent avoir peu d'influence sur la dégradation du PHB tandis que les organomodifiants affectent considérablement sa stabilité thermique. Ces observations ont pu être étayées par le calcul des énergies d'activation de dégradation selon le modèle cinétique connu de Coats & Redfern. Ces résultats nous ont conduits à tirer les conclusions suivantes : i) les mécanismes de dégradation du PHB purifié et des ammoniums quaternaires dans les systèmes polymère-organomodifiant sont liés, ii) le PHB, purifié ou non, i.e. avec ou sans résidus de fermentation, se dégrade selon une réaction du premier ordre tandis que les systèmes polymère-ammonium quaternaire se dégradent suivant une réaction d'avancement d'interface (type R), iii) S-Alk et S-Bz s'avèrent être les ammoniums quaternaires ayant le plus d'influence sur la dégradation du PHB. Par ailleurs, il a été démontré qu'il existe un effet de synergie entre les résidus de fermentation et l'ammonium quaternaire, diminuant davantage la stabilité thermique du polymère.

L'étude thermomécanique, qui simule la dégradation que peut subir le polymère lors de la mise en œuvre à l'état fondu des matériaux nanocomposites, a conduit aux mêmes conclusions.

Enfin, l'analyse de la cinétique et des produits de dégradation nous a également permis de proposer un mécanisme de dégradation. L'ammonium quaternaire se dégraderait en amine par une attaque nucléophile du contre-ion de l'ammonium ou par une réaction d'élimination d'Hofmann. L'amine et/ou le proton issu(s) de ces réactions joueraient le rôle de catalyseur de la scission aléatoire des chaînes PHB.

On peut donc considérer que, dans la préparation des nanocomposites par voie "fondu", la présence simultanée des résidus de fermentation et des ammoniums quaternaires affecte la masse molaire du PHB selon le même processus que celui décrit dans cette étude. Les propriétés du polyester vont donc être fortement altérées lors de la mise en œuvre. De plus, Xie et al. (Xie, 2001) ont montré que des sites catalytiques, type acides de Lewis, présents dans le feuillet inorganique

détériore la stabilité thermique des alkylammoniums quaternaires. Par conséquent, on peut facilement imaginer que la stabilité thermique de nos systèmes nanocomposites, i.e. en présence de feuillets inorganiques, d'ammoniums quaternaires et de résidus de fermentation, sera d'autant plus fragilisée.

Cherchant à minimiser ces problèmes de tenue en température, nous nous sommes intéressés aux copolymères poly(hydroxybutyrate-co-hydroxyvalérate) (PHBV), connus pour présenter une température de fusion et de mise en œuvre plus faible que l'homopolymère PHB. Il nous a donc paru intéressant d'étudier la stabilité thermique et thermomécanique de différents grades de PHBV (taux de HV de 4 et 8 %) dans des conditions similaires à la préparation des nano-biocomposites. Ce travail est présenté dans la **publication n°4** rapportée ci-dessous.

Publication n°4.

"Effect of clay organomodifiers on polyhydroxyalkanoates degradation"

P. Bordes, E. Hablot, E. Pollet, L. Avérous*

Macromolecular Chemistry and Physics, submitted.

A. Abstract

Ammonium surfactants are commonly used as clay organomodifiers in nanocomposites. Their effect on the thermal and thermo-mechanical degradation of polyhydroxyalkanoates (PHAs) is presently studied. Two poly(hydroxybutyrate-*co*-hydroxyvalerate) (PHBV) grades were tested and compared to polyhydroxybutyrate (PHB). Thermal stabilities were determined from thermogravimetric data and analyzed using the Coats & Redfern model. The results revealed that all surfactants greatly enhance the PHAs degradation since their decomposition products act as catalytic agents. This study also highlights the preponderant effect of the initial M_w rather than the HV content on the thermal stability. The thermo-mechanical study confirmed the role of surfactants and their different behaviour towards PHBV degradation.

*Keywords***:** ammonium surfactants ; biopolymers ; polyhydroxyalkanoates ; renewable resources ; thermal degradation.

* Corresponding author: Luc Averous.

Tel.:+33-3-90-242-707 - Fax: +33-3-90-242-716 - AverousL@ecpm.u-strasbg.fr

B. Introduction

Polyhydroxyalkanoates (PHAs) represent an interesting alternative to synthetic polymers due to many advantages. Not only they are biodegradable and biocompatible, but they can also be produced by bacterial fermentation from renewable resources like cane sugar. The poly(3-hydroxybutyrate) (PHB), the most common PHA, was first discovered in 1926 by Lemoigne (Lemoigne, 1926; Lenz, 2005) and is now produced at the industrial scale (Nonato, 2001). Nevertheless, this material shows some drawbacks compared to conventional polymers, such as a high stiffness, brittleness and shows poor thermal stability at temperature just above the melting point (Grassie, 1984a, 1984b, 1984c; Gain, 2005). To improve the properties of biodegradable polymers like PHAs, nano-biocomposites (Pandey, 2005; Chivrac, 2006) (nanocomposites based on biodegradable matrices) seem to be a good answer since they have raised great interest in recent years thanks to the enhancement of material properties. But in a preliminary study (Hablot), we have shown that organomodifiers (quaternary ammonium surfactants), used to compatibilize the nanoclays and the matrix, could dramatically enhance in certain cases the polymer degradation in the molten state.

To overcome the PHB sensitivity to temperature, one possible way is to insert hydroxyvalerate (HV) units along the polymer chain. The resulting copolymer, the poly(3-hydroxybutyrate-co-3-hydroxyvalerate), PHBV, will have a lower melting point and thus, the processing temperature window will be enlarged. Thereby, the materials are expected to be less prone to thermal degradation (He, 2001; Li, 2001; Carrasco, 2006).

Therefore, the aim of this article is to simulate nanocomposites systems in order to determine the montmorillonite organomodifiers effect on the degradation of the main PHAs, and finally, to understand the degradation mechanism in such multiphase systems. The PHBV degradation will be analyzed in the light of PHB one (Hablot). No attempt was reported regarding the degradation mechanism in such nanocomposite materials although the degradation of PHAs has been largely studied (Grassie, 1984a, 1984b, 1984c; Billingham, 1987; Kunioka, 1990; Kopinke, 1996; He, 2001; Lee, 2001; Li, 2001; Aoyagi, 2002; Li, 2003; Abe, 2006; Carrasco, 2006).

The thermal degradation activation energies were calculated for each system by applying the Coats & Redfern kinetic analytical model (Coats, 1964) to non-isothermal thermogravimetric (TG) measurements. This latter is based on a single step kinetic equation (Equation (1)).

$$\frac{d\alpha}{dt} = k(T) \cdot f(\alpha) \quad (6)$$

where α represents the fractional extent of conversion (i.e. weight loss), dα/dt is the rate of conversion and f(α) is a temperature-dependent function of conversion that depends on the degradation mechanism and k(T) is a temperature-dependent function.

Considering the Arrhenius equation leads to Equation (2).

$$\frac{d\alpha}{dt} = A \cdot \exp\left(-\frac{E_a}{RT}\right) \cdot f(\alpha) \quad (7)$$

where A is the pre-exponential factor independent of temperature, E_a the activation energy, R the gas constant and T the absolute temperature.

The representative equation of the Coats & Redfern method (Coats, 1964) (see Equation (3)) is obtained by multiple integration and combination of Equation (2), where g(α) is a function depending on the type of degradation mechanism and is related to f(α) by Equation (4). By plotting $\ln[g(\alpha)/T^2]$ as a function of 1/T, the slope of the obtained straight line is directly proportional to E_a.

$$\ln\left[\frac{g(\alpha)}{T^2}\right] = \ln\left(\frac{AR}{\beta E}\right) - \frac{E_a}{RT} \quad (3)$$

$$\text{where } g(\alpha) = \int_0^{\alpha} \left[f(\alpha)\right]^{-1} \cdot d\alpha \quad (4)$$

Eventually, to simulate the degradation of the PHA-based nano-biocomposites during processing, the thermo-mechanical degradation was also examined. The effect of different organomodifiers (surfactants) was studied by calculating the mechanical energy supplied to each system from the torque curves and by measuring the weight average molecular weight (M_w) at different processing times.

C. Experimental Section

C.I. Materials

Two types of poly(3-hydroxybutyrate-*co*-3-hydroxyvalerate) (PHBV) samples, produced by bacterial fermentation of sugar cane compounds, were kindly supplied by Biocycle PHB Industrial S/A, Brazil. The percentage of HV units in the copolymers was calculated from NMR spectra of PHA solutions in $CDCl_3$ (see Table 1). Table 1 gives also the weight average molecular weight (M_w) and the polydispersity index (PDI) determined by size exclusion chromatography (SEC), and the melting point (T_m) determined by differential scanning calorimetry (DSC). Both PHBV can be compared to a PHB which is used as a reference. This latter has been carefully

analysed and reported in a previous article (Hablot). Its main characteristics are also indicated in Table 1.

The clay organomodifiers selected were quaternary ammonium cations commonly used in commercial organo-modified montmorillonite (OMMT). Di(hydrogenated tallow)dimethylammonium chloride (S-Alk), (vegetable oil)benzyldimethylammonium chloride (S-Bz) and oleylbis(2-hydroxyethyl)methylammonium chloride (S-EtOH) in isopropyl alcohol - from Akzo Nobel - were kindly supplied by Brenntag Specialities (see Table 2). The tetramethylammonium chloride (TMA) (reagent grade, 97%) was supplied by Sigma-Aldrich.

Table 1. Characteristics of the PHA samples

Polymer	Reference	%HV	Mw	PDI	Tm (°C)
PHB	PHB	0	650,000	2.1	175
PHBV	PHBV4	4	930,000	1.7	173
PHBV	PHBV8	8	280,000	2.2	158

Table 2. Structure of the ammonium surfactants

Surfactants	Structure
S-Alk	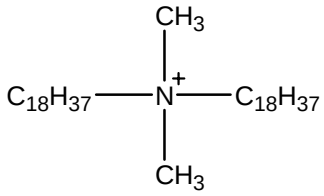
S- Bz	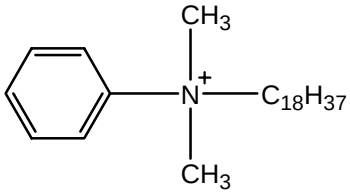
S-EtOH	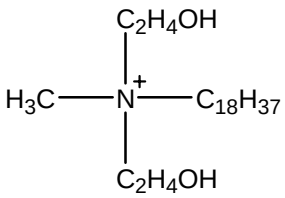

C.II. Polymer purification

Usually, since the PHAs are produced by bacterial fermentation, residues (phospholipids, fatty acids, proteins, amino acids, etc.) stemming from the bacteria cells still remain in the as-received biopolymers. To remove these fermentation residues, PHAs purification was performed by soxhlet extraction with diethyl ether (SDS Carlo Erba) for 24h. Purified PHA samples (PHBV4p, PHBV8p and PHBp) were recovered and dried at 80°C under vacuum. The liquid phase was collected and the extracted fermentation residues were recovered after solvent evaporation. The initial amount of fermentation residues in both raw PHBV samples is equal to ca. 1 wt.-%, as determined by gravimetry.

The nitrogen content in the extracted residues was determined. The titration leads to about 1% of nitrogen in the extract that corresponds to less than 60 ppm in the raw PHAs.

C.III. Samples preparation

To remove isopropyl alcohol and water from the commercial ammonium solutions, S-Alk and S-Bz were dispersed into diethyl ether, filtered and dried under vacuum in order to obtain white powders. Then, they were added and intimately mixed to the dried purified PHA. Regarding the S-EtOH surfactant, the pasty nature of this compound makes difficult the homogeneous mixing with the purified PHA powder. Thus, it has been dispersed into diethyl ether and mixed to the purified PHA. Then, once the solvent was evaporated, the mixture was dried under vacuum.

For the thermo-mechanical degradation study, the samples were prepared in an internal mixer Haake Rheocord 9000 at 160°C. Due to the limitation to obtain large amounts of purified PHA, this study was performed on samples prepared with the "as-received" raw PHA. Different processing times were tested, ranging from 3 to 15 min, respectively. The torque and the melt temperature were recorded during the processing. The mechanical energy was calculated using Equation (5) where N is the rotation speed ($rad \cdot s^{-1}$), M the sample mass (kg) introduced in the mixing chamber and S the area defined by the torque vs. time curve.

$$E_m\ (kJ/kg) = \left(\frac{N}{M}\right) \cdot S \quad (5)$$

All the PHA-surfactant systems contain 3 wt.-% of ammonium cations.

C.IV. Characterizations

Thermogravimetric analyses (TGA) were conducted under nitrogen flow using a Hi-Res TGA 2950 apparatus from TA Instruments. The surfactants, the neat polymers and the polymer-surfactants systems (10-20 mg placed in an aluminium pan) were heated up to 500°C at 5 and 10°C · min^{-1}. The characteristic degradation temperatures T_{dmax} and $T_{x\%}$, which are respectively, the temperature of the maximum of the DTG curve and the temperature at which the sample weight equals x% of the initial one, are determined.

Size Exclusion Chromatography (SEC) measurements were performed using a Shimadzu apparatus equipped with a RID-10A refractive index detector and a SPD-M10A UV detector. The columns used were PLGel Mixed-B 10 µm. The calibration was realized with PS standard from 580 to 1,650,000 g · mol^{-1}. Chloroform (puriss p.a. Riedel-de Haën) was the mobile phase and the analyses were carried out at 30°C with a solvent flow rate of 1 ml · min^{-1}. The SEC measurements were performed on the samples recovered after different processing times in the internal mixer.

D. Results and discussion

D.I. Thermal degradation

Thermal stability of PHA-surfactants systems has been investigated through the degradation mechanism, kinetics and characteristic temperatures determined by TG analyses.

D.I.1. Characteristic degradation temperatures

Figure 1 and 2 present the TG curves of purified PHBV/surfactant samples recorded at 10°C · min^{-1}. Table 3 summarizes the PHA characteristic temperatures (T_{dmax} and $T_{x\%}$). First, both purified PHBV samples (PHBV4p and PHBV8p) degrade within the same interval of temperature (285-298°C). Furthermore, their degradations seem to follow the same mechanism since the degradation occurs according to a single-step weight loss. Besides, the maxima of the DTG curves are very close since T_{dmax} equals 294°C and 293°C for PHBV4p and PHBV8p, respectively.

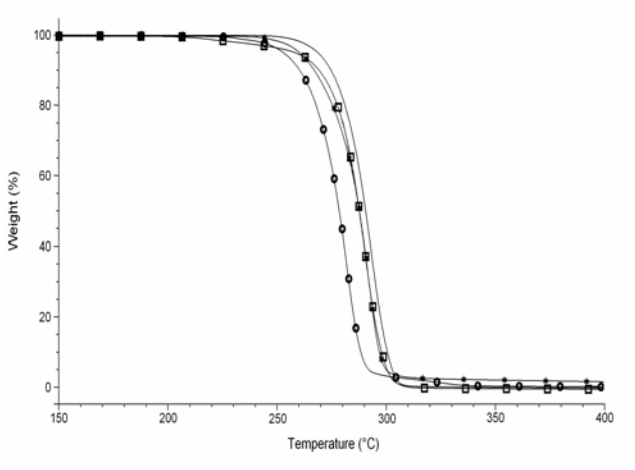

Figure 1. TG curves at 10°C · min^{-1} for PHBV4p (—), PHBV4p+S-Alk (O), PHBV4p+S-Bz (□) and PHBV4p+S-EtOH (✶).

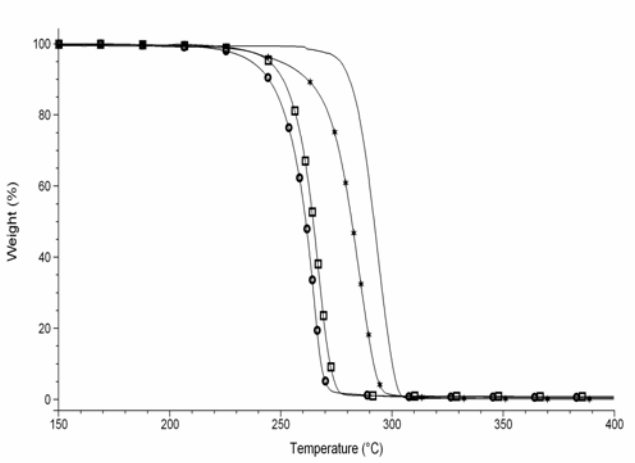

Figure 2. TG curves at 10°C · min^{-1} for PHBV8p (—), PHBV8p+S-Alk (O), PHBV8p+S-Bz (□) and PHBV8p+S-EtOH (✶).

Considering the PHBV4p-based systems, Table 3 shows that S-Bz and S-EtOH have low effect on polymer degradation, the characteristic temperatures being only shifted of few degrees compared to neat PHBV4p. Nevertheless, the $T_{80\%}$ shifts tend to be higher than the T_{dmax} and $T_{20\%}$ ones. This trend, observed for all the systems, means that the degradation starts at lower temperatures in the case of the PHA-surfactant systems. The onset temperature of the surfactants degradation are equal to 180°C, 185°C and 220°C for S-Alk, S-Bz and S-EtOH, respectively. If we consider these temperatures, one can reasonably affirm that the start of the PHA-surfactant degradation is affected by the surfactant degradation itself. Then, the $T_{80\%}$ will not be taken into account as a key parameter for monitoring the polymer degradation. In the case of PHBV4p+S-Alk, the temperature shifts (with respect to the neat matrix) on T_{dmax} and $T_{20\%}$ are higher (about -

11°C) compared to other systems. Obviously, PHBV4 presents a particular sensitivity to this surfactant.

Table 3. Degradation temperatures obtained from TG curves recorded at 10°C/min.

	PHBV4p			PHBV8p			PHBp		
	$T_{80\%}$ [a]	T_{dmax} [b]	$T_{20\%}$ [a]	$T_{80\%}$ [a]	T_{dmax} [b]	$T_{20\%}$ [a]	$T_{80\%}$ [a]	T_{dmax} [b]	$T_{20\%}$ [a]
Pure	285	294	297	285	293	298	285	295	298
S-Alk	269	282	286	252	264	266	259	275	277
S-Bz	279	291	295	257	267	270	275	292	294
S-EtOH	276	293	295	271	285	289	274	287	291

[a] $T_{x\%}$: temperature at which the weight sample equals x% of the initial value;
[b] T_{dmax}: temperature of the DTG curve maximum.

Regarding PHBV8p-surfactants systems, the degradations occur at lower temperatures compared to neat PHBV8p. On one hand, S-Alk and S-Bz have strong effects since temperature shifts are about -30°C. On the other hand, S-EtOH has a lower effect since the temperature shift is only around -10°C.

By comparing both PHBV, we can consider that all the surfactants studied have an effect on polymer degradation, S-Alk being the most degrading one. Nevertheless, PHBV4 seems less sensitive than PHBV8. This result is more likely due to the difference in molecular weight rather than the difference of HV content. Indeed, first, there is no difference in TG curves between both purified PHBV samples. Secondly, since the degradation is supposed to occur by random chain scission with or without surfactants as demonstrated recently for PHB (Hablot), the lower the initial M_w, the faster we obtain short chain lengths, and thus, the less thermally stable the PHA.

D.I.2. Dependence between PHA and surfactant degradation mechanisms

Before determining the activation energy of the degradation reactions, we have checked the possible dependence that could exist between the degradation mechanisms of both the polymer and the surfactant thanks to Equation (6) (Torre, 1998).

$$W = W_S \cdot x_S + W_{PHAp} \cdot x_{PHAp} \quad (6)$$

where W is the residual weight fraction of the PHA-surfactant system, W_s and W_{PHAp} the residual weight fractions of the surfactant and the purified PHA respectively, and eventually, x_s and x_{PHAp} the initial content of the corresponding compound in the PHA-surfactant system.
This equation allows to draw the calculated TG curve of a multicomponent system from the experimental TG data of each of its components, i.e. the polymer and the surfactant, when the degradations are considered independent. By comparing the calculated and the experimental TG curves of the studied system, we can determine whether the degradations of the compounds of a blend are chemically dependent. In our case, compared to the calculated TG curve, T_{dmax} measured from experimental data are lowered by 30°C, 27°C and 9°C for PHBV8p+S-Alk, PHBV8p+S-Bz and PHBV8p+S-EtOH respectively. In the case of PHBV4, these temperature shifts equal 12°C for PHBV4p+S-Alk and only few degrees for PHBV4p+S-Bz and PHBV4p+S-EtOH.

Thus, we can conclude that in such systems, polymer and surfactants degradations are dependant. This phenomenon highlights that surfactants, particularly S-Alk, play a key role in the PHBV thermal degradation. Moreover, this analysis confirms that initial M_w has a significant effect since the smaller the M_w, the greater the degrading effect.

D.I.3. Coats & Redfern model applied to TGA data

To better understand the thermal degradation of PHA-based systems and their related reaction mechanisms, we have evaluated the kinetic parameters (activation energy E_a and pre-exponential factor A) and the mechanism-dependent function g(α) by applying the Coats & Redfern model to the mass loss data obtained from dynamic thermogravimetric analyses. The studied systems are based on the most thermally sensitive PHBV sample, i.e. PHBV8.

The thermal degradation activation energy was obtained by plotting $\ln[g(\alpha)/T^2]$ as a function of 1/T. Table 4 presents twelve different probable forms of g(α) among the most commonly used functions of solid-state processes (Hatakeyama, 1999; Vyazovkin, 1999; Swain, 2005). Typically, for each TG curve, all the g(α) functions were tested and the one which presents the best linearity (r^2 closest to 1) is considered as the most probable reaction mechanism for the thermal degradation. The analysis has been performed from TG data obtained at the lowest heating rate ($5°C \cdot min^{-1}$) to better observe the degradation phenomenon and thus to have a better discrimination between the possible mechanisms.

Table 4. Set of solid-state reactions (g(α)) used for kinetic parameters calculation

Mechanism	Code	g(α)
Exponential law	-	$-\ln(\alpha)$
Avrami-Erofeev law	$A_{1.5}$	$[-\ln(1-\alpha)]^{2/3}$
	A_2	$[-\ln(1-\alpha)]^{1/2}$
	A_3	$[-\ln(1-\alpha)]^{1/3}$
	A_4	$[-\ln(1-\alpha)]^{1/4}$
Prout-Tompkins law	B_1	$\ln[\alpha/(1-\alpha)]$
Chemical reaction of n^{th} order (F_n)	F_1	$-\ln(1-\alpha)$
	F_2	$1/(1-\alpha)$
	F_3	$1/(1-\alpha)^2$
Phase boundary controlled reaction (contracting area)	R_2	$[1-(1-\alpha)^{1/2}]$
Phase boundary controlled reaction (contracting volume)	R_3	$[1-(1-\alpha)^{1/3}]$
Three dimensional diffusion spherical symmetry (Jander equation)	D_3	$[1-(1-\alpha)^{1/3}]^2$

The curves plotted according the Coats & Redfern model have highlighted that there is one main degradation step corresponding to the PHBV degradation but also secondary degradations corresponding to the degradation of surfactants before and/or after main degradation. This was previously mentioned when considering the onset temperature of the surfactants degradation and the $T_{80\%}$ characteristic temperature of PHA-surfactant systems. Table 5 shows the main results obtained with the Coats & Redfern method, i.e. the most suitable reaction mechanism and the related values for the activation energy E_a and the pre-exponential factor A for each system.

First, the reaction mechanism of PHBV8p thermal degradation follows a first order reaction (F1 type). This is on agreement with results obtained by Cyras et al. (Cyras, 2000) The PHBV8p activation energy, equal to 409 kJ · mol^{-1}, is higher than other systems for which the E_a values are ranging from 202 to 230 kJ · mol^{-1} (see Table 5). Thus, the purified PHBV8 is more stable than samples containing surfactants. Besides, from the most probable reaction mechanisms determined for these systems, one can conclude that the studied ammonium surfactants favour and enhance the PHBV8p thermal degradation through a phase boundary controlled process (R type).

Table 5. Kinetic parameters of the PHBV8p- and PHBp-based systems degradation according to the Coats & Redfern method

System	Temperature range		Model	E_a (kJ/mol)	r^2	A (s^{-1})
	Start (°C)	End (°C)				
PHBV8p	250	288	F1	409	0.9980	4.89E+35
PHBV8p+S-Alk	225	275	R2	230	0.9994	8.16E+30
PHBV8p+S-Bz	230	280	R2	226	0.9998	2.03E+30
PHBV8p+S-EtOH	215	285	R2	202	0.9964	8.52E+27
PHBp	230	305	F1	395	0.9962	3.25E+35
PHBp+S-Alk	200	240	R3	200	0.9948	1.07E+18
PHBp+S-Bz	220	290	R2	166	0.9796	1,47E+13
PHBp+S-EtOH	210	280	R2	161	0.9860	5,13E+12

D.I.4. Comparison between PHB and PHBV

Since PHB and PHBV are the main available PHAs, it is interesting to compare the results obtained for PHBV-based systems to the thermal behaviour of the corresponding PHB ones. TG analyses of purified PHB, PHBV4 and PHBV8 show that these samples degrade in the same temperature range with almost the same T_{dmax} (see Table 3) in spite of the difference of M_w and the increasing HV content.

Regarding the PHA-surfactant systems, the temperature shifts (with respect to the neat PHA) observed on $T_{80\%}$ and $T_{20\%}$ are lower for PHBV4 compared to PHB whatever the surfactant considered (see Table 3). For example, the temperature shift on $T_{20\%}$ equals -11°C for PHBV4p+S-Alk whereas a shift of -21°C is observed for PHBp+S-Alk. Furthermore, T_{dmax} are globally higher in the case of PHBV4-based systems indicating that PHBV4 is the most thermally stable matrix. Thus, we can sort the polymers according to their sensitivity towards the degrading effect of the surfactants as follows: PHBV8 > PHB > PHBV4.

In conclusion, an increase in the HV content has no effect on the neat polymer thermal stability whereas in presence of surfactants, the PHBV8 is more sensitive to thermal degradation. Consequently, this study does not allow us stating on the impact of HV units content but rather highlights the preponderant effect of the initial M_w.

The effect of surfactants on the thermal stability of PHBV samples is on agreement with the one observed in the case of PHB. Indeed, all the PHA-surfactant systems present lower activation energy of thermal degradation compared to neat polymer (see Table 5), indicating that all the surfactants have a significant degrading effect. Furthermore, all the PHA-surfactant systems degrade according to a phase boundary controlled process (R type). Eventually, S-Alk seems to enhance the most the PHAs degradation (see Table 3) even if the activation energies are similar to those of other PHA-surfactant systems.

D.II. Thermo-mechanical degradation

To simulate the degradation of the PHA-based nano-biocomposites during the processing, the thermo-mechanical degradation was also studied during a mixing step. The mixer torque values have been monitored during the experiments and the corresponding curves are presented in Figure 3 and 4. Samples have been taken from the mixer during the experiment at 5, 10 and 15 min to determine the weight average molecular weight by SEC. The M_w values of the different systems are reported in Table 6.

On one hand, the torque and the molecular weight evolutions follow globally the expected trends. On the other hand, we can notice some significant differences between PHBV with and without surfactants. Indeed, for both neat PHBV, the maximum torque value is higher and is reached earlier compared to the corresponding surfactants-based systems.

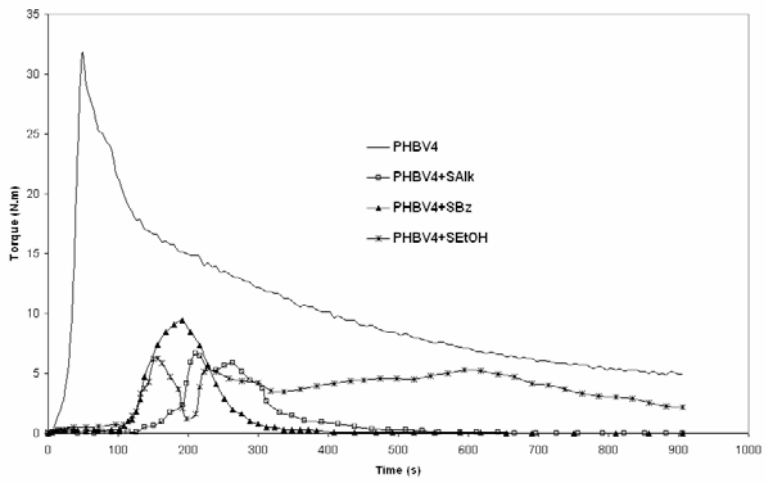

Figure 3. Evolution of the torque at 160°C and 50 rpm for 15 minutes for PHBV4-based systems.

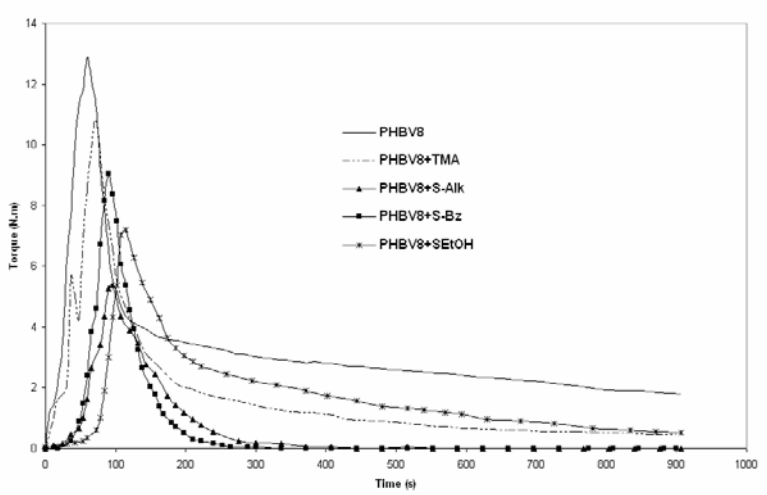

Figure 4. Evolution of the torque at 160°C and 50 rpm for 15 minutes for PHBV8-based systems.

Table 6. Weight average molecular weight ($M_w \times 10^{-3}$) of PHA-based systems processed at 160°C and 50 rpm for different times.

		$M_w \times 10^{-3}$				
		Surfactant				
Polymer	t (s)	∅	S-Alk	S-Bz	S-EtOH	TMA
PHBV4	300	660	180	91	679	-
	600	427	37	33	392	-
	900	327	21	21	184	-
PHBV8	300	185	90	56	163	174
PHB	300	412	106	39	263	117

In the case of PHBV8-based systems, the torque reaches a plateau at ca. 850 s and 800 s for neat PHBV8 and PHBV8+S-EtOH respectively, whereas a zero-torque is recorded after 300 s and 250 s for PHBV8+S-Alk and PHBV8+S-Bz, respectively (see Figure 4). This zero-torque can be attributed to the PHBV8 degradation enhanced by the surfactants. This is confirmed by SEC analyses results, presented in Table 6, showing that the samples collected after 5 min of processing already present a significant molecular weights decrease for PHBV8+S-Alk and PHBV8+S-Bz reaching -68% and -80%, respectively (compared to the initial M_w - see Table I) whereas this decrease is only of -34% and -42% for PHBV8 and PHBV8+S-EtOH, respectively. Furthermore, the mechanical energies (E_m) calculated from the torque curves correlate these observations since the mechanical energies of PHBV8+S-Alk and PHBV8+S-Bz systems are the lowest being

E_{m15}=54 and 59 kJ · kg^{-1}, respectively (see Table 7). Moreover, these values remain unchanged when increasing mixing time from 5 to 15 minutes, attesting to a decrease in viscosity.

Table 7. Mechanical energies provided to PHBV4- and PHBV8-based systems after 5 (E_{m5}) and 15 minutes (E_{m15}) of melt processing at 160°C and 50 rpm.

Polymer	PHBV4		PHBV8		PHB	
	E_{m5}	E_{m15}	E_{m5}	E_{m15}	E_{m5}	E_{m15}
Surfactant	(kJ · kg^{-1})		(kJ · kg^{-1})		(kJ · kg^{-1})	
∅	502	976	152	303	400	640
S-Alk	69	94	53	54	50	50
S-Bz	101	107	59	59	50	50
S-EtOH	83	335	88	160	70	130

As observed for PHBV8, the neat PHBV4 torque value is higher than PHBV4-surfactant systems, attesting to a greater degradation. Moreover, regarding PHBV4, one can notice that the torque value is considerably higher than the PHBV8 one (see Figure 3). This observation can be explained by the gap between its melting point (T_m=173°C, see Table I) and the temperature of processing (T=160°C), resulting in a high viscosity of the melt. Secondly, it can be seen that, even if the torque curves of PHBV4-based systems are globally in the same range and follow the same trends as PHBV8-based systems, differences in thermo-mechanical behaviour exist between the PHBV grades. First, the torque stabilizes later in the case of PHBV4-based systems, reaching a plateau after 900 s for PHBV4 whereas a zero-torque is recorded at around 450 and 350 s for PHBV4+S-Alk and PHBV4+S-Bz, respectively. These results tend to confirm the better thermal stability of PHBV4 during melt processing. Secondly, a remarkable torque curve was obtained in the case of PHBV4+S-EtOH system since the torque is maintained until 600 s. Consequently, the final mechanical energy is rather high (E_{m15}=335 kJ · kg^{-1}) compared to the other PHBV4-surfactant systems (see Table 7). This phenomenon could be explained by the difficulty of PHBV4+S-EtOH to melt. Therefore, the M_w drop seems limited until 600 s since the decrease for PHBV4+S-EtOH is in the same range as for the neat PHBV4 one (see Table 6). Eventually, a zero-torque value is observed in the early stage of processing for PHBV4-surfactant systems. This unusual phenomenon could be explained by lower T_m for PHBV4+S-Alk and PHBV4+S-Bz systems and by a possible lubricant behaviour of the corresponding surfactants. In contrast, for PHBV4+S-EtOH, the zero torque is more likely due to the difficulty to melt.

In conclusion, all these observations show that in the presence of surfactant, the melt is less viscous due to an enhanced degradation, except with S-EtOH. In this particular case, the degrading effect on the polymer seems limited, or at least, delayed.

D.II.1. Identification of the degradation chemical mechanism

To complement these results, PHBV8 was mixed to tetramethylammonium chloride (TMA) to determine whether the quaternary ammonium cation could favour the PHBV degradation as demonstrated in the case of PHB (Hablot). This system was processed in an internal mixer (160°C – 50 rpm – 15 min) and the PHBV8 weight average molecular weight after 5 minutes was determined by SEC. Table 6 compares the M_w of PHBV8+TMA with values obtained from different PHBV8-based samples processed in the same conditions.

As previously mentioned, the M_w of all the PHBV8-surfactant systems have considerably decreased compared to the PHBV8 sample. Such a M_w decrease is also observed for PHBV8+TMA since the M_w reaches 174,000. This result, combined with the torque curves trends, attests that the quaternary ammonium cation chemical entity has a significant effect on the thermo-mechanical degradation. Therefore, one can reasonably suppose that the surfactants enhance the PHBV degradation in the same manner as reported in the case of PHB (Hablot). The surfactant starts to decompose according to the Hofmann elimination (Xie, 2001) (see Scheme 1) or a nucleophilic attack of the ammonium counter-ion, generally the chloride ion, on the ammonium (see Scheme 2). The decomposition products, amines or acidic protons, could then enhance the random chain scission reaction of PHB or PHBV (see Scheme 3). The difference observed between surfactants only depends on the thermal stability of the ammonium cations, which is linked to their substituent groups.

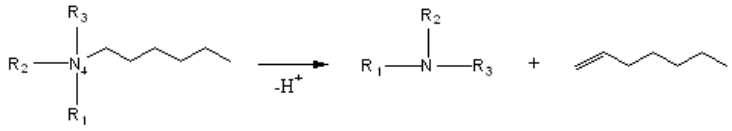

Scheme 1. Hofmann elimination

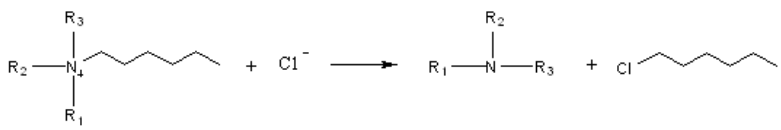

Scheme 2. Nucleophilic attack of chloride

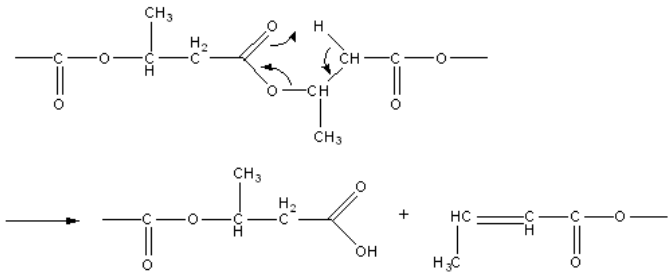

Scheme 3. PHB random chain scission

D.II.2. Comparison PHB and PHBV

Compared to PHB (Hablot), we observe the same surfactant degrading effect during processing in the case of PHBV samples, i.e. S-Alk and S-Bz have a higher impact than S-EtOH on the polymer degradation (see Table 6 & 7). Nevertheless, as the incorporation of HV units decreases the melting point, it is possible to process the PHBV samples at a lower temperature. This observation is appealing in the case of PHBV+S-EtOH, and particularly with PHBV4+S-EtOH, for which the degradation seems limited even after 15 minutes of processing.

E. Conclusions

This paper reports the thermal and thermo-mechanical degradation of the main PHAs, i.e. PHB and PHBV, in the presence of ammonium surfactants, commonly used as clay organomodifiers.

First, the thermal degradation studies based on TG data of PHBV with and without quaternary ammonium cations show that all surfactants have an effect on the polymer degradation. This effect is all the more pronounced since the initial M_w of the polymer is low. The results regarding the thermal stability in presence of surfactants were confirmed by the determination of kinetics parameters, particularly activation energies, using the Coats & Redfern method. They led to several conclusions: (i) the degradation mechanisms of both the purified PHBV and the surfactant in the blend are dependent, (ii) all the PHBV-surfactant systems degrade according to a phase boundary controlled mechanism, (iii) S-Alk appears to be the most degrading agent. These conclusions are totally on agreement with the results obtained for PHB.

The thermo-mechanical study has led to the same conclusions regarding the effect of surfactants since the mechanical energy, and thus the viscosity, is superior for neat PHBV. Moreover, S-Alk and S-Bz appear the most degrading surfactants. This study has revealed an

interesting thermo-mechanical behaviour for PHBV+S-EtOH systems, and particularly for PHBV4+S-EtOH since the torque, and thus the shear rate, is stable during the first ten minutes of processing while the decrease in M_w is limited. Therefore, this surfactant seems the most appropriate to prepare PHBV-based nanocomposites with organo-modified clays since it presents the adequate compromise between high shear rate, required to exfoliate layered silicates, and limited polymer degradation that could affect the material properties (Bordes, 2008).

Eventually, the possible mechanism of the surfactant degrading action on PHB proposed recently seems to be also valid for PHBV with low HV contents since all observations led to similar conclusions. Therefore, these studies could be expanded to other PHAs, and even, to other thermally sensitive biodegradable polyesters (polylactide…) for which the elaboration of nano-biocomposites based on organo-modified montmorillonites is also of major interest.

F. Acknowledgments

The authors thank the GMI-IPCMS (Institut de Physique et Chimie des Matériaux de Strasbourg, France) and Mrs Ducruet from the ENSIA-INRA in Massy (France) for their technical support. Biocycle (PHB Industrial, Brazil) is acknowledged for providing the PHA.

G. Discussion et commentaires

La dégradation thermique et thermomécanique des principaux PHAs en présence des ammoniums quaternaires, utilisés comme organomodifiants dans les systèmes nanocomposites, a été étudiée. Le but était de mieux comprendre le rôle de ces composés sur la stabilité des nano-biocomposites PHA/montmorillonites lors de la mise en œuvre. Afin de mieux se focaliser sur les effets des ammoniums quaternaires (organomodifiants) et des résidus de bioproduction (acides gras…), les systèmes étudiés l'ont été, dans ce cas, en l'absence de composé minéral (argile).

Les résultats de l'étude de la dégradation thermique des PHBV en présence des ammoniums quaternaires ont conduit globalement à des conclusions similaires à celles observées lors de l'étude de la stabilité thermique du PHB, à savoir :

i) les mécanismes de dégradation du polymère purifié et des ammoniums quaternaires dans les systèmes polymère-organomodifiant sont dépendants,
ii) tous les systèmes PHBV-ammonium quaternaire se dégradent selon le même mécanisme, i.e. une réaction d'avancement de l'interface (type R),
iii) S-Alk semble être l'ammonium quaternaire augmentant le plus la dégradation du PHBV.

Bien que l'étude de la dégradation thermomécanique confirme l'action néfaste des organomodifiants sur la stabilité thermique des PHBV, elle apporte également des informations intéressantes sur les systèmes PHBV+S-EtOH. En effet, la dégradation du polymère, en particulier celle du PHBV4, semble limitée ou du moins retardée au regard de l'évolution de la viscosité et des valeurs des masses molaires moyennes en poids durant les 10 premières minutes de mise en œuvre. Ainsi, il apparaît que l'ammonium quaternaire de type S-EtOH est le plus approprié en terme de stabilité thermique et thermomécanique en vue de la préparation de matériaux nanocomposites.

Par ailleurs, il faut noter qu'une étude comparable a été menée afin de déterminer le rôle des résidus de fermentation sur la dégradation du PHBV. Les résultats ont été confrontés aux conclusions tirées de l'étude similaire réalisée sur le PHB (cf. Publication n°3). De façon analogue, les résidus de fermentation ont été récupérés par extraction solide/liquide et ont été "rajoutés" dans le PHBV en proportion de 10 %pds. Il a été démontré que ces substances favorisent la dégradation du polymère de plus faible masse molaire tout comme les ammoniums quaternaires. En effet, les données thermogravimétriques ($T_{80\%}$, T_{dmax} et $T_{20\%}$) ont mis en évidence des décalages de l'ordre de -20°C pour le système PHBV8p+Rsd et de seulement quelques degrés

(-3°C) dans le cas du mélange PHBV4p+Rsd. De plus, dans le cas du système PHBV8+Rsd, T_{dmax} présente un écart de -19°C entre la courbe thermogravimétrique calculée par l'équation de Torre et al. (Torre, 1998) (cas où les dégradations des composants d'un mélange sont supposées indépendantes) et la courbe expérimentale. Quant au modèle cinétique de Coats & Redfern appliqué au système PHBV8p+Rsd, il donne une énergie d'activation égale à 246 kJ/mol c'est-à-dire proche des énergies d'activation relatives aux mélanges polymère-ammonium quaternaire. De plus, il a mis en évidence que la réaction de décomposition du système PHBV8p+Rsd suit le même mécanisme que les systèmes polymère-ammonium quaternaire (type R, i.e. réaction d'avancement d'interface).

L'influence des résidus de fermentation sur la stabilité thermique du PHBV existe donc bel et bien, et son effet est d'autant plus prononcé que les masses molaires moyennes du polymère sont faibles. Cependant, le mécanisme de dégradation reste indéterminé du fait de la variété des composants constituant les extraits de fermentation. L'étude relative au PHBV nous a donc permis de démontrer l'influence de ces résidus de fermentation sur la dégradation du polymère, effet qui n'avait pas été possible de mettre en évidence dans la publication n°3, probablement en raison de la haute masse molaire du PHB.

Conclusion du chapitre III et perspectives

En conclusion, il apparaît que les ammoniums quaternaires affectent grandement la stabilité thermique et thermomécanique du PHB et des PHBV à faibles taux d'unités HV selon un mécanisme identifié. Nous avons démontré que les résidus de fermentation, mélange très complexe de différents composés issus de la cellule bactérienne, participent également, mais dans une moindre mesure, à la dégradation de ces polymères. Du fait du manque de stabilité thermique et thermomécanique des PHAs étudiés, la masse molaire initiale du polymère s'avère être un paramètre plus influent que le taux d'unités HV. Ces études, réalisées sur des systèmes similaires aux nanocomposites évoqués au chapitre II, illustrent donc le rôle que peuvent jouer les organomodifiants, i.e. les ammoniums quaternaires, et les résidus de fermentation dans l'élaboration de tels matériaux..

Ces résultats pourraient facilement être étendus à d'autres matrices PHA. Des travaux analogues pourraient être menés sur d'autres polyesters thermosensibles comme le PLA qui est aussi actuellement un matériau d'avenir pour l'emballage à durée de vie contrôlée (compostage, recyclage) et issu de ressources renouvelables. Certains travaux très préliminaires menés par d'autres équipes de recherche semblent montrer que le même type de dégradation a lieu avec d'autres polyesters que les PHAs, mais avec un effet moindre.

Par ailleurs, il est vraisemblable que les sites acides de Lewis des feuillets inorganiques accroissent la sensibilité thermique et thermomécanique de ces PHAs. Mais, parce que différentes publications traitent largement cette question, les effets propres à l'argile sur la dégradation de la matrice n'ont pas été examinés lors de cette étude qui a porté préférentiellement sur les effets des différentes molécules organiques « additionnées » à la matrice PHA.

Le chapitre suivant va montrer les différentes approches exploratoires qui ont été tentées afin de pallier à ces phénomènes de dégradation de la matrice.

Bibliographie

Abe, H. (2006). Thermal Degradation of Environmentally Degradable Poly(hydroxyalkanoic acid)s. *Macromolecular Bioscience,* 6(7), 469-486.

Aoyagi, Y., Yamashita, K., Doi, Y. (2002). Thermal degradation of poly[(R)-3-hydroxybutyrate], poly[e-caprolactone], and poly[(S)-lactide]. *Polymer Degradation and Stability,* 76(1), 53-59.

Billingham, N. C., Henman, T. J., Holmes, P. A. (1987). Degradation and stabilisation of polyesters of biological and synthestic origin. *Developments in Polymer Degradation* pp. 81-121). London: Elsevier Applied Science.

Bordes, P., Pollet, E., Averous, L. (2008) Structure and properties of PHA/clay nano-biocomposites prepared by melt intercalation, ***submitted.***

Carrasco, F., Dionisi, D., Martinelli, A., Majone, M. (2006). Thermal stability of polyhydroxyalkanoates. *Journal of Applied Polymer Science,* 100(3), 2111-2121.

Chen, G. X., Hao, G. J., Guo, T. Y., Song, M. D., Zhang, B. H. (2002). Structure and mechanical properties of poly(3-hydroxybutyrate-co-3-hydroxyvalerate) (PHBV)/clay nanocomposites. *Journal of Materials Science Letters,* 21(20), 1587-1589.

Chen, G. X., Hao, G. J., Guo, T. Y., Song, M. D., Zhang, B. H. (2004). Crystallization kinetics of poly(3-hydroxybutyrate-co-3-hydroxyvalerate)/clay nanocomposites. *Journal of Applied Polymer Science,* 93(2), 655-661.

Chivrac, F., Kadlecova, Z., Pollet, E., Averous, L. (2006). Aromatic copolyester-based nano-biocomposites: Elaboration, structural characterization and properties. *Journal of Polymers and the Environment,* 14(4), 393-401.

Choi, W. M., Kim, T. W., Park, O. O., Chang, Y. K., Lee, J. W. (2003). Preparation and characterization of poly(hydroxybutyrate-co-hydroxyvalerate)-organoclay nanocomposites. *Journal of Applied Polymer Science,* 90(2), 525-529.

Coats, A. W., Redfern, J. P. (1964). Kinetics parameters from thermogravimetric data. *Nature,* 201(4914), 68.

Cyras, V. P., Vasquez, A., Rozsa, C., Galego Fernandes, N., Torre, L., Kenny, J. M. (2000). Thermal stability of P(HB-HV) and its blends with polyalcohols: Crystallinity, mechanical properties, and kinetics of degradation. *Journal of Applied Polymer Science,* 77(13), 2889-2900.

De Koning, G. J. M. (1993). Thesis.Prospects of bacterial poly[(R)-3-hydroxyalkanoates]. Center for Polymers and Composites (CPC) Eindhoven University of Technology Eindhoven

Erceg, M., Kovacic, T., Klaric, I. (2005). Thermal degradation of poly(3-hydroxybutyrate) plasticized with acetyl tributyl citrate. *Polymer Degradation and Stability,* 90(2), 313-318.

Fernandes, E. G., Pietrini, M., Chiellini, E. (2004). Thermo-mechanical and morphological characterization of plasticized poly[(R)-3-hydroxybutyric acid]. *Macromolecular Symposia* pp. 157-164).

Gain, O., Espuche, E., Pollet, E., Alexandre, M., Dubois, P. (2005). Gas barrier properties of poly(epsilon-caprolactone)/clay nanocomposites: Influence of the morphology and polymer/clay interactions. *Journal of Polymer Science Part B-Polymer Physics,* 43(2), 205-214.

Grassie, N., Murray, E. J., Holmes, P. A. (1984a). Thermal degradation of poly(-(D)- beta - hydroxybutyric acid): Part 3 - The reaction mechanism. *Polymer Degradation and Stability,* 6(3), 127-134.

Grassie, N., Murray, E. J., Holmes, P. A. (1984b). Thermal degradation of poly(-(D)- beta - hydroxybutyric acid): Part 1 - Identification and quantitative analysis of products. *Polymer Degradation and Stability,* 6(1), 47-61.

Grassie, N., Murray, E. J., Holmes, P. A. (1984c). Thermal degradation of poly(-(D)- beta - hydroxybutyric acid): Part 2 - Changes in molecular weight. *Polymer Degradation and Stability,* 6(2), 95-103.

Hablot, E., Bordes, P., Pollet, E., Avérous, L. (2007). Thermal and thermo-mechanical degradation of PHB-based multiphase systems. *Polymer Degradation and Stability*, In Press (doi: 10.1016/j.polymdegradstab.2007.11.018).

Hatakeyama, T., Quinn, F. X. (1999). *Thermal Analysis - Fundamentals and Applications to Polymer Science*. Wiley.

He, J.-D., Cheung, M. K., Yu, P. H., Chen, G.-Q. (2001). Thermal analyses of poly(3-hydroxybutyrate), poly(3-hydroxybutyrate-co-3-hydroxyvalerate), and poly(3-hydroxybutyrate-co-3-hydroxyhexanoate). *Journal of Applied Polymer Science,* 82(1), 90-98.

Kim, K. J., Doi, Y., Abe, H. (2006). Effects of residual metal compounds and chain-end structure on thermal degradation of poly(3-hydroxybutyric acid). *Polymer Degradation and Stability,* 91(4), 769-777.

Kopinke, F.-D., Remmler, M., Mackenzie, K. (1996). Thermal decomposition of biodegradable polyesters-I: Poly(beta-hydroxybutyric acid). *Polymer Degradation and Stability,* 52(1), 25-38.

Kunioka, M., Doi, Y. (1990). Thermal degradation of microbial copolyesters. Poly(3-hydroxybutyrate-co-3-hydroxyvalerate) and poly(3-hydroxybutyrate-co-4-hydroxybutyrate). *Macromolecules,* 23(7), 1933-1936.

Lee, M. Y., Lee, T. S., Park, W. H. (2001). Effect of side chains on the thermal degradation of poly(3-hydroxyalkanoates). *Macromolecular Chemistry and Physics,* 202(7), 1257-1261.

Lee, S. Y., Park, S. J. (2002). Fermentative production of SCL-PHAs. In Y. Doi, & A. Steinbüchel. *Biopolymers 3a - Polyesters I, Biological systems and biotechnological production* pp. 263-262). Weinheim, Germany: Wiley-VCH.

Lemoigne, M. (1926). Products of dehydration and of polymerization of b-hydroxybutyric acid. *Bulletin de la Société de Chimie Biologique,* 8, 770-782.

Lenz, R. W., Marchessault, R. H. (2005). Bacterial polyesters: Biosynthesis, biodegradable plastics and biotechnology. *Biomacromolecules,* 6(1), 1-8.

Li, S.-D., Yu, P. H., Cheung, M. K. (2001). Thermogravimetric analysis of poly(3-hydroxybutyrate) and poly(3-hydroxybutyrate-co-3-hydroxyvalerate). *Journal of Applied Polymer Science,* 80(12), 2237-2244.

Li, S.-D., He, J.-D., Yu, P. H., Cheung, M. K. (2003). Thermal degradation of poly(3-hydroxybutyrate) and poly(3-hydroxybutyrate-co-3-hydroxyvalerate) as studied by TG, TG-FTIR, and Py-GC/MS. *Journal of Applied Polymer Science,* 89(6), 1530-1536.

Lim, S. T., Hyun, Y. H., Lee, C. H., Choi, H. J. (2003). Preparation and characterization of microbial biodegradable poly(3-hydroxybutyrate)/organoclay nanocomposite. *Journal of Materials Science Letters,* 22(4), 299-302.

Maiti, P., Batt, C. A., Giannelis, E. P. (2003). Renewable plastics: Synthesis and properties of PHB nanocomposites. *Polymeric Materials Science and Engineering* pp. U665-U665).

Melik, D. H., Schechtman, L. A. (1995). Biopolyester melt behavior by torque rheometry. *Polymer Engineering & Science,* 35(22), 1795-1806.

Nonato, R. V., Mantelatto, P. E., Rossell, C. E. V. (2001). Integrated production of biodegradable plastic, sugar and ethanol. *Applied Microbiology and Biotechnology,* 57(1-2), 1-5.

Pandey, J. K., Kumar, A. P., Misra, M., Mohanty, A. K., Drzal, L. T., Singh, R. P. (2005). Recent advances in biodegradable nanocomposites. *Journal of Nanoscience and Nanotechnology,* 5(4), 497-526.

Ramsay, B. A., Ramsay, J. A. (2002). Poly(3-hydroxyalkanoates). *Encyclopedia of Polymer Science and Technology*. Weinheim, Germany: John Wiley & Sons.

Reddy, C. S. K., Ghai, R., Rashmi, Kalia, V. C. (2003). Polyhydroxyalkanoates: An overview. *Bioresource Technology,* 87(2), 137-146.

Renstad, R., Karlsson, S., Albertsson, A.-C. (1997). Influence of processing parameters on the molecular weight and mechanical properties of poly(3-hydroxybutyrate-co-3-hydroxyvalerate). *Polymer Degradation and Stability,* 57(3), 331-338.

Spychaj, T., Fabrycy, E., Spychaj, S., Kacperski, M. (2001). Aminolysis and aminoglycolysis of waste poly(ethylene terephthalate). *Journal of Material Cycles and Waste Management,* 3(1), 24-31.

Starink, M. J. (2003). The determination of activation energy from linear heating rate experiments: A comparison of the accuracy of isoconversion methods. *Thermochimica Acta,* 404(1-2), 163-176.

Swain, S. N., Rao, K. K., Nayak, P. L. (2005). Biodegradable polymers: Part II. Thermal degradation of biodegradable plastics cross-linked from formaldehyde-soy protein concentrate. *Journal of Thermal Analysis and Calorimetry,* 79(1), 33-38.

Tagushi, K., Tagushi, S., Sudesh, K., Maehara, A., Tsuge, T., Doi, Y. (2002). Metabolic pathways and engineering of PHA biosynthesis. In Y. Doi, & A. Steinbüchel. *Biopolymers 3a - Polyesters I, Biological systems and biotechnological production* pp. 217-248). Weinheim, Germany: Wiley-VCH.

Torre, L., Kenny, J. M., Maffezzoli, A. M. (1998). Degradation behaviour of a composite material for thermal protection systems Part I-Experimental characterization. *Journal of Materials Science,* 33(12), 3137-3143.

Vyazovkin, S., Wight, C. A. (1999). Model-free and model-fitting approaches to kinetic analysis of isothermal and nonisothermal data. *Thermochimica Acta,* 340-341, 53-68.

Wang, S., Song, C., Chen, G., Guo, T., Liu, J., Zhang, B., Takeuchi, S. (2005). Characteristics and biodegradation properties of poly(3-hydroxybutyrate-co-3-hydroxyvalerate)/organophilic montmorillonite (PHBV/OMMT) nanocomposite. *Polymer Degradation and Stability,* 87(1), 69-76.

Xie, W., Gao, Z., Pan, W.-P., Hunter, D., Singh, A., Vaia, R. (2001). Thermal degradation chemistry of alkyl quaternary ammonium montmorillonite. *Chemistry of Materials,* 13(9), 2979-2990.

Zanetti, M., Camino, G., Thomann, R., Mülhaupt, R. (2001). Synthesis and thermal behaviour of layered silicate-EVA nanocomposites. *Polymer,* 42(10), 4501-4507.

Chapitre IV
–
Les voies alternatives

Introduction

Nous avons vu dans les chapitres précédents que les PHAs subissent différents types de dégradation lors de la mise en œuvre en milieu fondu de systèmes nano-biocomposites. Le **chapitre II** a mis en évidence l'influence de cette dégradation sur la structure et les propriétés des matériaux. La comparaison des voies d'élaboration nous a tout de même confortés dans le choix de poursuivre l'étude en voie "fondu". En effet, cette dernière répond pleinement à une logique de développement industriel et de respect de l'environnement, et s'avère prometteuse au regard de la structure des matériaux PHA/C30B obtenus. Le **chapitre III** nous a permis d'identifier les composés mis en jeu dans la dégradation thermique et thermomécanique ainsi que de mieux comprendre les mécanismes réactionnels conduisant à la réduction des masses molaires des PHAs. Il apparaît donc nécessaire dans la poursuite de l'étude, de mieux contrôler et d'améliorer la stabilité de ces systèmes.

Ainsi, nous nous sommes tournés vers de nouvelles approches permettant d'augmenter la stabilité des PHAs dans le fondu, tout en préservant une bonne dispersion des feuillets de montmorillonites au sein de la matrice ; ceci afin que les nanocharges puissent entièrement jouer leur rôle de renfort mécanique et améliorer les propriétés thermiques et barrières. Billingham et al. (Billingham, 1987) avaient déjà fait état de différentes techniques pour résoudre ou compenser la faible stabilité thermique du PHB. L'utilisation d'agents de réticulation, de plastifiants, d'antioxydants etc., voire la combinaison de composés insaturés avec amorceur radicalaire dans le but de "repolymériser" après la β-scission aléatoire des chaînes, ont été envisagées avec plus ou moins de succès. Cependant, dans notre cas, les systèmes étudiés sont beaucoup plus complexes de par la présence des feuillets de montmorillonite et des organomodifiants. Aussi, nous nous sommes attachés à établir de nouveaux protocoles inspirés de procédés, déjà utilisés ou envisagés dans le domaine des nanocomposites conventionnels, qui seraient applicables à nos systèmes.

Dans ce **chapitre IV**, nous présenterons donc deux principales voies exploratoires tentant d'améliorer, d'une part la dispersion de la charge au sein de la matrice, et d'autre part, les propriétés des PHAs au travers de l'amélioration de leur stabilité. Ces études ont été principalement conduites sur la matrice PHB et mettent en jeu différentes approches, à savoir la préparation des matériaux par mélange maître, la compatibilisation par greffage de polymère et les mélanges de polymères.

La première méthode abordée dans ce chapitre vise à tirer indirectement avantage de la dégradation des PHAs au contact des montmorillonites, organo-modifiées ou non. Elle

s'intéresse plus particulièrement aux réactions de transestérification pouvant se produire à la surface des argiles. Celles-ci permettraient éventuellement de greffer les chaînes de PHA sur les feuillets de montmorillonites, améliorant ainsi la compatibilité polymère-argile, et donc de favoriser l'intercalation des chaînes PHA et l'exfoliation de la charge.

L'autre approche est basée sur la préparation d'un mélange maître de polycaprolactone (PCL) greffé à la surface de l'argile par polymérisation par ouverture de cycle. Nous avons vu au chapitre I que ce procédé est parfois utilisé pour favoriser l'exfoliation de la charge par compatibilisation charge-matrice. Elle présente également l'avantage de pouvoir combiner les propriétés du polymère greffé et de la matrice dans le cas d'une bonne miscibilité (Kim, 2001; Lepoittevin, 2003; Zheng, 2003; Kiersnowski, 2004; Gonzalez, 2006; Pollet, 2006).

Par ailleurs, ces deux approches permettent d'isoler les nanocharges, notamment par rapport aux sites acides de Lewis des feuillets qui accroissent la dégradation des PHAs.

A. Etude bibliographique

A.I. Transestérification

A.I.1. Généralités

La transestérification est une réaction organique classique qui transforme un ester en un autre ester par échange d'un groupe alkoxy (cf. Figure 1). Cette réaction peut être considérablement facilitée par la présence d'un acide fort ou d'une base forte jouant le rôle de catalyseur (Vollhardt, 1990).

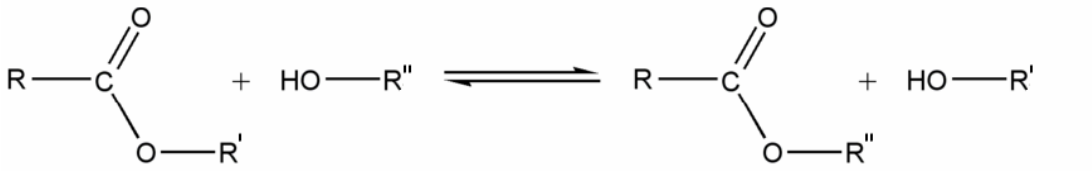

Figure 17 : Schéma de la réaction de transestérification entre un alcool et un ester

La transestérification est parfois utilisée comme alternative à l'estérification car plus pertinente lorsque l'alcool formé est volatile. Son champ d'application ne se limite pas à la recherche académique, plusieurs exemples de procédés industriels mettent en œuvre ce type de réaction. La transestérification d'huiles végétales ou de graisses animales est à l'origine de

biocarburants (Fukuda, 2001; Pinto, 2005). Dans le domaine des polymères, elle sert principalement à la synthèse de polyesters et copolyesters. Un des exemples les plus connus est la synthèse de polyéthylène téréphthalate (PET) par transestérification entre le diméthyltéréphthalate et l'éthylène glycol. La transestérification permet également de produire des esters acryliques (n-alkyl acrylates) à partir de l'acrylate de méthyle et d'un alcool (Rehberg, 1944a; Rehberg, 1944b). Ces derniers, en réagissant entre eux, conduisent à des homopolymères ou copolymères aux propriétés modulées, destinés à des applications dans le domaine des peintures, des revêtements et des adhésifs.

Pour augmenter les rendements de réaction et la sélectivité des produits (chemo-, stéréo- et régioséléctivité), d'autres types de catalyseurs ont été développés (Otera, 1993; Schuchardt, 1998). Ainsi, les principaux catalyseurs de transestérification utilisés, outre les acides forts et les bases fortes, sont les acétates (Tomita, 1975; Ma, 1998), les oxydes et les alcoolates de métaux (e.g. isopropanolate d'aluminium (Hammond, 1997), tetraalcoolates de titane (Hammond, 1997; Zhang, 2001a; Zhang, 2001b), et les alcoolates organostanneux (Poller, 1979)), les bases non ioniques et les enzymes.

A.I.2. Transestérification dans les systèmes nanocomposites à base de polyesters

Dans le cas des nanocomposites argile/polyester, les réactions de transestérification susceptibles de se produire mettent en jeu (i) les chaînes polyesters entre elles (transestérification polyester/polyester, cf. figure 2a), (ii) les chaînes polyesters et les groupes silanols situés à la surface des feuillets de montmorillonite (transestérification polyester/feuillets inorganique, cf. figure 2b), et enfin (iii) les chaînes polyesters et les groupes hydroxyles de l'organomodifiant (transestérification polyesters/organomodifiant, cf. figure 2c) dans le cas des montmorillonites organo-modifiées par des entités comportant des groupes hydroxyles telles que la Cloisite®30B (C30B).

Comme nous pouvons le voir sur la Figure 2, les deux dernières réactions permettent le greffage de chaînes polyesters à la surface de la montmorillonite.

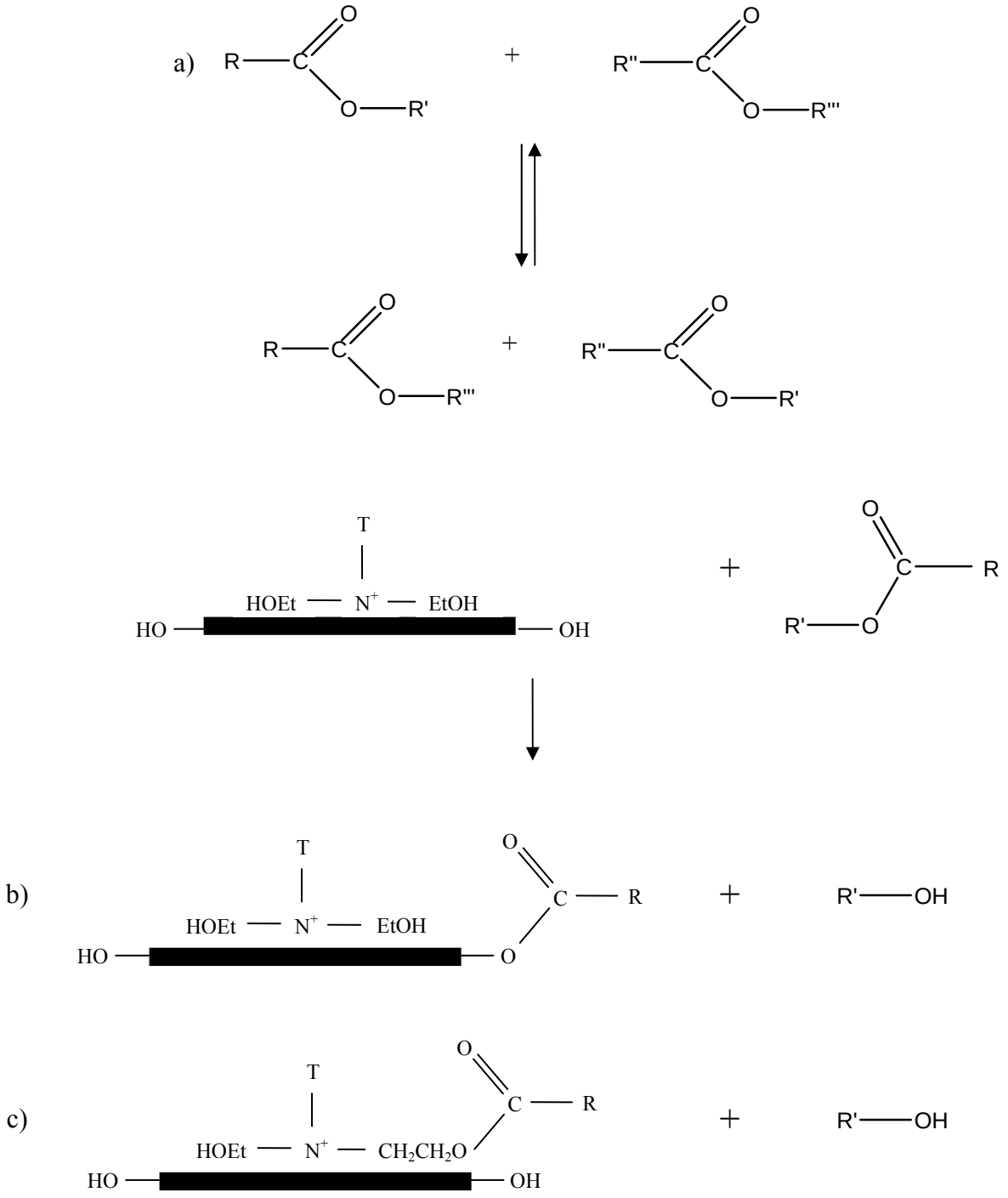

Figure 18 : Réactions de transestérification a) polyester/polyester, b) polyester/feuillets inorganiques et c) polyesters/organomodifiant

Pollet et al. (Pollet, 2006) ont ainsi utilisé différents catalyseurs afin de promouvoir les réactions de transestérification entre un biopolyester, en l'occurrence le Bionolle® - poly(butylene succinate) (PBS) -, et les fonctions hydroxyles de la C30B. Les auteurs ont démontré que le choix du catalyseur s'avère important puisque dans le cas de catalyseurs à base de titane et d'antimoine, respectivement le tétrabutanolate de titane ($Ti(OBu)_4$) et

l'oxyde d'antimoine (Sb_2O_3), la structure et les propriétés des matériaux étaient inchangées comparé aux propriétés du nanocomposite PBS/C30B. En revanche, l'utilisation d'un catalyseur à base d'étain, à savoir le dibutyle dilaurate d'étain ($Sn(Bu)_2(Lau)_2$), a permis d'obtenir une bien meilleure qualité de dispersion des feuillets de montmorillonites, i.e. un meilleur degré d'exfoliation. Ceci s'est notamment traduit par une amélioration des propriétés mécaniques du matériau (+27% pour le module d'Young). L'existence de réactions de transestérification, et donc d'un greffage du polymère, a été mise en évidence notamment par les analyses thermogravimétriques réalisées respectivement sur les parties organique et inorganique séparées et récupérées après extraction à partir du nanocomposite. La présence d'argile dans le polymère et inversement, de polymère dans la partie inorganique, chose qui n'est pas observée en l'absence de catalyseur, démontre clairement ce greffage.

Par la création de liaisons covalentes entre le polyester et l'organomodifiant situé en surface des feuillets, les réactions de transestérification permettent de mieux compatibiliser la charge et la matrice conduisant ainsi à une meilleure dispersion des feuillets de montmorillonite et à l'amélioration des propriétés du matériau.

Les systèmes étudiés à base de PHA étant similaires à ceux présentés par Pollet et al. (Pollet, 2006), cette dernière étude a servi d'appui pour l'élaboration des nano-biocomposites à base de PHA, et plus particulièrement de PHB. De façon analogue, notre but est de promouvoir les réactions de transestérification afin de greffer des chaînes de PHB à la surface de l'argile pour notamment améliorer la compatibilité PHB/montmorillonite et favoriser ainsi l'exfoliation de la charge.

A.II. Greffage et polymérisation par ouverture de cycle

Outre les propriétés intrinsèques des PHAs qu'il semble nécessaire d'améliorer, il s'agit également de favoriser l'exfoliation des nanocharges. Le choix de préparer un mélange maître par greffage de PCL à la surface de la montmorillonite par polymérisation par ouverture de cycle résulte d'un compromis entre miscibilité, ou compatibilité, avec le PHB, et les exigences de l'élaboration de matériaux techniquement compétitifs, biodégradables et biocompatibles.

A.II.1. Polymérisation par ouverture de cycles

Les polymérisations d'hétérocycles s'effectuent suivant différents mécanismes, relatifs à la nature du monomère, de l'amorceur, et peuvent ainsi conduire à de nombreux produits dont certains ont trouvé des applications industrielles importantes, comme par exemple le poly(caprolactame) ou Nylon 6, le poly(oxyde d'éthylène), etc. Par ailleurs, une large gamme d'amorceurs permettent aujourd'hui de polymériser divers monomères hétérocycliques et d'obtenir rapidement des macromolécules de masses molaires élevées dans des conditions relativement douces.

Plus spécifiquement, la polymérisation par ouverture de cycles oxygénés tels que les lactones permet d'obtenir des polyesters aux propriétés intéressantes. Parmi eux, le polycaprolactone (PCL) est synthétisé par ouverture de la liaison acyl-oxygène de l'ε-caprolactone, uniquement sous l'action de nucléophiles forts tels que les alcoolates (cf. Figure 3).

Nous avons vu au chapitre I que la polymérisation in-situ était une des techniques les plus pertinentes pour augmenter considérablement la distance interfeuillets, et obtenir des structures exfoliées. Selon l'amorceur et le catalyseur utilisés, il peut en résulter un greffage du polymère à la surface de l'argile (Lepoittevin, 2002c; Paul, 2003; Paul, 2005). La polymérisation par ouverture de cycle ou ROP (Ring-Opening Polymerization) dans les systèmes nanocomposites est maintenant bien maîtrisée que ce soit dans le cas du PLA ou du PCL (Kubies, 2002; Lepoittevin, 2002a, 2002b; Lepoittevin, 2002c; Pantoustier, 2002; Paul, 2003; Viville, 2003; Paul, 2005).

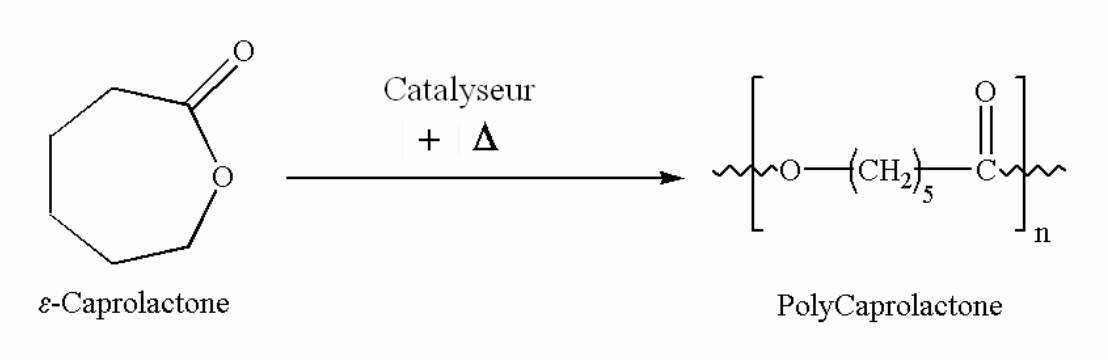

Figure 19 : Schéma de la polymérisation par ouverture de cycle dans le cas du polycaprolactone

A.II.2. Approche par association de polymères

A.II.2.1. Mélanges de polymères à base de PHA

L'association de deux polymères par mélange est une technique simple et peu coûteuse souvent utilisée pour combiner les propriétés de chaque constituant. Cependant, pour obtenir un mélange de polymères performant, la miscibilité de ces deux polymères doit être assurée. Celle-ci dépend notamment de la nature chimique des polymères et de leurs masses molaires. Il existe des mélanges dits compatibles, qui sont des matériaux partiellement hétérophasés mais qui présentent des structures et des propriétés suffisantes pour rencontrer de forts développement.

Un des critères permettant d'estimer la miscibilité est le phénomène de transition vitreuse. L'observation d'une transition unique atteste d'un mélange de polymères majoritairement miscibles. Sa valeur est notamment prédite par l'équation de Fox, suivant la formule classique :

$$\frac{1}{Tg_{AB}} = \frac{w_A}{Tg_A} = \frac{w_B}{Tg_B}$$

où w_A et w_B sont les fractions massiques des polymères A et B dans le mélange AB, et Tg_A, Tg_B et Tg_{AB}, sont les transitions vitreuses des polymères A, B, et du mélange AB.

De nombreux mélanges à base de PHB ont été étudiés afin d'améliorer ses propriétés (Avella, 2000; Yu, 2006). Selon la littérature, le PHB serait miscible avec le poly(oxyde d'éthylene) (PEO) (Avella, 1988), le poly(fluorure de vinylidène) (PVDF) (Marand, 1990), le polyacétate de vinyle (PVAc) (Kumagai, 1992), le polyméthacrylate de méthyle (PMMA) (An, 2000), et partiellement miscible avec, entre autres, le PLLA (Blumm, 1995), le PHBV (Organ, 1993) et le PCL (Gassner, 1994).

Les mélanges de polymères biodégradables et biocompatibles suscitent un intérêt tout particulier, et notamment le mélange PHB/PCL. En effet, le PCL joue en général un rôle de plastifiant augmentant la mobilité des chaines de PHB (Tg abaissée) et conférant ainsi au matériau un comportement plus ductile. Il présente aussi l'avantage d'avoir une température de fusion plus basse que le PHB (Tm_{PCL}=60°C). Cependant, les études menées sur ce type de mélange ont montré que le PHB et le PCL étaient peu miscibles à l'état amorphe (Kumagai,

1992; Gassner, 1994). Ce mélange est compatible lorsqu'il est mis en œuvre en milieu fondu (Gassner, 1994; Antunes, 2005) mais aucun effet synergique majeur au niveau des propriétés n'a pu être observé. Par ailleurs, la modification du PCL (Lovera, 2007) ou des mélanges réactifs (Avella, 1996) ont été également envisagés afin de mieux compatibiliser les deux polymères.

A.II.2.2. Préparation par mélange maître

Une autre approche a été développée sur des systèmes à base de mélange maître. Certains auteurs ont montré que la dispersion d'un mélange maître à forte concentration en charge minérale dans une matrice polymère pouvait conduire à une amélioration significative des propriétés du matériau final à condition de s'assurer de la bonne compatibilité entre les deux polymères présents (Lewitus, 2006; Pollet, 2006).

Pour cette approche et dans la suite de l'étude, nous nous focaliserons essentiellement sur l'effet des mélanges maîtres sur la structuration du matériau final.

B. Approche par transestérification

Comme nous l'avons vu dans le paragraphe A.I.2., les réactions de transestérification peuvent conduire au greffage de chaînes polyesters à la surface de la montmorillonite. L'idée est donc de tirer profit de la dégradation des PHAs, et en particulier du PHB, pour compatibiliser la charge avec la matrice et favoriser l'intercalation, voire l'exfoliation de la montmorillonite. Nous espérons également, en promouvant ce type de réactions, limiter la dégradation du polymère à la zone périphérique du feuillet et former ainsi une couche protectrice vis-à-vis de la matrice, autour des charges minérales.

Des mélanges à base de PHB et de montmorillonites, organomodifiées ou non, ont donc été préparés par voie "fondu". Plusieurs paramètres, tels que l'ajout de catalyseur, la préparation d'un mélange maître, ou encore la variation des vitesses de rotation ou des durées de mise en œuvre, ont été étudiés afin d'optimiser les réactions de transestérification. Bien sûr, dans tous les cas, nous avons essayé de mettre en évidence un éventuel greffage par analyse thermogravimétrique des parties organiques et inorganiques obtenues par extraction. La structure de ces matériaux et certaines de leurs propriétés ont quant à elles été déterminées pour quantifier l'impact d'une éventuelle transestérification.

B.I. Matériel et méthodes

B.I.1. Matériel

Le PHB ainsi que les charges organo-modifiées (Cloisite®30B, notée C30B) ou non (Dellite®HPS, notée HPS) sont préalablement séchés toute une nuit à l'étuve sous vide à 80°C. Le catalyseur testé est le dibutyle dilaurate d'étain (Sigma-Aldrich, noté SnLau). Les extractions par échange cationique sont réalisées en utilisant une solution de LiCl (Acros Organics). Le LiCl est séché et laissé à l'étuve sous vide à 30°C jusqu'à utilisation.

B.I.2. Préparation des nano-biocomposites

Les mélanges de référence que constituent les matériaux préparés par mélange direct sans catalyseur correspondent aux nano-biocomposites présentés au chapitre II et dont les résultats ont déjà été discutés. Ils sont reportés dans cette partie sous la série codée T0 à T5.

B.I.2.1. Par mélange direct

Le PHB et la charge (C30B ou HPS à 3 %pds) sont mélangés manuellement avant introduction dans le mélangeur interne Haake Rheocord 9000. Le mélange est ensuite mis en œuvre à 170°C pendant 5 minutes. La vitesse de rotation du mélangeur est soit maintenue à 100 rpm tout au long de la mise en œuvre, soit abaissée à 50 rpm après introduction de la matière (cf. Tableau 1)

Dans le cas où l'on souhaite promouvoir les réactions de transestérification par l'ajout d'un catalyseur (1 %pds SnLau – cf. Tableau 2, série 'TC'), ce dernier est directement déposé sur l'argile afin d'imprégner la charge et les sites réactifs.

Enfin, des mélanges non chargés mis en œuvre dans les mêmes conditions (i.e. en présence ou non de catalyseur) serviront de référence.

Tableau 4 : Conditions expérimentales de la préparation des nano-biocomposites par mélange direct SANS catalyseur

Code	Charge		T (°C)	N (rpm)	t (min)
	Type	Taux (%)			
T0	-	-	170	100	5
T1	HPS	3	170	100	5
T2	C30B	3	170	100	5
T3	-	-	170	100>50	5
T4	HPS	3	170	100>50	5
T5	C30B	3	170	100>50	5

Tableau 5 : Conditions expérimentales de la préparation des nano-biocomposites par mélange direct AVEC catalyseur

Code	Charge		Catalyseur		T (°C)	N (rpm)	t (min)
	Type	Taux (%pds)	Type	Taux (%pds)			
TC0	-	-	SnLau	1	170	100	5
TC1	HPS	3	SnLau	1	170	100	5
TC2	C30B	3	SnLau	1	170	100	5
TC3	-	-	SnLau	1	170	100>50	5
TC4	HPS	3	SnLau	1	170	100>50	5
TC5	C30B	3	SnLau	1	170	100>50	5

B.I.2.2. Par mélange maître

Les mélanges maîtres chargés à 15 %pds (C30B et HPS) sont mis en œuvre au mélangeur interne Haake Rheocord 9000 à 170°C et 100 rpm. Des temps de mélange de 5 et 20 minutes ont été testés. A la sortie du mélangeur et après refroidissement, la matière est broyée puis redispersée dans le PHB de façon à obtenir un taux de matière inorganique égal à 3 %pds (série 'TMB'). Deux protocoles de mise en œuvre ont alors été testés. Ils diffèrent par la vitesse de rotation des pales (constante à 100 rpm ou abaissée à 50 rpm après introduction).

La même série d'échantillons est préparée en présence de catalyseur (série 'TMBC'), ce dernier étant imprégné sur la charge avant mise en œuvre.

Tableau 6 : Conditions expérimentales de la préparation des matériaux par mélange maître SANS catalyseur

Mélange maître						Redispersion				
Code	Charge		T (°C)	N (rpm)	t (min)	Charge	T (°C)	N (rpm)	t (min)	Code
	Type	Taux (%pds)				Taux (%pds)				
TMB0a	-	-	170	100	5	3	170	100>50	5	TMB01a
TMB0b	-	-	170	100	20	3	170	100>50	5	TMB01b
TMB1	HPS	15	170	100	5	3	170	100>50	5	TMB11
TMB2	HPS	15	170	100	20	3	170	100>50	5	TMB21
TMB3	C30B	15	170	100	5	3	170	100>50	5	TMB31
TMB4	C30B	15	170	100	20	3	170	100>50	5	TMB41

Tableau 7 : Conditions expérimentales de la préparation des matériaux par mélange maître AVEC catalyseur

Mélange maître							Redispersion				
Code	Charge		Catalyseur	T (°C)	N (rpm)	t (min)	Charge	T (°C)	N (rpm)	t (min)	Code
	Type	Taux (%pds)	Type - Taux (%pds)				Taux (%pds)				
TMBC0a	-	-	SnLau - 1	170	100	5	3	170	100>50	5	TMBC01a
TMBC0b	-	-	SnLau - 1	170	100	20	3	170	100>50	5	TMBC01b
TMBC1	HPS	15	SnLau - 1	170	100	5	3	170	100>50	5	TMBC11
TMBC2	HPS	15	SnLau - 1	170	100	20	3	170	100>50	5	TMBC21
TMBC3	C30B	15	SnLau - 1	170	100	5	3	170	100>50	5	TMBC31
TMBC4	C30B	15	SnLau - 1	170	100	20	3	170	100>50	5	TMBC41

B.I.3. Caractérisations

Comme nous l'avons vu, les possibles réactions de transestérification entre le polymère et la charge via les groupes silanols du feuillet inorganique ou les groupes hydroxyles de l'organomodifiant de la C30B peuvent conduire au greffage de chaînes à la surface de la charge. Des protocoles consistant en l'extraction de la charge par solubilisation-centrifugation (Pollet, 2006) (appelée ici extraction simple), ou par échange cationique (Paul,

2003), ont permis de démontrer l'existence de liaisons covalentes entre la charge et la matrice (Pollet, 2006) suite à l'analyse thermogravimétrique des composants extraits.

Les structures des matériaux élaborés ont été étudiées par diffraction des rayons X aux petits angles et les propriétés mécaniques et thermiques de certains ont été déterminées.

B.I.3.1. Extraction

En cas de greffage de chaînes à la surface des argiles, le polymère est solidaire du feuillet inorganique lui-même ou de son organomodifiant. Ces extractions consistent à solubiliser les nanocomposites puis à centrifuger les suspensions afin de séparer la charge (culot) du polymère (surnageant). Dans le cas où ce dernier est greffé à la charge, l'analyse thermogravimétrique du culot révèlera la présence de matière organique. La perte de masse permettra de quantifier ces réactions de transestérification.

B.I.3.1.a. Extraction simple

Les extractions simples consistent dans un premier temps à solubiliser le matériau à base de PHB dans le chloroforme. Afin d'obtenir une quantité suffisante de matière inorganique, 0,2 g de l'échantillon sont prélevés et solubilisés dans ~25 ml de chloroforme à chaud (70°C) et dans des tubes sous pression.

Une fois le polymère solubilisé, les suspensions sont centrifugées à 6 000 tr/min pendant 20 minutes. Le surnageant est collecté et le culot redispersé dans environ 20 ml de chloroforme à chaud. Ces étapes de redispersion/centrifugation sont répétées 3 fois afin de s'assurer de l'élimination du polymère non greffé à la surface de l'argile.

Le culot est récupéré après redispersion dans un minimum de solvant. Ce dernier est ensuite évaporé et les feuillets inorganiques séchés à l'étuve à 30°C sous vide. Les surnageants collectés après les centrifugations sont mis en commun puis précipités goutte à goutte dans environ 10 volumes de n-heptane. La suspension est ensuite filtrée sur büchner et le polymère est séché à l'étuve à 30°C pendant une nuit.

Le taux de matière organique ($\mathbf{\Delta w_p}$) dans le culot ainsi que le taux de résidus à 600°C ($\mathbf{\Delta w_{600}}$) dans le polymère sont déterminés par analyse thermogravimétrique. Pour cela, les échantillons sont chauffés de la température ambiante à 600°C à une vitesse de 20°C/min sous flux d'azote.

B.I.3.1.b. Extraction par échange cationique

L'extraction par échange cationique est similaire au précédent protocole. En parallèle de la solubilisation, une solution de LiCl dans le THF à 1%g/ml est préparée, le LiCl n'étant pas soluble dans le $CHCl_3$. Après solubilisation du nanocomposite, la solution de LiCl est ajoutée dans les tubes sous pression. La quantité de LiCl nécessaire à l'échange est conditionnée par la quantité d'organomodifiants, elle-même fonction de la CEC de la montmorillonite et du taux de charge considérés. Les suspensions de charges dans le chloroforme sont laissées sous agitation magnétique à chaud et sous pression pendant 3 jours. A l'issue de cette étape, une succession de centrifugation/redispersion est effectuée de façon à séparer les culots des surnageants. Les culots sont collectés et séchés à l'étuve à 80°C sous vide, tout comme les surnageants après évaporation du $CHCl_3$. On procède ensuite aux analyses thermogravimétriques comme décrit dans le paragraphe précédent.

B.I.3.2. Diffraction des Rayons X aux petits angles

Avant toute caractérisation, les échantillons récupérés en sortie de mélangeur sont compressés à chaud (175°C) pendant 3 minutes afin d'obtenir un film. Le refroidissement jusqu'à température ambiante se fait à 200 bars pendant 3 minutes.

La caractérisation de ces films par diffraction des rayons X est effectuée sur un diffractomètre Siemens D5000 (Germany) en procédant à un balayage en 2θ allant de 1,5 à 10° à une vitesse de 0,03°/s. Les distances interfeuillets, notées $\mathbf{d_f}$ sont calculées à l'aide de la loi de Bragg à partir des pics de diffraction observés (cf. Annexe I).

B.I.3.3. Chromatographie d'Exclusion Stérique

Les mesures des masses molaires moyennes du PHB ont été réalisées sur les surnageants obtenus par centrifugation des nanocomposites dissous dans le chloroforme. Les analyses ont été effectuées à 40°C à un débit de 0,8 ml/min avec en sortie deux détecteurs, indice de réfraction et UV. Les colonnes utilisées sont des colonnes de type PLGel Mixed-B 10µm. La calibration a été réalisée avec des standards PS dans une gamme allant de 580 à 1 650 000 g/mol.

B.I.3.4. Analyse thermogravimétrique

La stabilité thermique des matériaux élaborés a été déterminée par analyse thermogravimétrique sous flux d'azote, suivant une montée en température allant de la température ambiante à 600°C à une vitesse de 20°C/min. Les températures de début et de fin de dégradation ainsi que la température correspondant au maximum de la vitesse de dégradation respectivement notées T_0, T_f et $T_{d\ max}$ sont relevées. Le taux de résidus (**Δw)** mesuré à 600°C nous donne le taux de matière inorganique compris dans l'échantillon analysé.

B.I.3.5. Traction

Pour chaque échantillon étudié, 5 éprouvettes ISO 527-2-5A injectées au Minijet Haake ($T_{cylindre}$=190°C, T_{moule}=60°C) ont été testées sur une machine de traction MTS 2/M à une vitesse de déplacement de 5 mm/min. Les caractéristiques mécaniques, à savoir module d'Young, contrainte au seuil et élongation à rupture, ont été déterminées par le calcul de la moyenne sur ces 5 éprouvettes.

B.II. Résultats et discussion

B.II.1. Structure des matériaux par DRX

La caractérisation par DRX nous permet de connaître le degré d'intercalation moyen des feuillets de montmorillonites, caractéristique de l'affinité polymère-charge. L'allure des diffractogrammes peut également être discutée pour apprécier qualitativement l'état de la dispersion de la charge au sein de la matrice.

Les distances interfeuillets relatives aux mélanges à base de HPS ne seront pas discutées puisque aucun des mélanges ne présente de pics de diffraction. Comme il l'a été mentionné au chapitre II, cette absence de pic de diffraction n'est pas du à une structure exfoliée mais plutôt au faible taux de montmorillonite et éventuellement à la mauvaise dispersion de gros tactoïdes.

B.II.1.1 Mélange direct

Dans le Tableau 5 sont reportées les valeurs des distances interfeuillets obtenues pour les nano-biocomposites déjà présentés au chapitre II. Le Tableau 6 rassemble les données relatives aux distances interfeuillets des matériaux préparés par mélange direct en présence de catalyseur de transestérification (série 'TC'). Dans le cas des mélanges à base de C30B avec catalyseur (TC2 et TC5), on constate que la distance interfeuillet est légèrement plus élevée qu'en l'absence de catalyseur. Mais la différence se fait surtout sur la définition et l'intensité des pics de diffraction en présence ou non de catalyseur (cf. Figure 4). Il semble donc que le catalyseur, ainsi qu'une vitesse de rotation plus élevée lors du mélange, favorisent la dispersion. Cependant, en présence de catalyseur, il semble que l'influence de la vitesse de rotation soit estompée puisque les diffractogrammes des matériaux TC2 et TC5 présentent le même profil.

Tableau 8 : Distances interfeuillets des nano-biocomposites élaborés par mélange direct

Code	Charge		T (°C)	N (rpm)	t (min)	d_f (Å)
	Type	Taux (%)				
T2	C30B	3	170	100	5	**42,3**
T5	C30B	3	170	100>50	5	**40,4**

Tableau 9 : Distances interfeuillets des nano-biocomposites élaborés par mélange direct en présence de catalyseur

Code	Charge		Catalyseur		T (°C)	N (rpm)	t (min)	d_f (Å)
	Type	Taux (%pds)	Type	Taux (%pds)				
TC2	C30B	3	SnLau	1	170	100	5	**42,8**
TC5	C30B	3	SnLau	1	170	100>50	5	**40,9**

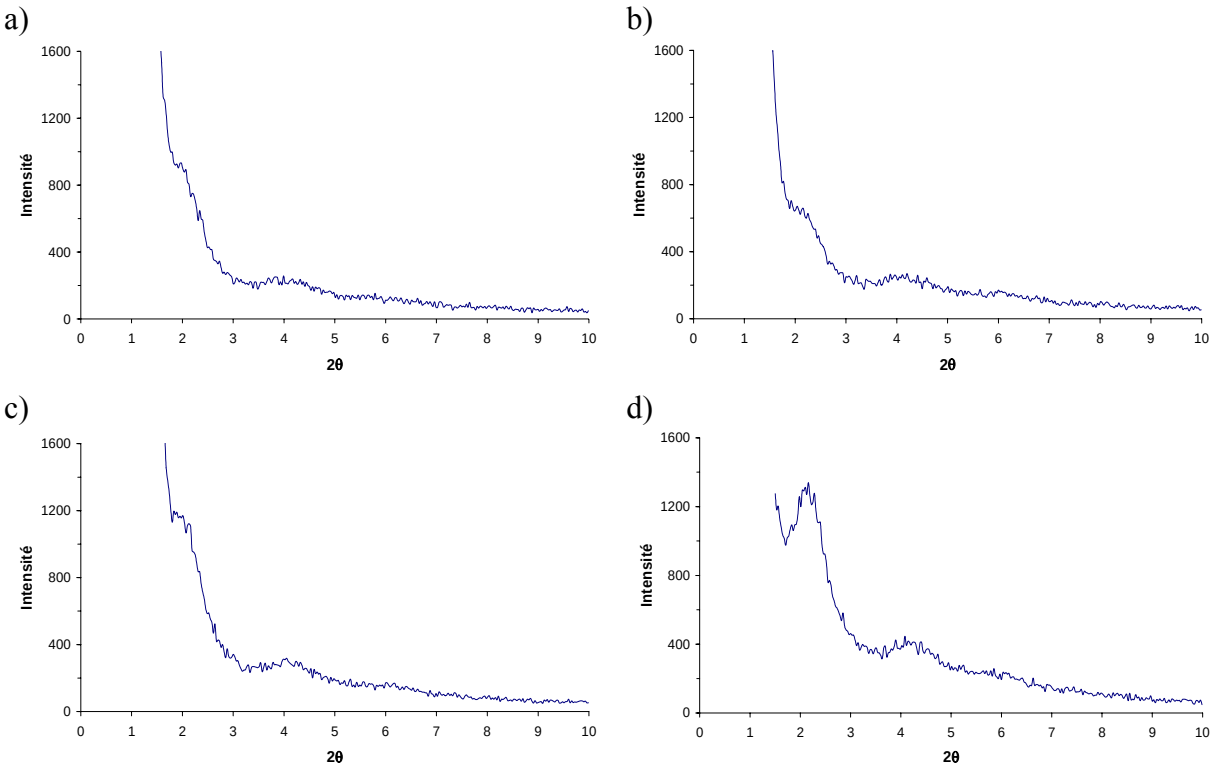

Figure 20 : Diffractogrammes RX des nano-biocomposites a) TC2, b) TC5, c) T2, d) T5

B.II.1.2. Par mélange maître sans catalyseur

La comparaison des résultats de DRX relatifs aux mélanges maître à base de C30B (TMB3 et TMB4), nous permet de mettre en évidence l'influence du temps de mise en œuvre sur la structure de la charge au sein de la matrice PHB (cf. Tableau 7). Au vu des distances interfeuillets similaires, le degré d'intercalation du PHB entre les feuillets est quasi équivalent. En revanche, la différence dans l'allure des DRX (cf. Figure 5) révèle, assez logiquement, une meilleure dispersion de la charge pour des temps de mis en œuvre plus élevés.

Tableau 10 : Distances interfeuillets des mélanges maîtres et des nano-biocomposites élaborés sans catalyseur

Code	Charge		T (°C)	N (rpm)	t (min)	d_f (Å)	Code	Taux de charge (%pds)	d_f (Å)
	Type	Taux (%pds)							
TMB3	C30B	15	170	100	5	**33,7**	TMB31	3	**42,0**
TMB4	C30B	15	170	100	20	**35,2**	TMB41	3	**43,6**

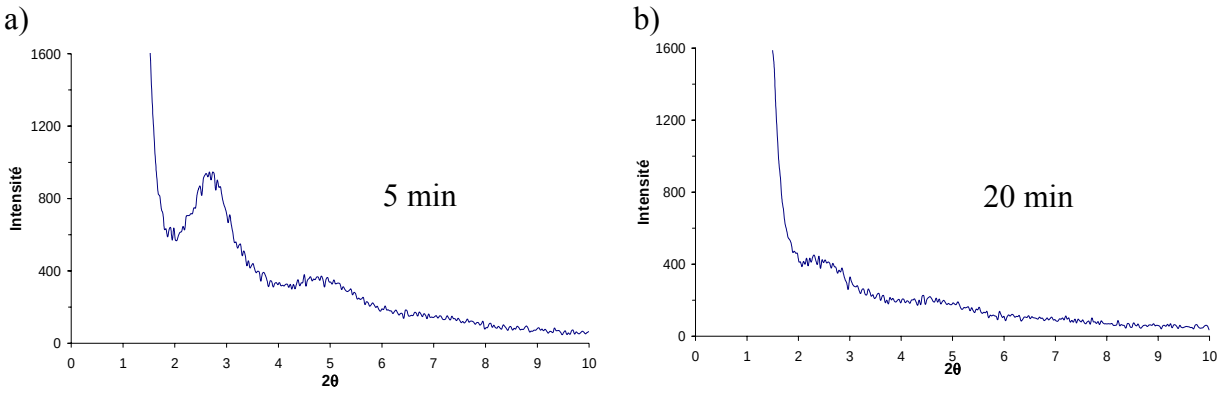

Figure 21 : Diffractogrammes RX des mélanges maîtres a) TMB3 et b) TMB4

De plus, ces résultats nous montrent que la redispersion des mélanges maîtres dans le PHB permet d'augmenter la distance interfeuillets d'environ 8 Å. Ceci est simplement dû à la diminution du taux de charge dans le matériau. Les observations faites sur les mélanges maîtres restent valables pour les mélanges redispersés (TM31 et TMB41, cf. Figure 6). En effet, les distances interfeuillets bien que voisines, tendent à montrer un meilleur degré d'intercalation dans le cas du matériau ayant été mis en œuvre pendant des temps plus longs (TMB4 et TMB41). L'allure des spectres révèle également une meilleure dispersion dans le cas de ces échantillons (pics de diffraction moins nets).

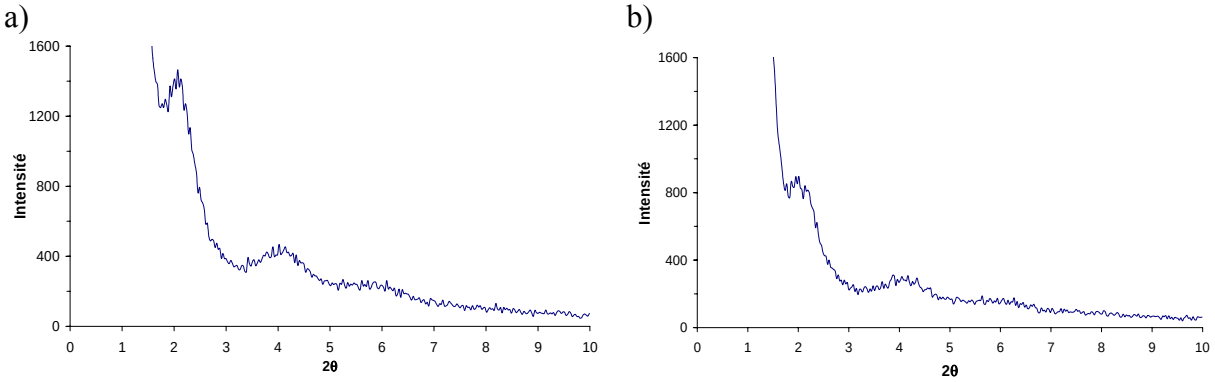

Figure 22 : Diffractogrammes RX des nano-biocomposites a) TMB31 et b) TMB41

Cependant, les matériaux obtenus par mélange direct de C30B (T5) présentent des degrés d'intercalation et une qualité de dispersion similaires à ce qui est obtenu via un mélange maître (TMB31), pour un même temps de mis en œuvre de 5 min. Ceci montre que, dans ces conditions, le passage par un mélange maître n'apporte pas d'amélioration notable.

B.II.1.3 Par mélange maître avec catalyseur

Comme observé précédemment, d'après l'allure des diffractogrammes, le mélange maître mis en œuvre pendant des temps plus long (20 min, i.e. TMBC4) semble présenter une meilleure dispersion que son homologue mis en œuvre pendant seulement 5 min (cf. Figure 7). Les nano-biocomposites issus de ces mélanges présentent cette même tendance (cf. Figure 8).

Les valeurs de distances interfeuillets des mélanges maîtres en présence de catalyseur (TMBC3 et TMBC4, cf. Tableau 8) ne sont pas plus élevées que celles obtenues sans catalyseur (33,7 et 35,2 Å pour TMB3 et TMB4, respectivement). Quant aux valeurs relatives aux nano-biocomposites (TMBC31 et TMBC41), elles sont du même ordre que celles des nanocomposites obtenus dans les mêmes conditions mais en l'absence de catalyseur (42,0 et 43,6 Å pour TMB31 et TMB41 respectivement).

Ces résultats, associés aux précédents, montrent que pour nos systèmes le passage par un mélange maître n'apporte aucune amélioration significative, que ce soit en présence ou non de catalyseur.

Tableau 11 : Distances interfeuillets des mélanges maîtres et des nano-biocomposites élaborés en présence de catalyseur

Code	Charge		Catalyseur	T (°C)	N (rpm)	t (min)	d_f (Å)	Code	Taux de charge (%pds)	d_f (Å)
	Type	Taux (%pds)								
TMBC3	C30B	15	SnLau - 1	170	100	5	**35,4**	TMBC31	3	**42,5**
TMBC4	C30B	15	SnLau - 1	170	100	20	**35,4**	TMBC41	3	**43,3**

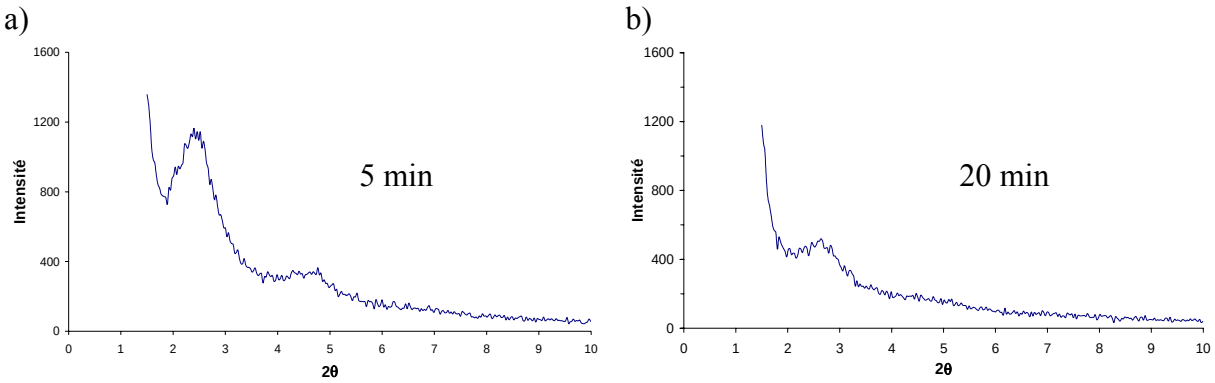

Figure 23 : Diffractogrammes RX des nano-biocomposites a) TMBC3 et b) TMBC4

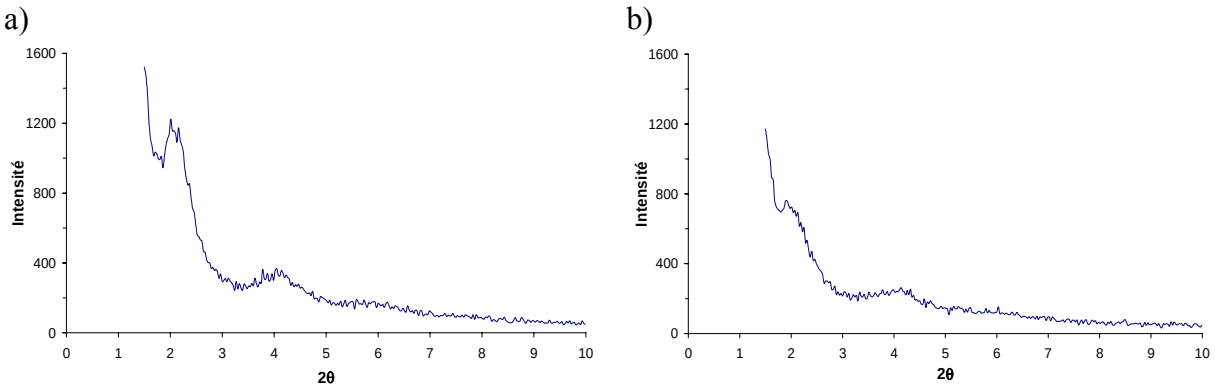

Figure 24 : Diffractogrammes RX des nano-biocomposites a) TMBC31 et b) TMBC41

Comparés aux autres nano-biocomposites à base de C30B, il semble que les matériaux élaborés par mélange direct, en présence de catalyseur (TC2 et TC5), présentent les meilleurs degrés d'intercalation et de dispersion de la charge au sein de la matrice PHB.

Pour conclure sur l'étude de la structure à partir des résultats DRX, tous les nanocomposites à base de C30B, avec ou sans masterbatch, et avec ou sans catalyseur, présentent une distance interfeuillet élevée comprise entre 40 et 43 Å. Bien que ces variations de distances interfeuillets soient peu significatives, l'allure des spectres nous permet de nous rendre compte des variations de la qualité de dispersion en fonction du protocole d'élaboration. En effet, il apparaît que l'ajout de catalyseur, un temps de mise en œuvre plus long ou une vitesse de rotation des pales plus élevée favorisent la dispersion des charges au sein de la matrice.

Cependant, avant d'imputer cet effet à un greffage du PHB et avant d'envisager d'entreprendre la caractérisation des propriétés de ces matériaux, il nous faut nous assurer de l'existence d'éventuelles liaisons covalentes entre la matrice et la charge (ou son organomodifiant).

B.II.2. Contrôle de la transestérification

Les premiers tests ont été menés sur les mélanges maîtres préparés en présence ou non de catalyseur. En effet, de par leur taux de charges élevé (~15 %pds), ces matériaux présentent les meilleures conditions pour être le support de ces réactions de transestérification.

Les résultats des analyses thermogravimétriques sont reportés dans le Tableau 9. Les paramètres caractéristiques qui ont été déterminés sont le taux de matière organique Δw_p dans le culot et le taux de résidus à 600°C Δw_{600} dans le polymère.

Tableau 12 : Résultats ATG des parties organiques et inorganiques issues de l'extraction simple

Echantillon	Charge		Culot	Polymère	
	Type	Taux (%pds)	Δw_p (%)	Δw_1 (%)	Δw_{600} (%)
TMB1	HPS	15	14,0	94,3	4,4
TMB3	C30B	15	13,7	94,6	4,5
TMBC1	HPS	15	13,0	103,1	-3,5
TMBC3	C30B	15	12,9	93,4	5,8

Ces résultats montrent que quelle que soit la charge et la présence ou non de catalyseur, la quantité de matière organique dans le culot reste quasi constante. Par ailleurs, la mesure du résidu à 600°C pour la fraction issue du surnageant n'apparaît pas assez précise pour évaluer la quantité de charge inorganique dans le polymère, et ce, malgré un nombre répété d'expériences. Le même phénomène a été observé dans le cas des extractions par échange cationique.

Bien que ces analyses ne nous permettent pas de conclure quant à un éventuel greffage de chaînes PHB à la surface de l'argile, nous avons déterminé certaines propriétés de ces matériaux. Nous espérons ainsi pouvoir statuer sur l'effet réel du catalyseur et du mélange maître sur les réactions de transestérification, et par conséquent sur la compatibilité polymère-charge.

B.II.3. Essais mécaniques

Les propriétés mécaniques des nanocomposites obtenus par mélange direct en présence de catalyseur (TC3 à TC5) ont été déterminées afin de les comparer aux résultats de

leurs homologues obtenus sans catalyseur (T3 à T5). Les résultats sont reportés dans le Tableau 10.

Si l'augmentation de la rigidité du matériau due à la dispersion de nanocharges peut toujours être observée au travers de l'augmentation du module d'Young, il s'avère que les propriétés mécaniques des matériaux préparés en présence de catalyseur sont affectées. En effet, les valeurs du module d'Young des nano-biocomposites préparés avec catalyseur restent sensiblement inférieures à leurs homologues. De plus, les variations des contraintes au seuil et des élongations à rupture ne sont pas significatives. Donc, malgré une meilleure dispersion des nanocharges (cf. résultats DRX), aucune amélioration des propriétés mécaniques n'est observée.

Tableau 13 : Propriétés mécaniques des nano-biocomposites obtenus par mélange direct avec (TC3 à TC5) ou sans catalyseur (T3 à T5) avec une vitesse de rotation réduite à 50 rpm après introduction (les nombres entre parenthèses représentent l'incertitude de mesure).

Système	Taux inorganique (%pds)	Module d'Young (MPa)	Contrainte seuil (MPa)	Elongation à la rupture (%)
T3	-	1884 (16)	24 (1)	1,56 (0,1)
T4	2,7	1913 (38)	25 (0,2)	2,2 (0,1)
T5	2,1	1981 (47)	27 (1)	1,56 (0,1)
TC3	-	1758 (34)	27 (4)	1,8 (0,3)
TC4	3,5	1804 (64)	22 (4)	1,4 (0,3)
TC5	2,8	1947 (29)	22 (2)	1,3 (0,1)

B.II.4. Stabilité thermique

Les analyses thermogravimétriques nous ont également permis de comparer les stabilités thermiques des matériaux élaborés suivant les différents protocoles.

Comme nous l'avons vu au chapitre II, les matériaux à base de montmorillonite non modifiée se dégradent à des températures plus faibles que les nanocomposites à base de C30B (cf. Figure 9 et 10). Nous retrouvons ce phénomène quel que soit le protocole considéré. Cela témoigne d'une meilleure affinité polymère-charge, et donc d'une meilleure dispersion, dans le cas de la C30B. Nous pouvons cependant remarquer que l'ajout du catalyseur dans le cas du mélange direct PHB/HPS, semble améliorer sensiblement la stabilité thermique puisque la courbe thermogravimétrique correspondante (TC4) est décalée de quelques degrés vers les

plus hautes températures. Le catalyseur aurait éventuellement permis d'améliorer la dispersion de la charge.

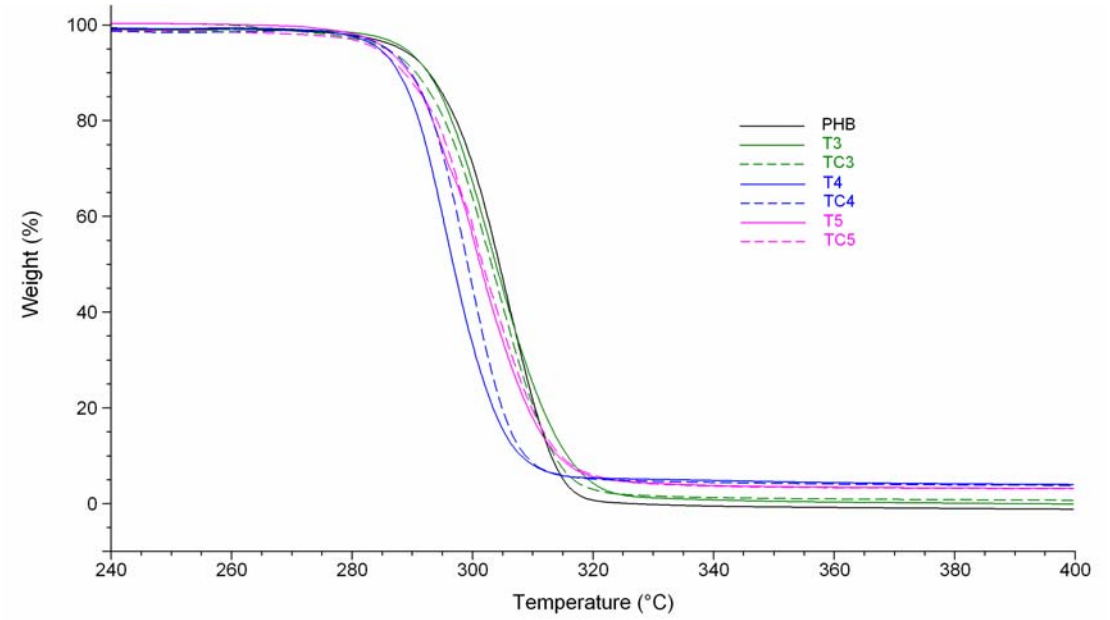

Figure 25 : Influence du catalyseur sur la stabilité thermique du PHB seul (T3 et TC3), en présence de 3%pds de HPS (T4 et TC4) ou de C30B (T5 et TC5) préparés par mélange direct

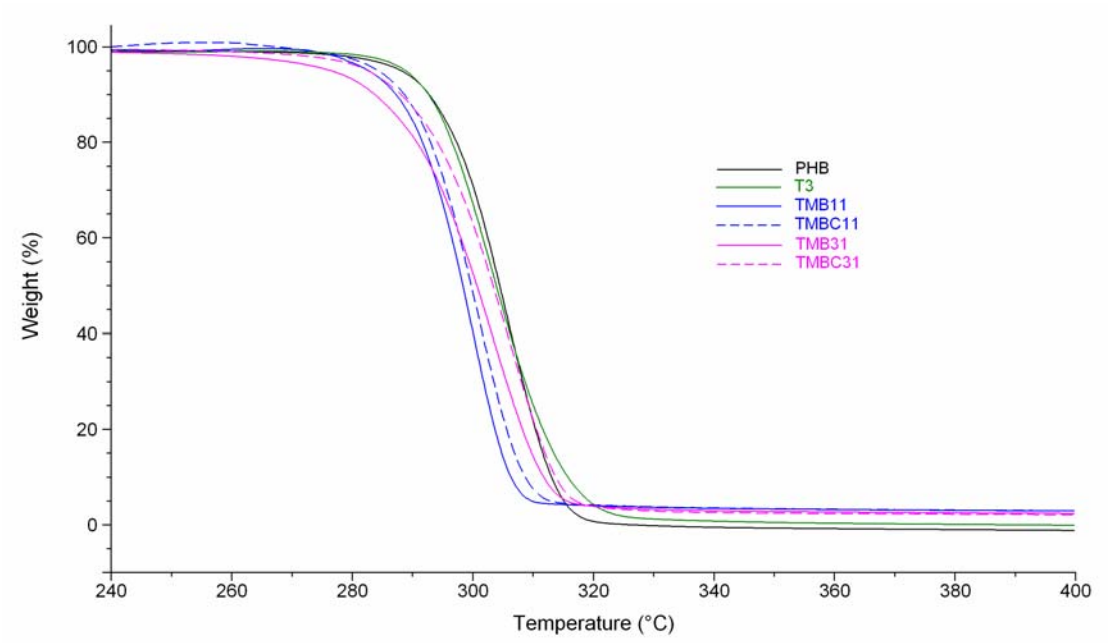

Figure 26 : Influence du catalyseur sur la stabilité thermique du PHB seul (T3 et TC3), en présence de 3%pds de HPS (TMB11 et TMBC11) ou de C30B (TMB31 et TMBC31) préparés via un mélange maître

Cependant, la stabilité thermique des nanocomposites à base de C30B reste plus faible que les matériaux non chargés, et ce, quel que soit le protocole considéré i.e. avec ou sans

catalyseur, et avec ou sans préparation de 'mélange maître'. En effet, l'étude comparative des courbes thermogravimétriques permettant d'étudier l'influence du 'mélange maître' et de sa durée de mise en œuvre (courbes non présentées ici), n'a pu mettre en évidence une quelconque influence de ces facteurs sur la stabilité thermique du PHB. Par ailleurs, même si la préparation de nano-biocomposites par mélange maître en présence de catalyseur semble réduire la diminution de la stabilité thermique des matériaux (cf. Figure 10), les températures caractéristiques de dégradation restent légèrement plus faibles que celles du polymère mis en œuvre (T3).

En conclusion, la diminution des propriétés mécaniques et thermiques n'étayent pas l'hypothèse selon laquelle des réactions de transestérification auraient pu greffer des chaînes PHB à la surface de la montmorillonite et donc mieux compatibiliser la charge et la matrice. En revanche, des phénomènes de dégradation du PHB pourraient expliquer cette perte des propriétés.

Nous nous sommes donc intéressés à la variation des masses molaires moyennes en fonction des protocoles de mise en œuvre testés. Il faut toutefois noter que ces mesures ont été réalisées sur les échantillons de polymère seul, mis en œuvre selon les différents protocoles présentés. L'analyse des masses molaires moyennes est donnée à titre indicatif ne pouvant présumer des réactions parallèles possibles en présence du feuillet inorganique et de l'organomodifiant.

B.II..5. Influence du protocole de préparation sur la dégradation

B.II.5.1. Mélange direct

Nous avons vu au chapitre II qu'une vitesse de mélange élevée avait un effet néfaste sur les Mw du PHB (-50% et -70% pour T3 et T0 après 5 minutes de mise en œuvre). Ceci est d'autant plus vrai en présence de catalyseur puisque la diminution de Mw atteint dans ce cas 68% et 75% de la valeur initiale pour les échantillons T3 et T0.

B.II.5.2 Par mélange maître

Dans le cas du PHB préparé via un mélange maître, on constate que la durée de mise en œuvre de ce dernier n'affecte pas les masses molaires moyennes en poids finales du nanocomposite. En effet, la diminution des Mw des échantillons TMB01a et TMB01b atteint

respectivement -58 et -61%, et -65 et -59% dans les cas des matériaux TMBC01a et TMBC01b. De plus, l'effet néfaste du catalyseur sur les masses molaires du PHB ne semble plus aussi marqué. Cependant, ces diminutions restent plus importantes que dans le cas d'un mélange direct lorsque la vitesse est abaissée à 50 rpm après introduction de la matière (-50% pour T3).

Il apparaît donc que l'ajout de catalyseur contribue à la dégradation du PHB. De plus, la préparation d'un mélange maître consistant à enrober dans un premier temps la charge dans la matrice ne semble pas limiter la dégradation du polymère dans lequel il est redispersé.

En conclusion, l'ajout de catalyseur et le procédé d'élaboration par mélange maître choisi ne semblent pas promouvoir les réactions de transestérification entre le PHB et la montmorillonite, via le feuillet inorganique ou l'organomodifiant. Les réactions de transestérification n'ont pas pu être mises en évidence, que ce soit par l'intermédiaire d'analyses thermogravimétriques sur les parties organiques et inorganiques issues des extractions, ou par la caractérisation des propriétés macroscopiques. De plus, il semble que les problèmes de stabilité thermique du PHB n'aient pu être résolus par ce type de procédé. Nous avons donc considéré une deuxième approche mettant enjeu un autre polymère biodégradable et biocompatible, le polycaprolactone.

C. Approche par greffage de PCL et mélange maître.

Cette partie présente l'élaboration de nano-biocomposites à base de PHA à partir d'un mélange-maître de chaînes PCL, greffées à la surface de l'argile par polymérisation par ouverture de cycle de l'ε-caprolactone. L'organisation de la charge au sein de la matrice sera étudiée par DRX aux petits angles et les propriétés thermiques seront déterminées.

C.I. Matériel et méthodes

L'élaboration des nano-biocomposites se fait donc en deux étapes : (i) préparation du mélange maître consistant au greffage à la surface des feuillets d'argile de PCL par polymérisation par ouverture de cycle de l'ε-CL par l'intermédiaire des groupes hydroxyles de l'organomodifiant, (ii) redispersion du mélange-maître dans la matrice PHA.

Concernant la préparation du mélange maître, le taux de charge, fixant la quantité de groupes hydroxyles, conditionne la longueur des chaînes polymères synthétisées (Lepoittevin, 2002b; Viville, 2004). Dans notre cas, un masterbatch chargé à 15 %pds d'argile a été préparé pour être ensuite redispersé de façon à obtenir un taux de charge final de 3 %pds dans la matrice PHA.

C.I.1. Matériel

Toutes les substances mises en jeu lors de cette réaction sont préalablement séchées afin d'éviter la présence d'eau dans le milieu réactionnel. L'ε-caprolactone (ε-CL, 99% pure, Acros Organics) est séchée sur tamis moléculaire, le toluène est distillé, quant à la C30B et au PHB, ils sont placés à l'étuve sous vide à 80°C toute une nuit.

C.I.2. Mélange-maître : Greffage de PCL par ouverture de cycle (**GPCL**)

C.I.2.1. Préparation

4,5 g de C30B séchée sont introduits dans un tricol de 500 ml fermé par 2 septum et une allonge à vide. Ce tricol est placé sous atmosphère inerte par une série de plusieurs cycles vide/argon. Le séchage de l'argile est prolongé pendant 3h en maintenant le ballon sous vide dans un bain d'huile à 70°C. Dans un deuxième temps, toujours sous atmosphère inerte, 21 g de ε-CL sont ajoutés à la C30B et laissés sous légère agitation pendant 1h pour permettre au monomère de gonfler la charge. Un réfrigérant est ensuite intégré au montage avant l'introduction de 600 ml de toluène distillé et de l'amorceur, l'octoate d'étain $Sn(Oct)_2$. La proportion de ce dernier est calculée de façon à avoir un rapport n(CL)/n(Sn)=200, soit 0,36 ml de $Sn(Oct)_2$. Après 1h sous agitation magnétique pour homogénéiser le milieu, le mélange est porté à 110°C afin d'amorcer la polymérisation par ouverture de cycle de CL à partir de la charge organo-modifiée. Cette étape de polymérisation in-situ est stoppée lorsque la consistance du milieu (viscosité, transparence) atteste d'une conversion quasi complète du monomère, dans notre cas après 5 jours.

Pour récupérer le masterbatch "PCL greffée sur C30B", noté GPCL, le solvant est partiellement évaporé de façon à concentrer le polymère tout en conservant la solution relativement fluide. Le polymère est ensuite précipité dans le n-heptane puis filtré sur

büchner. La poudre est séchée à l'étuve sous vide à 30°C toute une nuit. La masse finale du produit GPCL est de 22,1 g. Le taux effectif d'inorganique déterminé par thermogravimétrie est de 16%pds. En supposant une conversion totale du monomère, la masses molaire du PCL est estimée à 5 000 g/mol.

A cette étape, l'échantillon GPCL obtenu est analysé par DRX puis DSC et ATG de façon à déterminer le degré d'intercalation mais également de connaître le comportement en température du masterbatch.

C.I.2.2 Caractérisations

La distance interfeuillet est déterminée par DRX aux petits angles ($\mathbf{d_{GPCL}}$) en procédant à un balayage des angles 2θ de 1,5 à 10°C, à une vitesse de 0,03°/s.

L'analyse thermogravimétrique est réalisée selon une montée en température allant de la température ambiante à 600°C à une vitesse de 20°C/min sous flux d'azote.

Pour l'analyse DSC, le programme en température consiste à porter l'échantillon à 120°C de façon à "effacer son histoire thermique", à refroidir celui-ci jusqu'à 0°C puis à chauffer de nouveau l'échantillon à 120°C, tout ceci à une vitesse de 10°C/min.

C.I.3. Nano-biocomposites à base de PHA

C.I.3.1. Redispersion du mélange-maître

Le masterbatch est redispersé dans le PHB (ou le PHBV4) de façon à obtenir un nanocomposite PHA/GPCL à 3 %pds de matière inorganique.

Pour cela, 10,6 g du masterbatch sont mélangés manuellement à 42,4 g de PHB (ou PHBV). Ce mélange est introduit dans le mélangeur interne et mis en œuvre dans les mêmes conditions que les nanocomposites préparés par voie "fondue" (cf. Chapitre 2), i.e. à 170°C (160°C pour le PHBV4), avec une vitesse de rotation des pales de 100 rpm, réduite à 50 rpm après introduction et maintenue jusqu'à 5 minutes.

C.I.3.2. Caractérisations

Les analyses par DRX et par thermogravimétrie sont réalisées selon les mêmes protocoles qu'indiqués précédemment pour le masterbatch GPCL (cf §C.1.2.2).

En revanche, le programme en température de l'analyse par calorimétrie différentielle (DSC) est similaire aux nano-biocomposites préparés par voie "fondu" et rapportée au

Chapitre 2, i.e. une température maximale de 200°C à la chauffe et un refroidissement jusqu'à une température de -50°C. Le but est de nous renseigner sur l'éventuelle miscibilité du mélange PHB/PCL greffé par la détermination des principales caractéristiques (température, enthalpie, cristallinité) relatives aux différents phénomènes observés (cristallisation, fusion, transition vitreuse).

C.II. Résultats et discussion

C.II.1. Structure

Le diffractogramme RX du masterbatch GPCL présente un pic de diffraction correspondant à une distance interfeuillet de 32,0 Å (cf. Figure 11), soit une augmentation de 13,5 Å comparé au d_{001} de la C30B (d_{C30B}=18,5 Å). On peut donc considérer que les chaînes PCL se trouvent intercalées entre les feuillets inorganiques.

Une fois le mélange maître redispersé dans les matrices PHAs, cette distance interfeuillet augmente encore pour atteindre 41,4 Å dans la matrice PHB et 35,3 Å dans le cas du PHBV4. Cette augmentation démontre l'intercalation de chaînes PHA entre les feuillets de montmorillonites modifiées par le PCL, supposant donc une partielle compatibilité entre les deux polymères. Quant à l'intensité des pics de diffraction, cela nous laisse penser que l'argile est dispersée sous forme de petits tactoïdes. Les matériaux élaborés présentent clairement une structure intercalée. De plus, nous observons que le PHB conduit à une meilleure intercalation que le PHBV4, tout comme nous l'avions observé dans le cas des nanocomposites élaborés par voie "fondu" au chapitre II.

Cependant, les distances interfeuillets restent du même ordre, voire sont inférieures à celles des nano-biocomposites PHA/C30B obtenus par mélange direct ($d_{PHB/C30B}$=40,4 Å et $d_{PHBV4/C30B}$=38,5 Å). Au niveau de la nanostructure, cette approche ne semble donc présenter qu'un intérêt limité.

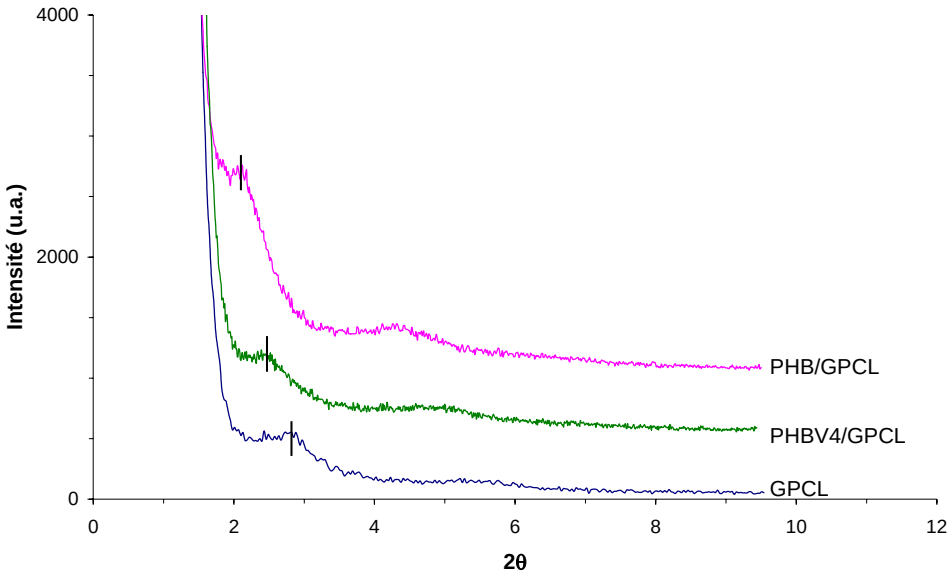

Figure 27 : Diffractogrammes RX du mélange maître GPCL et des nano-biocomposites PHA/GPCL

Quelques caractérisations complémentaires ont été toutefois menées pour tenter de mettre en évidence l'influence de l'ajout de PCL sur les propriétés du PHB.

C.II.2. Propriétés thermiques

C.II.2.1. Analyse thermogravimétrique

L'analyse thermogravimétrique nous permet d'une part de déterminer le taux effectif de charge dans le mélange maître et le matériau final, et d'autre part de connaître la stabilité thermique des nanocomposites élaborés.

Tout d'abord, le mélange maître présente un taux effectif de charge de 16 %pds. Sa dégradation se fait en deux étapes :

- la 1ère étape comprise entre 180 et 300°C, dont la perte de masse équivaut à à 8,5%, correspond à la dégradation des ammoniums quaternaires de la C30B (~3,5%pds) mais également à la première étape de la dégradation du PCL de faibles masses molaires (Persenaire, 2001) ;
- la 2e étape entre ~300 et 410°C correspond à la dégradation du PCL greffé à la surface de l'OMMT.

Quant aux nano-biocomposites à base de PHA, ils présentent un taux de matière inorganique respectivement de 2,4 et 3,0 %pds dans le cas du PHB et du PHBV4. Leur dégradation se fait également en deux étapes :

- dans un premier temps, environ 80% de la masse initiale est volatilisée dans un intervalle de température compris entre 267 et 338 °C pour l'échantillon PHB/GPCL et 267 et 334°C dans le cas de PHBV4/GPCL ; cette étape correspondant à la décomposition des PHAs ;
- dans un deuxième temps, une perte de masse de 16 %pds entre 335 et 400°C dans le cas de PHB/GPCL et entre 335 et 390°C dans le cas de PHBV4/GPCL.

Ces pertes de masse correspondent aux fractions massiques de PHA et de PCL dans les nanocomposites étudiés. En effet, le taux de matière inorganique dans le mélange maître (16%pds) nous donne un taux de C30B égal à 19% sachant que le taux d'organomodifiant dans la C30B est de 16%pds (cf. Annexe I). Ainsi, la proportion de PCL dans le mélange maître s'élève à 81%pds. Une fois le mélange maître redispersé dans les matrices PHAs, le taux de matière inorganique obtenu est d'environ 3%pds, soit une dilution d'environ 5,3. Ceci nous conduit donc à une fraction massique de PCL et de PHB respectivement égales à 15 et 82%.

Les courbes thermogravimétriques des nano-biocomposites PHA/GPCL reportées sur la Figure 12 présentent donc la même allure. Cependant, un léger décalage (~7°C) vers les hautes températures est observé dans la région de la dégradation du PCL pour l'échantillon PHB/GPCL. Cela peut s'expliquer par une meilleure intercalation et dispersion de la charge sans pour autant exclure un problème de précision dans la mesure.

En comparant ces résultats aux analyses thermogravimétriques relatives aux nanocomposites préparés par mélange direct (PHB/C30B et PHBV4/C30B), le PCL ne semble pas améliorer la stabilité thermique du PHB puisque les courbes sont superposées en début de dégradation, i.e. jusqu'à environ 300°C. Ainsi, l'incorporation de PCL permet seulement d'éviter une dégradation complète rapide en retardant la fin de la dégradation d'environ 70°C.

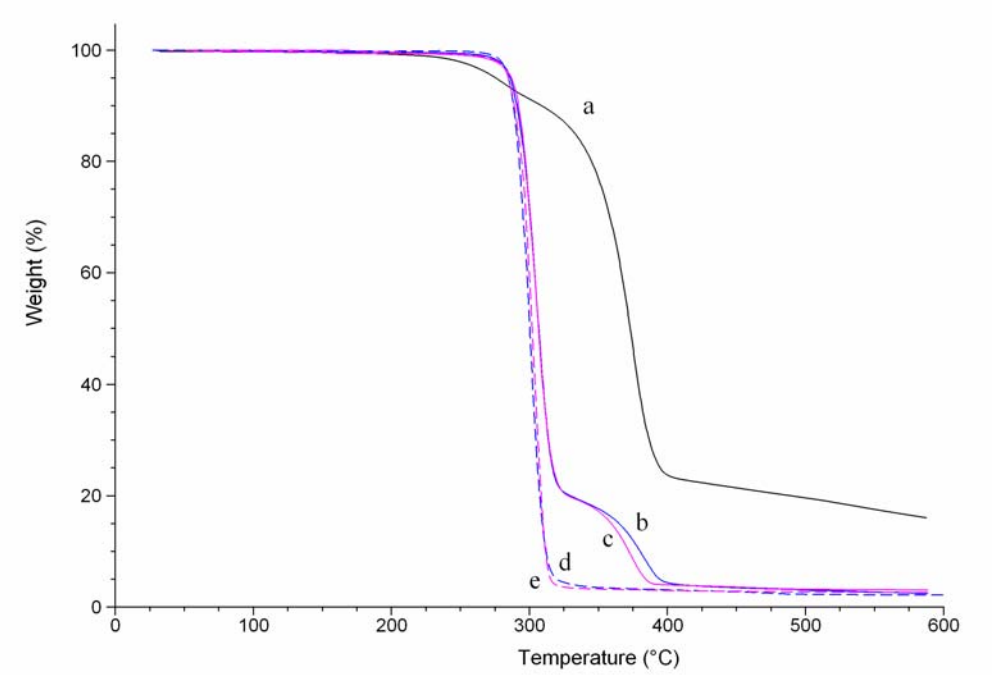

Figure 28 : Courbes thermogravimétriques a) du mélange maître GPCL et des nano-biocomposites b) PHB/GPCL, c) PHBV4/GPCL, d) PHB/C30B 3%pds et e) PHBV4/C30B 3%pds.

C.II.2.2. Analyse calorimétrique différentielle (DSC)

La miscibilité des mélanges polymères est souvent déterminée par DSC, et notamment par l'observation d'une transition vitreuse aux alentours de la température calculée selon l'équation 1. Dans notre cas, en considérant Tg_{PCL}=213 K (-60°C) et Tg_{PHB}=276 K (-3°C) ainsi que les fractions massiques déterminées à la suite des analyses ATG, la température de transition vitreuse du mélange miscible PHB/PCL serait de -1°C. Cependant, les températures de cristallisation et de fusion du PHB et les enthalpies correspondantes peuvent également nous donner des informations complémentaires.

Dans le Tableau 11, les résultats DSC des nanocomposites PHA/GPCL sont comparés aux mélanges directs PHA/C30B d'une part, et aux polymères seuls mis en œuvre d'autre part.

Concernant les matériaux PHA/GPCL, nous remarquons tout d'abord deux composantes relatives à chacun des polymères du mélange : d'une part, les températures de cristallisation et de fusion des PHAs respectivement égales à 82 et 167-175°C pour le PHB et 74 et 161/173°C pour le PHBV4, et d'autre part, les mêmes températures caractéristiques correspondant à la fraction de PCL, respectivement égales à ~30°C et 55°C. Il apparaît donc que les PHA et le PCL cristallisent selon deux phases distinctes. De plus, aucune température de transition vitreuse n'a pu être mise en évidence aux alentours des 0°C en raison du pic de

fusion du PCL masquant le phénomène. La DSC par modulation, une technique délicate à mettre en œuvre, aurait peut-être pu lever cette indétermination. Enfin, les températures de fusion des PHAs restent constantes quel que soit le mélange considéré, contrairement aux températures et enthalpies de cristallisation qui diminuent fortement.

Ces observations nous conduisent donc à penser que les PHAs et le PCL ainsi mélangés ne soient pas miscibles même si des interactions semblent apparaître entre les 2 polymères.

Tableau 14 : Résultats DSC des nano-biocomposites PHA/GPCL et PHA/C30B et des références PHB

	PHB/GPCL	PHB/C30B	PHB	PHBV4/GPCL	PHBV4/C30B	PHBV4
% charge	2,4	2,2	-	3,0	2,6	-
Tg (°C)	-	3	1,5	-	5	3
$Tc_{c\ PHA}$ (°C)	82	93	71	74	91	61
$\Delta Hc_{c\ PHA}$ (J/g)	38	63	50	34	59	40
Tm_{PHA} (°C)	168/175	167/173	169*/174	161/173	161/171	161*/172
$\Delta H_{m\ PHA}$ (J/g)	47	73	90	44	71	76
χ_{PHA}[a] (%)	32	50	62	30	49	52
$Tc_{c\ PCL}$ (°C)	7/14/29	-	-	32	-	-
$\Delta Hc_{c\ PCL}$ (J/g)	1	-	-	1	-	-
Tm_{PCL} (°C)	55	-	-	56	-	-
$\Delta H_{m\ PCL}$ (J/g)	2	-	-	2,1	-	-
χ_{PCL}[b] (%)	1	-	-	1,5	-	-

* épaulement du pic de fusion

[a] $\Delta H_{PCL\ 100\%\ crist.} = 136$ J/g

[b] $\Delta H_{PHB\ 100\%\ crist.} = \Delta H_{PHBV4\ 100\%\ crist.} = 146$ J/g

En conclusion, le mélange maître de PCL greffé à la surface de l'argile ne permet pas d'obtenir une meilleure nanostructuration de la charge au sein des matrices PHAs, et les premières propriétés déterminées nous laissent penser à une immiscibilité partielle des mélanges. Par conséquent, nous n'avons pas donné suite à cette approche.

Conclusion générale du chapitre IV

Dans ce chapitre, nous avons tenté de mettre en place de nouveaux procédés avancés d'élaboration des nano-biocomposites à base de PHA par voie "fondu". Le but était :

(i) d'améliorer la dispersion de la charge au sein de la matrice,

(ii) de limiter la dégradation du PHA lors de la mise en œuvre, responsable de la perte des propriétés du matériau final.

Pour cela, deux approches ont plus particulièrement été étudiées. La première consistait à promouvoir des réactions de transestérification entre les chaînes polymères et le feuillet inorganique ou l'organomodifiant. Nous espérions ainsi greffer des chaînes PHB à la surface de l'argile pour mieux compatibiliser la charge et la matrice et éventuellement limiter la dégradation du polymère à la couche périphérique de la montmorillonite. Cependant, ces réactions de transestérification n'ont pu être observées dans nos systèmes. De plus, malgré l'utilisation d'un catalyseur de transestérification, le dibutyle dilaurate d'étain, et/ou la préparation de mélange maître, nous n'avons pas constaté d'amélioration significative en terme de nanostructuration et de propriétés des matériaux. Il semblerait même qu'il y ait une possible augmentation de la dégradation en présence de catalyseur, phénomène classique déjà observé sur différents biopolyesters. On sait par exemple, que des résidus catalytiques favorisent la dégradation des polyesters.

Dans la deuxième approche, il s'agissait de préparer un mélange maître de PCL greffé à la surface de l'argile par polymérisation par ouverture de cycle et de redisperser ce mélange dans la matrice PHB. Aucune amélioration notable sur l'intercalation et la dispersion de la charge au sein du PHB n'a été mise en évidence et les propriétés déterminées tendent à montrer l'immiscibilité du mélange PHB/PCL.

L'élaboration de nano-biocomposites à base de PHA nécessitent donc d'utiliser d'autres approches novatrices afin d'améliorer la dispersion de la charge et/ou de prévenir la dégradation du polymère. Cependant, il faudra veiller à utiliser des composés biodégradables, et éventuellement biocompatibles, pour conserver les avantages majeurs des PHAs et s'assurer que les solutions proposées soient compatibles avec une perspective de développement industriel ultérieur. Les solutions proposées devront être intégrées au contexte de développement durable et être en accord avec la législation existante telle que la nouvelle réglementation européenne sur les substances chimiques (REACH) visant à améliorer la protection de la santé humaine et de l'environnement.

Bibliographie

An, Y., Dong, L., Li, G., Mo, Z., Feng, Z. (2000). Miscibility, crystallization kinetics, and morphology of poly(hydroxybutyrate) and poly(methyl acrylate) blends. *Journal of Polymer Science, Part B: Polymer Physics,* 38(14), 1860-1867.

Antunes, M. C. M., Felisberti, M. I. (2005). Blends of pol(hydroxybutyrate) and poly(e-caprolactone) obtained from melting mixture. *Polimeros: Ciencia e Tecnologia,* 15(2), 134-138.

Avella, M., Martuscelli, E. (1988). Poly-D-(-)(3-hydroxybutyrate)/poly(ethylene oxide) blends: Phase diagram, thermal and crystallization behaviour. *Polymer,* 29(10), 1731-1737.

Avella, M., Immirzi, B., Malinconico, M., Martuscelli, E., Volpe, M. G. (1996). Reactive blending methodologies for biopol. *Polymer International,* 39(3), 191-204.

Avella, M., Martuscelli, E., Raimo, M. (2000). Properties of blends and composites based on poly(3-hydroxy)butyrate (PHB) and poly(3-hydroxybutyrate-hydroxyvalerate) (PHBV) copolymers. *Journal of Materials Science,* 35(3), 523-545.

Billingham, N. C., Henman, T. J., Holmes, P. A. (1987). Degradation and stabilisation of polyesters of biological and synthestic origin. *Developments in Polymer Degradation* pp. 81-121). London: Elsevier Applied Science.

Blumm, E., Owen, A. J. (1995). Miscibility, crystallization and melting of poly(3-hydroxybutyrate) /poly(L-lactide) blends. *Polymer,* 36(21), 4077-4081.

Fukuda, H., Kondo, A., Noda, H. (2001). Biodiesel fuel production by transesterification of oils. *Journal of Bioscience and Bioengineering,* 92(5), 405-416.

Gassner, F., Owen, j. (1994). Physical properties of poly(ß-hydroxybutyrate)-poly(e-caprolactone) blends. *Polymer,* 35(10), 2233-2236.

Gonzalez, I., Eguiazabal, J. I., Nazabal, J. (2006). New clay-reinforced nanocomposites based on a polycarbonate/ polycaprolactone blend. *Polymer Engineering and Science,* 46(7), 864-873.

Hammond, T. (1997). *Polymer composition containing polyhydroxyalkanoate and metal compound*. US5646217, Zeneca Limited, London, England, United Kingdom

Kiersnowski, A., Piglowski, J. (2004). Polymer-layered silicate nanocomposites based on poly(e-caprolactone). *European Polymer Journal,* 40(6), 1199-1207.

Kim, S. W., Jo, W. H., Lee, M. S., Ko, M. B., Jho, J. Y. (2001). Preparation of clay-dispersed poly(styrene-co-acrylonitrile) nanocomposites using poly(e-caprolactone) as a compatibilizer. *Polymer,* 42(24), 9837-9842.

Kubies, D., Pantoustier, N., Dubois, P., Rulmont, A., Jerome, R. (2002). Controlled ring-opening polymerization of e-caprolactone in the presence of layered silicates and formation of nanocomposites. *Macromolecules,* 35(9), 3318-3320.

Kumagai, Y., Doi, Y. (1992). Enzymatic degradation and morphologies of binary blends of microbial poly(3-hydroxy butyrate) with poly(e-caprolactone), poly(1,4-butylene adipate) and poly(vinyl acetate). *Polymer Degradation and Stability,* 36(3), 241-248.

Lepoittevin, B., Pantoustier, N., Alexandre, M., Calberg, C., Jerome, R., Dubois, P. (2002a). Polyester layered silicate nanohybrids by controlled grafting polymerization. *Journal of Materials Chemistry,* 12(12), 3528-3532.

Lepoittevin, B., Pantoustier, N., Alexandre, M., Calberg, C., Jerome, R., Dubois, P. (2002b). Layered silicate/polyester nanohybrids by controlled ring-opening polymerization. *Macromolecular Symposia,* 183, 95-102.

Lepoittevin, B., Pantoustier, N., Devalckenaere, M., Alexandre, M., Kubies, D., Calberg, C., Jerome, R., Dubois, P. (2002c). Poly(e-caprolactone)/clay nanocomposites by in-situ intercalative polymerization catalyzed by dibutyltin dimethoxide. *Macromolecules,* 35(22), 8385-8390.

Lepoittevin, B., Pantoustier, N., Devalckenaere, M., Alexandre, M., Calberg, C., Jerome, R., Henrist, C., Rulmont, A., Dubois, P. (2003). Polymer/layered silicate nanocomposites by combined intercalative polymerization and melt intercalation: A masterbatch process. *Polymer,* 44(7), 2033-2040.

Lewitus, D., McCarthy, S., Ophir, A., Kenig, S. (2006). The effect of nanoclays on the properties of PLLA-modified polymers Part 1: Mechanical and thermal properties. *Journal of Polymers and the Environment,* 14(2), 171-177.

Lovera, D., Marquez, L., Balsamo, V., Taddei, A., Castelli, C., Muller, A. J. (2007). Crystallization, morphology, and enzymatic degradation of polyhydroxybutyrate/ polycaprolactone (PHB/PCL) blends. *Macromolecular Chemistry and Physics,* 208(9), 924-937.

Ma, D., Zhang, G., Huang, Z., Luo, X. (1998). Synthesis and chain structure of ethylene terephthalate-ε-caprolactone copolyesters. *Journal of Polymer Science Part A: Polymer Chemistry,* 36(16), 2961-2969.

Marand, H., Collins, M. (1990). Crystallization and morphology of poly(vinylidene fluoride)/poly(3-hydroxybutyrate) blends. *American Chemical Society, Polymer Preprints, Division of Polymer Chemistry* pp. 552-553).

Organ, S. J., Barham, P. J. (1993). Phase separation in a blend of poly(hydroxybutyrate) with poly(hydroxybutyrate-co-hydroxyvalerate). *Polymer,* 34(3), 459-467.

Otera, J. (1993). Transesterification. *Chemical Reviews,* 93(4), 1449-1470.

Pantoustier, N., Lepoittevin, B., Alexandre, M., Kubies, D., Calberg, C., Jerome, R., Dubois, P. (2002). Biodegradable polyester layered silicate nanocomposites based on poly(e-caprolactone). *Polymer Engineering and Science,* 42(9), 1928-1937.

Paul, M.-A., Alexandre, M., Degée, P., Calberg, C., Jerome, R., Dubois, P. (2003). Exfoliated polylactide/clay nanocomposites by in-situ coordination-insertion polymerization. *Macromolecular Rapid Communications,* 24(9), 561-566.

Paul, M.-A., Delcourt, C., Alexandre, M., Degée, P., Monteverde, F., Rulmont, A., Dubois, P. (2005). (Plasticized) polylactide/(organo-)clay nanocomposites by in situ intercalative polymerization. *Macromolecular Chemistry and Physics,* 206(4), 484-498.

Persenaire, O., Alexandre, M., Degée, P., Dubois, P. (2001). Mechanisms and kinetics of thermal degradation of poly(e-caprolactone). *Biomacromolecules,* 2(1), 288-294.

Pinto, A. C., Guarieiro, L. L. N., Rezende, M. J. C., Ribeiro, N. M., Torres, E. A., Lopes, W. A., De Pereira, P. A. P., De Andrade, J. B. (2005). Biodiesel: An overview. *Journal of the Brazilian Chemical Society,* 16(6 B), 1313-1330.

Poller, R. C., Retout, S. P. (1979). Organotin compounds as transesterification catalysts. *Journal of Organometallic Chemistry,* 173(3), C7-C8.

Pollet, E., Delcourt, C., Alexandre, M., Dubois, P. (2006). Transesterification catalysts to improve clay exfoliation in synthetic biodegradable polyester nanocomposites. *European Polymer Journal,* 42(6), 1330-1341.

Rehberg, C. E., Faucette, W. A., Fisher, C. H. (1944a). Preparation and properties of secondary and branched-chain alkyl acrylates. *Journal of the American Chemical Society,* 66(10), 1723-1724.

Rehberg, C. E., Fisher, C. H. (1944b). Preparation and properties of the n-alkyl acrylates. *Journal of the American Chemical Society,* 66(7), 1203-1207.

Schuchardt, U., Sercheli, R., Vargas, R. M. (1998). Transesterification of vegetable oils: A review. *Journal of the Brazilian Chemical Society,* 9(3), 199-210.

Tomita, K., Ida, H. (1975). Studies on the formation of poly(ethylene terephthalate): 3. Catalytic activity of metal compounds in transesterification of dimethyl terephthalate with ethylene glycol. *Polymer,* 16(3), 185-190.

Viville, P., Lazzaroni, R., Pollet, E., Alexandre, M., Dubois, P., Borcia, G., Pireaux, J.-J. (2003). Surface Characterization of Poly(e-caprolactone)-Based Nanocomposites. *Langmuir,* 19(22), 9425-9433.

Viville, P., Lazzaroni, R., Pollet, E., Alexandre, M., Dubois, P. (2004). Controlled polymer grafting on single clay nanoplatelets. *Journal of the American Chemical Society,* 126(29), 9007-9012.

Vollhardt, K. P. C. (1990). *Traité de chimie organique*. Bruxelles, Belgium: De Boeck et Editions Universitaires.

Yu, L., Dean, K., Li, L. (2006). Polymer blends and composites from renewable resources. *Progress in Polymer Science (Oxford),* 31(6), 576-602.

Zhang, Z., Luo, X., Lu, Y., Ma, D. (2001a). Transesterifications of poly(bisphenol A carbonate) with caprolactone segments in copolyester and poly(e-caprolactone) homopolymer. *European Polymer Journal,* 37(1), 99-104.

Zhang, Z., Luo, X., Lu, Y., Ma, D. (2001b). Transesterifications of poly(bisphenol A carbonate) with aromatic and aliphatic segments in ethylene terephthalate-caprolactone copolyester. *Journal of Applied Polymer Science,* 80(9), 1558-1565.

Zheng, X., Wilkie, C. A. (2003). Nanocomposites based on poly (e-caprolactone) (PCL)/clay hybrid: Polystyrene, high impact polystyrene, ABS, polypropylene and polyethylene. *Polymer Degradation and Stability,* 82(3), 441-450.

Conclusion générale
et
Perspectives

Conclusion générale

Ce travail très transversal, associant la chimie et les procédés d'élaboration des polymères, avait notamment pour but de développer des matériaux nanostructurés performants à base de polyhydroxyalcanoates (PHAs). Ces derniers sont des polymères issus de ressources renouvelables, obtenus par voie bactérienne, biodégradables et biocompatibles mais présentant notamment un comportement mécanique limité et une faible stabilité thermique. Parmi les principaux PHAs, on trouve le PHB et le PHBV. Par rapport aux approches classiques de modification chimique des polymères, la démarche retenue dans le cadre de cette thèse pour améliorer les propriétés de ces biopolymères est axée principalement sur la formulation, à savoir l'élaboration de nano-biocomposites à base de PHAs. Dans notre cas, la montmorillonite nous est apparue comme un choix judicieux en tant que nanocharge du fait de ses caractéristiques intrinsèques (facteur de forme important, surface interfaciale très élevée, possibilités d'organomodification, produit issu de ressources naturelles…) et de sa disponibilité. Cependant, l'amélioration des propriétés n'est possible que lorsque la charge se présente sous forme de feuillets individualisés (état exfolié), dispersés de façon homogène au sein de la matrice.

Notre démarche expérimentale se décompose en trois volets distincts :

(i) une approche formulation avec la compréhension des relations 'procédé-structure-propriétés' dans les systèmes nano-biocomposites PHA/Montmorillonite afin de déterminer les conditions optimales d'élaboration,

(ii) l'identification des composés et des mécanismes de dégradation mis en jeu dans ces systèmes, et enfin,

(iii) la recherche de nouvelles méthodes alternatives pour l'élaboration de ces matériaux.

Les facteurs clés contrôlant l'élaboration de matériaux nanostructurés, à savoir l'affinité polymère-argile, le taux de charge et la voie d'élaboration (voie "solvant" vs. "fondu") ont été mis en évidence au travers de l'étude de la (nano)structure et des propriétés des matériaux. Ces dernières ont été déterminées selon différentes techniques de caractérisation qui ont permis d'étudier le matériau à différentes échelles, du "nano" au "macro". Une technique particulièrement intéressante utilisant la RMN du solide a été

appliquée avec succès à nos systèmes. Elle nous a permis d'étayer et de compléter les résultats structuraux obtenus par des techniques avancées telles que la DRX et la MET.

(i) Dans le cas d'une bonne affinité polymère-charge (PHA/C30B), des nanocomposites présentant des petits tactoïdes (3 à 10 feuillets) dispersés au sein de la matrice ont été obtenus. En revanche, dans le cas d'une faible compatibilité polymère-charge (PHA/MMT-Na), les matériaux présentent de gros tactoïdes agrégés traduisant une structure de type microcomposite ;

(ii) Un taux croissant de charge tend à diminuer la qualité de la dispersion de la charge au sein de la matrice ;

(iii) Concernant l'influence du procédé de préparation des nanocomposites, nous avons pu mettre en exergue les limites de chacun d'eux. Ainsi, outre les problèmes environnementaux que pose l'utilisation de solvants organiques, la voie "solvant" n'est pas apparue comme étant une approche appropriée à la bonne dispersion d'argile au sein de la matrice PHB du fait du choix restreint des solvants des PHAs et de la mauvaise affinité polymère/solvant/OMMT. Par ailleurs, la faible stabilité thermique des PHAs lors de la mise en œuvre en milieu fondu limite l'amélioration des propriétés malgré une dispersion de la charge satisfaisante.

Suite à cela, une étude spécifique a été menée afin de mieux connaître les composés et les mécanismes mis en jeu dans les réactions de dégradation des PHAs dans des systèmes nanocomposites. Lors de la phase précédente, l'influence de certains composés liés à l'addition de nanocharges avait été mise en évidence comme favorisant la dégradation des PHAs. L'analyse plus approfondie de la cinétique de dégradation a permis de démontrer que les ammoniums quaternaires, utilisés pour compatibiliser le polymère et la charge, affectent grandement la stabilité thermique et thermo-mécanique du PHB et des PHBVs. Nous avons également établi que les résidus de fermentation, mélange complexe de différents composés issus du mode de bioproduction des PHAs, participent également, mais dans une moindre mesure, à la dégradation de ces polymères. Le mécanisme de dégradation des ammoniums quaternaires et l'influence de leurs produits de décomposition sur la stabilité thermique du polymère ont été identifiés.

Face à ces problèmes de stabilité thermique, d'autres approches ont été explorées afin d'améliorer la dispersion de la charge, de mieux compatibiliser la charge et la matrice, et enfin, de limiter la dégradation de la matrice d'origine bactérienne.

La première méthode cherchait à promouvoir des réactions de transestérification entre les chaînes polymères et le feuillet inorganique lui-même ou l'organomodifiant, pour greffer des chaînes polymères en surface du feuillet. Malheureusement, ces réactions de transestérification n'ont pu être démontrées et aucune amélioration significative de la structure et des propriétés des matériaux n'a été constatée. De même, le deuxième protocole testé consistant à préparer les nanocomposites PHA/Montmorillonite via un mélange maître de PCL greffé à la surface de l'argile n'a pas conduit à une meilleure dispersion de la charge. Par ailleurs, les propriétés déterminées tendent à montrer la faible miscibilité du mélange PHB/PCL.

Aucune de ces deux méthodes exploratoires testées n'ont permis d'améliorer significativement la nano-structuration et de manière générale les propriétés du matériau. Ceci permet d'envisager, dans le cadre des perspectives de ce travail, d'autres approches novatrices. Cependant, il faudra veiller à utiliser des composés biodégradables, et éventuellement biocompatibles, pour conserver les avantages majeurs des PHAs. De plus, les solutions proposées devront être compatibles avec une perspective de développement industriel ultérieur.

Perspectives

Au vu de ces résultats, bien que la nanostructuration des nano-biocomposites PHA/Montmorillonites soit prometteuse avec l'obtention de systèmes partiellement exfoliés, la faible stabilité thermique des PHAs en milieu fondu s'avère être un verrou majeur à l'élaboration de matériaux performants et techniquement très compétitifs. Ce verrou n'a été que partiellement levé dans le cadre de cette étude.

La maîtrise de cette dégradation passe par plusieurs approches à explorer : le changement du type de charge lamellaire (le mica par exemple) ou l'utilisation d'un autre organomodifiant (les phosphoniums) moins sensible à la température. De plus, l'ajout d'un additif tel qu'un plastifiant ou le mélange avec un autre polymère permettraient de travailler à des températures plus basses. Enfin, la modification chimique du polymère pourra également être envisagée bien que cette approche nuise souvent à l'Analyse du Cycle de Vie (ACV) et participe à l'augmentation du coût du matériau. Par ailleurs, l'ajout de nouvelles molécules au

système risque d'engendrer un problème d'intercalation préférentielle de petites molécules au détriment du polymère. Un contrôle particulier de la structure devra donc être mené ainsi qu'une étude de la mobilité de ces molécules dans un environnement contraint par la présence des nanocharges. La RMN du solide pourrait apporter ici quelques réponses. Il faudra veiller à ce que ces différentes approches soient compatibles avec un développement industriel ultérieur.

Au vu des différentes applications de ces nanocomposites, il apparait indispensable de déterminer les propriétés d'usage de ces matériaux. Par exemple, pour des applications dans le domaine de l'emballage compostable à courte durée de vie, il apparaît indispensable d'évaluer la perméabilité de ces matériaux à la vapeur d'eau et à l'oxygène, et de suivre l'impact du triptyque " procédé-structure-matériau" sur celles-ci. Il en sera de même dans l'étude de la biodégradation (environnementale) et de la compostabilité de ces matériaux qui, de plus, devrait être associée à l'analyse de l'écotoxicité des résidus de biodégradation.

Pour des applications dans le domaine biomédical, il faudra évaluer la biocompatibilité de ces matériaux au contact de tissus vivants ainsi que la biodégradation (non environnementale) tissulaire. Cette étude pourrait être menée en fonction des variables formées par les composants du matériau, le process utilisé et la structure qui en découle.

Annexes

Annexe I: Propriétés des matériaux utilisés

A. Les matrices polyhydroxyalcanoates

Polymère	Référence	%HV	Mw	Ip	densité	T_f (°C)
PHB	PHB ou PHB650	0	650 000	2,1	1,22	175
PHB	PHB470	0	470 000	2,3	1,25	172
PHBV	PHBV4	4	930 000	2,2	1,22	173
PHBV	PHBV8	8	280 000	2,7	1,19	158

B. Les montmorillonites commerciales

Argile		Organo-modifiant	Type	CEC (meq/100g)	Δw (%)[a]	Fournisseur
Cloisite	Na	-	MMT-Na		-	
	15A	2M2HT[b]	OMMT-Alk	125	29,4	Southern Clay
	20A	2M2HT[b]	OMMT-Alk	95	23,1	Products, Inc.
	30B	MT2EtOH[c]	OMMT-OH	90	16,0	
Dellite	LVF	-	MMT-Na		-	
	HPS	-	MMT-Na		-	Laviosa
	D43B	2MBHT[b]	OMMT-Bz	95[*]	29,2	Chimica
	D67G	2M2HT[d]	OMMT-Alk		29,2	

[a] Taux de matière organique mesuré par analyse thermogravimétrique en considérant la perte de masse entre 150 et 500°C
[b] 2M2HT : Dimethyl dihydrogenated tallow ammonium
[c] 2MBHT : Dimethylbenzylhydrogenated tallow ammonium
[d] MT2EtOH : Methyl bis-2-hydroxyethyl tallow ammonium
[*] données fournisseur avec d_{001}=18,6 Å; or nous obtenons expérimentalement d_{001}=37.2 Å mesuré par DRX ce qui laisse supposer que la valeur de CEC est supérieure à la CEC indiquée par le fournisseur.

Annexe II: Caractérisation par Diffraction des Rayons X (DRX)

C'est une technique d'analyse basée sur la diffraction des rayons X principalement utilisée pour caractériser la structure cristalline des matériaux.

La longueur d'onde des rayons X étant de l'ordre de grandeur des distances atomiques (quelques Å), les interférences des rayons diffusés vont être alternativement constructives ou destructives. Selon le matériau et la direction d'incidence des rayons X, le flux de RX diffractés varie (cf. Figure 1a). Les directions dans lesquelles les interférences sont constructives, appelées "pics de diffraction", peuvent être déterminées très simplement par la Loi de Bragg donnée ci–dessous.

$$n.\lambda = 2.d.\sin\theta$$

avec n= ordre de diffraction

λ : longueur d'onde des rayons X

d : distance inter-réticulaire i.e. distance entre les feuillets de montmorillonite

θ : demi-angle de déviation (moitié de l'angle faisceau incident-direction détecteur).

Cette technique peut être appliquée aux argiles, en particulier à la montmorillonite, du fait de la structure répétitive de l'empilement des feuillets. Grâce à cette relation, on peut donc déduire la distance d séparant deux feuillets (cf. Figure 1b). Dans le cas des montmorillonites, la distance est de l'ordre d'une à quelques dizaines d'angströms. Les pics de diffraction vont être détectés aux petits angles (1-10°). Au fur et à mesure que la distance interfeuillets augmente, le pic se déplace vers les petits angles.

On peut donc ainsi déterminer la structure de l'argile au sein de la matrice polymère. Si le polymère est intercalé entre les feuillets, un pic de diffraction sera observé et il sera plus ou moins décalé par rapport au pic de diffraction de la montmorillonite initiale. Si le procédé d'obtention du nanocomposite a permis d'obtenir une structure exfoliée, c'est-à-dire lorsqu'il y a déstructuration complète des tactoïdes en feuillets individuels, aucun pic de diffraction n'est décelé. Il faut cependant noter que la distance interfeuillets calculée par DRX n'est qu'une distance moyenne. C'est pourquoi, il est nécessaire de compléter cette analyse par des observations au microscope électronique à transmission (MET) ou d'autres méthodes de caractérisation (RMN du solide, ….).

a

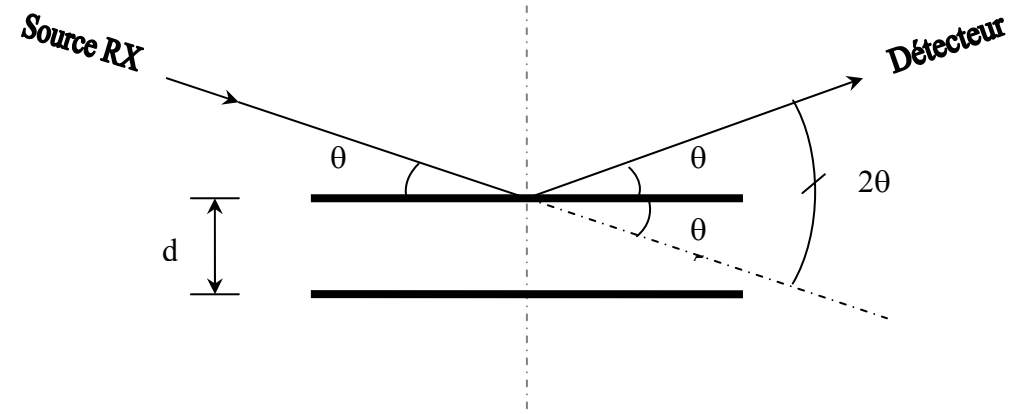

b

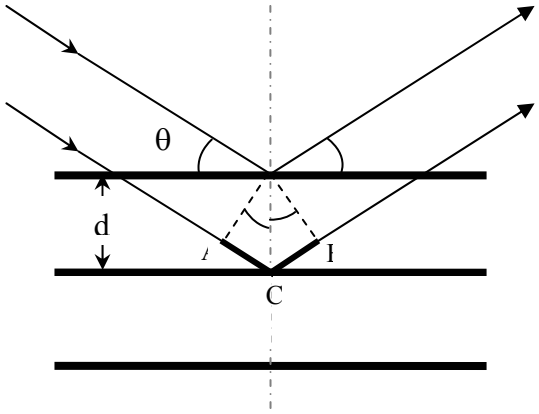

AC=BC=d.sinθ

Figure 1: Description du dispositif DRX (a) et illustration de la loi de Bragg (b)

Bibliographie générale

Abe, H. (2006). Thermal Degradation of Environmentally Degradable Poly(hydroxyalkanoic acid)s. *Macromolecular Bioscience,* 6(7), 469-486.

An, Y., Dong, L., Li, G., Mo, Z., Feng, Z. (2000). Miscibility, crystallization kinetics, and morphology of poly(?-hydroxybutyrate) and poly(methyl acrylate) blends. *Journal of Polymer Science, Part B: Polymer Physics,* 38(14), 1860-1867.

Antunes, M. C. M., Felisberti, M. I. (2005). Blends of pol(hydroxybutyrate) and poly(e-caprolactone) obtained from melting mixture. *Polimeros: Ciencia e Tecnologia,* 15(2), 134-138.

Albertsson, A.-C., Varma, I. K. (2002). Aliphatic polyesters: Synthesis, properties and applications. *Advances in Polymer Science,* 157, 1-40.

Amass, W., Amass, A., Tighe, B. (1998). A review of biodegradable polymers: Uses, current developments in the synthesis and characterization of biodegradable polyesters, blends of biodegradable polymers and recent advances in biodegradation studies. *Polymer International,* 47(2), 89-144.

Aoyagi, Y., Yamashita, K., Doi, Y. (2002). Thermal degradation of poly[(R)-3-hydroxybutyrate], poly[e-caprolactone], and poly[(S)-lactide]. *Polymer Degradation and Stability,* 76(1), 53-59.

Asrar, J., Mitsky, T. A., Shah, D. T. (2000). *Polyhydroxyalkanoates of narrow molecular weight distribution prepared in transgenic plants*. US6091002, Monsanto Company, St Louis, MO, United States

Asrar, J., Mitsky, T. A., Shah, D. T. (2001). *Polyhydroxyalkanoates of narrow molecular weight distribution prepared in transgenic plants*. US6228623, Monsanto Company, St Louis, MO, United States

Auras, R., Harte, B., Selke, S. (2004). An overview of polylactides as packaging materials. *Macromolecular Bioscience,* 4(9), 835-864.

Avella, M., Martuscelli, E. (1988). Poly-D-(-)(3-hydroxybutyrate)/poly(ethylene oxide) blends: Phase diagram, thermal and crystallization behaviour. *Polymer,* 29(10), 1731-1737.

Avella, M., Immirzi, B., Malinconico, M., Martuscelli, E., Volpe, M. G. (1996). Reactive blending methodologies for biopol. *Polymer International,* 39(3), 191-204.

Avella, M., Martuscelli, E., Raimo, M. (2000). Properties of blends and composites based on poly(3-hydroxy)butyrate (PHB) and poly(3-hydroxybutyrate-hydroxyvalerate) (PHBV) copolymers. *Journal of Materials Science,* 35(3), 523-545.

Averous, L., Moro, L., Dole, P., Fringant, C. (2000). Properties of thermoplastic blends: Starch-polycaprolactone. *Polymer,* 41(11), 4157-4167.

Averous, L. (2004). Biodegradable multiphase systems based on plasticized starch: A review. *Journal of Macromolecular Science-Polymer Reviews,* C44(3), 231-274.

Averous, L., Boquillon, N. (2004). Biocomposites based on plasticized starch: Thermal and mechanical behaviours. *Carbohydrate Polymers,* 56(2), 111-122.

Bastioli, C., Cerutti, A., Guanella, I., Romano, G. C., Tosin, M. (1995). Physical state and biodegradation behavior of starch-polycaprolactone systems. *Journal of Environmental Polymer Degradation,* 3(2), 81-95.

Bastioli, C. (1998). Biodegradable Materials - Present Situation and Future Perspectives. *Macromolecular Symposia,* 135, 193-204.

Bastioli, C. (1998). Properties and applications of mater-Bi starch-based materials. *Polymer Degradation and Stability,* 59(1-3), 263-272.

Bigg, D. M. (1996). Effect of copolymer ratio on the crystallinity and properties of polylactic acid copolymers. *Journal of Engineering and Applied Science,* 2, 2028-2039.

Billingham, N. C., Henman, T. J., Holmes, P. A. (1987). Degradation and stabilisation of polyesters of biological and synthestic origin. *Developments in Polymer Degradation* pp. 81-121). London: Elsevier Applied Science.

Blumm, E., Owen, A. J. (1995). Miscibility, crystallization and melting of poly(3-hydroxybutyrate) /poly(L-lactide) blends. *Polymer,* 36(21), 4077-4081.

Bonczek, J. L., Harris, W. G., Nkedi-Kizza, P. (2002). Monolayer to bilayer transitional arrangements of hexadecyltrimethylammonium cations on Na-montmorillonite. *Clays and clay minerals,* 50(1), 11-17.

Bordes, P., Hablot, E., Pollet, E., Avérous, L. (2008). Effect of clay organomodifiers on polyhydroxyalkanoates degradation, ***submitted.***

Bordes, P., Pollet, E., Averous, L. (2008). Nano-biocomposites: A review of biopolyester/clay systems, ***submitted.***

Bordes, P., Pollet, E., Averous, L. (2008). Structure and properties of PHA/clay nano-biocomposites prepared by melt intercalation, ***submitted.***

Bourbigot, S., VanderHart, D. L., Gilman, J. W., Awad, W. H., Davis, R. D., Morgan, A. B., Wilkie, C. A. (2003). Investigation of nanodispersion in Polystyrene-Montmorillonite nanocomposites by solid-state NMR. *Journal of Polymer Science - Part B Polymer Physics,* 41, 3188.

Bourbigot, S., Vanderhart, D. L., Gilman, J. W., Bellayer, S., Stretz, H., Paul, D. R. (2004). Solid state NMR characterization and flammability of styrene-acrylonitrile copolymer montmorillonite nanocomposite. *Polymer,* 45(22), 7627-7638.

Bruns, C., Gottschall, R., De Wilde, B. (2001). Ecotoxicological trials with BAK 1095 according to DIN V 54900. *Orbit J.,* 1(1), 1-10.

Burgentzlé, D., Duchet, J., Gerard, J. F., Jupin, A., Fillon, B. (2004). Solvent-based nanocomposite coatings: I. Dispersion of organophilic montmorillonite in organic solvents. *Journal of Colloid and Interface Science,* 278(1), 26-39.

Calberg, C., Jerome, R., Grandjean, J. (2004). Solid-state NMR study of poly(e-caprolactone)/clay nanocomposites. *Langmuir,* 20(5), 2039-2041.

Carrasco, F., Dionisi, D., Martinelli, A., Majone, M. (2006). Thermal stability of polyhydroxyalkanoates. *Journal of Applied Polymer Science,* 100(3), 2111-2121.

Cartier, L., Okihara, T., Ikada, Y., Tsuji, H., Puiggali, J., Lotz, B. (2000). Epitaxial crystallization and crystalline polymorphism of polylactides. *Polymer,* 41(25), 8909-8919.

Chandra, R., Rustgi, R. (1998). Biodegradable polymers. *Progress in Polymer Science (Oxford),* 23(7), 1273-1335.

Chang, J.-H., An, Y. U., Cho, D., Giannelis, E. P. (2003). Poly(lactic acid) nanocomposites: Comparison of their properties with montmorillonite and synthetic mica (II). *Polymer,* 44(13), 3715-3720.

Chang, J.-H., An, Y. U., Sur, G. S. (2003). Poly(lactic acid) nanocomposites with various organoclays. I. Thermomechanical properties, morphology, and gas permeability. *Journal of Polymer Science, Part B: Polymer Physics,* 41(1), 94-103.

Chen, B., Evans, J. R. G. (2006). Poly(e-caprolactone)-clay nanocomposites: Structure and mechanical properties. *Macromolecules,* 39(2), 747-754.

Chen, G. X., Hao, G. J., Guo, T. Y., Song, M. D., Zhang, B. H. (2002). Structure and mechanical properties of poly(3-hydroxybutyrate-co-3-hydroxyvalerate) (PHBV)/clay nanocomposites. *Journal of Materials Science Letters,* 21(20), 1587-1589.

Chen, G. X., Hao, G. J., Guo, T. Y., Song, M. D., Zhang, B. H. (2004). Crystallization kinetics of poly(3-hydroxybutyrate-co-3-hydroxyvalerate)/clay nanocomposites. *Journal of Applied Polymer Science,* 93(2), 655-661.

Chen, G., Yoon, J.-S. (2005). Nanocomposites of poly[(butylene succinate)-co-(butylene adipate)] (PBSA) and twice-functionalized organoclay. *Polymer International,* 54(6), 939-945.

Chen, G.-X., Kim, E.-S., Yoon, J.-S. (2005). Poly(butylene succinate)/twice functionalized organoclay nanocomposites: Preparation, characterization, and properties. *Journal of Applied Polymer Science,* 98(4), 1727-1732.

Chen, G.-X., Kim, H.-S., Kim, E.-S., Yoon, J.-S. (2005). Compatibilization-like effect of reactive organoclay on the poly(L-lactide)/poly(butylene succinate) blends. *Polymer,* 46(25), 11829-11836.

Chen, G.-X., Yoon, J.-S. (2005). Thermal stability of poly(L-lactide)/poly(butylene succinate)/clay nanocomposites. *Polymer Degradation and Stability,* 88(2), 206-212.

Chen, G.-X., Yoon, J.-S. (2005). Non-isothermal crystallization kinetics of poly(butylene succinate) composites with a twice functionalized organoclay. *Journal of Polymer Science, Part B: Polymer Physics,* 43(7), 817-826.

Chiellini, E., Solaro, R. (1996). Biodegradable polymeric materials. *Advanced Materials,* 8(4), 305-313.

Chivrac, F., Kadlecova, Z., Pollet, E., Averous, L. (2006). Aromatic copolyester-based nano-biocomposites: Elaboration, structural characterization and properties. *Journal of Polymers and the Environment,* 14(4), 393-401.

Chivrac, F., Pollet, E., Averous, L. (2007). Nonisothermal crystallization behavior of poly(butylene adipate-co-terephthalate)/clay nano-biocomposites. *Journal of Polymer Science, Part B: Polymer Physics,* 45(13), 1503-1510.

Choi, W. M., Kim, T. W., Park, O. O., Chang, Y. K., Lee, J. W. (2003). Preparation and characterization of poly(hydroxybutyrate-co-hydroxyvalerate)-organoclay nanocomposites. *Journal of Applied Polymer Science,* 90(2), 525-529.

Coats, A. W., Redfern, J. P. (1964). Kinetics parameters from thermogravimetric data. *Nature,* 201(4914), 68.

Connelly, J., Van Duijneveldt, J. S., Klein, S., Pizzey, C., Richardson, R. M. (2006). Effect of surfactant and solvent properties on the stacking behavior of non-aqueous suspensions of organically modified clays. *Langmuir,* 22(15), 6531-6538.

Cyras, V. P., Vasquez, A., Rozsa, C., Galego Fernandes, N., Torre, L., Kenny, J. M. (2000). Thermal stability of P(HB-HV) and its blends with polyalcohols: Crystallinity, mechanical properties, and kinetics of degradation. *Journal of Applied Polymer Science,* 77(13), 2889-2900.

De Koning, G. J. M. (1993). Thesis. Prospects of bacterial poly[(R)-3-hydroxyalkanoates]. Center for Polymers and Composites (CPC) Eindhoven University of Technology Eindhoven

Di Maio, E., Iannace, S., Sorrentino, L., Nicolais, L. (2004). Isothermal crystallization in PCL/clay nanocomposites investigated with thermal and rheometric methods. *Polymer,* 45(26), 8893-8900.

Di, Y., Iannace, S., Di Maio, E., Nicolais, L. (2003). Nanocomposites by melt intercalation based on polycaprolactone and organoclay. *Journal of Polymer Science, Part B: Polymer Physics,* 41(7), 670-678.

Doi, Y. (1990). *Microbial polyesters*. New York: John Wiley & Sons, Inc.

Dos Santos Rosa, D., Calil, M. R., Fassina Guedes, C. d. G., Rodrigues, T. C. (2004). Biodegradability of thermally aged PHB, PHB-V, and PCL in soil compostage. *Journal of Polymers and the Environment,* 12(4), 239-245.

Drzal, L. T., Misra, M., Mohanty, A. K. (2004). Sustainable Biodegradable Green Nanocomposites From Bacterial Bioplastic for Automotive Applications. *U.S. EPA STAR Progress Review Workshop - Nanotechnology and the Environment II* (p. 23). Philadelphia.

El-Hadi, A., Schnabel, R., Straube, E., Müller, G., Henning, S. (2002). Correlation between degree of crystallinity, morphology, glass temperature, mechanical properties and biodegradation of poly(3-hydroxyalkanoate) PHAs and their blends. *Polymer Testing,* 21(6), 665-674.

Ema, Y., Ikeya, M., Okamoto, M. (2006). Foam processing and cellular structure of polylactide-based nanocomposites. *Polymer,* 47(15), 5350-5359.

Erceg, M., Kovacic, T., Klaric, I. (2005). Thermal degradation of poly(3-hydroxybutyrate) plasticized with acetyl tributyl citrate. *Polymer Degradation and Stability,* 90(2), 313-318.

Fernandes, E. G., Pietrini, M., Chiellini, E. (2004). Thermo-mechanical and morphological characterization of plasticized poly[(R)-3-hydroxybutyric acid]. *Macromolecular Symposia* pp. 157-164).

Flynn, J., Wall, L. A. (1966). A quick, direct method for the determination of activation energy from thermogravimetric data. *Journal of Polymer Science Part B: Polymer Letters,* 4(5), 323-328.

Fritz, J. (1999). Thesis.Ecotoxicity of Biogenic Materials During and After their Biodegradation. University of Agriculture Vienna, Austria

Fujimaki, T. (1998). Processability and properties of aliphatic polyesters, 'Bionolle', synthesized by polycondensation reaction. *Polymer Degradation and Stability,* 59(1-3), 209-214.

Fujita, M., Sawayanagi, T., Tanaka, T., Iwata, T., Abe, H., Doi, Y., Ito, K., Fujisawa, T. (2005). Synchrotron SAXS and WAXS studies on changes in structural and thermal properties of poly[(R)-3-hydroxybutyrate] single crystals during heating. *Macromolecular Rapid Communications,* 26(9), 678-683.

Fukuda, H., Kondo, A., Noda, H. (2001). Biodiesel fuel production by transesterification of oils. *Journal of Bioscience and Bioengineering,* 92(5), 405-416.

Gain, O., Espuche, E., Pollet, E., Alexandre, M., Dubois, P. (2005). Gas barrier properties of poly(epsilon-caprolactone)/clay nanocomposites: Influence of the morphology and polymer/clay interactions. *Journal of Polymer Science Part B-Polymer Physics,* 43(2), 205-214.

Gardebien, F., Gaudel-Siri, A., Bredas, J.-L., Lazzaroni, R. (2004). Molecular dynamics simulations of intercalated poly(e-caprolactone)-montmorillonite clay nanocomposites. *Journal of Physical Chemistry B,* 108(30), 10678-10686.

Gardebien, F., Bredas, J.-L., Lazzaroni, R. (2005). Molecular dynamics simulations of nanocomposites based on poly(e-caprolactone) grafted on montmorillonite clay. *Journal of Physical Chemistry B,* 109(25), 12287-12296.

Garlotta, D. (2001). A literature review of poly(lactic acid). *Journal of Polymers and the Environment,* 9(2), 63-84.

Gassner, F., Owen, j. (1994). Physical properties of poly(ß-hydroxybutyrate)-poly(e-caprolactone) blends. *Polymer,* 35(10), 2233-2236.

Gonzalez, I., Eguiazabal, J. I., Nazabal, J. (2006). New clay-reinforced nanocomposites based on a polycarbonate/ polycaprolactone blend. *Polymer Engineering and Science,* 46(7), 864-873.

Gorrasi, G., Tortora, M., Vittoria, V., Pollet, E., Lepoittevin, B., Alexandre, M., Dubois, P. (2003). Vapor barrier properties of polycaprolactone montmorillonite nanocomposites: Effect of clay dispersion. *Polymer,* 44(8), 2271-2279.

Grassie, N., Murray, E. J., Holmes, P. A. (1984a). Thermal degradation of poly(-(D)- beta - hydroxybutyric acid): Part 3 - The reaction mechanism. *Polymer Degradation and Stability,* 6(3), 127-134.

Grassie, N., Murray, E. J., Holmes, P. A. (1984b). Thermal degradation of poly(-(D)- beta - hydroxybutyric acid): Part 1 - Identification and quantitative analysis of products. *Polymer Degradation and Stability,* 6(1), 47-61.

Grassie, N., Murray, E. J., Holmes, P. A. (1984c). Thermal degradation of poly(-(D)- beta - hydroxybutyric acid): Part 2 - Changes in molecular weight. *Polymer Degradation and Stability,* 6(2), 95-103.

Grigat, E., Koch, R., Timmermann, R. (1998). BAK 1095 and BAK 2195: Completely biodegradable synthetic thermoplastics. *Polymer Degradation and Stability,* 59(1-3), 223-226.

Hablot, E., Bordes, P., Pollet, E., Avérous, L. (2007). Thermal and thermo-mechanical degradation of PHB-based multiphase systems, *Polymer Degradation and Stability*, In Press (doi: 10.1016/j.polymdegradstab.2007.11.018).

Hammond, T. (1997). *Polymer composition containing polyhydroxyalkanoate and metal compound*. US5646217, Zeneca Limited, London, England, United Kingdom

Hasook, A., Tanoue, S., Lemoto, Y., Unryu, T. (2006). Characterization and mechanical properties of poly(lactic acid)/poly(e-caprolactone)/organoclay nanocomposites prepared by melt compounding. *Polymer Engineering and Science,* 46(8), 1001-1007.

Hatakeyama, T., Quinn, F. X. (1999). Thermal Analysis - Fundamentals and Applications to Polymer Science. Wiley.

He, H., Galy, J., Gérard, J.-F. (2005). Molecular simulation of the interlayer structure and the mobility of alkyl chains in HDTMA+/montmorillonite hybrids. *Journal of Physics and Chemistry,* 109(27), 13301-13306.

He, J.-D., Cheung, M. K., Yu, P. H., Chen, G.-Q. (2001). Thermal analyses of poly(3-hydroxybutyrate), poly(3-hydroxybutyrate-co-3-hydroxyvalerate), and poly(3-hydroxybutyrate-co-3-hydroxyhexanoate). *Journal of Applied Polymer Science,* 82(1), 90-98.

Heinz, H., Koerner, H., Anderson, K. L., Vaia, R. A., Farmer, B. L. (2005). Force field for mica-type silicates and dynamics of octadecylammonium chains grafted to montmorillonite. *Chemistry of Materials,* 17(23), 5658-5669.

Heinz, H., Vaia, R. A., Farmer, B. L. (2006). Interaction energy and surface reconstruction between sheets of layered silicates. *Journal of Chemical Physics,* 124, 224713.

Ho, D. L., Glinka, C. J., Ho, D. L. (2003). Effects of solvent solubility parameters on organoclay dispersions. *Chemistry of Materials,* 15(6), 1309-1312.

Hori, Y., Suzuki, M., Yamaguchi, A., Nishishita, T. (1993). Ring-opening polymerization of optically active β-butyrolactone using distannoxane catalysts: synthesis of high-molecular-weight poly(3-hydroxybutyrate). *Macromolecules,* 26(20), 5533.

Hori, Y., Takahashi, Y., Yamaguchi, A., Nishishita, T. (1993). Ring-opening copolymerization of optically active β-butyrolactone with several lactones catalyzed by distannoxane complexes: synthesis of new biodegradable polyesters. *Macromolecules,* 26(16), 4388.

Hori, Y., Hagiwara, T. (1996). Ring-opening polymerisation of β-butyrolactone catalysed by distannoxane complexes: study of the mechanism. *International Journal of Biological Macromolecules,* 25(1-3), 235-247.

Hrobarikova, J., Robert, J.-L., Calberg, C., Jerome, R., Grandjean, J. (2004). Solid-state NMR study of intercalated species in poly(e-caprolactone)/clay nanocomposites. *Langmuir,* 20(22), 9828-9833.

Hsu, S.-F., Wu, T.-M., Liao, C.-S. (2007). Nonisothermal crystallization behavior and crystalline structure of poly(3-hydroxybutyrate)/layered double hydroxide nanocomposites. *Journal of Polymer Science, Part B: Polymer Physics,* 45(9), 995-1002.

Jacobsen, S., Fritz, H. G. (1999). Plasticizing polylactide - the effect of different plasticizers on the mechanical properties. *Polymer Engineering and Science,* 39(7), 1303-1310.

Jordan, J. W. (1949). Organophilic bentonites: I - Swelling in organic liquids. *Journal of Physics and Colloid Chemistry,* 53(2), 294-306.

Jimenez, G., Ogata, N., Kawai, H., Ogihara, T. (1997). Structure and thermal/mechanical properties of poly(e-caprolactone)-clay blend. *Journal of Applied Polymer Science,* 64(11), 2211-2220.

Juzwa, M., Jedlinski, Z. (2006). Novel Synthesis of Poly(3-hydroxybutyrate). *Macromolecules,* 39(13), 4627.

Kadar, F., Szazdi, L., Fekete, E., Pukanszky, B. (2006). Surface characteristics of layered silicates: Influence on the properties of clay/polymer Nanocomposites. *Langmuir,* 22(18), 7848-7854.

Kalambur, S. B., Rizvi, S. S. (2004). Starch-based nanocomposites by reactive extrusion processing. *Polymer International,* 53(10), 1413-1416.

Kaplan, D. L., Mayer, J. M., Ball, D., McCassie, J., Allen, A. L., Stenhouse, P. (1993). Fundamentals of biodegradable polymers. In C. Ching, D. L. Kaplan, & E. L. Thomas. *Biodegradable Polymers and Packaging* pp. 1-42): Lancaster, Technomic Pub. Co.

Kaplan, D. L. (1998). *Biopolymers from Renewable Resources*. Berlin: Springer Verlag.

Karlsson, S., Albertsson, A.-C. (1998). Biodegradable polymers and environmental interaction. *Polymer Engineering and Science,* 38(8), 1251-1253.

Kiersnowski, A., Dabrowski, P., Budde, H., Kressler, J., Piglowski, J. (2004). Synthesis and structure of poly(e-caprolactone)/synthetic montmorillonite nano-intercalates. *European Polymer Journal,* 40(11), 2591-2598.

Kiersnowski, A., Piglowski, J. (2004b). Polymer-layered silicate nanocomposites based on poly(e-caprolactone). *European Polymer Journal,* 40(6), 1199-1207.

Kim, K. J., Doi, Y., Abe, H. (2006). Effects of residual metal compounds and chain-end structure on thermal degradation of poly(3-hydroxybutyric acid). *Polymer Degradation and Stability,* 91(4), 769-777.

Kim, S. W., Jo, W. H., Lee, M. S., Ko, M. B., Jho, J. Y. (2001). Preparation of clay-dispersed poly(styrene-co-acrylonitrile) nanocomposites using poly(e-caprolactone) as a compatibilizer. *Polymer,* 42(24), 9837-9842.

Kobayashi, T., Yamaguchi, A., Hagiwara, T., Hori, Y. (1995). Synthesis of poly(3-hydroxyalkanoate)s by ring-opening copolymerization of (R)-β-butyrolactone with other four-membered lactones using a distannoxane complex as a catalyst. *Polymer,* 36(24), 4707-4710.

Koenig, M. F., Huang, S. J. (1994). Evaluation of crosslinked poly(caprolactone) as a biodegradable, hydrophobic coating. *Polymer Degradation and Stability,* 45(1), 139-144.

Kopinke, F.-D., Remmler, M., Mackenzie, K. (1996). Thermal decomposition of biodegradable polyesters-I: Poly(beta-hydroxybutyric acid). *Polymer Degradation and Stability,* 52(1), 25-38.

Kotnis, M. A., O'Brien, G. S., Willett, J. L. (1995). Processing and mechanical properties of biodegradable poly(hydroxybutyrate-co-valerate)-starch compositions. *Journal of Environmental Polymer Degradation,* 3(2), 97-105.

Kranz, H., Ubrich, N., Maincent, P., Bodmeier, R. (2000). Physicomechanical properties of biodegradable poly(D,L-lactide) and poly(D,L-lactide-co-glycolide) films in the dry and wet states. *Journal of Pharmaceutical Sciences,* 89(12), 1558-1566.

Krikorian, V., Pochan, D. J. (2003). Poly (L-Lactic Acid)/Layered Silicate Nanocomposite: Fabrication, Characterization, and Properties. *Chemistry of Materials,* 15(22), 4317-4324.

Krikorian, V., Pochan, D. J. (2004). Unusual crystallization behavior of organoclay reinforced poly(L-lactic acid) nanocomposites. *Macromolecules,* 37(17), 6480-6491.

Krikorian, V., Pochan, D. J. (2005). Crystallization behavior of poly(L-lactic acid) nanocomposites: Nucleation and growth probed by infrared spectroscopy. *Macromolecules,* 38(15), 6520-6527.

Krishnamoorti, R., Giannelis, E. P. (1997). Rheology of end-tethered polymer layered silicate nanocomposites. *Macromolecules,* 30(14), 4097-4102.

Krook, M., Albertsson, A.-C., Gedde, U. W., Hedenqvist, M. S. (2002). Barrier and mechanical properties of montmorillonite/polyesteramide nanocomposites. *Polymer Engineering and Science,* 42(6), 1238-1246.

Krook, M., Morgan, G., Hedenqvist, M. S. (2005). Barrier and mechanical properties of injection molded montmorillonite/polyesteramide nanocomposites. *Polymer Engineering and Science,* 45(1), 135-141.

Kubies, D., Pantoustier, N., Dubois, P., Rulmont, A., Jerome, R. (2002). Controlled ring-opening polymerization of e-caprolactone in the presence of layered silicates and formation of nanocomposites. *Macromolecules,* 35(9), 3318-3320.

Kumagai, Y., Doi, Y. (1992). Enzymatic degradation and morphologies of binary blends of microbial poly(3-hydroxy butyrate) with poly(e-caprolactone), poly(1,4-butylene adipate) and poly(vinyl acetate). *Polymer Degradation and Stability,* 36(3), 241-248.

Kunioka, M., Doi, Y. (1990). Thermal degradation of microbial copolyesters. Poly(3-hydroxybutyrate-co-3-hydroxyvalerate) and poly(3-hydroxybutyrate-co-4-hydroxybutyrate). *Macromolecules,* 23(7), 1933-1936.

Kwak, S.-Y., Oh, K. S. (2003). Effect of thermal history on structural changes in melt-intercalated poly(e-caprolactone)/organoclay nanocomposites investigated by dynamic viscoelastic relaxation measurements. *Macromolecular Materials and Engineering,* 288(6), 503-508.

Labrecque, L. V., Kumar, R. A., Dave, V., Gross, R. A., McCarthy, S. P. (1997). Citrate esters as plasticizers for poly(lactic acid). *Journal of Applied Polymer Science,* 66(8), 1507-1513.

Lagaly, G. (1986). Interaction of alkylamines with different types of layered compounds. *Solid State Ionics,* 22(1), 43-51.

Lagaly, G. (1993). From clay mineral crystals to colloidal clay mineral dispersions. In B. Dobias. *Coagulation and floculation - Theory and applications* (p. 427). New York: Dekker, M.

Laszlo, P. (1987). Chemical reactions on clays. *Science,* 235(4795), 1473-1477.

Lee, C. H., Lim, S. T., Hyun, Y. H., Choi, H. J., Jhon, M. S. (2003). Fabrication and viscoelastic properties of biodegradable polymer/organophilic clay nanocomposites. *Journal of Materials Science Letters,* 22(1), 53-55.

Lee, C. H., Kim, H. B., Lim, S. T., Choi, H. J., Jhon, M. S. (2005). Biodegradable aliphatic polyester-poly(epichlorohydrin) blend/organoclay nanocomposites: Synthesis and rheological characterization. *Journal of Materials Science,* 40(15), 3981-3985.

Lee, J. H., Park, T. G., Park, H. S., Lee, D. S., Lee, Y. K., Yoon, S. C., Nam, J.-D. (2003). Thermal and mechanical characteristics of poly(L-lactic acid) nanocomposite scaffold. *Biomaterials,* 24(16), 2773-2778.

Lee, M. Y., Lee, T. S., Park, W. H. (2001). Effect of side chains on the thermal degradation of poly(3-hydroxyalkanoates). *Macromolecular Chemistry and Physics,* 202(7), 1257-1261.

Lee, S.-R., Park, H.-M., Lim, H., Kang, T., Li, X., Cho, W.-J., Ha, C.-S. (2002). Microstructure, tensile properties, and biodegradability of aliphatic polyester/clay nanocomposites. *Polymer,* 43(8), 2495-2500.

Lee, S. Y., Park, S. J. (2002). Fermentative production of SCL-PHAs. In Y. Doi, & A. Steinbüchel. *Biopolymers 3a - Polyesters I, Biological systems and biotechnological production* pp. 263-262). Weinheim, Germany: Wiley-VCH.

Lee, Y. H., Lee, J. H., An, I.-G., Kim, C., Lee, D. S., Lee, Y. K., Nam, J.-D. (2005). Electrospun dual-porosity structure and biodegradation morphology of Montmorillonite reinforced PLLA nanocomposite scaffolds. *Biomaterials,* 26(16), 3165-3172.

Lehermeier, H. J., Dorgan, J. R., Way, J. D. (2001). Gas permeation properties of poly(lactic acid). *Journal of Membrane Science,* 190(2), 243-251.

Lemoigne, M. (1926). Products of dehydration and of polymerization of b-hydroxybutyric acid. *Bulletin de la Société de Chimie Biologique,* 8, 770-782.

Lenz, R. W., Marchessault, R. H. (2005). Bacterial polyesters: Biosynthesis, biodegradable plastics and biotechnology. *Biomacromolecules,* 6(1), 1-8.

Lepoittevin, B., Devalckenaere, M., Pantoustier, N., Alexandre, M., Kubies, D., Calberg, C., Jerome, R., Dubois, P. (2002). Poly(e-caprolactone)/clay nanocomposites prepared by melt intercalation: mechanical, thermal and rheological properties. *Polymer,* 43(14), 4017-4023.

Lepoittevin, B., Pantoustier, N., Alexandre, M., Calberg, C., Jerome, R., Dubois, P. (2002). Polyester layered silicate nanohybrids by controlled grafting polymerization. *Journal of Materials Chemistry,* 12(12), 3528-3532.

Lepoittevin, B., Pantoustier, N., Alexandre, M., Calberg, C., Jerome, R., Dubois, P. (2002). Layered silicate/polyester nanohybrids by controlled ring-opening polymerization. *Macromolecular Symposia,* 183, 95-102.

Lepoittevin, B., Pantoustier, N., Devalckenaere, M., Alexandre, M., Kubies, D., Calberg, C., Jerome, R., Dubois, P. (2002). Poly(e-caprolactone)/clay nanocomposites by in-situ intercalative polymerization catalyzed by dibutyltin dimethoxide. *Macromolecules,* 35(22), 8385-8390.

Lepoittevin, B., Pantoustier, N., Devalckenaere, M., Alexandre, M., Calberg, C., Jerome, R., Henrist, C., Rulmont, A., Dubois, P. (2003). Polymer/layered silicate nanocomposites by combined intercalative polymerization and melt intercalation: A masterbatch process. *Polymer,* 44(7), 2033-2040.

Lewitus, D., McCarthy, S., Ophir, A., Kenig, S. (2006). The effect of nanoclays on the properties of PLLA-modified polymers Part 1: Mechanical and thermal properties. *Journal of Polymers and the Environment,* 14(2), 171-177.

Li, S.-D., Yu, P. H., Cheung, M. K. (2001). Thermogravimetric analysis of poly(3-hydroxybutyrate) and poly(3-hydroxybutyrate-co-3-hydroxyvalerate). *Journal of Applied Polymer Science* pp. 2237-2244).

Li, S.-D., He, J.-D., Yu, P. H., Cheung, M. K. (2003). Thermal degradation of poly(3-hydroxybutyrate) and poly(3-hydroxybutyrate-co-3-hydroxyvalerate) as studied by TG, TG-FTIR, and Py-GC/MS. *Journal of Applied Polymer Science,* 89(6), 1530-1536.

Lim, S. T., Hyun, Y. H., Choi, H. J., Jhon, M. S. (2002). Synthetic biodegradable aliphatic polyester/montmorillonite nanocomposites. *Chemistry of Materials,* 14(4), 1839-1844.

Lim, S. T., Hyun, Y. H., Lee, C. H., Choi, H. J. (2003). Preparation and characterization of microbial biodegradable poly(3-hydroxybutyrate)/organoclay nanocomposite. *Journal of Materials Science Letters,* 22(4), 299-302.

Lim, S. T., Lee, C. H., Choi, H. J., Jhon, M. S. (2003). Solidlike transition of melt-intercalated biodegradable polymer/clay nanocomposites. *Journal of Polymer Science, Part B: Polymer Physics,* 41(17), 2052-2061.

Lim, S. T., Lee, C. H., Kim, H. B., Choi, H. J., Jhon, M. S. (2004). Polymer/organoclay nanocomposites with biodegradable aliphatic polyester and its blends: Preparation and characterization. *E-Polymers*(026).

Liu, W. J., Yang, H. L., Wang, Z., Dong, L. S., Liu, J. J. (2002). Effect of nucleating agents on the crystallization of poly(3-hydroxybutyrate-co-3-hydroxyvalerate). *Journal of Applied Polymer Science,* 86(9), 2145-2152.

Ljungberg, N., Andersson, T., Wesslen, B. (2003). Film extrusion and film weldability of poly(lactic acid) plasticized with triacetine and tributyl citrate. *Journal of Applied Polymer Science,* 88(14), 3239-3247.

Lovera, D., Marquez, L., Balsamo, V., Taddei, A., Castelli, C., Muller, A. J. (2007). Crystallization, morphology, and enzymatic degradation of polyhydroxybutyrate/ polycaprolactone (PHB/PCL) blends. *Macromolecular Chemistry and Physics,* 208(9), 924-937.

Lunt, J. (1998). Large-scale production, properties and commercial applications of polylactic acid polymers. *Polymer Degradation and Stability,* 59(1-3), 145-152.

Ma, D., Zhang, G., Huang, Z., Luo, X. (1998). Synthesis and chain structure of ethylene terephthalate-ε-caprolactone copolyesters. *Journal of Polymer Science Part A: Polymer Chemistry,* 36(16), 2961-2969.

Marand, H., Collins, M. (1990). Crystallization and morphology of poly(vinylidene fluoride)/poly(3-hydroxybutyrate) blends. *American Chemical Society, Polymer Preprints, Division of Polymer Chemistry* pp. 552-553).

Madison, L. L., Huisman, G. W. (1999). Metabolic engineering of poly(3-hydroxyalkanoates): From DNA to plastic. *Microbiology and Molecular Biology Reviews,* 63(1), 21-53.

Maiti, P., Giannelis, E. P., Batt, C. A. (2002). Biodegradable polyester/layered silicate nanocomposites. *Materials Research Society Symposium - Proceedings,* 740, 141-145.

Maiti, P., Yamada, K., Okamoto, M., Ueda, K., Okamoto, K. (2002). New polylactide/layered silicate nanocomposites: Role of organoclays. *Chemistry of Materials,* 14(11), 4654-4661.

Maiti, P. (2003a). Influence of miscibility on viscoelasticity, structure, and intercalation of oligo-poly(caprolactone)/layered silicate nanocomposites. *Langmuir,* 19(13), 5502-5510.

Maiti, P., Batt, C. A., Giannelis, E. P. (2003). Renewable plastics: Synthesis and properties of PHB nanocomposites. *Polymeric Materials Science and Engineering* pp. U665-U665).

Martin, O., Averous, L. (2001). Poly(lactic acid): Plasticization and properties of biodegradable multiphase systems. *Polymer,* 42(14), 6209-6219.

McCarthy, S. P., Ranganthan, A., Ma, W. (1999). Advances in properties and biodegradabilility of co-continuous, immiscible, biodegradable, polymer blends. *Macromolecular Symposia,* 144, 63-72.

Melik, D. H., Schechtman, L. A. (1995). Biopolyester melt behavior by torque rheometry. *Polymer Engineering & Science,* 35(22), 1795-1806.

Messersmith, P. B., Giannelis, E. P. (1993). Polymer-layered silicate nanocomposites: In situ intercalative polymerization of e-caprolactone in layered silicates. *Chemistry of Materials,* 5(8), 1064-1066.

Messersmith, P. B., Giannelis, E. P. (1995). Synthesis and barrier properties of polycaprolactone-layered silicate nanocomposites. *Journal of Polymer Science: Part A: Polymer Chemistry,* 33(7), 1047-1057.

Misra, M., Desai, S. M., Mohanty, A. K., Drzal, L. T. (2004). Novel solvent-free method for functionalization of polyhydroxyalkanoates: Synthesis and characterizations. *Annual Technical Conference - ANTEC, Conference Proceedings* pp. 2442-2446).

Moon, S. I., Lee, C. W., Miyamoto, M., Kimura, Y. (2000). Melt polycondensation of L-lactic acid with Sn(II) catalysts activated by various proton acids: A direct manufacturing route to high molecular weight poly(L-lactic acid). *Journal of Polymer Science, Part A: Polymer Chemistry,* 38(9), 1673-1679.

Moon, S.-I., Lee, C.-W., Taniguchi, I., Miyamoto, M., Kimura, Y. (2001). Melt/solid polycondensation of L-lactic acid: An alternative route to poly(L-lactic acid) with high molecular weight. *Polymer,* 42(11), 5059-5062.

Moraru, V. N. (2001). Structure formation of alkylammonium montmorillonites in organic media. *Applied Clay Science,* 19(1-6), 11-26.

Muller, R.-J., Witt, U., Rantze, E., Deckwer, W.-D. (1998). Architecture of biodegradable copolyesters containing aromatic constituents. *Polymer Degradation and Stability,* 59(1-3), 203-208.

Nam, J. Y., Sinha Ray, S., Okamoto, M. (2003). Crystallization behavior and morphology of biodegradable polylactide/layered silicate nanocomposite. *Macromolecules,* 36(19), 7126-7131.

Nam, P. H., Fujimori, A., Masuko, T. (2003). Flocculation characteristics of OM clay particles in PLA-MMT hybrid systems. *E-Polymers*(5).

Nam, P. H., Fujimori, A., Masuko, T. (2004). The dispersion behavior of clay particles in poly(L-lactide)/organo-modified montmorillonite hybrid systems. *Journal of Applied Polymer Science,* 93(6), 2711-2720.

Nistor, D., Miron, N. D., Surpateanu, G. G., Azzouz, A. (2004). Study by thermal programmed desorption of the properties of modified clays on their impact on environmental pollution. *Journal of Thermal Analysis and Calorimetry,* 76(3), 913-920.

Nobes, G. A. R., Kazlauskas, R. J., Marchessault, R. H. (1996). Lipase-catalyzed ring-opening polymerization of lactones: a novel route to poly(hydroxyalkanoate)s. *Macromolecules,* 29(14), 4829.

Noda, I., Green, P. R., Satkowski, M. M., Schechtman, L. A. (2005). Preparation and properties of a novel class of polyhydroxyalkanoate copolymers. *Biomacromolecules,* 6(2), 580-586.

Nonato, R. V., Mantelatto, P. E., Rossell, C. E. V. (2001). Integrated production of biodegradable plastic, sugar and ethanol. *Applied Microbiology and Biotechnology,* 57(1-2), 1-5.

Ogata, N., Jimenez, G., Kawai, H., Ogihara, T. (1997). Structure and thermal/mechanical properties of poly(L-lactide)-clay blend. *Journal of Polymer Science, Part B: Polymer Physics,* 35(2), 389-396.

Okada, M. (2002). Chemical syntheses of biodegradable polymers. *Progress in Polymer Science (Oxford),* 27(1), 87-133.

Okamoto, K., Ray, S. S., Okamoto, M. (2003). New poly(butylene succinate)/layered silicate nanocomposites. II. Effect of organically modified layered silicates on structure, properties, melt rheology, and biodegradability. *Journal of Polymer Science, Part B: Polymer Physics,* 41(24), 3160-3172.

Organ, S. J., Barham, P. J. (1993). Phase separation in a blend of poly(hydroxybutyrate) with poly(hydroxybutyrate-co-hydroxyvalerate). *Polymer,* 34(3), 459-467.

Otera, J. (1993). Transesterification. *Chemical Reviews,* 93(4), 1449-1470.

Ozawa, T. (1965). A New Method of Analyzing Thermogravimetric Data. *Bulletin of the Chemical Society of Japan,* 38, 188.

Padermshoke, A., Katsumoto, Y., Sato, H., Ekgasit, S., Noda, I., Ozaki, Y. (2005). Melting behavior of poly(3-hydroxybutyrate) investigated by two-dimensional infrared correlation spectroscopy. *Spectrochimica Acta - Part A: Molecular and Biomolecular Spectroscopy,* 61(4), 541-550.

Pandey, J. K., Kumar, A. P., Misra, M., Mohanty, A. K., Drzal, L. T., Singh, R. P. (2005). Recent advances in biodegradable nanocomposites. *Journal of Nanoscience and Nanotechnology,* 5(4), 497-526.

Pantoustier, N., Alexandre, M., Degée, P., Calberg, C., Jerome, R., Henrist, C., Cloots, R., Rulmont, A., Dubois, P. (2001). Poly(e-caprolactone) layered silicate nanocomposites: effect of clay surface modifiers on the melt intercalation process. *E-Polymers,* 009.

Pantoustier, N., Lepoittevin, B., Alexandre, M., Kubies, D., Calberg, C., Jerome, R., Dubois, P. (2002). Biodegradable polyester layered silicate nanocomposites based on poly(e-caprolactone). *Polymer Engineering and Science,* 42(9), 1928-1937.

Pantoustier, N., Alexandre, M., Degée, P., Kubies, D., Jerome, R., Henrist, C., Rulmont, A., Dubois, P. (2003). Intercalative polymerization of cyclic esters in layered silicates: thermal vs. catalytic activation. *Composite Interfaces,* 10(4), 423-433.

Parikh, M., Gross, R. A., McCarthy, S. P. (1998). The influence of injection molding conditions on biodegradable polymers. *Journal of Injection Molding Technology,* 2(1), 30.

Paul, M.-A., Alexandre, M., Degée, P., Calberg, C., Jerome, R., Dubois, P. (2003). Exfoliated polylactide/clay nanocomposites by in-situ coordination-insertion polymerization. *Macromolecular Rapid Communications,* 24(9), 561-566.

Paul, M.-A., Alexandre, M., Degée, P., Henrist, C., Rulmont, A., Dubois, P. (2003). New nanocomposite materials based on plasticized poly(L-lactide) and organo-modified montmorillonites: Thermal and morphological study. *Polymer,* 44(2), 443-450.

Paul, M.-A., Delcourt, C., Alexandre, M., Degée, P., Monteverde, F., Dubois, P. (2005). Polylactide/montmorillonite nanocomposites: study of the hydrolytic degradation. *Polymer Degradation and Stability,* 87(3), 535-542.

Paul, M.-A., Delcourt, C., Alexandre, M., Degée, P., Monteverde, F., Rulmont, A., Dubois, P. (2005). (Plasticized) polylactide/(organo-)clay nanocomposites by in situ intercalative polymerization. *Macromolecular Chemistry and Physics,* 206(4), 484-498.

Perego, G., Cella, G. D., Bastioli, C. (1996). Effect of molecular weight and crystallinity on poly(lactic acid) mechanical properties. *Journal of Applied Polymer Science,* 59(1), 37-43.

Persenaire, O., Alexandre, M., Degée, P., Dubois, P. (2001). Mechanisms and kinetics of thermal degradation of poly(e-caprolactone). *Biomacromolecules,* 2(1), 288-294.

Philip, S., Keshavarz, T., Roy, I. (2007). Polyhydroxyalkanoates: Biodegradable polymers with a range of applications. *Journal of Chemical Technology and Biotechnology,* 82(3), 233-247.

Pinto, A. C., Guarieiro, L. L. N., Rezende, M. J. C., Ribeiro, N. M., Torres, E. A., Lopes, W. A., De Pereira, P. A. P., De Andrade, J. B. (2005). Biodiesel: An overview. *Journal of the Brazilian Chemical Society,* 16(6 B), 1313-1330.

Pluta, M., Galeski, A., Alexandre, M., Paul, M.-A., Dubois, P. (2002). Polylactide/montmorillonite nanocomposites and microcomposites prepared by melt blending: Structure and some physical properties. *Journal of Applied Polymer Science,* 86(6), 1497-1506.

Pluta, M. (2004). Morphology and properties of polylactide modified by thermal treatment, filling with layered silicates and plasticization. *Polymer,* 45(24), 8239-8251.

Pluta, M., Paul, M.-A., Alexandre, M., Dubois, P. (2006). Plasticized polylactide/clay nanocomposites. I. The role of filler content and its surface organo-modification on the physico-chemical properties. *Journal of Polymer Science, Part B: Polymer Physics,* 44(2), 299-311.

Pluta, M., Paul, M.-A., Alexandre, M., Dubois, P. (2006). Plasticized polylactide/clay nanocomposites. II. The effect of aging on structure and properties in relation to the filler content and the nature of its organo-modification. *Journal of Polymer Science, Part B: Polymer Physics,* 44(2), 312-325.

Poirier, Y. (2002). Polyhydroxyalknoate synthesis in plants as a tool for biotechnology and basic studies of lipid metabolism. *Progress in Lipid Research,* 41(2), 131-155.

Poller, R. C., Retout, S. P. (1979). Organotin compounds as transesterification catalysts. *Journal of Organometallic Chemistry,* 173(3), C7-C8.

Pollet, E., Delcourt, C., Alexandre, M., Dubois, P. (2006). Transesterification catalysts to improve clay exfoliation in synthetic biodegradable polyester nanocomposites. *European Polymer Journal,* 42(6), 1330-1341.

Pucciariello, R., Villani, V., Langerame, F., Gorrasi, G., Vittoria, V. (2004). Interfacial effects in organophilic montmorillonite-poly(e- caprolactone) nanocomposites. *Journal of Polymer Science, Part B: Polymer Physics,* 42(21), 3907-3919.

Pucciariello, R., Villani, V., Gorrasi, G., Vittoria, V. (2005). Phase behavior of blends of poly(e-caprolactone) and a modified montmorillonite-poly(e-caprolactone) nanocomposite. *Journal of Macromolecular Science - Physics,* 44 B(1), 79-92.

Ramkumar, D. H. S., Bhattacharya, M. (1998). Steady shear and dynamic properties of biodegradable polyesters. *Polymer Engineering and Science,* 38(9), 1426-1435.

Ramsay, B. A., Ramsay, J. A. (2002). Poly(3-hydroxyalkanoates). *Encyclopedia of Polymer Science and Technology*. Weinheim, Germany: John Wiley & Sons.

Ratto, J. A., Stenhouse, P. J., Auerbach, M., Mitchell, J., Farrell, R. (1999). Processing, performance and biodegradability of a thermoplastic aliphatic polyester/starch system. *Polymer,* 40(24), 6777-6788.

Rehberg, C. E., Faucette, W. A., Fisher, C. H. (1944a). Preparation and properties of secondary and branched-chain alkyl acrylates. *Journal of the American Chemical Society,* 66(10), 1723-1724.

Rehberg, C. E., Fisher, C. H. (1944b). Preparation and properties of the n-alkyl acrylates. *Journal of the American Chemical Society,* 66(7), 1203-1207.

Reddy, C. S. K., Ghai, R., Rashmi, Kalia, V. C. (2003). Polyhydroxyalkanoates: An overview. *Bioresource Technology,* 87(2), 137-146.

Renstad, R., Karlsson, S., Albertsson, A.-C., Werner, P.-E., Westdahl, M. (1997). Influence of processing parameters on the mass crystallinity of poly(3-hydroxybutyrate-co-3-hydroxyvalerate). *Polymer International,* 43(3), 201-209.

Renstad, R., Karlsson, S., Albertsson, A.-C. (1997). Influence of processing parameters on the molecular weight and mechanical properties of poly(3-hydroxybutyrate-co-3-hydroxyvalerate). *Polymer Degradation and Stability,* 57(3), 331-338.

Schuchardt, U., Sercheli, R., Vargas, R. M. (1998). Transesterification of vegetable oils: A review. *Journal of the Brazilian Chemical Society,* 9(3), 199-210.

Shibata, M., Someya, Y., Orihara, M., Miyoshi, M. (2006). Thermal and mechanical properties of plasticized poly(L-lactide) nanocomposites with organo-modified montmorillonites. *Journal of Applied Polymer Science,* 99(5), 2594-2602.

Shibata, M., Teramoto, N., Someya, Y., Tsukao, R. (2007). Nanocomposites based on poly(e-caprolactone) and the montmorillonite treated with dibutylamine-terminated e-caprolactone oligomer. *Journal of Applied Polymer Science,* 104(5), 3112-3119.

Shih, Y. F., Wang, T. Y., Jeng, R. J., Wu, J. Y., Teng, C. C. (2007). Biodegradable nanocomposites based on poly(butylene succinate)/organoclay. *Journal of Polymers and the Environment,* 15(2), 151-158.

Shogren, R. (1997). Water vapor permeability of biodegradable polymers. *Journal of Environmental Polymer Degradation,* 5(2), 91-95.

Shogren, R. L. (1995). Poly(ethylene oxide)-coated granular starch-poly(hydroxybutyrate-co-hydroxyvalerate) composite materials. *Journal of Environmental Polymer Degradation,* 3(2), 75-80.

Sinclair, R. G. (1996). The case for polylactic acid as a commodity packaging plastic. *Journal of Macromolecular Science - Pure and Applied Chemistry*, 33(5), 585-597.

Sinha Ray, S., Maiti, P., Okamoto, M., Yamada, K., Ueda, K. (2002). New Polylactide/Layered Silicate Nanocomposites. 1. Preparation, Characterization, and Properties. *Macromolecules,* 35(8), 3104-3110.

Sinha Ray, S., Okamoto, K., Maiti, P., Okamoto, M. (2002). New Poly(butylene succinate)/Layered Silicate Nanocomposites: Preparation and Mechanical Properties. *Journal of Nanoscience and Nanotechnology,* 2(2), 171-176.

Sinha Ray, S., Okamoto, K., Yamada, K., Okamoto, M. (2002). Novel Porous Ceramic Material via Burning of Polylactide/Layered Silicate Nanocomposite. *Nano Letters,* 2(4), 423-425.

Sinha Ray, S., Yamada, K., Ogami, A., Okamoto, M., Ueda, K. (2002). New polylactide/layered silicate nanocomposite: Nanoscale control over multiple properties. *Macromolecular Rapid Communications,* 23(16), 943-947.

Sinha Ray, S., Yamada, K., Okamoto, M., Ueda, K. (2002). Polylactide-Layered Silicate Nanocomposite: A Novel Biodegradable Material. *Nano Letters,* 2(10), 1093-1096.

Sinha Ray, S., Okamoto, K., Okamoto, M. (2003a). Structure-property relationship in biodegradable poly(butylene succinate)/layered silicate nanocomposites. *Macromolecules,* 36(7), 2355-2367.

Sinha Ray, S., Okamoto, M. (2003). Polymer/layered silicate nanocomposites: A review from preparation to processing. *Progress in Polymer Science (Oxford),* 28(11), 1539-1641.

Sinha Ray, S., Okamoto, M. (2003). New Polylactide/Layered Silicate Nanocomposites. 6. Melt Rheology and Foam Processing. *Macromolecular Materials and Engineering,* 288(12), 936-944.

Sinha Ray, S., Okamoto, M. (2003). Biodegradable polylactide and its nanocomposites: Opening a new dimension for plastics and composites. *Macromolecular Rapid Communications,* 24(14), 815-840.

Sinha Ray, S., Yamada, K., Okamoto, M., Fujimoto, Y., Ogami, A., Ueda, K. (2003). New polylactide/layered silicate nanocomposites. 5. Designing of materials with desired properties. *Polymer,* 44(21), 6633-6646.

Sinha Ray, S., Yamada, K., Okamoto, M., Ogami, A., Ueda, K. (2003). New Polylactide/Layered Silicate Nanocomposites. 3. High-Performance Biodegradable Materials. *Chem. Mater.,* 15(7), 1456-1465.

Sinha Ray, S., Yamada, K., Okamoto, M., Ogami, A., Ueda, K. (2003). New polylactide/layered silicate nanocomposites. 4. Structure, properties and biodegradability. *Composite Interfaces,* 10(4-5), 435-450.

Sinha Ray, S., Yamada, K., Okamoto, M., Ueda, K. (2003). Biodegradable polylactide/montmorillonite nanocomposites. *Journal of Nanoscience and Nanotechnology,* 3(6), 503-510.

Sinha Ray, S., Yamada, K., Okamoto, M., Ueda, K. (2003). Control of biodegradability of polylactide via nanocomposite technology. *Macromolecular Materials and Engineering,* 288(3), 203-208.

Sinha Ray, S., Yamada, K., Okamoto, M., Ueda, K. (2003). New polylactide-layered silicate nanocomposites. 2. Concurrent improvements of material properties, biodegradability and melt rheology. *Polymer,* 44(3), 857-866.

Sinha Ray, S., Bousmina, M. (2005). Poly(butylene sucinate-co-adipate)/montmorillonite nanocomposites: Effect of organic modifier miscibility on structure, properties, and viscoelasticity. *Polymer,* 46(26), 12430-12439.

Sinha Ray, S., Bousmina, M., Okamoto, K. (2005). Structure and properties of nanocomposites based on poly(butylene succinate-co-adipate) and organically modified montmorillonite. *Macromolecular Materials and Engineering,* 290(8), 759-768.

Sinha Ray, S., Bousmina, M. (2006). Crystallization behavior of poly[(butylene succinate)-co-adipate] nanocomposite. *Macromolecular Chemistry and Physics,* 207(14), 1207-1219.

Sinha Ray, S., Okamoto, K., Okamoto, M. (2006). Structure and properties of nanocomposites based on poly(butylene succinate) and organically modified montmorillonite. *Journal of Applied Polymer Science,* 102(1), 777-785.

Sinha Ray, S., Bandyopadhyay, J., Bousmina, M. (2007). Effect of organoclay on the morphology and properties of poly(propylene)/poly[(butylene succinate)-co-adipate] blends. *Macromolecular Materials and Engineering,* 292(6), 729-747.

Sinha Ray, S., Bandyopadhyay, J., Bousmina, M. (2007). Thermal and thermomechanical properties of poly[(butylene succinate)-co-adipate] nanocomposite. *Polymer Degradation and Stability,* 92(5), 802-812.

Someya, Y., Nakazato, T., Teramoto, N., Shibata, M. (2004). Thermal and mechanical properties of poly(butylene succinate) nanocomposites with various organo-modified montmorillonites. *Journal of Applied Polymer Science,* 91(3), 1463-1475.

Slabaugh, W. H., Hiltner, A. (1968). The swelling of alkylammonium montmorillonites. *Journal of Physical Chemistry,* 72(12), 4295-4298.

Someya, Y., Kondo, N., Teramoto, N., Shibata, M. (2005). Studies of biodegradation of poly (butylene adipate-co-butylene terephtharate) / layered silicatenanocomposites. *Polymer Preprints, Japan* (p. 5362).

Someya, Y., Sugahara, Y., Shibata, M. (2005). Nanocomposites based on poly(butylene adipate-co-terephthalate) and montmorillonite. *Journal of Applied Polymer Science,* 95(2), 386-392.

Sposito, G., Skipper, N. T., Sutton, R., Park, S.-H., Soper, A. K., Greathouse, J. A. (1999). Surface geochemistry of the clay minerals. *Proceedings of the National Academy of Sciences of the United States of America,* 96(7), 3358-3364

Spychaj, T., Fabrycy, E., Spychaj, S., Kacperski, M. (2001). Aminolysis and aminoglycolysis of waste poly(ethylene terephthalate). *Journal of Material Cycles and Waste Management,* 3(1), 24-31.

Starink, M. J. (2003). The determination of activation energy from linear heating rate experiments: A comparison of the accuracy of isoconversion methods. *Thermochimica Acta,* 404(1-2), 163-176.

Steinbuchel, A., Doi, Y. (2002). *Polyesters III - Applications and Commercial Products*. Wiley-VCH, Weinheim, Germany.

Steinbuchel, A. (2003). *Biopolymers, General Aspects and Special Applications*. Wiley-VCH, Weinheim, Germany.

Swain, S. N., Rao, K. K., Nayak, P. L. (2005). Biodegradable polymers: Part II. Thermal degradation of biodegradable plastics cross-linked from formaldehyde-soy protein concentrate. *Journal of Thermal Analysis and Calorimetry,* 79(1), 33-38.

Tagushi, K., Tagushi, S., Sudesh, K., Maehara, A., Tsuge, T., Doi, Y. (2002). Metabolic pathways and engineering of PHA biosynthesis. In Y. Doi, & A. Steinbüchel. *Biopolymers 3a - Polyesters I, Biological systems and biotechnological production* pp. 217-248). Weinheim, Germany: Wiley-VCH.

Tanoue, S., Hasook, A., Iemoto, Y., Unryu, T. (2006). Preparation of poly(lactic acid)/poly(ethylene glycol)/ organoclay nanocomposites by melt compounding. *Polymer Composites,* 27(3), 256-263.

Tokiwa, Y., Suzuki, T. (1977). Hydrolysis of polyesters by lipases. *Nature,* 270(5632), 76-78.
Tortora, M., Vittoria, V., Galli, G., Ritrovati, S., Chiellini, E. (2002). Transport properties of modified montmorillonite-poly(e-caprolactone) nanocomposites. *Macromolecular Materials and Engineering,* 287(4), 243-249.

Tomita, K., Ida, H. (1975). Studies on the formation of poly(ethylene terephthalate): 3. Catalytic activity of metal compounds in transesterification of dimethyl terephthalate with ethylene glycol. *Polymer,* 16(3), 185-190.

Torre, L., Kenny, J. M., Maffezzoli, A. M. (1998). Degradation behaviour of a composite material for thermal protection systems Part I-Experimental characterization. *Journal of Materials Science,* 33(12), 3137-3143.

Tuominen, J., Kylma, J., Kapanen, A., Venelampi, O., Itävaara, M., Seppälä, J. (2002). Biodegradation of lactic acid based polymers under controlled composting conditions and evaluation of the ecotoxicological impact. *Biomacromolecules,* 3(3), 445-455.

Urbanczyk, L., Hrobarikova, J., Calberg, C., Jerome, R., Grandjean, J. (2006). Motional heterogeneity of intercalated species in modified clays and poly(e-caprolactone)/clay nanocomposites. *Langmuir,* 22(10), 4818-4824.

Utracki, L. A., Sepehr, M., Boccaleri, E. (2007). Synthetic, layered nanoparticles for polymeric nanocomposites (PNCs). *Polymers for Advanced Technologies,* 18(1), 1–37.

Vaia, R. A., Teukolsky, R. K., Giannelis, E. P. (1994). Interlayer structure and molecular environment of alkylammonium layered silicates. *Chemistry of Materials,* 6(7), 1017-1022.

Vaia, R. A., Liu, W., Koerner, H. (2003). Analysis of Small-Angle Scattering of Suspensions of Organically Modified Montmorillonite: Implications to Phase Behavior of Polymer Nanocomposites. *Journal of Polymer Science: Part B: Polymer Physics,* 41, 3214–3236.

Valentin, H. E., Broyles, D. L., Casagrande, L. A., Colburn, S. M., Creely, W. L., DeLaquil, P. A., Felton, H. M., Gonzalez, K. A., Houmiel, K. H., Lutke, K., Mahadeo, D. A., Timothy A. Mitsky, Padgette, S. R., Reiser, S. E., Slater, S., Stark, D. M., Stock, R. T., Stone, D. A., Taylor, N. B., Thorne, G. M., Tran, M., Gruys, K. J. (1999). PHA production, from bacteria to plants. *International Journal of Biological Macromolecules,* 25(1-3), 303-306.

VanderHart, D. L., Asano, A., Gilman, J. W. (2001). Solid-state NMR investigation of paramagnetic nylon-6 clay nanocomposites. 1. Crystallinity, morphology, and the direct influence of Fe3+ on nuclear spins. *Chemistry of Materials,* 13(10), 3781-3795.

VanderHart, D. L., Asano, A., Gilman, J. W. (2001). NMR measurements related to clay-dispersion quality and organic-modifier stability in nylon-6/clay nanocomposites. *Macromolecules,* 34(12), 3819-3822.

VanderHart, D. L., Asano, A., Gilman, J. W. (2001). Solid-state NMR investigation of paramagnetic nylon-6 clay nanocomposites. 2. Measurement of clay dispersion, crystal stratification, and stability of organic modifiers. *Chemistry of Materials,* 13(10), 3796-3809.

Van Tuil, R., Fowler, P., Lawther, M., Weber, C. J. (2000). Properties of biobased packaging materials. *Biobased Packaging Materials for the Food Industry - Status and Perspectives* pp. 8-33): KVL, Frederiksberg, Denmark.

Velho, L., Velho, P. (2006). Innovation in Resource-Based Technology Clusters: Investigating the Lateral Migration Thesis - The development of a sugar-based plastic in Brazil. *Employment growth & development initiative*: Human Science Research Council.

Vert, M., Schwarch, G., Coudane, J. (1995). Present and future of PLA polymers. *J. Macromol. Sci., Pure Appl. Chem.,* A32(4), 787-796.

Viville, P., Lazzaroni, R., Pollet, E., Alexandre, M., Dubois, P., Borcia, G., Pireaux, J.-J. (2003). Surface Characterization of Poly(e-caprolactone)-Based Nanocomposites. *Langmuir,* 19(22), 9425-9433.

Viville, P., Lazzaroni, R., Pollet, E., Alexandre, M., Dubois, P. (2004). Controlled polymer grafting on single clay nanoplatelets. *Journal of the American Chemical Society,* 126(29), 9007-9012.

Vollhardt, K. P. C. (1990). *Traité de chimie organique*. Bruxelles, Belgium: De Boeck et Editions Universitaires.

Torre, L., Kenny, J. M., Maffezzoli, A. M. (1998). Degradation behaviour of a composite material for thermal protection systems Part I-Experimental characterization. *Journal of Materials Science,* 33(12), 3137-3143.

Wang, S., Song, C., Chen, G., Guo, T., Liu, J., Zhang, B., Takeuchi, S. (2005). Characteristics and biodegradation properties of poly(3-hydroxybutyrate-co-3-hydroxyvalerate)/organophilic montmorillonite (PHBV/OMMT) nanocomposite. *Polymer Degradation and Stability,* 87(1), 69-76.

Wee, Y.-J., Kim, J.-N., Ryu, H.-W. (2006). Biotechnological production of lactic acid and its recent applications. *Food Technology and Biotechnology,* 44(2), 163-172.

Williams, S. F., Martin, D. P., Horowitz, D. M., Peoples, O. P. (1999). PHA applications: addressing the price performance issue I. Tissue engineering. *International Journal of Biological Macromolecules,* 25(1-3), 111–121.

Witt, U., Einig, T., Yamamoto, M., Kleeberg, I., Deckwer, W.-D., Muller, R.-J. (2001). Biodegradation of aliphatic-aromatic copolyesters: Evaluation of the final biodegradability and ecotoxicological impact of degradation intermediates. *Chemosphere,* 44(2), 289-299.

Wu, T.-M., Wu, C.-Y. (2006). Biodegradable poly(lactic acid)/chitosan-modified montmorillonite nanocomposites: Preparation and characterization. *Polymer Degradation and Stability,* 91(9), 2198-2204.

Xi, Y., Ding, Z., He, H., Frost, R. L. (2004). Structure of organoclays - An X-ray diffraction and thermogravimetric analysis study. *Journal of Colloid and Interface Science,* 277(1), 116–120.

Xi, Y., Frost, R. L., He, H., Kloprogge, T., Bostrom, T. (2005). Modification of Wyoming montmorillonite surfaces using a cationic surfactant. *Langmuir,* 21(19), 8675-8680.

Xie, W., Gao, Z., Pan, W.-P., Hunter, D., Singh, A., Vaia, R. (2001). Thermal degradation chemistry of alkyl quaternary ammonium montmorillonite. *Chemistry of Materials,* 13(9), 2979-2990

Yokota, Y., Marechal, H. (1999). Processability of biodegradable poly(butylene) succinate and its derivates. A case study. *Biopolymer Conference*. Wurzburg, Germany.

Yoshida, O., Okamoto, M. (2006). Direct melt intercalation of polylactide chains into nano-galleries: Interlayer expansion and nano-composite structure. *Macromolecular Rapid Communications,* 27(10), 751-757.

Yoshioka, M., Takabe, K., Sugiyama, J., Nishio, Y. (2006). Newly developed nanocomposites from cellulose acetate/layered silicate/poly(e-caprolactone): Synthesis and morphological characterization. *Journal of Wood Science,* 52(2), 121-127.

Yu, L., Dean, K., Li, L. (2006). Polymer blends and composites from renewable resources. *Progress in Polymer Science (Oxford),* 31(6), 576-602.

Zanetti, M., Camino, G., Thomann, R., Mülhaupt, R. (2001). Synthesis and thermal behaviour of layered silicate-EVA nanocomposites. *Polymer,* 42(10), 4501-4507.

Zhang, Z., Luo, X., Lu, Y., Ma, D. (2001). Transesterifications of poly(bisphenol A carbonate) with caprolactone segments in copolyester and poly(e-caprolactone) homopolymer. *European Polymer Journal,* 37(1), 99-104.

Zhang, Z., Luo, X., Lu, Y., Ma, D. (2001). Transesterifications of poly(bisphenol A carbonate) with aromatic and aliphatic segments in ethylene terephthalate-caprolactone copolyester. *Journal of Applied Polymer Science,* 80(9), 1558-1565.

Zheng, X., Wilkie, C. A. (2003). Nanocomposites based on poly (e-caprolactone) (PCL)/clay hybrid: Polystyrene, high impact polystyrene, ABS, polypropylene and polyethylene. *Polymer Degradation and Stability,* 82(3), 441-450.

Zinn, M., Witholt, B., Egli, T. (2001). Occurrence, synthesis and medical application of bacterial polyhydroxyalkanoate. *Advanced Drug Delivery Reviews,* 53(1), 5-21.

Liste des Figures

Chapitre I

Publication n°1

Chapitre II

Publication n°2

Chapitre III

Publication n°3

Publication n°4

Chapitre IV

Liste des Tableaux

Chapitre I

Publication n°1

Chapitre II

Publication n°2

Chapitre III

Publication n°3

Publication n°4

Chapitre IV

RESUME "Nano-biocomposites : Etude de systèmes structurés à base de polyhydroxyalcanoates et montmorillonites"

Les polyhydroxyalcanoates (PHAs) étudiés sont des polyesters biodégradables et biocompatibles synthétisés par fermentation bactérienne de produits dérivés de la canne à sucre. Ces biopolymères présentent notamment une bonne rigidité et un taux de cristallinité très important. Cependant, leur comportement mécanique fragile et leur faible stabilité thermique limitent encore leur développement. L'élaboration de nano-biocomposites, i.e. l'incorporation et la dispersion de charges de taille nanométrique telles que les montmorillonites dans la matrice PHA vise donc à pallier ces déficiences. L'analyse des relations "procédé-structure-propriétés" ont montré que les facteurs clés contrôlant l'élaboration de ces matériaux nanostructurés sont l'affinité polymère-argile, le taux de charge et la voie d'élaboration (voie "solvant" vs. "fondu"). Par ailleurs, une étude spécifique a montré que les organomodifiants utilisés pour compatibiliser le polymère et la charge, et dans une moindre mesure, les résidus de fermentation, affectent la stabilité thermique et thermo-mécanique des PHAs. Différentes approches (enrobage des feuillets d'argile par greffage de biopolyester, redispersion de masterbatch…) ont donc été explorées afin de limiter la dégradation de la matrice mais également d'améliorer la dispersion de la charge et de mieux compatibiliser la charge et la matrice. Ces études ont montré que la dispersion directe d'un faible taux de Cloisite®30B (< 3%pds) dans le PHA à l'état fondu présente le meilleur compromis en terme de dégradation limitée, de qualité de dispersion et donc de propriétés du matériau final.

ABSTRACT "Nano-biocomposites : Study of structured systems based on polyhydroxyalkanoates and montmorillonites"

Polyhydroxyalkanoates (PHAs) are biodegradable and biocompatible polyesters produced from renewable resources by bacterial fermentation. These biopolymers are stiff and highly crystalline. Nevertheless, they are not fully competitive compared to conventional polymers since they exhibit brittleness and poor thermal stability. Therefore, to improve their properties, PHA-based nano-biocomposites were prepared by adding nano-sized fillers such as montmorillonites (a clay layered silicate). The process-structure-properties relationships have been investigated. They have shown that the polymer-clay affinity, the filler content and the elaboration route (solvent vs. melt intercalation) are key factors for elaboration of these nano-structured materials. Moreover, a specific study evidenced that organomodifiers used as polymer-clay compatibilizers and, in a less extent, the fermentation residues affect the thermal and thermo-mechanical PHAs stability. Different approaches (biopolyester grafting on the clay surface, masterbatch route,) were thus considered to limit the matrix degradation, but also to improve the clay nanodispersion and the polymer-clay affinity. This work has revealed that melt mixing of less than 3 wt% of Cloisite®30B with PHA leads to better results in terms of limited degradation, clay dispersion and thus properties of the final material.

MOTS-CLES

Nanocomposite, biopolymère, polyhydroxyalcanoate, argile, montmorillonite, organomodifiant, relations "procédé-structure-propriétés", dégradation, stabilité thermique.

LABORATOIRE

Laboratoire d'Ingénierie des Polymères pour les Hautes Technologies (LIPHT) - UMR CNRS 7165 – 25 Rue Becquerel – 67 087 Strasbourg Cedex 2.